

**Functional characterisation of
alkane-degrading monooxygenases
in *Rhodococcus jostii* strain 8**

Jindarat Ekprasert

**A thesis submitted to the School of Environmental
Sciences in fulfilment of the requirements for the
degree of Doctor of Philosophy**

September 2014

**University of East Anglia
Norwich, UK**

Contents

List of figures	viii
List of tables	xiii
Declaration	xv
Acknowledgements	xvi
Abbreviations	xvii
Abstract	xxi
Chapter 1 introduction	1
1.1. Significance of alkanes in the environment	2
1.1.1. Chemistry of alkanes	2
1.2. The <i>Rhodococcus</i> genus	3
1.2.1. Common characteristics of <i>Rhodococcus</i> spp.	3
1.2.2. <i>Rhodococcus</i> spp. are capable of degrading gaseous alkanes	4
1.2.3. Potential applications of <i>Rhodococcus</i> in biotechnology	5
1.3. Bacterial enzymes responsible for alkane degradation	6
1.3.1. Integral membrane, non-heme iron alkane hydroxylases (AlkB)	6
1.3.2. Soluble di-iron monooxygenases (SDIMO)	8
1.3.2.1. SDIMO classification	10
1.3.2.2. Molecular genetics of SDIMOs	13
1.3.2.3. Mutagenesis of soluble methane monooxygenase	13
1.3.3. Cytochrome P450 alkane hydroxylases	14
3.3.1. Class I P450	14
3.3.2. Class II P450 (CYP52)	15
3.3.3. Class II P450 (CYP2E, CYP4B)	15
1.3.4. Membrane bound copper-containing (and possibly iron-containing) monooxygenases	15
1.4. Alkane metabolisms in <i>Rhodococcus</i> spp.	16
1.4.1. Aerobic metabolism of C ₂ -C ₄ gaseous alkanes in bacteria	16
1.4.1.1. Ethane (C ₂ H ₆) metabolism	16
1.4.1.2. Propane (C ₃ H ₈) metabolism	17

1.4.1.3. Butane (C ₄ H ₁₀) metabolism	21
1.4.2. Alcohol dehydrogenases (ADH)	22
1.4.2.1. Pyrroloquinoline quinone (PQQ) dependent alcohol dehydrogenase	23
1.4.2.2. Nicotinamide adenine dinucleotide (NAD(P)) dependent alcohol dehydrogenase	23
1.4.2.3. <i>N,N</i> -dimethyl-4-nitrosoaniline (NDMA) dependent alcohol dehydrogenase	24
1.5. Previous studies on mutagenesis of alkane-degrading enzymes in <i>Rhodococcus</i> species	25
1.5.1. The development of <i>E. coli</i> – <i>Rhodococcus</i> shuttle vectors and transformation procedures	25
1.5.2. Mutagenesis of propane monooxygenases	27
1.5.3. Mutagenesis of <i>alkB</i> -type alkane monooxygenases	28
Project aims	29
Chapter 2 Materials and methods	32
2.1. Bacterial strains, plasmids and primers used in this study	33
2.2. Chemicals	33
2.3. Antibiotics	33
2.4. Growth conditions	34
2.4.1. <i>Rhodococcus jostii</i> strain 8	35
2.4.2. <i>Escherichia coli</i>	36
2.5. Maintenance of bacterial strains	36
2.6. Cell dry weight measurement	36
2.7. Light microscopy	36
2.8. General purpose buffers and solutions	37
2.9. Extraction of nucleic acids	37
2.9.1. Extraction of genomic DNA from <i>Rhodococcus jostii</i> strain 8	38
2.9.2. Small-scale extraction of plasmids from <i>E. coli</i>	38
2.9.3. Extraction of RNA from <i>Rhodococcus jostii</i> strain 8	38
2.10. Nucleic acid manipulation techniques	38
2.10.1. DNA/RNA quantification	38
2.10.2. DNA purification	38
2.10.3. RNA purification	38
2.10.4. RNase treatment of genomic DNA	39
2.10.5. DNA restriction digests	39

2.11. Polymerase chain reaction (PCR)	39
2.11.1. Design of PCR primers	39
2.12. Agarose gel electrophoresis	43
2.13. Dephosphorylation of DNA	43
2.14. DNA ligations	43
2.15. Cloning of PCR products	43
2.16. Clone library construction and restriction fragment length polymorphism (RFLP)	43
2.17. Sequencing of DNA	44
2.18. Reverse transcriptase PCR (RT-PCR)	44
2.19. Reverse transcriptase quantitative PCR (RT-qPCR)	44
2.20. Genome sequencing	45
2.21. Bacterial transformations	45
2.21.1. Preparation and transformation of chemically competent <i>E. coli</i>	45
2.21.2. Preparation and transformation of electrocompetent <i>E. coli</i>	46
2.21.3. Preparation and transformation of electrocompetent <i>Rhodococcus jostii</i> strain 8	47
2.22. Harvesting of cells	47
2.23. Bacterial purity checks	48
2.24. Calculation of specific growth rates	48
2.25. Preparation of cell-free extracts	48
2.26. Protein quantification	48
2.27. Sodium Dodecyl Sulfate-Polyacrylamide Gel Electrophoresis (SDS-PAGE)	49
2.28. Mass spectrometry analysis of polypeptides	50
2.29. Oxygen electrode experiments	51
2.29.1. Preparation of cell suspension	51
2.29.2. Measurement of oxygen uptake by cell suspensions in the presence of substrates	51
2.30. Enzyme assays	53
2.30.1. PQQ-dependent alcohol dehydrogenase	53
2.30.2. NAD(P) ⁺ -dependent alcohol dehydrogenase	53
2.30.3. NDMA-dependent alcohol dehydrogenase	53
2.30.4. sMMO activity using the naphthalene assay	54
Chapter 3 Growth and Oxidation studies	55
3.1. Introduction	56
3.1.1. General characteristics of <i>Rhodococcus jostii</i> strain 8	62
3.1.2. Cloning of SDIMO α -subunit genes of <i>R. jostii</i> strain 8	63
3.2. Growth profiles of <i>R. jostii</i> strain 8 and <i>R. jostii</i> RHA1	67

3.3. Growth curves of <i>R. jostii</i> strain 8 grown on glucose and alkanes	69
3.4. Oxidation studies using the oxygen electrode	71
3.1.3. Alkane-oxidising enzymes are inducible during growth on alkanes	71
3.1.4. Oxygen consumption by whole cells in response to alcohols	73
3.1.5. Oxygen consumption by whole cells in response to other potential intermediates of alkane oxidation	76
3.5. Alcohol dehydrogenase assays	78
3.5.1. PQQ-dependent alcohol dehydrogenase assays	79
3.5.2. NAD(P)H-dependent alcohol dehydrogenases	80
3.5.3. NDMA-dependent alcohol dehydrogenases	82
3.6. Discussion and conclusion	88
Chapter 4 The genome of <i>Rhodococcus jostii</i> strain 8	90
4.1. Introduction	91
4.2. Genome sequencing for <i>Rhodococcus jostii</i> strain 8	94
4.3. Subsystems in the genome of <i>R. jostii</i> strain 8	94
4.4. Plasmids and transposable elements	96
4.5. The genes encoding a putative naphthalene 1, 2-dioxygenase	97
4.6. The biphenyl dioxygenase and ethylbenzene dioxygenase gene clusters	99
4.7. Analysis of propane monooxygenase gene sequences in the genome of <i>Rhodococcus jostii</i> strain 8	102
4.8. Analysis of <i>alkB</i> -type alkane hydroxylase gene sequences in the <i>Rhodococcus jostii</i> strain 8 genome	109
4.9. Cytochrome P450 monooxygenases in <i>Rhodococcus jostii</i> strain 8	114
4.10. Metabolic pathway analysis for <i>Rhodococcus jostii</i> strain 8	115
4.10.1. Nitrogen metabolism: reduction and fixation	116
4.10.2. Sulfur metabolism	118
4.10.3. Propanoate metabolism	120
4.10.4. Butanoate metabolism	122
4.11. Discussion and conclusions	124

Chapter 5 Expression of propane monooxygenase and <i>alkB</i>-type alkane monooxygenase	126
5.1. Introduction	127
5.2. Polypeptide analysis: Expression of propane monooxygenase polypeptides during growth on propane	129
5.3. Discussion for polypeptide analysis	141
5.4. RT-qPCR: transcription of <i>alkB</i> and <i>prmA</i> in <i>Rhodococcus jostii</i> strain 8 grown on glucose, ethane, propane, butane and octane	145
5.4.1. RNA extraction and assessment of RNA quality	145
5.4.2. Reverse Transcriptase PCR targeting <i>prmA</i> and <i>alkB</i>	146
5.4.3. Primer optimisation for RT-qPCR	148
5.4.4. Expression of propane monooxygenase and alkane hydroxylase in <i>R. jostii</i> strain 8 during different growth conditions	152
5.5. Discussion for expression of <i>prmA</i> and <i>alkB</i>	158
5.6. Conclusions	160
Chapter 6 Mutagenesis of <i>prmA</i> and <i>alkB</i> in <i>Rhodococcus jostii</i> strain 8	161
6.1. Introduction	162
6.2. Optimisation of electroporation conditions for use in mutagenesis of <i>prmA</i> and <i>alkB</i> in <i>R. jostii</i> strain 8	163
6.2.1. Optimal voltage for electroporation of <i>R. jostii</i> strain 8	163
6.2.2. Optimal resistance for electroporation conditions of <i>Rhodococcus jostii</i> strain 8	165
6.2.3. Optimal competent cell culture density, recovery medium and recovery time for transformants	167
6.3. Marker exchange mutagenesis using the vector pK18 <i>mobsacB</i> introduced by electroporation	168
6.3.1. Construction of mutants	168

6.4. Introduction of mutated <i>prmA</i> and <i>alkB</i> into the chromosome of <i>R. jostii</i> strain 8 by electroporation	172
6.4.1. Electroporation of pAGB and pXGY	172
6.4.2. Electroporation of mutated <i>prmA</i> and <i>alkB</i> fragments	172
6.5. Screening for a <i>prmA</i> -deficient strain	175
6.6. Screening for <i>alkB</i> mutants	178
6.7. Discussion and conclusions	181
Chapter 7 Conclusions and future prospects	184
7.1. Conclusions	185
7.1.1. Growth and oxidation studies	185
7.1.2. The genome of <i>Rhodococcus jostii</i> strain 8	186
7.1.3. Expression studies	186
7.1.4. Mutagenesis of <i>prmA</i> and <i>alkB</i>	187
7.2. Future prospects	187
References	190

List of figures

Figure 1.1: The crystal structure of soluble methane monooxygenase from <i>Methylococcus capsulatus</i> Bath	9
Figure 1.2: A phylogenetic tree showing the relationship of SDIMOs is based on alignment of 600 amino acids from the α -subunit of the hydroxylase components	11
Figure 1.3: Amino acid alignments show conserved regions of SDIMO alpha subunits targeted for PCR primer design and the expected PCR amplicon sizes from various primer combinations	12
Figure 1.4: the sMMO operon of <i>Methylosinus trichosporium</i> OB3b	13
Figure 1.5: Ethane metabolism by non-methane oxidising bacteria	17
Figure 1.6: The possible propane oxidation pathway by <i>Rhodococcus rhodochrous</i> PNKb1	19
Figure 1.7: Proposed terminal (left) oxidation and subterminal (right) of butane in butane-degrading bacteria (adapted from Arp, 1999)	23
Figure 1.8: The plasmid map of pK18 <i>mobsacB</i>	27
Figure 3.1: Phylogenetic tree showing relationship between 6 selected isolates and their relatives	60
Figure 3.2: cell morphology of <i>R. jostii</i> strain 8 grown on NMS medium with 10% (v/v) propane in the headspace	62
Figure 3.3: Diagram demonstrating NVC and <i>mmoX</i> primer sites within the SDIMO α -subunit gene	64
Figure 3.4: Phylogenetic relationship between amino acid sequences of the putative SDIMO α -subunit from strain 8 and those from other organisms	66
Figure 3.5: Growth curves of <i>R. jostii</i> strain 8 grown on NMS with 10 mM glucose or 10% (v/v) ethane, propane or butane as sole carbon source	70

Figure 3.6: Oxygen consumption rates (nmol/min/mg dry cell weight) of whole-cell <i>R. jostii</i> strain 8 grown on glucose, ethane, propane and butane induced by primary alcohols which are potential intermediates in alkane metabolism pathways	74
Figure 3.7: Oxygen consumption rates (nmol/min/mg dry cell weight) of whole-cell <i>R. jostii</i> strain 8 grown on glucose, ethane, propane and butane induced by secondary alcohols and diols which are potential intermediates in alkane metabolism pathways	74
Figure 3.8: Specific activities of NDMA-linked enzymes in cell-free extracts, from glucose-, ethane-, propane- and butane-grown cells, corresponding to the addition of methanol	83
Figure 3.9: Specific activities of NDMA-linked enzymes in cell-free extracts, from glucose-, ethane-, propane- and butane-grown cells, corresponding to the addition of ethanol	84
Figure 3.10: Specific activities of NDMA-linked enzymes in cell-free extracts, from glucose-, ethane-, propane- and butane-grown cells, corresponding to the addition of 1-propanol	84
Figure 3.11: Specific activities of NDMA-linked enzymes in cell-free extracts, from glucose-, ethane-, propane- and butane-grown cells, corresponding to the addition of 2-propanol	85
Figure 3.12: Specific activities of NDMA-linked enzymes in cell-free extracts, from glucose-, ethane-, propane- and butane-grown cells, corresponding to the addition of 1-butanol	86
Figure 3.13: Specific activities of NDMA-linked enzymes in cell-free extracts from glucose-, ethane-, propane- and butane-grown cells, corresponding to the addition of 2-butanol	87
Figure 4.1: the naphthalene 1,2-dioxygenase gene clusters of <i>R. jostii</i> strain 8 and those of other <i>Rhodococcus</i> spp.	98

Figure 4.2: Gene arrangement of propane monooxygenase operon found in <i>R. jostii</i> strain 8 compared to its two close relatives	103
Figure 4.3: Neighbour-joining phylogenetic tree of the α -subunit hydroxylase (PrmA) of the propane monooxygenase in <i>R. jostii</i> strain 8 and its close relatives	106
Figure 4.4: Comparison of partial hydroxylase regions (residues 77-301) of the propane monooxygenase amino acid sequences of <i>R. jostii</i> strain 8 and the other known PrmA sequences -- <i>R. jostii</i> RHA1, <i>Gordonia</i> TY-5, <i>Mycobacterium</i> TY-6 and <i>Pseudonocardia</i> TY-7	108
Figure 4.5: Gene arrangement of <i>alkB</i> -type alkane monooxygenase operon found in <i>R. jostii</i> strain 8 compared to its three close relatives	110
Figure 4.6: Neighbour-joining phylogenetic tree of the hydroxylase subunit of the <i>alkB</i> -type alkane monooxygenase in <i>R. jostii</i> strain 8 and its close relatives	112
Figure 4.7: Comparison of partial hydroxylase regions (residue 153-376) of <i>alkB</i> -type alkane monooxygenases	113
Figure 4.8: Kegg recruitment plot of genes involved in nitrogen metabolism: reduction and fixation from the <i>R. jostii</i> strain 8 genome	116
Figure 4.9: Kegg recruitment plot of genes involved in sulfur metabolism from the <i>R. jostii</i> strain 8 genome	118
Figure 4.10: Kegg recruitment plot of genes involved in propanoate metabolism from the <i>R. jostii</i> strain 8 genome	120
Figure 4.11: Kegg recruitment plot of genes involved in butanoate metabolism from the <i>R. jostii</i> strain 8 genome	122
Figure 5.1: SDS-PAGE analysis of cell-free extracts from <i>R. jostii</i> strain 8 grown on glucose, ethane, propane and butane	130
Figure 5.2: SDS-PAGE analysis of cell-free extracts from <i>R. jostii</i> strain 8 grown on glucose, ethane, propane, butane, succinate and octane	135

Figure 5.3: SDS-PAGE analysis of cell-free extracts (extracted by boiling preparation) from strain 8 grown on glucose, ethane, propane, butane, succinate and octane	139
Figure 5.4: Total RNA (5 µl each lane) extracted from cells grown on glucose, ethane, propane, butane, succinate and octane	146
Figure 5.5: Reverse transcription followed by PCR reactions targeting <i>prmA</i>	147
Figure 5.6: Reverse transcription followed by PCR reactions targeting <i>alkB</i>	148
Figure 5.7: Melting curves showing fluorescent signals detected when using different concentrations of primers targeting <i>prmA</i>	151
Figure 5.8: Transcription of <i>rpoB</i> during growth on glucose, ethane, propane, butane, succinate and octane	153
Figure 5.9: qPCR reactions targeting <i>rpoB</i> . Standard curve showing Ct value (y-axis) against quantity of template in log scale (x-axis)	154
Figure 5.10: qPCR reactions targeting <i>alkB</i> Standard curve showing Ct value (y-axis) against quantity of template in log scale (x-axis)	155
Figure 5.11: qPCR reactions targeting <i>prmA</i> Standard curve showing Ct value (y-axis) against quantity of template in log scale (x-axis)	155
Figure 5.12: Fold changes in the expression of <i>alkB</i> in <i>R. jostii</i> strain 8 grown on ethane, propane, butane, succinate and octane compared to that of strain 8 grown on glucose	156
Figure 5.13: Fold changes in the expression of <i>prmA</i> in <i>R. jostii</i> strain 8 grown on ethane, propane, butane and octane compared to that of strain 8 grown on glucose	157
Figure 6.1: A diagram showing pK18 <i>mobsacB</i>	169
Figure 6.2: Construction of pAGB, a plasmid carrying a disrupted <i>prmA</i> and pXGY, a plasmid carrying a disrupted <i>alkB</i> gene	170

Figure 6.3: The diagram showing primer binding sites on the wild-type and the mutated <i>prmA</i> fragments	175
Figure 6.4: Gel analysis of PCR amplification using outAGBf/r primers on 28 colonies checking for mutated <i>prmA</i> using outAGBf/r primers	176
Figure 6.5: Gel analysis of PCR amplification using outAGBf/r primers on colonies grown from 10 ⁵ -fold dilution cultures	177
Figure 6.6: The diagram showing primer binding sites on the wild-type and the mutated <i>alkB</i> fragments	178
Figure 6.7: Gel analyses of PCR amplification on 28 colonies using outXGYf/r primers	179
Figure 6.8: Gel analysis of PCR amplification using outXGYf/r primers on colonies grown from 10 ⁵ -fold dilution cultures	180

List of tables

Table 2.1 Bacterial strains used in this study	31
Table 2.2 Plasmids used in this study	32
Table 2.3 Antibiotics used in this study	33
Table 2.4 Primers used in this study	40
Table 2.5 Henry's constants used for calculation gas solubility in water	52
Table 3.1: List of 6 selected isolates with genus identification based on 16S rRNA gene sequences (754 nucleotides within the region covered by 27f/1492r PCR primers)	57
Table 3.2: Growth tests of the selected isolates on alkanes and alkenes	58
Table 3.3: Comparison of growth profiles of <i>R. jostii</i> strain 8 and <i>R. jostii</i> RHA1	68
Table 3.4: Oxygen consumption rates of glucose- and alkane-grown cells in response to alkanes and alkenes	72
Table 3.5: Oxygen consumption rates (nmol/min/mg dry cell weight) in response to potential intermediates in gaseous alkane metabolisms of whole-cell <i>R. jostii</i> strain 8 grown on glucose, ethane, propane and butane	77
Table 4.1: A list of non-pathogenic <i>Rhodococcus</i> strains whose genomes have been published	92
Table 4.2: The number of genes within each subsystem category in the genome of <i>Rhodococcus jostii</i> strain 8	95
Table 4.3: The list of putative genes and proteins of naphthalene 1, 2-dioxygenase in <i>R. jostii</i> strain8 and their close relatives	97
Table 4.4: The list of genes involved in the degradation of biphenyl and ethylbenzene in <i>R. jostii</i> RHA1 compared to the genes in <i>R. jostii</i> strain 8	100
Table 4.5: The amino acid sequence identity of structural genes in the propane monooxygenase gene cluster of <i>R. jostii</i> strain 8 compared to its relatives, <i>R. jostii</i> RHA1	104
Table 4.6: The amino acid sequence identity of structural genes in the <i>alkB</i> -type alkane monooxygenase gene cluster of <i>R. jostii</i> strain 8 compared to its relatives	111

Table 5.1: Mass spectrometry analysis of polypeptides identifications of gel bands (shown in Figure 4.2.1.) after comparison with the <i>R. jostii</i> RHA1 genome	132
Table 5.2: Mass spectrometry analysis of polypeptides identifications of gel bands (shown in Figure 5.2) after comparison with the <i>R. jostii</i> strain 8 genome	136
Table 5.3: Primers used in RT-qPCR assays	149
Table 6.1: The viability of competent <i>R. jostii</i> strain 8 cells after electroporation using different voltages	164
Table 6.2: Growth of transformants on NMS containing 10 mM glucose and kanamycin (100µg/ml) medium after electroporation with pNV18 using different voltages	165
Table 6.3: The viability of competent <i>R. jostii</i> strain 8 cells after electroporation using different resistances	166
Table 6.4: Growth of transformants on NMS containing 10 mM glucose and kanamycin (100µg/ml) medium after electroporation with pNV18 using different resistances	167
Table 6.5: The list of PCR primers used for screening of colonies containing a gentamicin cassette and disrupted <i>prmA</i> and <i>alkB</i>	173
Table 6.6: Electroporation of disrupted <i>prmA</i> and <i>alkB</i> fragments, pAGB and pXGY into <i>R. jostii</i> strain 8	174

Declaration

I declare that the work entitled ‘Functional characterization of alkane-degrading monooxygenases in *Rhodococcus jostii* strain 8’ has not previously been submitted for any other degree at the University of East Anglia or other institution. The content of this work was undertaken and completed by me under the supervision of my supervisor, Prof. Colin Murrell, unless otherwise acknowledged.

Jindarat Ekprasert

Acknowledgements

I owe my deep gratitude to my supervisor, Prof. Colin Murrell. Without his professional supervising experience and his exceptionally extensive knowledge, this project would not have been possible.

I would like to thank Dr. Andrew Crombie for his patience and helpful guidance and discussions throughout my PhD. I would also like to thank my second supervisor, Prof. Andy Johnston for his great advices on this thesis. I thank Dr. H el ene Moussard who guided me with lab techniques. She spent her hard time patiently helping me with this project during my first year. I would like to thank all lab members both at University of Warwick and University of East Anglia.

I would like to express my gratitude to the Royal Thai Government for providing funding to support my study in UK. Without their encouragement and supportive advices, my life would not have been through this state.

I also wish to thank my beloved family for being supportive and giving me caring advices. I thank my best friend, Poemwai for always sharing good experience. My life in the UK is worth memorizing because of him. I would also like to thank my friends both at Warwick and Norwich for providing me the best and most relaxed social life. Their inspiration to me is gratefully acknowledged.

Abbreviations

Amp ^R	ampicillin resistance
ADH	alcohol dehydrogenase
BIS	<i>N,N'</i> -methylenebisacrylamide
BLAST	basic local alignment search tool
bp	base pairs
BSA	bovine serum albumin
cDNA	complementary DNA
cm	centimeter
Da	Dalton
DCPIP	2,6-dichlorophenolindophenol
DEPC	diethylpyrocarbonate
DMSO	dimethylsulfoxide
DNA	deoxyribonucleic acid
DNase	deoxyribonuclease
dNTP	deoxynucleotide triphosphate
dO ₂	dissolved oxygen
dw	dry weight
EDTA	ethylenediaminetetraacetic acid
<i>e.g.</i>	<i>exempli gratia</i>
<i>etc.</i>	<i>et cetera</i>
FAD	flavin-adenine dinucleotide
g	gram/ acceleration due to gravity
GC	gas chromatography
Gm ^R	gentamicin resistance
h	hour
<i>i.e.</i>	<i>id est</i>

IPTG	isopropyl β -D-thiogalactopyranoside
kb	kilobases
Km ^R	kanamycin resistance
kV	kilovolt
l	litre
LacZ	β -galactosidase
LB	Luria Bertani medium
LC/ESI	liquid chromatography electrospray ionisation
M	molar
MCS	multiple cloning site
MDH	methanol dehydrogenase
mg	milligram
min	minute
ml	millilitre
μ F	microfarad
μ g	microgram
μ l	microliter
MM	theoretical molecular mass
mM	millimolar
mol	mole
MOPS	3-(N-morpholino)propanesulfonic acid
mRNA	messenger RNA
MS/MS	tandem mass spectrometry
MTBE	methyl <i>tert</i> -butyl ether
NAD ⁺	nicotinamide adenine dinucleotide (oxidised form)
NADH	nicotinamide adenine dinucleotide (reduced form)
NDMA	4-nitroso-N,N-dimethylaniline

NADP+	nicotinamide adenine dinucleotide phosphate (oxidised form)
NADPH	nicotinamide adenine dinucleotide phosphate (reduced form)
NCBI	National Center for Biotechnology Information
ng	nanogram
nm	nanometer
NMS	nitrate mineral salts
NTC	no-template control
OD ₅₄₀	optical density at 540 nm
<i>orf</i>	open reading frame
Ω	ohms
<i>ori</i>	origin of replication
<i>oriT</i>	origin of transfer
PAGE	polyacrylamide electrophoresis
PCR	polymerase chain reaction
PIPES	Piperazine-N,N'-bis(2-ethanesulfonic acid)
PMS	phenazine methosulfate
pMMO	particulate methane monooxygenase
PQQ	pyroloquinoline quinone
PrMO	propane monooxygenase
psi	pounds per square inch
RFLP	restriction fragment length polymorphism
RNA	ribonucleic acid
RNase	ribonuclease
rpm	revolutions per minute
rRNA	ribosomal ribonucleic acid
RT-PCR	reverse transcriptase PCR
s	seconds

SDIMO	soluble diiron monooxygenase
SDS	sodium dodecyl sulphate
Sm ^R	streptomycin resistance
sMMO	soluble methane monooxygenase
SOB	super optimal broth
SOC	super optimal broth with catabolite repression
sp.	specie
spp.	species
Sp ^R	spectinomycin resistance
<i>Taq</i>	<i>Thermus aquaticus</i>
TBE	tris borate EDTA
TCA	tricarboxylic acid
TE	tris EDTA
TEMED	<i>N,N,N',N'</i> -tetramethyl-ethane-1,2-diamine
Tris	tris(hydroxymethyl)aminomethane
UV	ultraviolet
v/v	volume to volume
w/v	weight to volume
X-gal	5-bromo-4-chloro-3-indoyl-β-D-galactoside

Abstract

Short-chain alkanes are gaseous hydrocarbons that contribute to photochemical pollution and ozone production in the atmosphere. A number of studies have shown that *Rhodococcus* species possess the ability to metabolite a wide range of hydrocarbons since they contain multiple hydrocarbon-degrading enzymes such as soluble diiron monooxygenases (SDIMOs) and *alkB*-type alkane monooxygenases. This study aimed to investigate the role of multiple alkane-degrading enzymes in the metabolism of gaseous alkanes in *Rhodococcus jostii* strain 8. *R. jostii* strain 8 was isolated from a propane enrichment culture using petroleum-contaminated soil as an inoculum. *R. jostii* strain 8 could grow on ethane, propane, butane, octane, naphthalene and some potential intermediates in alkane metabolism. Oxidation studies showed that *R. jostii* strain 8 is likely to oxidise propane via both terminal and sub-terminal oxidation of propane and that these activities are induced in propane-grown cells. Alcohol dehydrogenase assays were carried out in order to determine cofactor and substrate ranges of these enzymes. Results showed that alcohol dehydrogenases involved in the metabolism of gaseous alkanes are NDMA-dependent. The size of the genome sequence of *R. jostii* strain 8 is 8.5 Mbp with a G+C content of 67%. The closest relative of *R. jostii* strain 8, based on 16S rRNA sequence, is *Rhodococcus jostii* RHA1 with 99% identity. However, growth profiles and a number of catabolic genes in the genome of *R. jostii* strain 8 clearly indicated that this bacterium is different from *R. jostii* RHA1. *R. jostii* strain 8 contains two alkane-degrading enzyme systems – a propane monooxygenase and an *alkB*-type alkane monooxygenase. Polypeptide analysis on cell-free extracts from cells grown on gaseous alkanes using SDS-PAGE indicated that propane monooxygenase is inducible during growth on propane. Expression studies using RT-qPCR of *prmA* and *alkB* showed that *prmA* was highly expressed during growth on propane. The exact involvement of *alkB*-type alkane monooxygenase in the degradation of alkanes was still unclear. A gene transfer system for *R. jostii* strain 8 was established. Marker-exchanged mutagenesis of *prmA* and *alkB* was attempted. Construction of mutated-*prmA* and mutated-*alkB* plasmids was achieved. Electroporation conditions were successfully optimised in order to transfer linear DNA into *R. jostii* strain 8. However, mutants lacking active *prmA* or *alkB* are still needed to further study their phenotypes and to provide more evidence supporting the role of these two enzymes.

Chapter 1

Introduction

1.1. Significance of alkanes in the environment

Non-methane hydrocarbons play an important role in tropospheric chemistry and ozone formation (Poizzer et al., 2010). Short-chain alkanes and alkenes, which can be found as components of crude oil, are gaseous at ambient temperature. Hydrocarbon gases are present in all petroleum reservoirs in significant amount for sufficient distribution and diffusion through subsurface environments (Shennan, 2006). Ethane, propane, butane and methane are components of natural gas. They are also produced by a variety of organisms such as plants, animals and even bacteria (Rojo, 2009). Therefore, alkanes are widespread in the environment. Some microorganisms have evolved to utilise these compounds as a carbon source. Low molecular weight alkanes are still soluble enough for those microorganisms to directly take up alkanes into the cells.

1.1.1. Chemistry of alkanes

Alkanes are saturated hydrocarbon compounds with the general chemical formula C_nH_{2n+2} . They are comprised of carbon and hydrogen atoms in their molecules. Alkanes can be found in the form of linear, branched or cyclic compounds. Those with one to four carbon atoms, methane, ethane, propane and butane, are gaseous at ambient temperature. Alkanes of higher number of carbon atoms ($\geq C_5$) are liquid or solid. These compounds are very insoluble in water. Solubility decreases as molecular weight increases (Eastcott et al., 1988). Alkanes are chemically inert and require activation in order to be metabolised (Labinger and Bercaw, 2002). Propane and butane are moderately soluble in water.

Alkanes can be metabolised both aerobically and anaerobically. Due to the low solubility of alkanes in water, potential accumulation of compounds in cell membranes and the energy required for the activation, microorganisms possessing the ability to degrade alkanes are of great interest. In aerobic degradation of alkanes, oxygen acts as a reactant to activate alkane molecules so that alkanes can be metabolised by alkane degraders. Alkanes with two or more carbon atoms are usually degraded by the oxidation of terminal or sub-terminal methyl groups resulting in primary or secondary alcohols (Rojo, 2009). Degradation of gaseous

alkanes has been studied and numerous bacterial strains possessing the ability to degrade these compounds have been discovered. Details are described in the next section.

1.2. The *Rhodococcus* genus

Rhodococcus are categorised into the suborder *Corynebacterineae* within the phylum *Actinobacteria*. They are widespread in a broad range of environments including soils and seawater. There was some confusion in the taxonomic position of *Rhodococcus* species for many years until Goodfellow resolved it (Goodfellow et al., 1990). Since then, classification of members of the genus *Rhodococcus* is based on the presence of long-chain mycolic acid in the cell walls and 16S rRNA sequences (Rainey et al., 1995). Based upon those criteria, *Rhodococcus* is taxonomically closed to the genus *Nocardia*. The changes in the classification of actinomycetes have been established due to an increase in the use of 16S rRNA sequences. It is noteworthy that the classification of any novel strains of *Rhodococcus* without considering the 16S rRNA sequences may result in them belonging to other genera and the classification may be incorrect. Therefore, the classification of novel isolates in this study mainly relied on 16S rRNA sequence analysis. In depth details on the biology of the genus *Rhodococcus* has been described by Alvarez et al., 2010, where most of the information in this section was derived from.

A better understanding in the molecular genetics of *Rhodococcus* species and *Nocardia* has shown that these organisms possess many features which are common features of *Streptomyces* (Larkin et al., 1998). Recently, because genome sequencing has become extensively used for studying the versatile metabolic potential of *Rhodococcus*, the genome sequences of a number of *Rhodococcus* strains are available (see Table 1, Section 4.1., Chapter 4).

1.2.1. Common characteristics of *Rhodococcus* spp.

Members of the genus *Rhodococcus* are aerobic, non-motile, non-sporulating, Gram-positive bacteria with a high G+C content. *Rhodococcus* cells contain mycolic

acid. Common characteristics of the genus *Rhodococcus* were described by Goodfellow (Goodfellow et al., 1990). *Rhodococcus* spp. are aerobic chemoorganotrophic bacteria that use a wide range of substrates as sole carbon and energy sources. Morphological changes from rods to cocci occur during each stage of growth depending on the strain. Some *Rhodococcus* spp. can form branched filaments which may develop into extensive aerial filaments. These various forms of morphology then fragment and become short rods or cocci. The colony colour can vary, depending on the strain, from colourless to cream, yellow, orange, pink and red.

1.2.2. *Rhodococcus* spp. are capable of degrading gaseous alkanes

Some *Rhodococcus* species can use gaseous hydrocarbons as a sole carbon source. For example, *R. rhodochrous* and *R. ruber* can utilize propane, butane and acetylene (Ivshina et al., 1994). Several strains of *R. rhodochrous* and *R. ruber* which are propane- and butane degraders were isolated from various environments such as soil, rock and groundwater (Ivshina et al., 1981). This is an indication of the presence of subterranean hydrocarbon deposits. *Rhodococcus ruber* ENV425 is capable of cometabolising *N*-nitrosodimethylamine (NDMA), which is a potent carcinogen sometimes contaminating groundwater, after growth on propane (Fournier et al., 2009). *Rhodococcus rhodochrous* PNKb1 is a propanotroph and its propane metabolism has been well-characterised (Ashraf et al., 1994). It was found that in *R. rhodochrous* PNKb1, propane is metabolized via both terminal and subterminal pathway (see Figure 5, Section 4.1.2.).

The other example of a *Rhodococcus* strain which is able to degrade gaseous hydrocarbons is *R. jostii* RHA1, for which the complete genome is available (McLeod et al., 2006). *R. jostii* RHA1 can degrade propane as a sole carbon source (McLeod et al., 2006). Similar to *R. ruber* ENV425, the propane monooxygenase of *R. jostii* RHA1 is also responsible for the degradation of NDMA (Sharp et al., 2007). As mentioned earlier, there were a limited number of *Rhodococcus* strains which possess the ability to degrade gaseous alkanes, so in this project, a propane-degrading *Rhodococcus* strain capable of also degrading ethane and butane was isolated.

1.2.3. Potential applications of *Rhodococcus* in biotechnology

Many *Rhodococcus* species are interesting in terms of their applications in biotechnology because of their broad metabolic versatility (Warhurst and Fewson, 1994). It was found that *Rhodococcus* spp. possess a wide range of oxygenases which allow them to metabolise various aromatic compounds (Larkin et al., 2005). *Rhodococcus* spp. are suitable for bioremediation and biocatalysis because they can persist in highly contaminated environment and even oxygen- and nutrient-limited conditions (Alvarez et al., 2010). *Rhodococcus* spp. can be isolated directly from environmental samples and enriched with mixed or pure cultures incubated with the particular contaminant of interest. This is, therefore, beneficial in preparation of inocula for bioremediation.

The most successful industrial application of *Rhodococcus* spp. is the production of acrylamide by the Nitto Chemical Industry, Co. in Japan (Hughes et al., 1998). The conversion of acrylonitrile to acrylamide by *Rhodococcus rhodochrous* PA-34 was first reported in 2006 (Raj et al., 2006). Later in 2008, an industrial-scale synthesis of acrylamide was carried out in a partitioned fed batch reactor by using agar entrapped cells of *Rhodococcus rhodochrous* PA-34 (Raj et al., 2008). It was found that some *Rhodococcus* strains were able to produce vanillin, which is widely used as flavouring agent in foods, beverages and pharmaceuticals, from ferrulic acid and eugenol (Plaggenborg et al., 2006). The production of vanillin from the breakdown of lignin was found in *Rhodococcus jostii* RHA1 (Sainsbury et al., 2013). In this work, the vanillin dehydrogenase gene was deleted in *R. jostii* RHA1 in order to allow an accumulation of vanillin when grown on a minimal medium containing 2.5% wheat straw lignocellulose and 0.05% glucose. This resulted in the yield of up to 96 mg/l after 144 h of incubation. Some *Rhodococcus* strains such as *Rhodococcus opacus* PD630 are also capable of producing energy-rich triacylglycerols which are compounds used for the production bio-diesel (Holder et al., 2011b).

Due to the versatile catabolic diversity of *Rhodococcus* spp., there have been substantial numbers of reports suggesting that *Rhodococcus* species are suitable for bioremediation of toxic compounds in contaminated environments. Chlorophenols are one of the most dangerous contaminants in the environment because they are

recalcitrant, carcinogenic and toxic to humans (Proudfoot, 2003). A number of microorganisms, particularly *Rhodococcus* spp., have been isolated from phenol and/or chlorophenol contaminated environments in order to be used in remediating contaminated sites. Examples of phenol-degrading *Rhodococcus* spp. are described as follows. *Rhodococcus* sp. CS1, which was isolated from industrial effluents and polluted sediments, showed a high ability to degrade phenol in synthetic media (Paisio et al., 2012; Paisio et al., 2013). This bacterium was also able to tolerate and metabolise different phenolic compounds such as methoxy- and chlorophenols (Paisio et al., 2014). *Rhodococcus erythropolis* M1 was able to degrade phenol, 2-chlorophenol and *p*-cresol in a co-culture with *Pseudomonas fluorescens* P1 (Goswami et al., 2005). The study of the ability of *R. erythropolis* M1 to degrade phenolic compounds in the presence of a competitor, *P. fluorescens* P1, showed that its degradative ability was similar to its ability when it was used in pure culture. Immobilised cells of *Rhodococcus erythropolis* UPV-1 were used for removal of phenolic compounds in effluent from a resin industry (Begoña Prieto et al., 2002).

Finally, this research could be applied for the remediation of hydrocarbon-contaminated environment due to, for example, oil spills (e.g. the report in On scene coordinator report Deepwater Horizon oil spill, 2011) or fracking (e.g. Ridlington, 2013) in which large amounts of natural gas are released. Once collected in the Earth's atmosphere, the extra gas definitely enhances greenhouse effect and represents the danger to the environment. We discuss in the final chapter the possibility of using *R. jostii* strain 8 as a biocatalyst to degrade gaseous alkanes (e.g. ethane, propane and butane) and to prevent them from reaching the atmosphere. Therefore, this application would provide an alternative method to minimise the environmental impact causing by hydrocarbon contamination.

1.3. Bacterial enzymes responsible for alkane degradation

The first step of alkane degradation in bacteria is catalysed by enzymes converting alkanes into alcohols. These enzymes have been characterized into four main groups – integral membrane alkane hydroxylases, soluble diiron monooxygenases, cytochrome P450 and membrane-bound copper containing monooxygenases. Details of these four groups of enzymes are described below.

1.3.1. Integral membrane, non-heme iron alkane hydroxylases (AlkB)

The integral membrane, non-heme iron alkane hydroxylases requires one or two rubredoxins and a rubredoxin reductase for providing electrons to the integral membrane monooxygenase (AlkB). Substrate range for this type of alkane monooxygenase includes C₅-C₁₆ alkanes. Genes with high sequence similarity to the gene encoding alkane hydroxylase were found in many bacteria isolated from oil-contaminated environments (Sotsky et al., 1994). Multiple copies of *alkB*-type alkane monooxygenases were also found in many bacteria. There are probably because of four reasons for this. The first explanation is because different alkane monooxygenases have different substrate ranges. Some may oxidise C₁₀-C₁₆ alkanes, while some oxidise C₅-C₁₂ alkanes (van Beilen et al., 1994; Smits et al., 2003). Another reason is that different alkane monooxygenases might be expressed during different growth phases. Also, different alkane monooxygenases might have a different affinity towards different forms of alkanes such as branched, aliphatic, non-linear and to aromatic compounds. The last possible explanation for redundancy of alkane monooxygenases is that some *alkB* genes maybe pseudogenes (van Beilen and Funhoff, 2005).

The first and most well characterized *alkB*-related alkane monooxygenase was found in an octane degrader, *Pseudomonas putida* GPo1 (Chakrabarty et al., 1973). *P. putida* GPo1 could grow on a range of alkanes from pentane to dodecane (Schwartz and McCoy, 1973). The *alkB*-type alkane monooxygenase in *P. putida* GPo1 oxidised C₅-C₁₂ alkanes to 1-alkanols (Peterson et al., 1966). C₁-C₄ alkanes were not recognized as growth substrates for *P. putida* GPo1 (Smith and Hyman, 2004). Recent molecular studies showed that there are many strains of bacteria which possess gene homologues to *alkB* in *P. putida* GPo1 and they are usually present in the chromosome (Smits et al., 1999). In contrast, *alk* genes of *P. putida* GPo1 are located on a large plasmid, named the OCT plasmid, and grouped into two clusters (Chakrabarty et al., 1973). The OCT plasmid encodes the genes required for the assimilation of C₃-C₁₃ alkanes (van Beilen et al., 1994; Johnson and Hyman, 2006).

Branched-chain alkanes are considered to be more difficult to degrade than linear alkanes (Pirnik et al., 1974). Interestingly, *Alcanivorax borkumensis* SK2 possesses the ability to metabolise isoprenoid hydrocarbons (Schneiker et al., 2006).

It was found that *A. borkumensis* SK2 possesses two copies of *alkB*-type alkane monooxygenases which are essential in the degradation of alkanes as this bacterium could only grow on a very limited range of carbon sources (Smits et al., 2002). The growth properties of an *alkB1*-disrupted mutant of *A. borkumensis* SK2 clearly showed that this gene is involved in the degradation of *n*-hexane (Hara et al., 2004). The mutant containing mutations in both *alkB1* and *alkB2* could still grow on medium-chain alkanes. This indicated that the degradation of medium-chain alkanes in *A. borkumensis* SK2 depended on the function of other enzyme systems rather than AlkB1 or AlkB2 (Hara et al., 2004). It is therefore likely that a different enzyme system is responsible for the degradation of medium-chain alkanes in this bacterium.

This type of alkane monooxygenase has been found to be useful as biocatalyst to convert inexpensive compounds into valuable products in the pharmaceutical and chemical industries (Furuhashi, 1992). For example, alkane-grown cells of *Rhodococcus rhodochrous* NCIMB12566 are able to stereoselectively metabolise substituted phenoxypropane to phenoxy propanoic acids, which is a compound used in the production of herbicides. Another example is *Rhodococcus erythropolis* NRRL B-16531 which is capable of stereoselectively converting cumene to 2-phenyl-1-propionic acids, which are used for the production of pharmaceuticals such as ibuprofen (Hou et al., 1994).

1.3.2. Soluble di-iron monooxygenases (SDIMO)

SDIMOs are multicomponent enzymes comprising of three main components which are: a $\alpha_2\beta_2\gamma_2$ hydroxylase, a FAD-containing reductase, and a coupling protein (Coleman et al., 2006). The oxidation of hydrocarbons occurs at the alpha subunit of the hydroxylase component, working together with the reductase component which is responsible for electron transfer facilitated by a coupling protein. The catalytic center of the SDIMO enzyme comprises of two iron atoms linked by a carboxylate bridge in a 4-helix bundle structure within the α -subunit (Rosenzweig et al., 1997). Soluble methane monooxygenase (sMMO) is considered to be the most well-characterised SDIMO and knowledge about sMMO is useful for the study of other SDIMOs. The crystal structure of soluble methane monooxygenase hydroxylase

(MMOH) from *Methylococcus capsulatus* Bath is shown in Figure 1.1 (taken from Dalton, 2005).

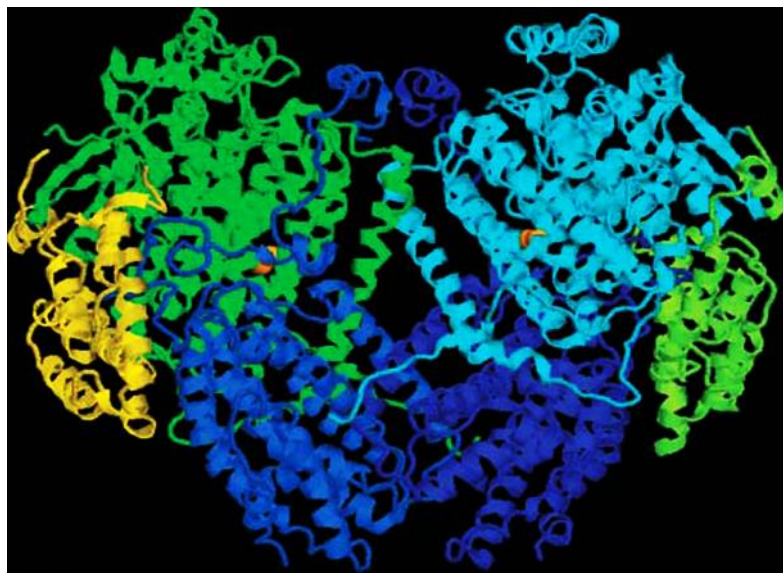


Figure 1.1: The crystal structure of soluble methane monooxygenase from *Methylococcus capsulatus* Bath. The α -subunits are shown in pale blue and green, the β -subunits are shown in royal blue and mid-blue, and the γ -subunits are shown in yellow-green and yellow. The iron atoms are shown as orange spheres (taken from Dalton, 2005).

Soluble diiron monooxygenases (SDIMOs) are involved in aerobic degradation of short-chain alkanes, short-chain alkenes and aromatic compounds (Holmes and Coleman, 2008). A number of studies have mentioned prospecting applications of SDIMO in bioremediation and biocatalysis. These are, for example, the degradation of alkanes and alkenes contaminating soils and marine environments. SDIMOs are also promising enzymes which possess regio- and stereoselective properties towards carbon substrates for the production of epoxides used industrially use as monomers in the production of plastics (www.dow.com/propyleneoxide/app/index.htm). Moreover, the application of SDIMO enzymes can probably be exploited for pharmaceutical synthesis such as the

production of naphthol which possesses antiseptic properties and is also a precursor for insecticide production (Baichwal et al., 1958; Khorana et al., 1967).

1.3.2.1. SDIMO classification

Recently, SDIMO enzymes have been characterised into six distinct lineage subgroups based on gene sequences, genetic organisation of operons and phylogenetic analyses (Leahy et al., 2003; Coleman et al., 2006; Holmes and Coleman, 2008). A phylogenetic tree showing the relationship between SDIMO subgroups is given in Figure 1.2. The characterised enzymes, which are affiliated to the same subgroup, are able to oxidise a relatively similar group of substrates. Also, the gene arrangement is conserved within the SDIMO of the same subgroup, but not between different subgroups (Leahy et al., 2003).

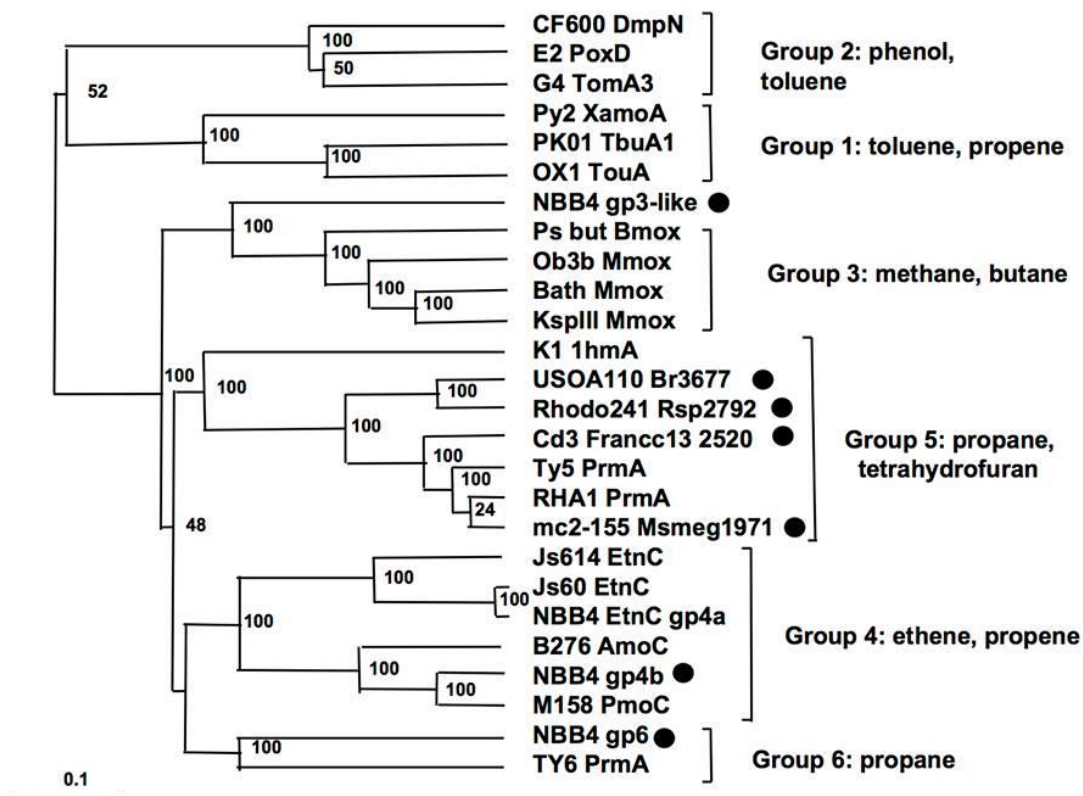


Figure 1.2: A phylogenetic tree showing the relationship of SDIMOs is based on alignment of 600 amino acids from the alpha subunit of the hydroxylase components. The black dots represent uncharacterised SDIMOs and their roles in the degradation of alkanes and/or alkenes have not been studied (Holmes and Coleman, 2008).

PCR amplification of the alpha subunit hydroxylase SDIMO gene has been accomplished by using a set of PCR primers known as NVC primers, degenerate PCR primers targeting conserved region in the gene encoding the hydroxylase component (Coleman et al., 2006). Figure 1.3 shows the conserved region in the alpha subunit SDIMO gene which the NVC primers bind to.

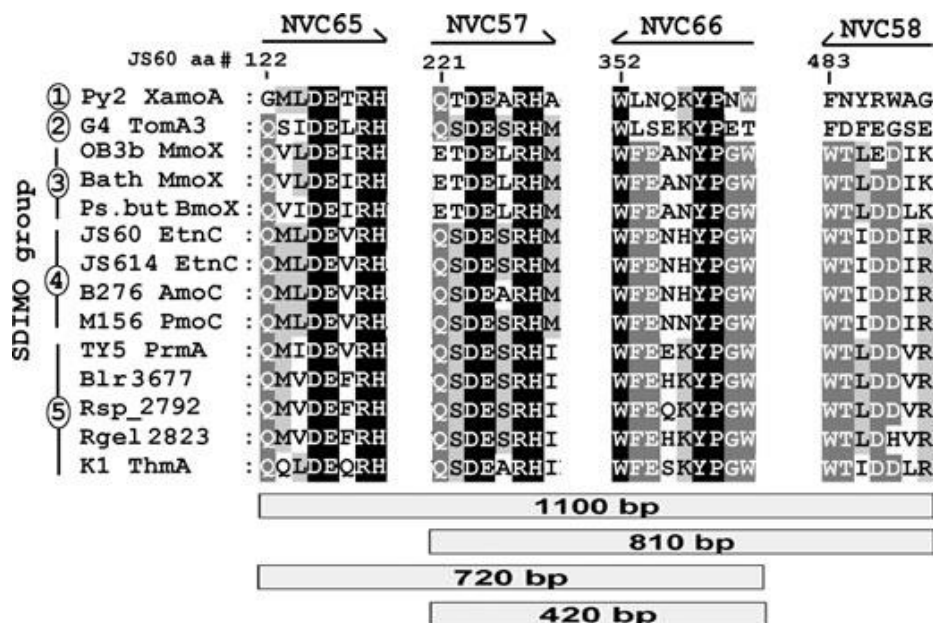


Figure 1.3: Amino acid alignments show conserved regions of SDIMO alpha subunits targeted for PCR primer design and the expected PCR amplicon sizes from various primer combinations. Black shading indicates highly conserved amino acids. Dark grey shading indicates >75% conserved amino acids. Light grey shading indicates >50% conserved amino acids. Representative sequences from each SDIMO group are shown. The representatives are alkene monooxygenase from *Xanthobacter* PY-2, toluene-o-monooxygenase from *Burkholderia cepacia* G4, soluble methane monooxygenase from *Methylosinus trichosporium* OB3b, soluble methane monooxygenase from *Methylococcus capsulatus* Bath, butane monooxygenase from *Pseudomonas butanovora*, ethene monooxygenase from *Mycobacterium* sp. JS60, ethene monooxygenase from *Nocardioides* sp. JS614, alkene monooxygenase from *Rhodococcus rhodochrous* B-276, propene monooxygenase from *Mycobacterium* sp. M156, propane monooxygenase from *Gordonia* sp. TY-5, predicted monooxygenase from *Bradyrhizobium japonicum* USDA 110, predicted monooxygenase from *Rhodobacter sphaeroides* 2.4.1, predicted monooxygenase from *Rubrivivax gelatinosus* PM1 and tetrahydrofuran monooxygenase from *Pseudonocardia* K1. (taken from Coleman et al., 2006)

1.3.2.2. Molecular genetics of SDIMOs

The most well characterised SDIMO is the sMMO from methanotrophs, so molecular information aspect on SDIMOs are mostly based on the molecular genetics of sMMO. The genes encoding sMMO in *Methylococcus capsulatus* Bath and *Methylosinus trichosporium* OB3b have been extensively studied (Murrell et al., 2000). The genetic organisation of sMMO in *Methylosinus trichosporium* OB3b is indicated in Figure 4. *mmoX*, *mmoY*, and *mmoZ* encode the α -, β -, and γ -subunits, respectively, which make up the hydroxylase component of the enzyme (Cardy et al., 1991; Murrell et al., 2000). A coupling protein is encoded by *mmoB* gene, while the reductase component is encoded by *mmoC* (Murrell et al., 2000).

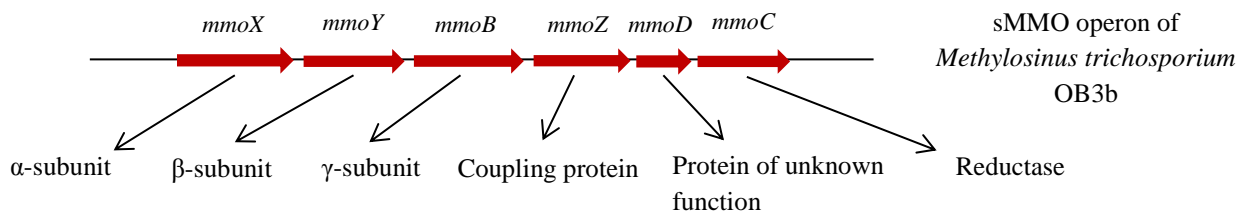


Figure 1.4: the sMMO operon of *Methylosinus trichosporium* OB3b, a well-studied SDIMO, showing the gene arrangement and encoded proteins.

1.3.2.3. Mutagenesis of soluble methane monooxygenase

Mutagenesis of soluble methane monooxygenase was not easily achieved. It was found that there was no appropriate expression system for protein engineering of sMMO. Moreover, Murrell's team in 1992 found that the sMMO hydroxylase component, where the catalytic site of this enzyme locates, is inactive when expressed in *E.coli* (West et al., 1992). Less than a decade later, the same team developed a homologous expression system for sMMO, which is called mutant F (Lloyd et al., 1999). The mutant F, which is a mutated *Methylosinus trichosporium* OB3b, allows good yields of highly active wild-type sMMO, and provides a system for the expression of mutant sMMO hydroxylases (Smith et al., 2002). This was a groundbreaking step for allowing sMMO mutagenesis to be exploited to study

catalytic properties of this enzyme. This then led to the development of even more tractable expression systems. A few years later, there was substantial development of expression vectors for protein engineering of sMMO hydroxylase component (Smith et al., 2002). These researchers also demonstrated that this new expression system functioned well in mutant F. Recently, Borodina in Murrell's group in 2007 studied the role of leucine residue 110 of the hydroxylase α -subunit encoded by *mmoX* using site-directed mutagenesis (Borodina et al., 2007). They found that this leucine residue plays an important role in controlling regioselectivity with aromatic substrates of sMMO. Interestingly, they developed a new strain of *M. trichosporium* called SMDM (soluble methane monooxygenase deleted mutant) for use as a homologous expression host for mutant sMMO genes. The strain SMDM allows mutagenesis of all components of sMMO operon except the reductase encoded by *mmoC*.

1.3.3. Cytochrome P450 alkane hydroxylases

Cytochrome P450 alkane hydroxylases were found in both eukaryotes and prokaryotes (Sariaslani, 1991). The most well characterized P450 enzymes in prokaryotes are P450cam, an enzyme involved in the metabolism of camphor in *Pseudomonas putida* (Dus et al., 1970), and P450 BM-3, an enzyme involved in fatty acid metabolism in *Bacillus megaterium* (Li et al., 1991). Cytochrome P450 alkane hydroxylases have been categorized into ten classes, but P450 alkane hydroxylases are mostly belonged to only three classes – Class I P450, Class II P450 (CYP52) and Class II P450 (CYP2E, CYP4B). Details of each class of cytochrome P450 alkane hydroxylases are discussed in the following section.

1.3.3.1. Class I P450

This type of P450 enzymes is involved in the degradation of C₄-C₁₆ alkanes. The class I P450 enzymes are soluble and driven by ferredoxin and ferredoxin reductases. Examples of bacteria containing this type of cytochrome P450 enzyme are *Sphingomonas* sp. HXN-200, *Mycobacterium* sp. HXN-1500 and *Acinetobacter* sp. EB104 (Maier et al., 2001).

1.3.3.2. Class II P450 (CYP52)

Most of class II P450 enzymes belong to the CYP52 family. The class II P450 (CYP52) enzymes are microsomal and driven by a reductase. Substrate range for this type of P450 is C₁₀-C₁₆ alkanes. Examples of microorganisms containing this type of P450 are *Candida tropicalis* and *Yarrowia lipolytica* (Craft et al., 2003).

1.3.3.3. Class II P450 (CYP2E, CYP4B)

The Class II P450 (CYP2E, CYP4B) enzymes are driven by reductase. Most of the P450 enzymes belonging to this class are found in human and rabbits. Class II P450 (CYP2E, CYP4B) enzymes oxidise C₆-C₁₀ alkanes (Fisher et al., 1998; Iba et al., 2000; Bolt et al., 2003).

1.3.4. Membrane bound copper-containing (and possibly iron-containing) monooxygenases

One of the well-studied members belonging to this family is particulate methane monooxygenases (pMMO) from *Methylococcus capsulatus* (Bath) (Nguyen et al., 1998). The pMMO comprises of three subunits which are α -subunit, β -subunit and γ -subunit encoded by *pmoB*, *pmoA* and *pmoC* genes, respectively (Semrau et al., 1995; Stolyar et al., 1999). The pMMO catalyse the oxidation of methane under high copper-to-biomass ratio growth conditions (Dalton et al., 1984; Prior and Dalton, 1985). Ammonia monooxygenases (AMO), found only in ammonia oxidizing nitrifiers, are one of the members of this family. Analysis of *pmo* and *amo* gene sequences from a diverse range of organisms suggested that pMMO and AMO are evolutionarily related (Holmes et al., 1995). Membrane bound copper-containing monooxygenases play a crucial role in the oxidation of ammonia, methane, small alkanes and chlorinated hydrocarbons (Bédard and Knowles, 1989; Conrad, 1996). A copper-containing membrane-bound monooxygenase was also found in *Mycobacterium chubuense* NBB4 (Coleman et al., 2011). This membrane-bound monooxygenase is responsible for the hydroxylation of C₂-C₄ hydrocarbons (Coleman et al., 2012). The membrane-bound monooxygenase of *Mycobacterium chubuense* NBB4 showed activity towards ethane, propane and butane, but not

methane. A membrane-associated monooxygenase was also found in the butane degrader *Nocardia* sp. CF8 (Sayavedra-Soto et al., 2011). The activity of this enzyme towards the oxidation of butane in *Nocardia* sp. CF8 was inhibited by the Cu-selective chelator allylthiourea, which is also known as an inhibitor of pMMO and AMO (Hamamura et al., 1999). It is known that acetylene also acts as an inhibitor for membrane bound monooxygenases (Hyman and Wood, 1985).

1.4. Alkane metabolisms in *Rhodococcus* spp.

A number of studies demonstrated that *Rhodococcus* spp. contain a variety of hydrocarbon-degrading enzymes which allow the ability to metabolise a wide range of organic compounds such as alkanes, alkenes, aromatic compounds and even toxic compounds like acrylamide (Holmes & Coleman, 2008; Larkin et al., 2005; van Beilen et al., 2002; Arai et al., 1981). One of the most well studied areas of alkane metabolism by *Rhodococcus* species is propane metabolism.

1.4.1. Aerobic metabolism of C₂-C₄ gaseous alkanes in bacteria

1.4.1.1. Ethane (C₂H₆) metabolism

Ethane can be oxidised to ethanol by a monooxygenase. Ethanol is then converted to acetaldehyde and acetate. These two compounds then enter central metabolic pathways in bacterial cells (Linton et al., 1980, Davies et al., 1974). Ethane metabolism of non-methane oxidising bacteria is shown in Figure 1.5.

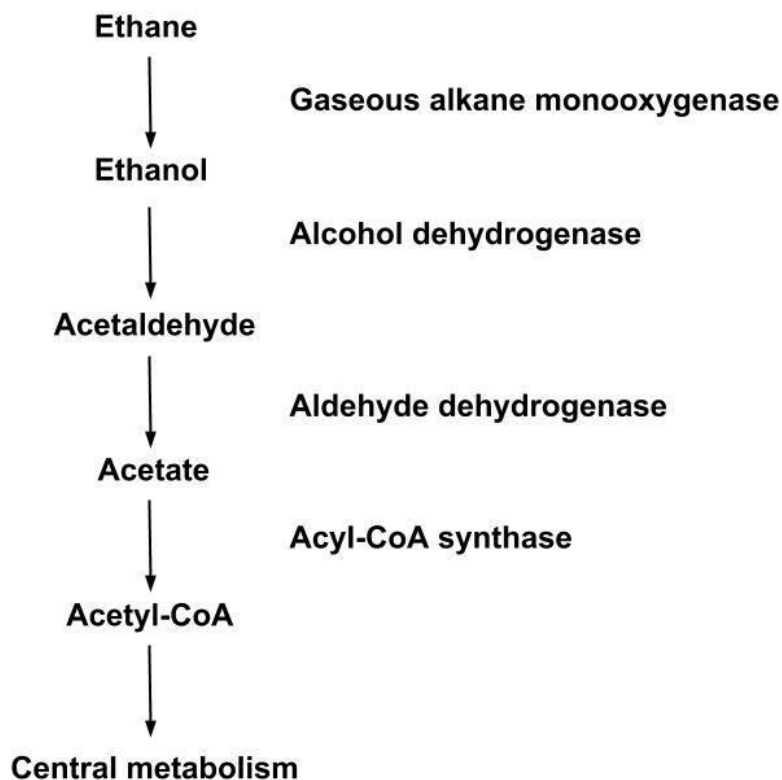


Figure 1.5: Ethane metabolism by non-methane oxidising bacteria

Mycobacterium paraffinicum was isolated from an ethane-enriched soil. It was tested for its ability to grow on a range of alkanes (Chase et al., 1956). This bacterium could grow well on ethane and liquid alkanes, but not on methane. *M. paraffinicum* lacks the ability to grow on bacteriological media such as yeast extract, peptone or glucose, but it will grow readily on these media in the presence of ethane. This suggested that this bacterium is an obligate alkane utilizer. Ethane-grown cells of *M. paraffinicum* could also oxidise propane and butane. They could also oxidise ethene, ethanol, acetaldehyde and acetate. The authors suggested, based on these results, that ethene, ethanol, acetaldehyde and acetate are intermediates in the ethane oxidation pathway. However, slow ethene oxidation rates with ethane-grown cells suggested that ethene is unlikely to be an intermediate of the ethane oxidation pathway.

1.4.1.2. Propane (C₃H₈) metabolism

There is a number of *Rhodococcus* spp. that can degrade propane (Perry, 1980; Woods & Murrell, 1989; Kulikova et al., 2001; Fournier et al., 2009). These studies suggested that *Rhodococcus* spp. can aerobically oxidise propane through either terminal or sub-terminal pathways or through both pathways in some cases. The proposed propane oxidation pathways in *Rhodococcus rhodochrous* PNKb1 are shown in Figure 1.6.

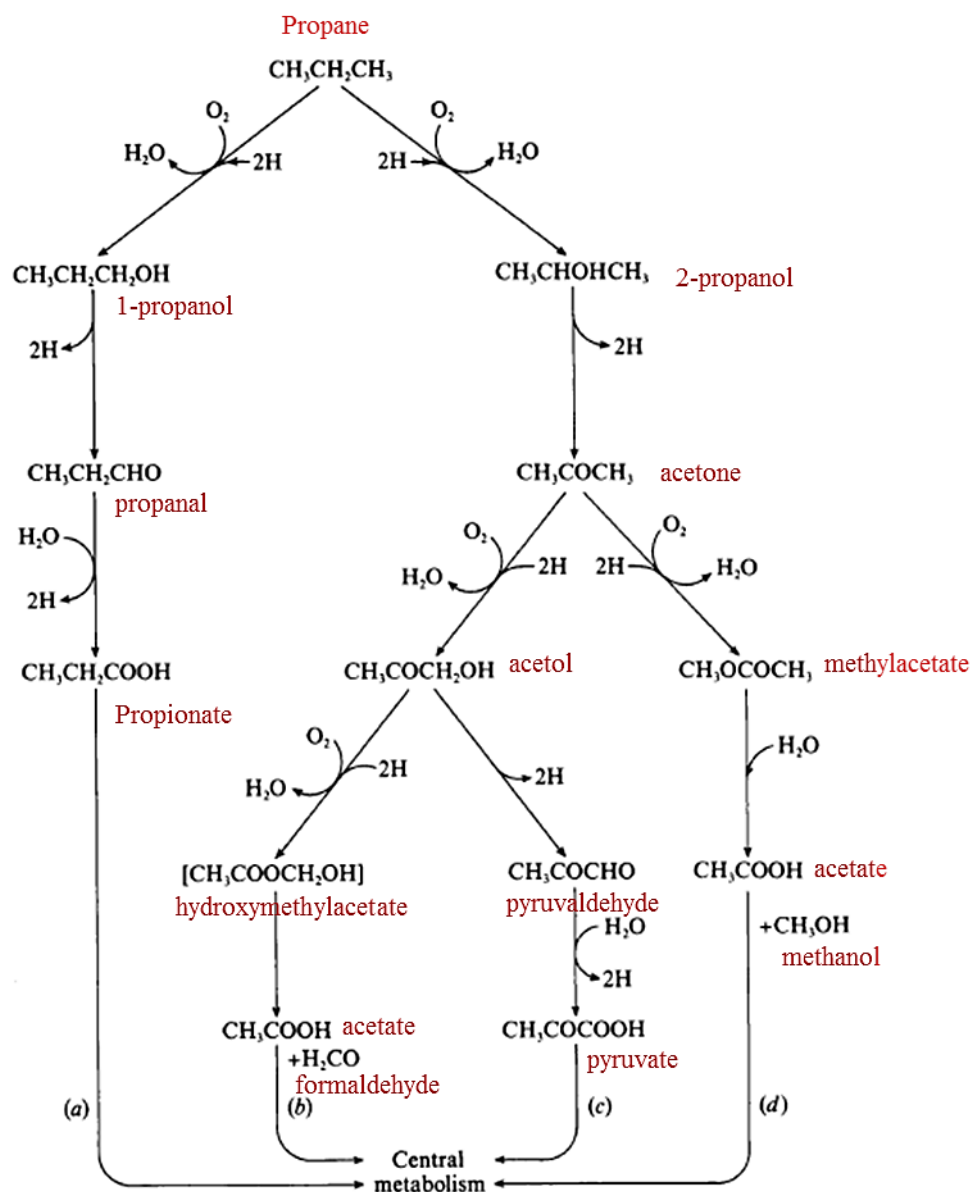


Figure 1.6: The possible propane oxidation pathway by *Rhodococcus rhodochrous* PNKb1. (a) terminal oxidation via propanoate; (b) sub-terminal oxidation via acetol and hydroxymethylacetate; (c) sub-terminal oxidation via pyruvate; (d) sub-terminal oxidation via methyl acetate (adapted from Woods & Murrell, 1989)

Terminal oxidation occurs via a primary alcohol (1-propanol) which is oxidised by alcohol and aldehyde dehydrogenases to the corresponding fatty acid. Fatty acid is then converted to acetyl-CoA by the β -oxidation (Wegener et al., 1968; Kunau et al., 1995). Sub-terminal oxidation occurs via a secondary alcohol (2-

propanol) which is oxidised via the corresponding ketone by a Baeyer-Villiger monooxygenase to fatty acids (Forney and Markovetz, 1970; Van Beilen et al., 2003). Another pathway for bacterial oxidation of propane could occur via 1,2-propanediol catalysed by a dioxygenase (Ashraf et al., 1994). However, propane oxidation by a dioxygenase has not been observed in propane-utilising bacteria, but propanediol metabolism is observed in enteric bacteria (Bobik, 2006).

The study of propane metabolism in *R. rhodochrous* PNKb1 suggested that propane monooxygenase does not have preference in the insertion of oxygen into the propane molecule (Ashraf & Murrell, 1992). Specificity was observed at the stage of the primary or secondary alcohol dehydrogenase. The ability of *R. rhodochrous* PNKb1 to grow on potential intermediates of both terminal and sub-terminal propane oxidation pathways suggested that this strain could oxidise propane via both pathways (Woods & Murrell, 1989). Oxidation studies on potential intermediates of propane metabolism by *R. rhodochrous* PNKb1 suggested that propane oxidation was inducible only by growth on propane. Propane oxygenase in *R. rhodochrous* PNKb1 was induced during growth on propane. This enzyme was also able to oxidise ethane and butane, but not other longer-chain alkanes (up to C₈ alkane). However, propane is the only growth substrate for this strain. NADH-dependent propane oxygenase activity in *R. rhodochrous* PNKb1 was detected by using propene as substrate and measuring the formation of 1,2-epoxypropane (Woods and Murrell, 1990). These researchers found that purification of this enzyme was difficult due its unstable nature. Cell-free extracts of *R. rhodochrous* PNKb1 cells grown on propane and its potential propane oxidation intermediates were assayed for alcohol dehydrogenase activities (Ashraf and Murrell, 1992). The highest 1-propanol and 2-propanol dehydrogenase activities were detected in cell-free extract of cells grown on propane. Such activities were also detected in cell-free extracts of cells grown on potential intermediates of propane oxidation, except propanoate. The increase in both NAD⁺-linked 1-propanol and 2-propanol dehydrogenase activities after growth on propane suggested that *R. rhodochrous* PNKb1 contained two alcohol dehydrogenases involved in propane metabolism (Ashraf and Murrell, 1992).

Mycobacterium sp. TY-6 and *Pseudonocardia* sp. TY-7 were able to grow well on propane and other *n*-alkanes (Kotani et al., 2006). *Mycobacterium* sp. TY-6 was able to grow on C₃-C₆ and C₁₀-C₁₉ alkanes while *Pseudonocardia* sp. TY-7

could grow on C₂-C₆ and C₁₃-C₁₉ alkanes. The growth of these two propanotrophs on possible products (alcohols) of gaseous alkane metabolism was tested. It was found that *Mycobacterium* sp. TY-6 could not consume methanol, 2-propanol and 2-butanol. This suggested that it is likely that this bacterium metabolise propane and butane mainly via the terminal oxidation pathway. Whole-cell assays were carried out in order to determine products of gaseous alkane metabolism by *Mycobacterium* sp. TY-6 (Kotani et al., 2006). The results showed that 1-butanol and 1-propanol were detected as products of butane and propane metabolisms, respectively. This confirmed that in *Mycobacterium* sp. TY-6 propane and butane are metabolised via terminal pathways. Differently, *Pseudonocardia* sp. TY-7 was able to consume a range of primary and secondary alcohols, but not methanol. This suggested that methane was not oxidised by this bacterium. In order to investigate possible pathways for the degradation of gaseous alkanes by *Pseudonocardia* sp. TY-7, the oxidation products of propane and butane were determined (Kotani et al., 2006). It was found that 1-propanol and acetone were detected as products of propane oxidation. The 1-butanol, 2-butanol and 2-butanone were detected as products of butane metabolism. These results suggested that *Pseudonocardia* sp. TY-7 oxidised propane and butane through both terminal and sub-terminal pathways.

In *Flavobacterium* sp. NCIB 11171, 1,2-propanediol metabolism was determined (Willettts, 1979). The pathway of 1,2-propanediol in this bacterium was influenced by the amount of aeration during growth. Under aerobic conditions, 1,2-propanediol was metabolized to lactaldehyde which was converted to pyruvate. Pyruvate was subsequently oxidized to carbon dioxide by tricarboxylic acid cycle. Under microaerophilic conditions, some diol was catabolized by an inducible diol hydratase to propionaldehyde which was then converted to propanol as an end product, while some diol was metabolized via the same pathway as when growing under aerobic conditions.

It was also found that some strains of the propane-oxidising *Rhodococcus* spp. are capable of oxidising other compounds (Steffan et al., 1997; Kulikova and Bezborodov, 2000; Sharp et al., 2007; Fournier et al., 2009). One example is propane monooxygenase from *Rhodococcus jostii* RHA1, which is the closest relative of *R. jostii* strain 8 obtained in this study. It is responsible for the degradation of *N*-nitrosodimethylamine (NDMA) which is a carcinogenic groundwater pollutant

(Sharp et al., 2007). *R. jostii* RHA1 is capable of removing NDMA when grown on pyruvate, soy broth, LB medium or propane. *Rhodococcus ruber* ENV425, isolated from turf soil which propane was used as sole carbon source, could catabolise NDMA (Fournier et al., 2009). This *Rhodococcus* strain was also able to oxidise methyl tertiary-butyl ether (MTBE) and gasoline oxygenates (Steffan et al., 1997). Propane-grown cells of *Rhodococcus* sp. RR1 performed the ability to transform NDMA (Sharp et al., 2010). According to genomic and transcriptional studies, it was found that propane monooxygenase in *Rhodococcus* sp. RR1 was responsible for the degradation of NDMA. These data suggested that other propanotrophs may also possess the ability to metabolise NDMA. Therefore, alkane-degrading *Rhodococcus* spp. are potential sources for biotechnological applications, particularly for bioremediation and biocatalysis.

1.4.1.3. Butane (C₄H₁₀) metabolism

As with propane, butane can be metabolized via both terminal and sub-terminal pathways by a monooxygenase, resulting in primary or secondary butanol. 1-butanol is then converted to butyraldehyde by butanol dehydrogenase. Butyraldehyde is then metabolized to butyrate. The most well-studied butane degrader is *Pseudomonas butanovora*, recently named *Thauera butanivorans* (Arp, 1999; Cooley et al., 2009). Growth substrates of *P. butanovora* are C₂-C₈ alkanes (Takahashi, 1980). Butane metabolism in *P. butanovora* via the terminal oxidation pathway was proposed via 1-butanol, butyraldehyde and butyrate (Arp, 1999). Butane metabolism in *Pseudomonas butanovora* ATCC 43655 was regulated independently at each step in the pathway. Butane oxidation via the terminal pathway was also observed in *Mycobacterium vaccae* JOB5 (Phillips and Perry, 1974). Proposed butane metabolism in butane-degrading bacteria is shown in Figure 1.7.

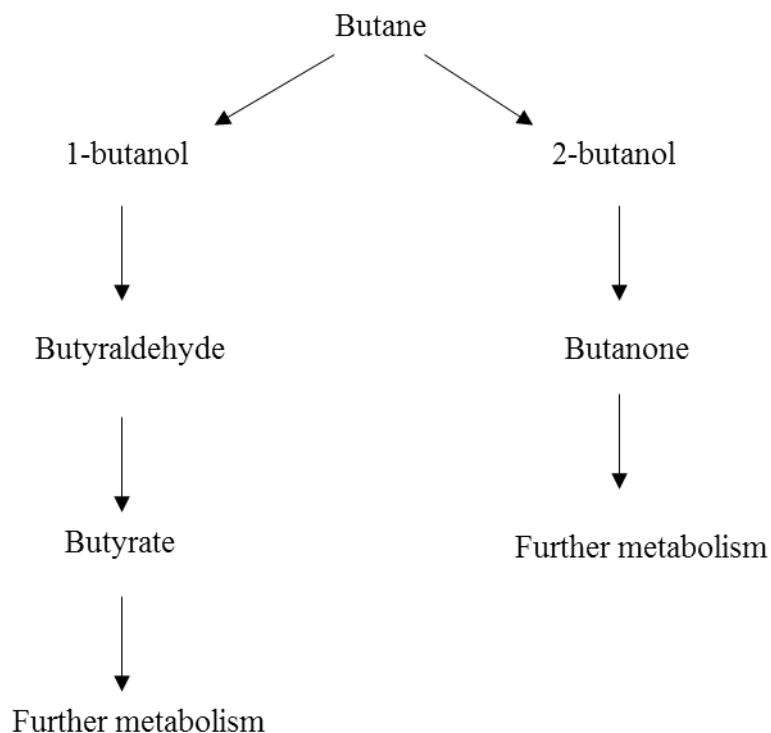


Figure 1.7: Proposed terminal (left) oxidation and subterminal (right) of butane in butane-degrading bacteria (adapted from Arp, 1999)

As mentioned earlier, it was found that *Mycobacterium vaccae* JOB5 metabolised butane via the terminal oxidation pathway (Phillips and Perry, 1974). This was indicated because cells grown on butane or butyrate expressed isocitrate lyase activity resulting in further metabolism of butyrate. In contrast, cells grown on butanone did not express isocitrate lyase activity. Similarly, *Nocardia* TB1 metabolised butane via the terminal pathway (van Ginkel et al., 1987). The proposed butane metabolism pathway in this bacterium is that butane was oxidized to 1-butanol which was converted to butyraldehyde and then butyrate. The sub-terminal pathway for the degradation of butane was proposed for propane-grown *Mycobacterium smegmatis* 422 (Lukins and Foster, 1963).

Mycobacterium sp. NBB4 contains multiple monooxygenases including a novel type SDIMO, a soluble methane monooxygenase (sMMO)-like enzyme which can oxidise butane (Martin et al., 2014). In this study, a gene cluster encoding a novel type of SDIMO was expressed in *Mycobacterium smegmatis* mc²-155, which

does not metabolise tested alkanes and alkenes under control conditions for this assay. The novel SDIMO enzyme showed highest activity with ethane and ethene. Low activity of the enzyme was detected with propane and butane. Activity towards methane was not detected. These results suggested that the enzyme activity increased as substrate size increased.

Multiple alcohol dehydrogenases have been found in *P. butanovora*. The reasons why *P. butanovora* required more than one alcohol dehydrogenase to oxidise 1-butanol was not known (Vangnai and Arp, 2001; Vangnai et al., 2002a; Vangnai et al., 2002b). The possibility of the presence of more than one alcohol dehydrogenase in one organism is usually because those enzymes that are expressed have different substrate ranges. A study on the roles of two distinct alcohol dehydrogenases in *P. butanovora* suggested that one was required for energy production while another was required for detoxification of 1-butanol (Vangnai et al., 2002b).

1.4.2. Alcohol dehydrogenases (ADH)

Alcohol dehydrogenases are responsible for the conversion of alcohols to aldehydes or ketones, which is the second step of alkane metabolism. Alcohol dehydrogenases were categorized into three main types regarding to their cofactors.

1.4.2.1. Pyrroloquinoline quinone (PQQ) dependent alcohol dehydrogenase

Most of the methanol dehydrogenases commonly found in Gram-negative methylotrophs use pyrroloquinoline quinone (PQQ) as cofactor (Duine et al., 1980). Unlike Gram-negative methylotrophs, limited studies on methanol oxidation in Gram-positive methylotrophs suggested that methanol dehydrogenases of these bacteria do not contain PQQ (Hektor H.J., 2000). Methanol dehydrogenase in Gram-negative methylotrophs is not only specific to methanol, but also able to catalyze aliphatic alcohols (Anthony and Zatman, 1964). This type of enzyme can be assayed for activity by using phenazine methosulphate (PMS) as an artificial electron acceptor. The activities of the enzyme can be spectrophotometrically measured from

the rate of reduction of 2, 6-dichlorophenolindophenol (DCPIP). The reaction is initiated by the addition of ammonia. The most well studied PQQ-containing alcohol dehydrogenase is the methanol dehydrogenase from *Pseudomonas* sp. M 27 (Anthony and Zatman, 1964b). The other examples of PQQ-containing alcohol dehydrogenases are butanol dehydrogenase from *Pseudomonas butanovora*, methanol dehydrogenase from *Methylocella silvestris* BL2 and acetaldehyde dehydrogenase from *Rhodococcus erythropolis* EK-1 (Pirog et al., 2009).

1.4.2.2. Nicotinamide adenine dinucleotide (NAD(P)) dependent alcohol dehydrogenase

NAD(P)-dependent alcohol dehydrogenases have been categorized into three families (Jörnvall et al., 1987; Reid and Fewson, 1994). Members of Family I are zinc-dependent, di- or tetrameric quaternary structures. Alcohol dehydrogenases belonging to this Family do not have activities with methanol. The only exception is methanol dehydrogenase of *Bacillus stearothermophilus* DSM 2334 (Sheehan et al., 1988). Members of Family II are metal-independent. They possess broad substrate specificity. Similar to members of Family I, members of this Family are not involved in methanol oxidation in methanotrophs. Members of Family III are initially known as iron-dependent. However, with increasing number of members, iron dependency is no longer common among members of this Family. Other metal ions such as zinc and magnesium were detected instead of iron. A variety of alcohol dehydrogenases from various types of organisms e.g. Gram-positive bacteria, Gram-negative bacteria, aerobic and anaerobic bacteria, yeasts, archaea, was classified into this Family based on their sequence similarity (de Vries et al., 1992). These enzymes can sometimes be involved in the oxidation of methanol to formaldehyde.

1.4.2.3. *N,N*-dimethyl-4-nitrosoaniline (NDMA) dependent alcohol dehydrogenase

This novel type of cofactor-containing alcohol dehydrogenases was first discovered in the thermotolerant methanol oxidizer, *Bacillus methanolicus* C1 (Arfman and Dijkhuizen, 1990). Methanol dehydrogenase from *B. methanolicus* C1

could oxidise C₁-C₄ primary alcohols and 1, 3- propanediol (Arfman and Dijkhuizen, 1990). The presence of both zinc and magnesium in each subunit of NDMA-dependent alcohol dehydrogenases is the feature which distinguish these enzymes from the other types of alcohol dehydrogenases (Vonck et al., 1991). Members of this type of alcohol dehydrogenase showed enzyme activity when coupling the oxidation of alcohols to the reduction of NDMA, but were not active with free NAD(P)⁺ (Bystrykh et al., 1993). The advantage of NDMA-dependent alcohol dehydrogenases over the other types of these enzymes is that the activities are not affected by redox balance (NAD/NADP ratio) of the cells (Schenkels and Duine, 2000). This property could benefit bioconversion in industrial scale. Limited details have been discovered to this type of alcohol dehydrogenase due to its limited occurrence. Other examples of bacteria possessing NDMA-dependent alcohol dehydrogenase are the Gram-positive methylotrophs, *Amycolatopsis methanolica*, *Mycobacterium gastri* MB19, a methanogen, *Methanosarcina barkeri* DSM 804, *Rhodococcus* sp. NI86/21 and *Rhodococcus erythropolis* DSM 1069 (Bystrykh et al., 1993; Nagy et al., 1995; Dausmann et al., 1997; Schenkels and Duine, 2000). It was found that NDMA-dependent alcohol dehydrogenase was also able to oxidise ethanol to acetaldehyde (Schenkels and Duine, 2000).

1.5. Previous studies on mutagenesis of alkane-degrading enzymes in *Rhodococcus* species

1.5.1. The development of *E. coli* – *Rhodococcus* shuttle vectors and transformation procedures

The first *E. coli* – *Rhodococcus* shuttle vector, pMVS301 was developed for the purpose of cloning. The plasmid pMVS301 contains ampicillin and thiostrepton resistance genes (Singer and Finnerty, 1988). The recombinant plasmid pMVS301 was transferred into *Rhodococcus* sp. AS-50 by polyethylene glycol-assisted transformation and by selection for thiostrepton resistant transformants. Optimisation of the polyethylene glycol-assisted transformation was carried out. The transformation frequency obtained by this transformation procedure was 10⁵

transformants/ μg DNA. The plasmid pMVS301 was applied for use in other strains of *Rhodococcus* such as *R. erythropolis*, *R. globerulus* and *R. equi* (Singer and Finnerty, 1988). The use of this plasmid in *R. rhodochrous* was not successful (Singer and Finnerty, 1988). Later, several plasmids such as a cadmium-resistance plasmid (pD188) from *R. fascians* and an arsenate-resistance plasmid (pD37) used for transformation of *R. erythropolis* and *R. equi* have been constructed in order to allow transformation of foreign DNA into *Rhodococcus* species (Desomer et al., 1988; Dabbs et al., 1990). However, recently one of the most widely used *E. coli*-*Rhodococcus* shuttle vectors is pK18*mobsacB* (Schäfer et al., 1994). The plasmid map of pK18*mobsacB* is shown in Figure 1.6 below.

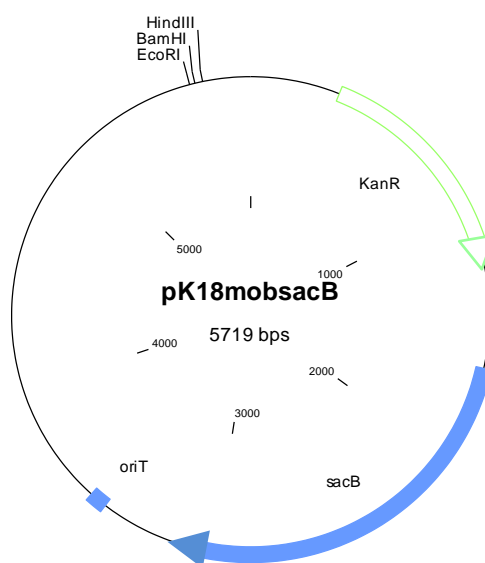


Figure 1.8: The plasmid map of pK18*mobsacB*, an *E. coli*-*Rhodococcus* shuttle vector used in this study

The pK18*mobsacB* plasmid can replicate in *E. coli* and closely related species. This plasmid also contains the broad host range transfer elements from the plasmid RP4 (Datta et al., 1971) which allows the transfer of this plasmid between *E. coli* and other bacterial genera. pK18*mobsacB* also contains a modified *sacB* gene

from *Bacillus subtilis* which is lethal to the cells in the presence of sucrose (Selbitschka et al., 1993). In the presence of sucrose in the medium, levansucrase is released, resulting in sucrose hydrolysis and levan synthesis (Steinmetz et al., 1985). The toxicity of levan, which has a high molecular weight, to the cells could be due to accumulation in the periplasm or a transfer of fructose residues to unsuitable acceptor molecules causing toxic effect to the cells (Steinmetz et al., 1983). The use of the lethal effect of *sacB* in the presence of sucrose in order to select for the transposition of insertion sequences has been achieved in several genera of Gram-positive bacteria (Gay et al., 1985; Jäger et al., 1995).

A number of nucleic acid manipulation techniques have been developed for transferring plasmid DNA into *Rhodococcus* spp. Electrotransformation (protoplast and electroporation) techniques have been widely used for the transformation of various plasmids into various *Rhodococcus* strains. Preparation of protoplasts was firstly developed for used with *Streptomyces* (Hopwood et al., 1985). However, the protoplast transformation technique did not work with some *Rhodococcus* species (Desomer et al., 1990). The adaptation of electrotransformation techniques led to the development of electroporation methods for transformation of *Rhodococcus* spp. (Desomer et al., 1990). This technique has become widely used for introducing DNA into various *Rhodococcus* strains (Nagy et al., 1995; Shao et al., 1995; Sekizaki et al., 1998). As with electroporation, conjugation has been used as another approach to transfer plasmid DNA into *Rhodococcus* spp. (Desomer et al., 1988; Dabbs, 1998; van Hylckama Vlieg et al., 2000).

1.5.2. Mutagenesis of propane monooxygenases

There have been a few studies on the mutagenesis of propane monooxygenases in *Gordonia* sp. TY-5 and *Methylocella silvestris* BL2. The deletion of the α -subunit hydroxylase of the propane monooxygenase was carried out in *Methylocella silvestris* BL2, a facultative methanotroph which can also grow on propane as sole source of carbon and energy (Crombie and Murrell, 2014). In the genome of *M. silvestris* BL2, there are two different SDIMOs – one is soluble methane monooxygenase (sMMO) and another is propane monooxygenase belonging to Group 5 SDIMO (Chen et al., 2010). It was found that in *M. silvestris*

BL2, propane was metabolized via both terminal and sub-terminal pathways resulting in the detection of both 1- and 2-propanol. The role of propane monooxygenase in *M. silvestris* BL2 was studied by deleting *prmA*, the gene encoding the hydroxylase α -subunit of propane monooxygenase (Crombie and Murrell, 2014). The *prmA*-deleted mutant was still able to grow on propane, but with slower growth rates than the wild-type strain. This is because of the oxidation of propane by active sMMO. It was found that 2-propanol was detected in the medium of the *prmA*-deleted mutant when grown on propane. This suggested that 2-propanol is the product of propane metabolism by sMMO. In contrast, 2-propanol was not detected in the medium of sMMO-deficient strain grown on propane. This suggested that 2-propanol is not a major product of propane metabolism by propane monooxygenase. The ability of propane monooxygenase in *M. silvestris* BL2 to oxidise methane was evaluated by comparing methane consumption of the wild-type strain with that of sMMO-deficient strain. The study showed that there was no detectable consumption of methane by the sMMO-deficient strain. This suggested the inability of propane monooxygenase to metabolise methane.

In *Gordonia* TY-5, *prmB*, a gene encoding β -subunit of propane monooxygenase and *adh1*, a gene encoding alcohol dehydrogenase were inactivated by homologous recombination with gene disruption plasmids (Kotani et al., 2003). Both mutants were tested for their ability to grow on propane and potential intermediates in propane metabolism. The results showed that both the *prmB*-deleted mutant and the *adh1*-deleted mutant were not able to grow on propane. This suggested that both genes are essential in propane oxidation in this bacterium. Both mutant strains were still able to grow on 1-propanol as well as the wild-type strain. This indicated that there might be other enzymes involved in the oxidation of 1-propanol. The growth of *prmB*-deleted mutant and the *adh1*-deleted mutant on 2-propanol was reduced. However, both mutant strains could still grow on 2-propanol. This suggested that there are probably other enzymes responsible for the oxidation of 2-propanol. Other evidence supporting this claim is the presence of two alcohol dehydrogenase genes, *adh2* and *adh3* located on the chromosome. The expression of *adh1* in the *prmB*-deleted mutant was investigated by northern blot analysis. Results showed that *adh1* was not transcribed in *prmB*-deleted mutant. This suggested that the insertion of kanamycin-resistant gene in the *prmB* affected the transcription of

adh1, which is located downstream of *prmB* in the propane monooxygenase gene cluster of *Gordonia* sp. TY-5.

1.5.3. Mutagenesis of *alkB*-type alkane monooxygenases

The role of *alkB*-type alkane monooxygenase (alkane hydroxylase or alkane-1-monooxygenase) has been extensively studied in *Pseudomonas oleovorans* GPo1, recently named as *Pseudomonas putida* GPo1 (van Beilen et al., 2001). The alkane hydroxylase system in *P. putida* GPo1 was identified as being responsible for the first step in the oxidation of alkanes. Site-directed mutagenesis of *alkB* gene in the *alkB*-type alkane monooxygenase of *Pseudomonas putida* GPo1 was recently carried out (Alonso et al., 2014). In this study, a lysine residue which is one of the highly conserved amino acid residues near active site of the enzyme was substituted with alanine. It was found that the mutant protein completely lacked enzyme activity. This indicated that the lysine residue plays an essential role in the function of the *alkB*-type alkane monooxygenase. The observation of the 3D structure of the mutant protein comparing with the wild-type protein showed that substitution of lysine with alanine leads to the loss of integrity of the structure of the enzyme.

Two *alkB*-type alkane monooxygenases were found in *Alcanivorax borkumensis* SK2 (Hara et al., 2004). The role of the two alkane monooxygenases in *A. borkumensis* SK2 was investigated by the disruption of *alkB1* and *alkB2*. Results suggested that the *alkB1* gene is responsible for the degradation of *n*-hexane. A mutant in which both *alkB1* and *alkB2* were disrupted was still able to grow on medium-chain alkanes. This suggested that the metabolism of medium-chain alkanes depends on the hydroxylation of the enzyme system rather than the *alkB1* and *alkB2* (Hara et al., 2004).

Project aim

This PhD project aims to test the hypotheses that there is more than one enzyme system which is responsible for the oxidation of alkanes in *Rhodococcus jostii* strain 8 or if there is only one versatile enzyme system. To achieve this goal, the ranges of carbon substrates which *R. jostii* strain 8 can grow and oxidise was investigated. The potential pathways of alkane metabolism were also determined. The development of a system for mutagenesis of *prmA* and *alkB* in *R. jostii* strain 8 was carried out in order to make the deleted mutants to further determine the role of alkane-degrading enzymes.

Chapter 2

Materials and methods

2.1. Bacterial strains, plasmids and primers used in this study

Table 2.1: Bacterial strains used in this study. Abbreviations, Gm^R, gentamicin resistance; Km^R, kanamycin resistance; Ap^R, ampicillin resistance

Bacterial strains	Description	Reference/source
<i>Rhodococcus jostii</i> RHA1	wild-type strain	Prof. Tim Bugg, University of Warwick
<i>Rhodococcus jostii</i> strain 8	wild-type strain	This study
<i>Escherichia coli</i> JM109	<i>endA1, recA1, gyrA96, thi, hsdR17</i> (r_k^- , m_k^+ , <i>relA1, supE44</i> , $\Delta(lac-proAB)$, [F' <i>traD36, proAB, laqI^qZ</i> Δ M15]	Promega
<i>Escherichia coli</i> Top10	F- <i>mcrA</i> $\Delta(mrr-hsdRMS-mcrBC)$ $\phi 80lacZ$ Δ M15 $\Delta lacX74$ <i>recA1 araD139</i> $\Delta(ara leu)7697$ <i>galU galK rpsL (strR) endA1 nupG</i>	Invitrogen

Table 2.2: Plasmids used in this study

Plasmids	Description	Reference/source
pGEM-T	Ap ^R , TA cloning vector	Promega
pNV18	Km ^R	(Chiba et al., 2007)
pK18 <i>mobsacB</i>	Km ^R , RP4-mob, mobilisable cloning vector containing <i>sacB</i> from <i>Bacillus subtilis</i>	(Schäfer, et al., 1994)
p34S-Gm	Source of Gm ^R cassette	(Dennis & Zylstra, 1998)
pAGB	Km ^R , Gm ^R , pK18 <i>mobsacB</i> containing insertion of gentamicin cassette inserted into a fragment of <i>prmA</i> of <i>R. jostii</i> strain 8	This study
pXGY	Km ^R , Gm ^R , pK18 <i>mobsacB</i> containing insertion of gentamicin cassette inserted into a fragment of <i>alkB</i> of <i>R. jostii</i> strain 8	This study

2.2. Chemicals

Chemicals, enzymes and media components were of analytical grade and were obtained from the following manufacturers:

Sigma-Aldrich Corporation (St Louis, MO, USA), Melford laboratories Ltd (Ipswich, UK), Fisher Scientific UK (Loughborough, UK), Oxoid Ltd (Basingstoke, Hampshire, England), Formedium Ltd (Hunstanton, England), Merck (Darmstadt, Germany).

Methane and propane were used at 99.5% purity grade. Ethane, butane, ethane, propene and butane were used at 99+% purity grades. Gases were from the following manufacturers:

BOC (Manchester, UK), Air Liquide UK (Birmingham, UK), Sigma-Aldrich.

2.3. Antibiotics

Stock antibiotic solutions were prepared by filter sterilized through 0.2 μm pore-size disposable Minisart syringe filter (Sartorius, Göttingen, Germany). Concentrations of antibiotics which were used in growth media are shown in Table 2.3.

Table 2.3: Antibiotics used in this study

Antibiotics	Stock concentration (mg/ml)	Working concentration ($\mu\text{g/ml}$)
ampicillin	100	100
kanamycin	50	50, 100
spectinomycin	50	25
streptomycin	50	25
gentamicin	5	2.5, 5

2.4. Growth conditions

All solutions for growth media were prepared with deionized water and sterilized by autoclaving at 15 psi for 15 minutes at 121°C. Any solutions which were sensitive to autoclaving (*e.g.* glucose) were sterilized using 0.2 μm pore-size

disposable Minisart syringe filter (Sartorius, Göttingen, Germany), and were then added to cooled autoclaved media.

2.4.1. *Rhodococcus jostii* strain 8

Cultures of strain 8 using gaseous alkanes and volatile substrates of the putative propane oxidation pathway were grown in batch culture in 120 ml, 250 ml or 2 L quick-fit flasks containing 20 ml, 50 ml or 500 ml of NMS medium, respectively. Cultures were inoculated with a loopful of cells from a plate or 10% (v/v) of an exponential phase liquid culture. Flasks were closed with suba seals. The air in the headspace was withdrawn prior to the addition of an equivalent volume of gaseous alkanes by using a sterile needle and syringe, resulting in 10% (v/v) of gaseous alkanes in the headspace. When using liquid substrates i.e. volatile substrates involved in the propane oxidation pathway, an appropriate volume of substrate was added to batch cultures to give a final substrate concentration of 10 mM. Flasks were incubated at 30°C, with shaking at 150 rpm.

Preparation of Nitrate Mineral Salts Medium (NMS)

Solution 1: Salt solution (x10 stock)

Potassium nitrate	(KNO ₃)	10 g
Magnesium sulfate	(MgSO ₄ .7H ₂ O)	10 g
Calcium chloride	(CaCl ₂ .2H ₂ O)	2 g

Dissolve the above in approximately 700 ml of deionised water and make up to 1 L

Solution 2: Iron EDTA solution (x10,000 stock)

Ferric-EDTA	(Fe-EDTA)	3.8 g
-------------	-----------	-------

Dissolve in deionised water to a final volume of 100 ml

Solution 3: Sodium Molybdate solution (x1,000 stock)

Sodium Molybdate	(NaMO ₃ .2H ₂ O)	0.26 g
------------------	--	--------

Dissolve in deionised water to a final volume of 1 L

Solution 4: Trace Elements solution (x1,000 stock)

Copper sulphate	(CuSO ₄ .5H ₂ O)	1 g
Ferric sulphate	(FeSO ₄ .7H ₂ O)	2.5 g
Zinc sulphate	(ZnSO ₄ .7H ₂ O)	2 g
Orthoboric acid	(H ₃ BO ₃)	0.075 g
Cobalt chloride	(CoCl ₂ .6H ₂ O)	0.25 g
Disodium EDTA	(Na ₂ EDTA.2H ₂ O)	1.25 g
Manganese chloride	(MnCl ₂ .4H ₂ O)	0.1 g
Nickel sulfate	(NiSO ₄ .7H ₂ O)	0.05 g

Dissolve the above in the specified order in deionised water and dilute to a final volume of 5 L. Store in the dark at 4°C.

Solution 5: Phosphate buffer solution (x100 stock)

Disodium orthophosphate	(Na ₂ HPO ₄ .12H ₂ O)	71.6 g
Potassium orthophosphate	(KH ₂ PO ₄)	26 g

Dissolve the above in the specified order in 800 ml of deionised water. Adjust pH to 6.8 and dilute to 1 L.

NMS medium was prepared by diluting 100 ml of solution 1 to 1 L and then adding 1 ml of solution 3, 1 ml of solution 4 and 0.1 ml of solution 2. 10 ml of sterile solution 5 was then added to the cooled medium (<50°C) after autoclaving. When preparing solid medium, 1.5% (w/v) of bacteriological agar (Oxoid, Basingstoke, Hampshire, UK) was added prior to autoclaving.

2.4.2. *Escherichia coli*

E. coli was routinely cultured in Luria Broth (LB) (Sambrook & Russell, 2001). The cultures were grown in universal vials or flasks at 37°C with shaking at 200 rpm. Antibiotics were added to the medium at the concentrations indicated in Table 2.3 when appropriate. Solid media were prepared by the addition of 1.5% (w/v) bacteriological agar (Formedium Ltd.) prior to autoclaving.

2.5. Maintenance of bacterial strains

E. coli and *R. jostii* strain 8 were stored in LB medium + 20% (v/v) glycerol. The cultures were stored at -80°C until use.

2.6. Cell dry weight measurement

Dry weights of *R. jostii* strain 8 cells were estimated by constructing a standard curve of dry weights against optical density values at 540 nm. Dry weight measurements were carried out using a filtration method (Gerhardt, 1981). Cultures of different known optical densities were filtered under vacuum through pre-weighed, dried filters of pore size 0.2 µm. Filters and cells were then dried in an oven at 90°C to constant weight.

2.7. Light microscopy

Purity of cultures was routinely checked by microscopy and growth on R2A agar. A drop of bacterial culture was placed on a slide and was then retained with a coverslip. The culture was observed using a phase contrast microscope (Zeiss, Axio observer, UK) at a magnification of 1,000x.

2.8. General purpose buffers and solutions

Agarose gel loading buffer (6X)

Bromophenol blue	0.0025 g
EDTA	2.92 g
Glycerol	2.5 ml
Deionised water to	5 ml

The buffer was stored at room temperature.

TE buffer (pH8.0)

Tris-HCl	10 mM
Sodium EDTA	1 mM

Prepared from 1 M Tris-HCl (pH8.0) and 0.5 M sodium EDTA (pH8.0) which were adjusted to pH 8.0 with HCl

TBE electrophoresis buffer (10X)

Tris base	108 g
Boric acid	55 g
0.5 M Sodium EDTA solution (pH 8.0)	40 ml

Volume was adjusted to 1 L with deionised water.

2.9. Extraction of nucleic acids

2.9.1. Extraction of genomic DNA from *Rhodococcus jostii* strain 8

High-molecular mass genomic DNA was extracted from *R. jostii* strain 8 for subsequent sequencing by The Genome Analysis Center (TGAC), Norwich UK and for use during this project. Cells from a 50 ml culture, grown on NMS with 10% (v/v) propane in the headspace, were centrifuged at 8,500g for 15 min. The cell pellet was resuspended in a minimum volume of TE buffer pH 8.0. Extraction of genomic DNA from this cell suspension was carried out using a Fast DNA Spin kit for Soil (MPBio, Solon, OH, USA). The extraction procedure was conducted according to the manufacturer's instructions. Quality and quantity of DNA was assessed by running it on a 1% (w/v) agarose gel alongside a 1 kb ladder (Fermentas). It should be noted that the extraction of genomic DNA from *R. jostii* strain 8 by phenol-chloroform extraction did not yield sufficiently high quality DNA nor sufficient DNA for Illumina genome sequencing.

2.9.2. Small-scale extraction of plasmids from *E. coli*

Plasmids were routinely extracted from *E. coli* by using the GeneJET Plasmid Miniprep Kit (Fermentas). Plasmid extraction was carried out according to the manufacturer's instructions.

2.9.3. Extraction of RNA from *Rhodococcus jostii* strain 8

R. jostii strain 8 was grown in 50 ml NMS medium with 10 mM glucose or 10% (v/v) of ethane, propane or butane in the headspace. Total RNA was extracted from cultures grown to an OD₅₄₀ of 0.8-1.0 (mid-exponential phase) using the hot-phenol method as described previously (Gilbert *et al.*, 2000). All solutions, water and glassware which were used for RNA manipulations were treated with diethylpyrocarbonate (DEPC)-treated water by adding 0.1% (v/v) DEPC solution and incubated with shaking overnight at 37°C. All plasticware and tips were RNase-free.

2.10. Nucleic acid manipulation techniques

2.10.1. DNA/RNA quantification

DNA and RNA concentration and purity was estimated by using a Nanodrop 2000 (Thermo Fisher Scientific) Spectrophotometer or by agarose gel analysis and comparison with a known amount of 1 kb DNA ladder (Fermentas).

2.10.2. DNA purification

PCR products or DNA samples excised from gels were purified using NucleoSpin gel and PCR clean-up kits (Macherey Nagel, Düren, Germany) according to the manufacturer's instructions.

2.10.3. RNA purification

Removal of DNA from RNA was carried out using DNase I solution. DNase treatment was carried out using RNase-free DNase set (Qiagen) according to the manufacturer's instructions. Quality of RNA was assessed by running 5 µl of RNA on a 1% (w/v) agarose gel. The absence of DNA contamination in RNA was confirmed by performing PCR amplification of 16S rRNA genes on 3 µl of RNA

using 27f/1492r primers. RNA was judged to be DNA-free if no PCR product was obtained after 40 rounds of PCR amplification.

2.10.4. RNase treatment of genomic DNA

Removal of RNA from genomic DNA was carried out by adding 100 µg/ml of RNase solution. The DNA was incubated at 37°C for 30 minutes. RNase was then removed by extraction with an equal volume of chloroform: IAA (isoamyl alcohol). Quality of DNA after RNase treatment was assessed by running on a 1% (w/v) agarose gel.

2.10.5. DNA restriction digests

DNA restriction enzymes were supplied by Fermentas. Restriction digests were carried out according to the manufacturer's instructions.

2.11. Polymerase chain reaction (PCR)

PCR amplifications were performed in 50 µl total volume in 0.5 ml microcentrifuge tubes using a Tetrad thermocycler (Bio-Rad). The PCR mixtures contained 1.5 mM MgCl₂, 0.2 mM of each dNTP, 0.07% (w/v) BSA, 2.5 units of *Taq* DNA polymerase (DreamTaq) (Fermentas), 0.4 µM of forward and reverse primer (equivalent to 10 pmol per 50 µl reaction) and an appropriate amount of DNA template. For direct amplification of any gene from colonies, 5% (v/v) DMSO was included in the reactions. Amplification conditions were typically: initial denaturation at 95°C, 30 s; annealing step (temperature dependent on primers), 30 s; elongation at 72°C, 1min/kb; final elongation at 72°C, 7 min. For direct amplification of any gene from colonies, initial denaturation was extended to 10 min. Reactions without DNA templates were included in all cases as a negative control.

2.11.1. Design of PCR primers

Primers were designed using The Primer Designer (v. 5.04) in the Clone Manager Professional Suite (Scientific & Educational Software) or Primer 3 online software. All primers used in this study are listed in Table 2.4.

Table 2.4: Primers used in this study

Primers	Target gene and description	Sequences (5' to 3')	References
27f	16S rRNA	AGAGTTTGATCMTGGCTCAG	(Lane, 1991)
1492r	16S rRNA	TACGGYTACCTTGTTACGACTT	(Lane, 1991)
M13f	insert gene in pGEM-T and pK18 <i>mobsacB</i>	GTAAAACGACGGCCAG	Invitrogen
M13r	insert gene in pGEM-T and pK18 <i>mobsacB</i>	CAGGAAACAGCTATGAC	Invitrogen
NVC57	degenerate primer targeting gene encoding α -subunit of SDIMO	CAGTCNGAYGARKCSCGNCAAYAT	(Coleman et al., 2006)
NVC58	degenerate primer targeting gene encoding α -subunit of SDIMO	CGDATRTRCRTC DATNGTCCA	(Coleman et al., 2006)
NVC65	degenerate primer targeting gene encoding α -subunit of SDIMO	CCANCCNGGRTAYTTRTTYTCRAACCA	(Coleman et al., 2006)
NVC66	degenerate primer targeting gene encoding α -subunit of SDIMO	CARATGYTNGAYGARGTNCGNCA	(Coleman et al., 2006)
alkBf	primer for qPCR of gene encoding for hydroxylase subunit of alkane hydroxylase (alkB)	CACACGAGATGGGTCACAAGA	This study
alkBr	primer for qPCR of gene encoding for hydroxylase subunit of alkane hydroxylase (alkB)	GGTCTGCGCGAGAGTGATC	This study
rpoBf_RT	reference gene for qPCR targeting <i>rpoB</i>	ACATCATCAAGCTGCACCAC	This study
rpoBr_RT	reference gene for qPCR targeting <i>rpoB</i>	ACAAGTTGATGCCAGGTTT	This study
pmAf	ArmA of <i>prmA</i>	CATGGAATTCGCGTGTACGGCGCCATGGAC	This study
pmAr	ArmA of <i>prmA</i>	CATGGGATCCGACTGCACCGAGTGGAAGAC	This study
pmBf	ArmB of <i>prmA</i>	GATCGGATCCCATCGAGTACGGCACGAAGG	This study
pmBr	ArmB of <i>prmA</i>	GATCAAGCTTCGGCGTCCGGTCCAGTAGCAG	This study

Table 2.4: (continued) Primers used in this study

Primers	Target genes and Descriptions	Sequences (5' to 3')	References
prmAf	gene encoding α -subunit of propane monooxygenase in <i>R. jostii</i> strain 8, for the amplification of partial <i>prmA</i> from cDNA	TCAAACAGATCATGCGGTCCTA	This study
prmAr	gene encoding α -subunit of propane monooxygenase in <i>R. jostii</i> strain 8, for the amplification of partial <i>prmA</i> from cDNA	CGTACACGCGGTTGTCCTT	This study
AlkBf	gene encoding hydroxylase subunit of alkane hydroxylase in <i>R. jostii</i> strain 8, for the amplification of partial <i>prmA</i> from cDNA	CCGTAGTGCTCGAGGTAGTT	This study
AlkBr	gene encoding hydroxylase subunit of alkane hydroxylase in <i>R. jostii</i> strain 8, for the amplification of partial <i>prmA</i> from cDNA	GACCTTCTACGGCCACTTCT	This study
PrMOf	gene encoding α -subunit of propane monooxygenase in <i>R. jostii</i> strain 8	TCTCCAACGGCTACTCGATC	This study
PrMOr	gene encoding α -subunit of propane monooxygenase in <i>R. jostii</i> strain 8	GGTACTTGTGCTCGAACCAC	This study
Gmf	gentamicin resistant gene	TAAGACATTCATCGCGCTTG	This study
Gmr	gentamicin resistant gene	TCGTCACCGTAATCTGCTTG	This study
Kmf	kanamycin resistant gene	CTGTGCTCGACGTTGTCACT	This study
Kmr	kanamycin resistant gene	AGCCAACGCTATGTCCTGAT	This study
rpoBf	reference gene for amplification of any gene from cDNA, target gene is <i>rpoB</i>	CGGACCCGCGTTTCG	This study

Table 2.4: (continued) Primers used in this study

Primers	Target genes and Descriptions	Sequences (5' to 3')	References	
rpoBr	reference gene for amplification of any gene from cDNA, target gene is <i>rpoB</i>	GCCGCGTAGGTCATGTCTTT	This study	
206f	<i>mmoX</i> } gene encoding α -subunit of sMMO <i>mmoX</i> }	ATCGCBAARGAATAYGCSCG	(Hutchens et al., 2004)	
886r		ACCCANGGCTCGACYTTGAA	(Hutchens et al., 2004)	
out_AGBr	downstream region of 'ArmB' of <i>prmA</i>	CGTCGAGAGTCCACATCTTC	This study	
out_AGBf	upstream region of 'ArmA' of <i>prmA</i>	TGTCATGGGATCCGACATTC	This study	
alkXf	'ArmX' of <i>alkB</i>	} used for mutagenesis of <i>alkB</i>	This study	
alkXr	'ArmX' of <i>alkB</i>		TCGATCCGCCAGTAGTTCAC	This study
alkYf	'ArmY' of <i>alkB</i>		CACACGAGATGGGTCACAAG	This study
alkYr	'ArmY' of <i>alkB</i>		GCAGGTGGTACAGGAAGATG	This study
Out_XGYf	upstream region of 'ArmX' of <i>alkB</i>	AGCGCTACCTGTGGCTGATG	This study	
Out_XGYr	downstream region of 'ArmY' of <i>alkB</i>	GAACTCCGCCGCTGTACTTG	This study	
SDIMOgr3r	gene encoding α -subunit of group 3 SDIMO in <i>R. jostii</i> strain 8	GGATACTTGCCACGGAGTGT	This study	

2.12. Agarose gel electrophoresis

Agarose gels were prepared with 1x TBE electrophoresis buffer containing between 0.7%-2% (w/v) agarose and 0.5 µg/ml ethidium bromide. DNA samples were prepared by addition of DNA loading buffer (10x) at 1/5 volume per volume of DNA samples. Agarose gel electrophoresis was performed using a Power Pac Basic (Power Pak, Bio-Rad). Gels were visualized on a UV transilluminator (Molecular imager gel doc XR⁺) (BioRad), and photographs were taken using Image Lab software (Bio-Rad).

2.13. Dephosphorylation of DNA

DNA ends were dephosphorylated using shrimp alkaline phosphatase (SAP) (Fermentas). The dephosphorylation was carried out according to the manufacturer's instructions.

2.14. DNA ligations

The ligation of DNA was carried out in a total volume of 20 µl using T4 DNA ligase (Fermentas) according to the manufacturer's instructions. Typically, total amount of DNA used in each ligation reaction was 500 ng.

2.15. Cloning of PCR products

PCR products were cloned into the pGEM-T Easy vector (Promega, Madison, WI, USA) according to the manufacturer's instructions. Successful insertion of PCR products into the vector was confirmed by sequencing using M13f or M13r primers.

2.16. Clone library construction and restriction fragment length polymorphism (RFLP)

A clone library of genes encoding the α -subunit of SDIMO was constructed using PCR products from the amplification by using NVC57f and NVC66r primers (Coleman et al., 2006). PCR products were cloned as described in section 10.10. Inserts were directly amplified from colonies by PCR using M13f and M13r primers. PCR products were digested with *EcoRI* and *MspI*, and resolved by running on a 2%

(w/v) agarose gel. One or two representatives of each set of clones containing identical restriction patterns were selected for sequence analysis.

2.17. Sequencing of DNA

Purified DNA was submitted, with 5.5 pmol of the appropriate primer, for Sanger sequencing at the University of Warwick Genomics Facility or Source Bioscience Company (Cambridge, UK). DNA sequences from the University of Warwick were analysed using Chromas (Technelysium Pty Ltd, Brisbane, Australia). Sequences were aligned by Clustal W using MEGA 5 software (Tamura et al., 2011)

2.18. Reverse transcriptase PCR (RT-PCR)

Reverse transcription was performed, on RNA obtained from *R. jostii* strain 8 grown on different carbon sources, using Superscript II or Superscript III (Invitrogen) with random hexamer, according to the manufacturer's instructions. Between 500 ng and 1 µg RNA was used for the first strand cDNA synthesis with 200 ng random hexamer. Reactions in which water was used in place of reverse transcriptase were included as negative controls. Reverse transcription was carried out at 42°C or 55°C for Superscript II or Superscript III, respectively. 2 µl of cDNA was used as template in PCR reactions, together with cDNA synthesis reactions where reverse transcriptase was omitted. Reactions with DNA template were included as positive control, and also without template as a negative control.

2.19. Reverse transcriptase quantitative PCR (RT-qPCR)

Quantitative PCR amplification on cDNA was carried out using the StepOnePlus Real-Time PCR system (Applied Biosystems, Invitrogen, UK). cDNA synthesis was carried out as described in section 10.13. The reactions were set up in 96-well plates. The reactions were performed in a total volume of 20 µl containing 200 nmol of forward and reverse primers, 100 ng of cDNA templates and SYBR Green qPCR mastermix (Applied Biosystems, Invitrogen, UK) or Precision Fast 2x mastermix with SYBR Green (Primer Design, Southampton, UK). The reactions with DNA template and with water in place of cDNA template were included as a positive and negative control, respectively. Amplification conditions were typically: enzyme activation (hot start) at 95°C, 20 s, denaturation at 95°C, 1s, annealing at 60°C, 20 s. The data were analysed using StepOne software v 2.2.2.

2.20. Genome sequencing

Genomic DNA of *R. jostii* strain 8 was prepared as described in section 9.1. The DNA was submitted to The Genome Analysis Center (TGAC) (Norwich, UK) for Illumina sequencing using the MiSeq system. The MiSeq runs included 150 bp paired-end runs and 250 bp paired-end runs. The reads were trimmed based on quality and assembled using ABySS. SSPACE was used for scaffolding pre-assembled contigs using paired-read data. The whole procedure for generating assemblies was repeated for combining both 150 bp and 250 bp paired-end runs. Annotation procedures and comparison of the data were carried out by me at UEA. Annotation of the open reading frames was performed using RAST (Rapid Annotation using Subsystem Technology) and by comparison with data from COG, KEGG and Swiss-Prot databases.

2.21. Bacterial transformations

2.21.1. Preparation and transformation of chemically competent *E. coli*

Solutions which were used for preparation of chemically competent *E. coli* are listed below.

SOB medium:

Yeast extracts	5 g
Tryptone	20 g
NaCl	0.5 g
KCl solution (250 mM)	10 ml

The above components were dissolved in 900 ml deionized water, the pH was adjusted to 7.0 with 5 M NaOH and the solution made up to a volume of 1 L with water. The solution was sterilized by autoclaving. Sterile MgCl₂ (2 M stock solution) was added to 10 mM prior to use.

Transformation buffer:

MnCl ₂ .4H ₂ O	10.88 g
CaCl ₂ .2H ₂ O	2.2 g
KCl	18.65 g
Piperazine-N,N'-bis(2-ethanesulfonic acid) (PIPES) buffer (0.5 M, pH 6.7)	10 ml

The above components were dissolved in 800 ml deionized water and made up to 1 L with water. The solution was then sterilized by filtration through a 0.2 μm filter.

SOC medium:

Filter-sterilised glucose solution was added to SOB medium to a final concentration of 20 mM.

Chemically competent *E. coli* was prepared according to the method of (Inoue et al., 1990). *E. coli* was grown in 125 ml SOB medium in 500 ml flask to an OD_{600} of 0.55. A flask was cooled on ice, and centrifuged at 2,500g for 10 min at 4°C. The supernatant was removed, and cells were washed in 40 ml ice-cold Inoue buffer. Cells were resuspended in 10 ml ice-cold Inoue buffer and 750 μl of dimethylsulfoxide (DMSO) were gently added. The cell suspension was cooled on ice for 10 min and 50 μl aliquots were dispensed into microcentrifuge tubes. Tubes were frozen in liquid nitrogen and stored at -80°C.

For transformation, cells were thawed on ice and then approximately 1-50 ng of plasmid DNA was added and gently mixed with the cells. Cells were 'heat shocked' at 42°C for 50 s and cooled on ice for 2 min. SOC medium (1 ml) was added to allow recovery of cells at 37°C, with shaking at 200 rpm, for 1.5 hours. Cells were spread on selective LB plates containing X-Gal and IPTG (as appropriate). Plates were incubated at 37°C for 16-24 hours.

2.21.2. Preparation and transformation of electrocompetent *E. coli*

Electrocompetent *E. coli* cells were prepared from a 500 ml culture grown on LB medium to an OD_{540} of 0.5-0.6. The flask containing the culture was chilled on ice for 15 min prior to precipitation of cells by centrifugation at 4,000g for 15 min at 4°C. Supernatant was removed and the cell pellet was first washed with 500 ml cold sterile deionized water. The pellet was washed again with 250 ml of cold sterile deionized water and finally washed with 2.5 ml of cold 10% (v/v) glycerol after centrifugation as above. Electrocompetent cells were resuspended in cold 10% (v/v) glycerol and 100 μl aliquots were dispensed into microcentrifuge tubes. Tubes were immediately frozen in liquid nitrogen and stored at -80°C.

Electrocompetent *E. coli* were transformed by adding up to 2 μl of plasmid DNA or ligation mix each containing a 500 ng DNA. Cells were incubated on ice for

15 min and then transferred into a chilled 1 cm electroporation cuvette (Plus BTX, Harvard Apparatus, Holliston, MA, USA). Cells were transformed by electroporation using an electric field pulse applied using a GenePulser Electroporation system (Bio-Rad, Hemel Hempstead, UK) at the setting 1.8 kV, 25 μ F, 200 Ω . Cells were immediately transferred into 1 ml SOC medium for recovery with shaking at 200 rpm for 1 hour. Appropriate volumes of culture (50 – 100 μ l) were spread onto selective LB agar plates. Transformant colonies usually developed after overnight incubation at 37°C.

2.21.3. Preparation and transformation of electrocompetent

***Rhodococcus jostii* strain 8**

Electrocompetent *R. jostii* strain 8 was prepared from 50 ml culture grown on NMS medium + 10 mM glucose to OD₅₄₀ of 0.4-0.5 (early exponential phase). Flask was chilled on ice for 20 min and then centrifuged at 2,500g for 15 min at 4°C. Supernatant was removed and the cells were washed firstly in 25 ml cold sterile deionized water, then in 25 ml cold 10% (v/v) glycerol, with centrifugation as above. The cells were resuspended in 500 μ l of cold 10% (v/v) glycerol, dispensed in 100 μ l aliquots into microcentrifuge tubes and store on ice until use. No long term storage of the cells was carried out in case the cells lost their competency after the freeze-thaw process.

Electrocompetent *R. jostii* strain 8 was transformed by adding plasmid DNA up to 3 μ l containing 500 ng – 1 μ g of DNA. Cells were chilled on ice for 15 min before transferring them into a chilled 0.2 cm electroporation cuvette. An electric field pulse were applied to the cells by using a GenePulser Electroporation system set at 2.5 kV, 25 μ F, 800 Ω . Cells were immediately recovered in 1 ml NMS + 10 mM glucose medium on a rotary shaker at 30°C for 16 hours. Aliquots (50–100 μ l) were spread onto selective NMS + 10 mM glucose plates. Transformant colonies developed after 3 days of incubation at 30°C.

2.22. Harvesting of cells

R. jostii strain 8 cultures were harvested by centrifugation at 8,500g for 15 min. Supernatant was removed and cell pellets were washed with appropriate buffer or growth medium without substrate. Cells were either used immediately or, in most cases, drop frozen in liquid nitrogen and stored at -80°C.

2.23. Bacterial purity checks

Purity of bacterial cultures was examined by streaking out on R2A plates and observation of subsequent growth and also by examination under a phase contrast microscope at x1,000 magnification.

2.24. Calculation of specific growth rates

Cultures of *R. jostii* strain 8 were grown in 20 ml NMS in 120 ml serum vials. The cultures were grown in triplicate for each growth substrate. Culture density was determined every 12 hours by measuring optical density at 540 nm. The natural logarithm of culture density was plotted against time. Growth rates were determined from a minimum of three data points obtained during exponential phase using Microsoft Excel.

2.25. Preparation of cell-free extracts

R. jostii strain 8 was grown on 500 ml NMS medium with 10 mM glucose or 10% (v/v) ethane or propane or butane in the headspace. The cultures were grown to an OD₅₄₀ of 0.8-1.0 or during late-exponential phase. Cells were pelleted by centrifugation at 8,500g for 15 min at 4°C. Cell pellets were washed twice with 500 ml of 25 mM MOPS (3-(N-morpholino) propanesulfonic acid) solution pH 7.2. Cells were resuspended in a minimal volume (usually 2-4 ml) of MOPS solution and immediately drop frozen in liquid nitrogen.

Cells were mixed with freshly prepared benzamidine solution (working concentration of 1 mM) as a protease inhibitor. Cells were then disrupted by passaging three times into a French pressure cell (Aminco, Silver Spring, Maryland, USA) at a pressure of 20,000 psi or 138 MPa. The disrupted cells were cooled to 4°C. Cell extracts were collected by centrifugation at 8,500g for 15 min at 4°C. Cell debris was discarded and supernatant (crude extract) was stored at -80°C.

2.26. Protein quantification

Protein concentration of cell extracts was determined using the Bio-Rad Protein Assay (Bio-Rad Laboratories Inc., Hercules, CA, USA) according to the manufacturer's instructions. Protein concentrations were analysed against standards prepared with bovine serum albumin (BSA).

2.27. Sodium Dodecyl Sulfate-Polyacrylamide Gel Electrophoresis (SDS-PAGE)

SDS-PAGE was carried out using an X-cell II Mini-Cell apparatus (Novex) in order to separate polypeptides in cell-free extracts. A stacking gel (4% (w/v)) and a resolving gel (12.5% (w/v)) were used and prepared as follows, using premixed 40% (w/v) acrylamide/bis (37:5:1) (Amresco, Solon, OH, USA).

Stacking gel:

Water	3.17 ml
Acrylamide/bis	0.5 ml
0.5M Tris-HCl, pH 6.8	1.25 ml
10% (w/v) SDS	50 μ l
10% (w/v) Ammonium persulfate	25 μ l
TEMED (<i>N,N,N',N'</i> -tetramethylethane-1,2-diamine)	5 μ l

Resolving gel:

Water	5.41 ml
Acrylamide/bis	3.125 ml
3M Tris-HCl pH 8.8	1.25 ml
10% (w/v) SDS	100 μ l
10% (w/v) Ammonium persulfate	75 μ l
TEMED (<i>N,N,N',N'</i> -tetramethylethane-1,2-diamine)	5 μ l

SDS-PAGE sample buffer:

Tris-HCl pH 6.8	63 mM
Glycerol	10% (v/v)
β -mercaptoethanol	5% (v/v)
SDS	2% (w/v)
Bromophenol blue	0.00125% (w/v)

Running buffer:

Glycine	72 g/L
Tris base	15 g/L
SDS	5 g/L

SDS-PAGE was performed with cell-free extracts prepared using the French Press method. Cell extracts were mixed with $\frac{1}{4}$ volume of 5x sample buffer. The mixtures were heated for 8 minutes in a boiling water bath and cooled on ice. Approximately 15 μ g protein was loaded per lane. Electrophoresis was carried out at 90V through the stacking gel and 120V during separation through the resolving gel, using Tris-glycine running buffer. PageRuler Plus prestained protein ladder (Fermentas) was used as molecular mass marker. Gels were stained with Coomassie brilliant blue staining solution (0.1% w/v). Staining solution was prepared by dissolving Coomassie Brilliant Blue destained solution (40% (v/v) methanol and 10% (v/v) acetic acid) in water.

2.28. Mass spectrometry analysis of polypeptides

Protein identification from Coomassie stained gels was conducted by means of tryptic digest and nanoLC-ESI-MS/MS. Gel pieces were tryptically digested, using the manufacturer's recommended protocol, on the MassPrep robotic protein

handling system (Waters). The extracted peptides from the samples were then analysed by means of nanoLC-ESI-MS/MS using the NanoAcquity/Synapt G2 HDMS instrumentation (Waters) using a 30 minute LC gradient. The data were analysed against the entire amino acid sequences from the *R. jostii* strain 8 genome using ProteinLynx Global Server v 2.5.1. This was done by Dr. Susan E. Slade at the University of Warwick, UK.

2.29. Oxygen electrode experiments

2.29.1. Preparation of cell suspension

Cell suspensions of *R. jostii* strain 8 were prepared from 500 ml cultures grown on NMS + 10% (v/v) ethane, propane or butane or NMS + 10 mM glucose in 2L flasks. The cultures were grown to mid-exponential phase at an OD₅₄₀ of 0.6-0.8. Cells were harvested by centrifugation at 8,500g for 15 min at 4°C. Cell pellets were washed twice with 500 ml of 0.1 mM phosphate buffer (pH 7.0). Supernatant was removed and the pellets were resuspended in a minimal volume of 0.1 mM phosphate buffer (pH 7.0). Cell suspensions were immediately frozen in liquid nitrogen and stored at -80°C.

2.29.2. Measurement of oxygen uptake by cell suspensions in the presence of substrates

The ability of *R. jostii* strain 8 to oxidise a variety of carbon compounds was investigated by measuring oxygen consumption when adding the substrate to cell suspension placed in a Clark-type oxygen electrode (Rank Brothers, Bottisham, Cambridge, UK). Assays were conducted in 3 ml of 0.1 mM phosphate buffer (pH 7.0). The temperature of the assays was maintained at 30°C using a circulating water bath (Churchill Co. Ltd, Perivale, UK). Air-saturated buffer was added to the oxygen electrode chamber, the plunger was then inserted to allow the system to equilibrate. Then, an appropriate volume of cells, equivalent to 5 mg dry weight, was added into the chamber. Endogenous rates of oxygen uptake were measured. Substrates were then added to a final concentration of 200 µM or, for some substrates, 200 µl of gaseous alkane/alkene-saturated water was added. Stimulation of oxygen uptake was

recorded. Oxygen consumption rates were estimated by subtraction of endogenous rates prior to calculation of oxygen-stimulated substrate oxidation rates in terms of nmol of oxygen $\text{min}^{-1}\text{mg cell dry weight}^{-1}$.

The dissolved oxygen concentration of air-saturated buffer was calculated using the method described by Robinson and Cooper, 1970. Gaseous alkane- or alkene-saturated water was prepared by passing the gas contained within an inflated football bladder through 10 ml of distilled water in a 120 ml serum vial in a fume hood. The final concentrations of gaseous alkanes and alkenes used in experiments were calculated according to Henry's Law constants obtained from Sander, 1999. Henry's constant for gaseous alkanes and alkenes are shown in Table 5 (Sander, 1999).

Table 2.5: Henry's constants used for calculation gas solubility in water

Henry's constant at 25°C	
Substance	$kH/(\text{M/atm})$
methane	1.5×10^{-3}
ethane	2.0×10^{-3}
propane	1.4×10^{-3}
butane	1.1×10^{-3}
hexane	7.7×10^{-4}
heptane	3.7×10^{-4}
octane	2.0×10^{-4}
ethene	4.8×10^{-3}
propene	4.8×10^{-3}
<i>cis</i> -2-butene	4.0×10^{-3}
<i>trans</i> -2-butene	4.0×10^{-3}

2.30. Enzyme assays

2.30.1. PQQ-dependent alcohol dehydrogenase

PQQ-dependent alcohol dehydrogenase activity was measured spectrophotometrically by following the change in absorbance at 600 nm due to the reduction of DCPIP (dichlorophenol indophenol) by reduced PMS (phenazine methosulfate). Assays were carried out in 1 ml solution in a cuvette containing 20 mM Tris-NaOH, pH 9.0, 0.11 μmol of PMS, 0.13 μmol DCPIP, 45 μmol NH_4Cl and an appropriate amount of cell extracts. The reactions were started by the addition of NH_4Cl . Changes in absorbance were monitored using a Shimadzu UV-1800 spectrophotometer and the rates were calculated by using a molar absorption coefficient for DCPIP at 600 nm of $1.91 \times 10^4 \text{ M}^{-1}\text{cm}^{-1}$ (Day & Anthony, 1990).

2.30.2. NAD(P)⁺-dependent alcohol dehydrogenase

NAD(P)⁺-dependent alcohol/aldehyde dehydrogenase activity was measured spectrophotometrically by following the change in absorbance at 340 nm. Assays were carried out in 1 ml solution in a cuvette containing 20 mM Tris-NaOH, pH 10.0, 0.2 μmol of NAD^+ and an appropriate amount of cell extract. The reactions were started by the addition of substrates (alcohols/aldehydes) to a final concentration of 10 mM. Changes in absorbance were monitored for 4 minutes, and the rates were calculated by using a molar absorption coefficient at 340 nm for NAD(P)H of $6.22 \times 10^3 \text{ M}^{-1}\text{cm}^{-1}$.

2.30.3. NDMA-dependent alcohol dehydrogenase

4-nitroso-N,N-dimethylaniline (NDMA)-dependent alcohol dehydrogenase activity was assayed by measuring the rate of decrease in absorbance at 440 nm of NDMA as described in Schenkel & Duine (2002). The reactions contained NDMA (28 μM final concentration), 10 mM potassium phosphate buffer pH7.0, 1 mM substrates and water made up to 1 ml. The reactions were started by the addition of cell extract (25 $\mu\text{g}/\text{ml}$ final concentration). Changes in absorbance were followed for 3 min and the rates were calculated by using a molar absorption coefficient for NDMA at 440 nm of $3.54 \times 10^3 \text{ M}^{-1}\text{cm}^{-1}$.

2.30.4. sMMO activity using the naphthalene assay

Naphthalene oxidizing activity was assayed colorimetrically as described by (Graham et al., 1992). Approximately 1 ml of active cells grown to exponential phase ($OD_{540} = 0.5$) was incubated at 30°C for 30 min with a few crystals of naphthalene. A few drops of freshly prepared tetrazotized-*o*-dianisidine (5 mg/ml) were added. Cells with naphthalene oxidizing activity will immediately formed a pink or purple color. In case of the naphthalene assay using colonies on agar plates, a few crystals of naphthalene were placed inside the lid of the agar plate. Plates were incubated at 30°C for 30 min. A few drops of freshly prepared tetrazotized-*o*-dianisidine (5 mg/ml) were added directly onto colonies. Immediate development of a pink or purple color was the result of naphthalene oxidizing activity.

Chapter 3

Growth and oxidation studies

3.2. Introduction

Prior to the commencement of this project, Kristin Schultz, a research exchange student from the University of Bayreuth, Germany, carried out the isolation and characterisation of alkane/alkene-degrading bacteria from petroleum contaminated soils in Kenilworth, UK. Historically, soils had been exposed to trace amount of petroleum leakage from the industrial site nearby for more than a decade. In her research project, soil samples were incubated with NMS medium and enriched with the short-chain alkanes and alkenes -- methane, ethane, propane, butane, ethene, propene and butene. The reduction of alkanes/alkenes concentration in enrichment cultures was investigated using gas chromatography (GC). After 1 month of incubation, alkane/alkene degraders were screened from enrichment cultures by serial dilutions and plating on NMS agar medium with the corresponding alkane/alkene. Single colonies were transferred into liquid NMS medium and incubated with alkane or alkene which was the carbon source for the isolates when they were enrichment cultures. The consumption of corresponding gaseous alkane/alkene was confirmed by following a decrease in alkane/alkene concentration using GC. The culture purity was routinely tested by streaking on R2A plates and by microscopic observation. The isolates were stored at -80°C. DNA was also extracted from the isolates for further identification and characterization using molecular biological approaches. The PCR amplification of 16S rRNA genes and genes encoding the α -subunit hydroxylase of the SDIMO (Coleman et al., 2006) from DNA of isolates, followed by DNA sequencing, was carried out for strain identification and characterisation. Results (done by Kristin) showed that some of the isolates affiliated to the same genus, some took longer than 2 weeks to grow on alkanes and/or alkenes and some possessed similar SDIMOs and/or carbon substrate degradation profiles. Therefore, I only selected 6 distinct isolates for initial study in my project. The list of isolates and their SDIMO group affiliations is shown in Table 3.1. These isolates were tested for growth on various alkanes and alkenes by growing them in 20 ml of NMS in 120 ml serum vials with 10% (v/v) of gaseous alkanes or alkenes in the headspace. The tests were carried out in triplicate for each substrate. The cultures were incubated at 30°C with shaking at 150 rpm for 2 weeks. Growth profiles of the selected isolates are shown in Table 3.2.

Isolate no.	16S rRNA gene affiliation	% identity
4	<i>Rhodococcus erythropolis</i> strain MJ2	98
8	<i>Rhodococcus jostii</i> strain RHA1	99
13	<i>Rhodococcus wratislaviensis</i> strain FPA1	99
15	<i>Mycobacterium isoniacini</i>	98
16	<i>Mycobacterium</i> sp.	97
21	<i>Methylocystis</i> sp.	95

Table 3.1: List of 6 selected isolates with genus identification based on 16S rRNA gene sequences (754 nucleotides within the region covered by 27f/1492r PCR primers)

Isolate number	16S rRNA gene affiliation	Growth substrates							
		Methane	Ethane	Propane	Butane	Ethene	Propene	<i>trans</i> -2-butene	<i>cis</i> -2-butene
4	<i>Rhodococcus erythropolis</i> MJ2	No	Yes	Yes	No	No	No	No	No
8	<i>Rhodococcus jostii</i> RHA1	No	Yes	Yes	Yes	No	No	No	No
13	<i>Rhodococcus wratislaviensis</i> FPA1	No	Yes	Yes	Yes	No	No	No	No
15	<i>Mycobacterium isoniacini</i>	No	No	No	No	No	No	No	No
16	<i>Mycobacterium</i> sp.	No	No	No	No	No	Yes	No	No
21	<i>Methylocystis</i> sp.	Yes	No	No	No	No	No	No	No

Table 3.2: Growth tests of the selected isolates on alkanes and alkenes

At the beginning of this project, revival, repurification and reconfirmation of the 16S rRNA gene identification of the 6 selected isolates was carried out. The initial objective of this work was to carry out gene mining for potentially novel SDIMOs from these isolates. The purity of the isolates was re-affirmed several times by serial dilutions, two-subcultures by streaking on R2A plates and by observing under the microscope with assistance from experts in the lab. The phylogenetic relationship between 16S rRNA sequences from the 6 selected isolates is shown in Figure 3.1.

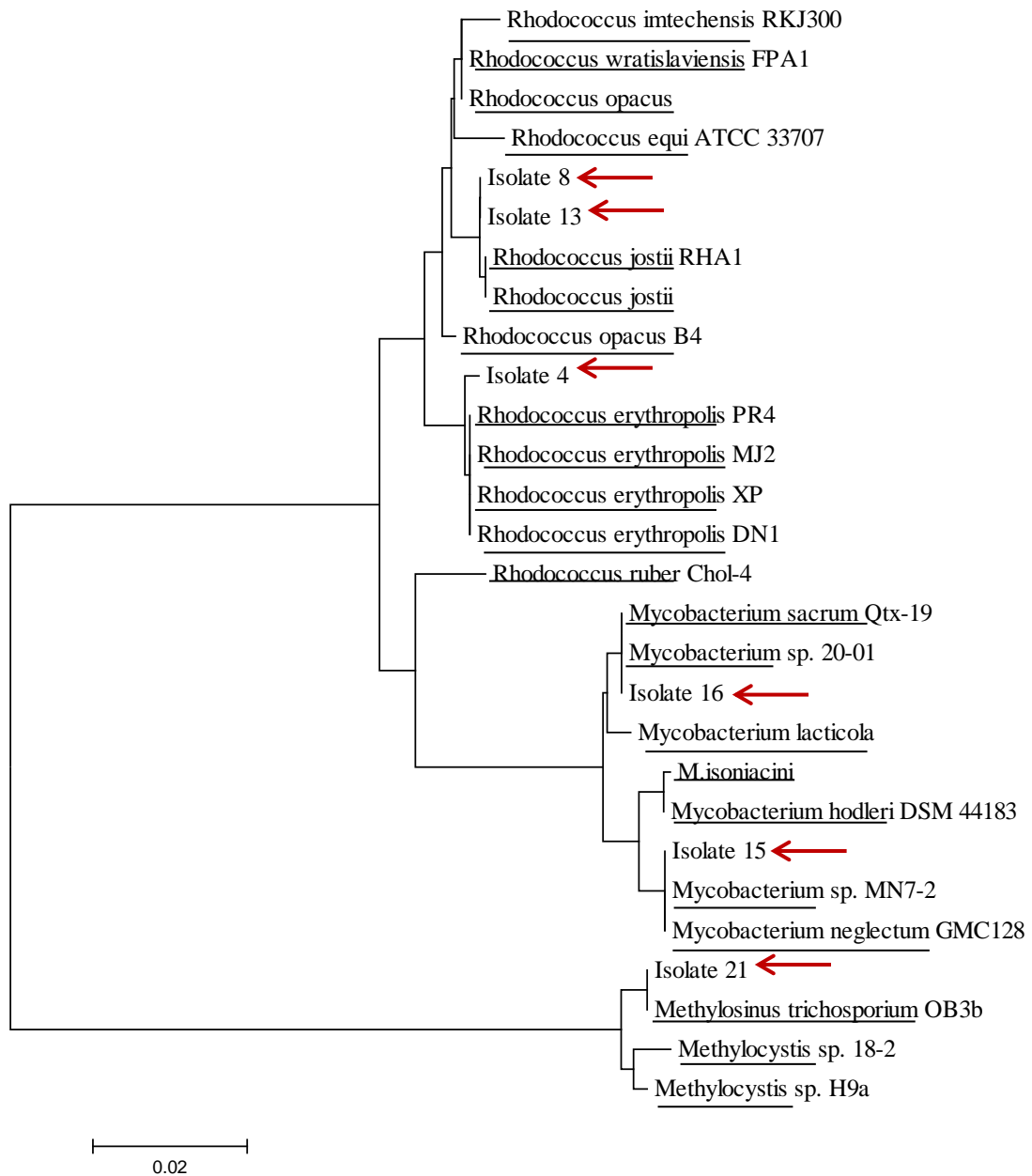


Figure 3.1: Phylogenetic tree showing relationship between 6 selected isolates and their relatives. The tree, constructed using the Neighbour-joining method, is based on 1200-1300 nucleotide sequences. The sequences were aligned using ClustalW. The tree was constructed using MEGA5 software (Tamura et al., 2011). Accession numbers: *Rhodococcus imtechensis* RKJ300, NR042946.1; *Rhodococcus wratislaviensis* FPA1, FM999002.1; *Rhodococcus opacus*, AF095715; *Rhodococcus equi* ATCC33707, X80594.1; *Rhodococcus jostii* RHA1, NR074610.1; *Rhodococcus jostii*, AB458522.1; *Rhodococcus opacus* B4, AB192962.1; *Rhodococcus erythropolis* PR4, NR074622.1; *Rhodococcus erythropolis* MJ2, GU991529.1; *Rhodococcus erythropolis* XP, DQ074453.1; *Rhodococcus erythropolis* DN1, NZ_AUZK01000073.1; *Rhodococcus ruber* Chol-4, EU878550.1; *Mycobacterium sacrum* Qtx-19, GU201853.1; *Mycobacterium* sp. 20-01, EU167966.1; *Mycobacterium lacticola*, AF480582.1; *Mycobacterium isoniacini*, X80768.1; *Mycobacterium hodleri*, NR026286.1; *Mycobacterium* sp. MN7-2, JQ396585.1; *Mycobacterium neglectum* GMC128, AB741467.1; *Methylosinus trichosporium* OB3b, NR044947.1; *Methylocystis* sp. 18-2, AB007841.1; *Methylocystis* sp. H9a, AJ458490.1.

Isolate numbers 8 and 13 appeared to be exactly the same strain, where their 16S rRNA gene sequence is 99% identical to the sequence of *Rhodococcus jostii* RHA1 (McLeod et al., 2006), in which biphenyl and ethylbenzene degradation pathways are well-characterised. Isolate number 15, after several attempts, failed to grow on any alkanes or alkenes. This might be due to poor storage or the loss of culturability before and/or after storage. According to the growth profile of the selected isolates (shown in Table 3.2), propene is the only hydrocarbon which isolate 16 could grow on, hence isolate 16 was not an appropriate strain to further the study in terms of application for biocatalysis and bioremediation due to its narrow range in substrate specificity. Regarding isolate 21, the colony morphology, gene encoding α -subunit hydroxylase of SDIMO sequence and 16S rRNA sequence of this isolate indicated that it is 100% identical to *Methylosinus trichosporium* OB3b, whose physiology and the ability to grow and oxidise alkanes, alkenes and aromatic compounds has been thoroughly studied (Strom et al., 1974; Green and Dalton, 1989; Sullivan et al., 1998; Rodrigues and Salgado, 2009). Unfortunately, even though several attempts were made to purify isolate number 4, it was still contaminated with a long-rod-shaped organism. The sequencing results of 16S rRNA gene of isolate number 4 came out as a messy sequence even with repeated sequencing. This is probably because the culture was a mixed culture. Hence, to progress the work and avoid time consuming processes on the re-purification of all strains, isolate number 8, which is closely related to *Rhodococcus jostii* RHA1 (99% identity at the 16S rRNA level), was the only organism considered for further study in this project. The aim was therefore to investigate whether isolate number 8 (now known as *R. jostii* strain 8 or strain 8 throughout this thesis) utilized one versatile alkane-degrading enzyme system or if it had more than one enzyme system which allowed it to grow on different alkanes.

This chapter describes the growth profile of *R. jostii* strain 8 compared to the growth profile of *R. jostii* RHA1, whose genome sequence is available (McLeod et al., 2006). The aim was to distinguish *R. jostii* strain 8 from *R. jostii* RHA1, and once it was confirmed that it was different, to characterize strain 8 at the physiological and genomic levels. Also, the investigation of a range of carbon compounds which *R. jostii* strain 8 could utilize and/or oxidise was conducted using growth tests and oxygen electrode experiments. The enzyme(s) responsible for the

growth of strain 8 on alkanes was then examined by the analysis of polypeptide profiles of cells grown on different alkanes using SDS-PAGE. The expression of alkane oxidation genes was also investigated, and in particular transcription of *prmA* and *alkB*, using reverse transcriptase-quantitative PCR (RT-qPCR).

3.2.1. General characteristics of *Rhodococcus jostii* strain 8

At the start of this project, *R. jostii* strain 8 was grown on 20 ml NMS in 120 ml serum vials with 10% (v/v) propane in the headspace or grown on NMS agar plates incubated with propane in a gas-tight jar. The liquid cultures were incubated at 30°C with shaking at 150 rpm. Liquid cultures became turbid after 3 days of incubation and colonies started to develop on plates after 5 days of incubation. Purity of cultures was examined by microscopy and checking on R2A agar for colony morphology, uniform colony size, colour, etc. Cell morphology of strain 8 under the light microscope is shown in Figure 3.2.

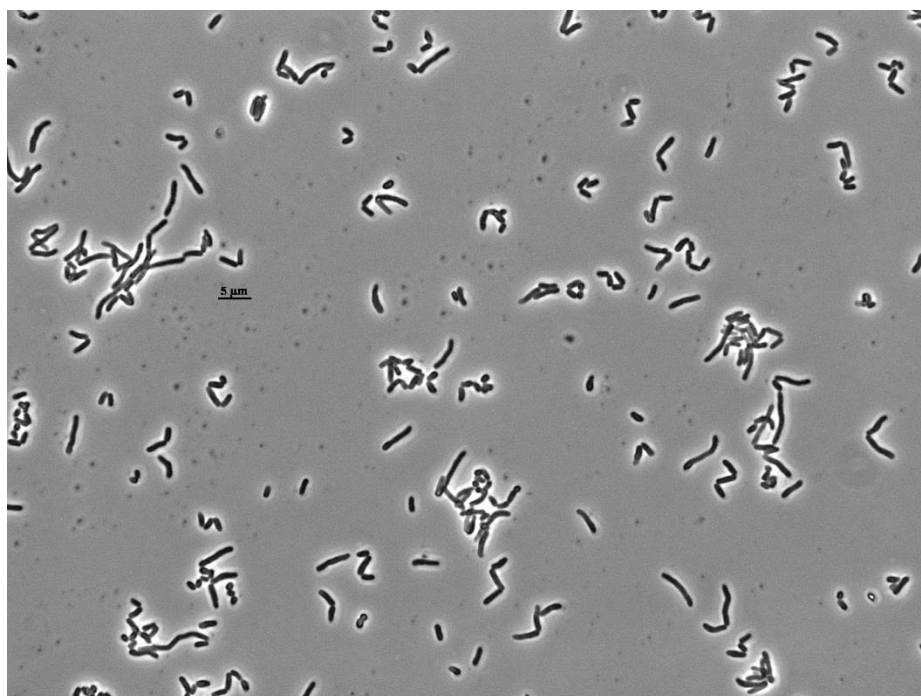


Figure 3.2: cell morphology of *R. jostii* strain 8 grown on NMS medium with 10% (v/v) propane in the headspace. The culture was observed under the microscope at x1,000 magnification. A scale bar of 5 μm is indicated in the picture.

Rhodococcus jostii strain 8 is a Gram-positive, non-motile, short-rod shaped bacterium. Cell morphology of this organism varied *i.e.* coccoid, short-rod and long-rod (approximately 5 μm in length), depending on its stage of growth. The cells are chains of short rods at early stage of growth and form cocci and short –rods during exponential and stationary phase. A colony of strain 8 grown on NMS agar incubated with propane had a light pink colour. The colony is in a circular form with a smooth edge and a slightly raised surface. Cells grow optimally at 30°C, but do not grow at 37°C.

The morphological properties of *R. jostii* strain 8 were considered characteristic of other *R. jostii* strains. There were a few *R. jostii* strains whose cell morphology has been reported. One example is *R. jostii* sp. nov. which was isolated from a medieval human grave (Takeuchi et al., 2002). The cells formed filaments which then fragmented into irregular rods and coccoids. Cocci and short rods were formed in early growth phase and exponential phase, respectively. This morphology in relation to growth phase is similar to what was found in *R. jostii* strain 8. The other well-characterised *R. jostii* strain is *R. jostii* RHA1, isolated from biphenyl enrichment of lindane contaminated soil (Seto et al., 1995). The study of Seto et al. (1995) showed that *R. jostii* RHA1 also formed both rods and cocci depending on its stage of growth.

3.2.2. Cloning of SDIMO α -subunit genes of *R. jostii* strain 8

PCR amplification of SDIMO α -subunit genes from genomic DNA of *R. jostii* strain 8 was carried out using the NVC primer set (Coleman et al., 2006). A diagram illustrating target regions in the SDIMO α -subunit gene for the NVC primer set is shown in Figure 3.3.

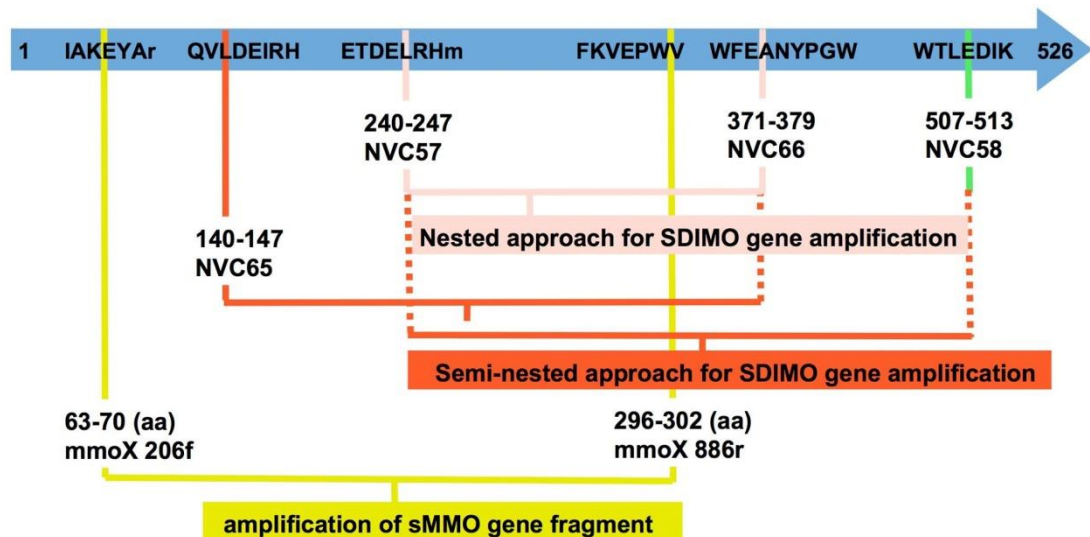


Figure 3.3: Diagram demonstrating NVC and *mmoX* primer sites within the SDIMO α -subunit gene. Amino acid sequences of the soluble methane monooxygenase in *Methylosinus trichosporium* OB3b are indicated at the primer sites. The names of the primers and positions of amino acids at primer binding sites are shown.

The first round of PCR amplification was conducted using the NVC65f/NVC58r primers. Then, two semi-nested PCR amplifications were carried out using NVC65f/NVC66r and NVC57f/NVC58r primers, which resulted in two overlapping fragments of SDIMO α -subunit genes. Each of the fragments was individually ligated into the pGEM-T Easy vector and then transformed into *E. coli* Top10 cells. Clones containing SDIMO α -subunit genes were selected based on blue/white selection. The gene fragments were then amplified directly from 20 colonies from each transformation by PCR using M13f/M13r primers, followed by RFLP analysis using *EcoRI* and *MspI* restriction enzymes. RFLP profiles were analysed on a 2% (w/v) agarose gel. pGEM-T plasmids were extracted (MiniPrep) from a representative clone from each different RFLP profile and SDIMO α -subunit genes were then sequenced using M13f/r primers.

The translated SDIMO α -subunit sequences of strain 8 were aligned to the corresponding sequences from other organisms obtained from the NCBI database. The alignment was used to construct a phylogenetic tree by using MEGA5 software.

A phylogenetic tree of amino acid sequences of SDIMO α -subunit from strain 8 aligned with sequences from other organisms is shown in Figure 3.4.

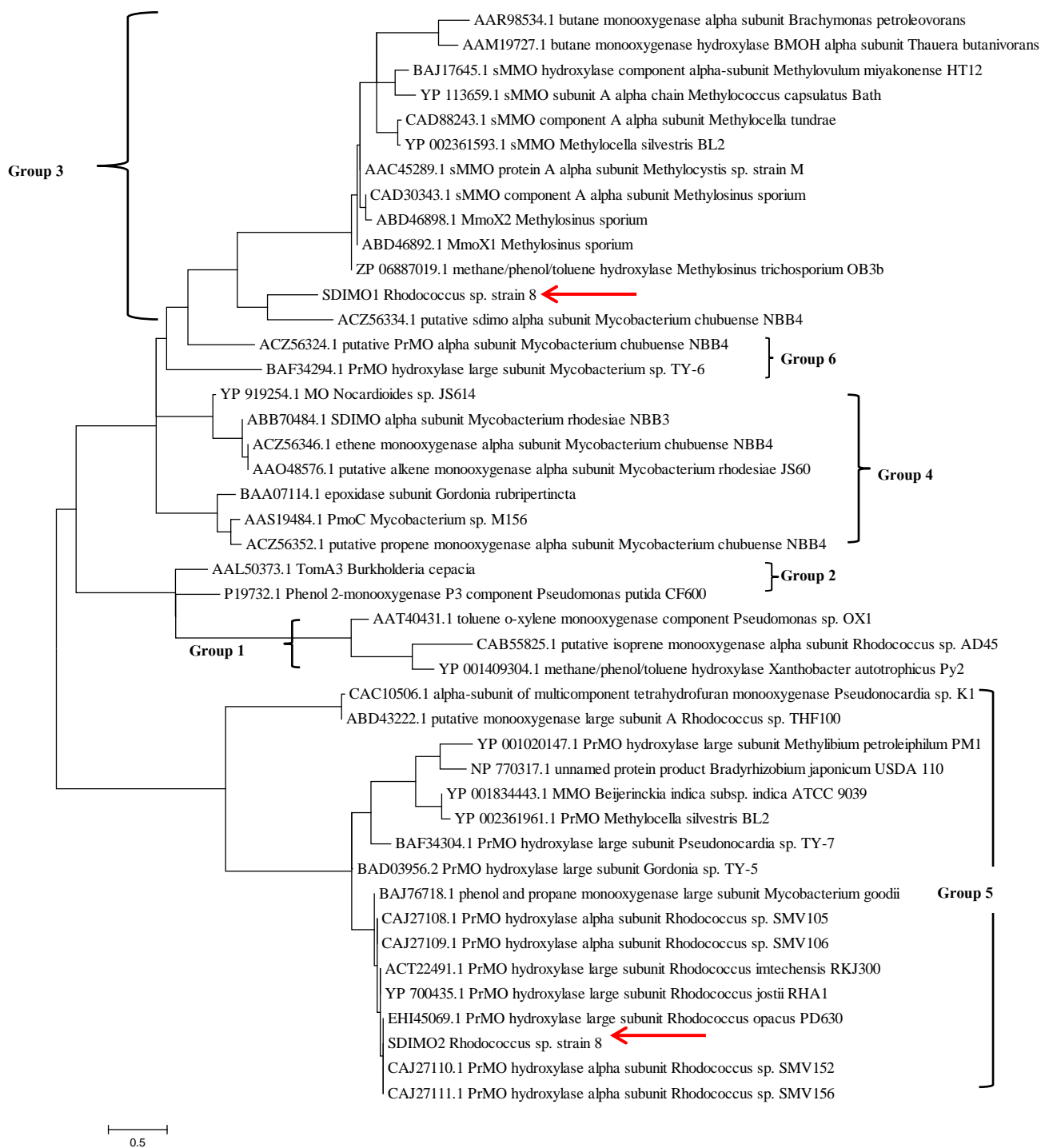


Figure 3.4: Phylogenetic relationship between amino acid sequences of the putative SDIMO α -subunit from strain 8 and those from other organisms. The tree was constructed using Maximum Likelihood method based on amino acid alignment using ClustalW. The tree was constructed from sequences containing at least 250 amino acids using MEGA5 software (Tamura et al., 2011).

According to the SDIMO cloning and sequence analysis, there are two different types of α -subunits from SDIMOs in *R. jostii* strain 8. One of them (indicated as SDIMO1 in the phylogenetic tree) clusters in Group 3 of the SDIMOs and is 80% (192/240 amino acids) identical to the α -subunit SDIMO of *Mycobacterium chubuense* NBB4 (Coleman et al., 2011). Another SDIMO (indicated as SDIMO2 in Figure 3.4) clusters in Group 5 of the SDIMOs and is 98% (241/246 amino acids) identical to propane monooxygenase found in the genome of *Rhodococcus jostii* RHA1 (McLeod et al., 2006).

After the genome of *R. jostii* strain 8 became available, it was found that the sequence of SDIMO1 was not present in the genome. Primers which specifically target SDIMO1 sequence were designed to amplify the SDIMO1 gene in order to investigate whether the gene was lost due to incomplete genome sequence or the absence of the gene. It was found that there was no PCR product. This is probably because there was a loss of this gene operon which might be a plasmid-encoded during multiple subcultures. Although the genome sequence revealed that *R. jostii* strain 8 contain one SDIMO, the other potential alkane-degrading enzyme, an *alkB*-type alkane monooxygenase was also found. Therefore, it is still worth further studies on the roles of the two potential alkane-degrading enzymes in *R. jostii* strain 8.

3.3. Growth profiles of *R. jostii* strain 8 and *R. jostii* RHA1

Due to the close relationship of the 16S rRNA gene of *Rhodococcus jostii* strain 8 to *Rhodococcus jostii* RHA1, both Rhodococci were tested for growth on various substrates in order to distinguish their ability to degrade a wide variety of potential growth substrates. The growth profile of *R. jostii* strain 8 compared to that of *R. jostii* RHA1 is shown in Table 3.3.

Substrates	Concentrations	Growth	
		<i>R.jostii</i> strain 8	<i>R.jostii</i> RHA1
acetate	5 mM	Yes	Yes
succinate	5mM	Yes	Yes
acetone	0.1%	Yes	Yes
1-propanol	0.1%	Yes	Yes
2-propanol	0.1%	Yes	Yes
heptane	0.1%	No	No
hexane	0.1%	No	No
glycerol	0.1%	Yes	Yes
octane	0.1%	<u>Yes</u>	<u>No</u>
ethanol	0.1%	Yes	Yes
glutamate	5 mM	Yes	Yes
glucose	5 mM	Yes	Yes
1-butanol	0.1%	Yes	Yes
methanol	0.1%	No	No
propanal	0.1%	Yes	Yes
propionate	5 mM	Yes	Yes
glycine	5mM	Yes	Yes
methane	10%	No	No
ethane	10%	<u>Yes</u>	<u>No</u>
propane	10%	Yes	Yes
butane	10%	Yes	No
ethene	10%	No	No
propene	10%	No	No
<i>trans</i> -2-butene	10%	No	No
isoprene	10%	No	No
naphthalene*	few crystals	<u>Yes</u>	<u>No</u>
ethylbenzene	0.1%	<u>No</u>	<u>Yes</u>
biphenyl*	few crystals	<u>No</u>	<u>Yes</u>

NB: The concentrations of naphthalene and biphenyl used in the test were not determined because these substrates are mostly insoluble.

Table 3.3: Comparison of growth profiles of *R. jostii* strain 8 and *R. jostii* RHA1

Both *R. jostii* strain 8 and *R. jostii* RHA1 could grow well on alcohols such as ethanol and butanol and the potential intermediates of propane metabolism such as 1-propanol, 2-propanol and propionate. Interestingly, *R. jostii* strain 8 could also grow well on ethane and butane whereas propane was the only alkane which *R. jostii*

RHA1 could grow on. Also, *R. jostii* strain 8 was able to grow on naphthalene and octane, but *R. jostii* RHA1 could not. Conversely, *R. jostii* RHA1 could grow on biphenyl and ethylbenzene, but strain 8 could not. These results indicated that *R. jostii* strain 8 is different from *R. jostii* RHA1. This fact was also confirmed when the genome of *R. jostii* strain 8 and *R. jostii* RHA1 were compared (see Chapter 4).

3.4. Growth curves of *R. jostii* strain 8 grown on glucose, ethane, propane and butane

R. jostii strain 8 can grow on the gaseous alkanes -- ethane, propane and butane. In order to determine growth rates for *R. jostii* strain 8 grown on gaseous alkanes, strain 8 was grown on NMS medium in 120 ml serum vials with 10% (v/v) of ethane, propane or butane or 10 mM glucose. Cultures were started using 10% (v/v) inoculum. Serum vials were closed with crimp-top rubber stoppers. The cultures were incubated at 30°C with shaking at 150 rpm for 5 days or until the culture reached stationary phase. 1 ml of the cultures was sampled daily using a syringe and needle in order to follow optical density at 540 nm using a spectrophotometer. The cultures were grown in triplicate for each substrate. Growth curves of *R. jostii* strain 8 grown on glucose, ethane, propane and butane are shown in Figure 3.5.

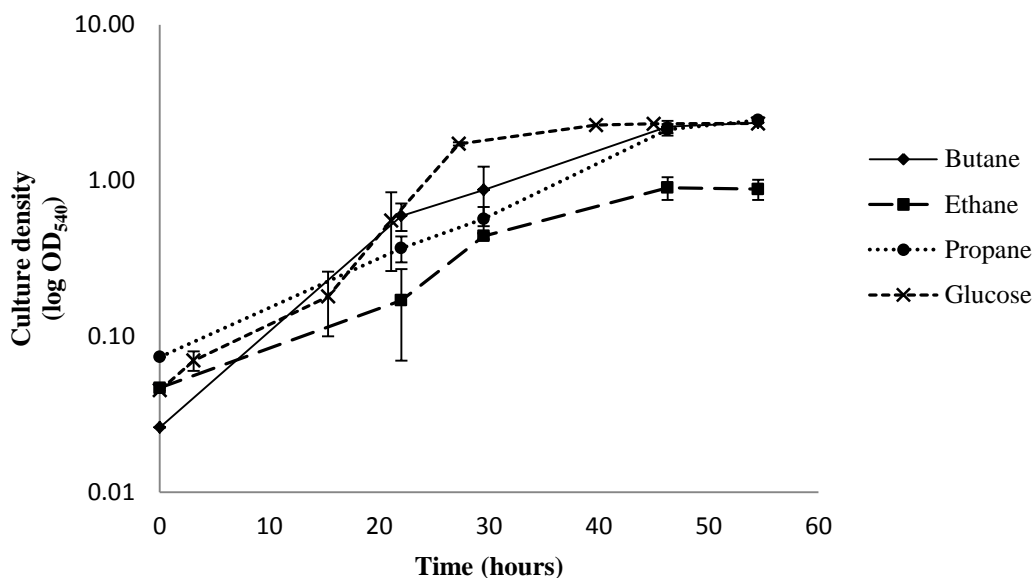


Figure 3.5: Growth curves of *R. jostii* strain 8 grown on NMS with 10 mM glucose or 10% (v/v) ethane, propane or butane as sole carbon source. Error bars indicated the standard deviations of triplicate data.

Specific growth rates for each growth condition were calculated from the data at the exponential phase. The growth rates of strain 8 grown on glucose, ethane, propane and butane were 0.92, 0.11, 0.07 and 0.10 hr⁻¹, respectively. The growth rates showed that strain 8 could grow better on glucose than on ethane, propane and butane, whereas it could grow on ethane as well as on propane and butane. This is not surprising because glucose can be metabolized rapidly by *Rhodococcus* spp.

Due to this distinct alkane-degrading ability and the presence of more than one alkane-degrading enzyme systems in *R. jostii* strain 8, this organism was worthy of further study. Therefore, functional characterization of the enzymes degrading alkanes in this organism and also genome mining were undertaken. The following sections of this chapter will describe substrate-oxidising capability of *R. jostii* strain 8, polypeptide analysis by SDS-PAGE, alcohol dehydrogenase(s) involved in alkane metabolism and transcription of key genes in *R. jostii* strain 8 grown under specific growth conditions.

3.4. Oxidation studies using the oxygen electrode

This experiment aimed to investigate the ability of potential intermediates in gaseous alkane metabolism to induce oxygen consumption in whole-cells of *R. jostii* strain 8. The ability of whole-cells of *R. jostii* strain 8 grown on ethane, propane and butane to oxidise potential intermediates in the corresponding alkane metabolism pathways was investigated by using an oxygen electrode (see Chapter 2, section 17). Oxygen consumption by whole cells in response to the addition of substrates, which are potential intermediates in alkane metabolisms (e.g. ethanol, propanal, acetone etc.) was investigated. Saturated solutions of gaseous alkanes and alkenes were prepared by passing gas from a football bladder inflated with the gas through 20 ml water in 120 ml serum vials. Other substrates were prepared as 0.5M solutions. Stability of alkane-oxidising enzymes in whole cells was compared by measuring substrate-stimulated oxygen consumption rates with fresh cells and freeze-thaw cells. The oxygen consumption rates were investigated with propane-grown cells using saturated propane solution as a substrate. Propane-grown cells were used because it was known from polypeptide analysis that propane-grown cells contained propane monooxygenase, which is believed to be responsible for propane oxidation. It was found that the oxygen consumption rate with propane by fresh propane-grown cells was generally equivalent to the rate by freeze-thawed cells (14.4 ± 0.3 nmol/min/mg dry cell weight), thus the activity of the enzyme responsible for alkane metabolism was not destroyed by the freeze-thaw process. Therefore, cells were stored frozen and thawed when used throughout these oxygen electrode experiments.

3.4.1. Alkane-oxidising enzymes are inducible during growth on alkanes

Gaseous alkanes and alkenes were prepared as saturated solutions in water. The volume of solutions used in each reaction was 200 μ l. It should be noted that the measured oxidation rates were not the rates at substrate concentrations approaching k_m because the solubility of these gases in water was very low. The inducible oxidation rates of alkane-grown cells in response to alkanes and alkenes are shown in Table 3.4.

Assay substrate	Growth substrate			
	Glucose	Ethane	Propane	Butane
methane	ND	ND	ND	ND
ethane	ND	13.6 ± 0.1	7.5 ± 0.2	25.8 ± 0.2
propane	ND	7.4 ± 0.2	14.4 ± 0.3	36.9 ± 0.0
butane	ND	2.0 ± 0.3	8.3 ± 0.1	46.6 ± 0.3
propene	ND	2.3 ± 0.4	4.5 ± 0.1	16.8 ± 0.3
ethene	ND	1.2 ± 0.2	2.1 ± 0.1	5.8 ± 0.1
butene	ND	1.5 ± 0.3	3.0 ± 0.2	4.8 ± 0.2

NB: ND: Not Detectable

Table 3.4: Oxygen consumption rates of glucose- and alkane-grown cells in response to alkanes and alkenes. The rates are determined as nmol of oxygen consumed per min per mg dry cell weight. Standard deviations of triplicate data are also indicated.

The oxidation rates of alkane-grown cells in response to ethane, propane and butane were significantly higher than the rates of glucose-grown cells in response to those alkanes. This suggested that oxidation of ethane, propane and butane was inducible during growth on these alkanes. The alkane-induced rates of butane-grown cells were significantly higher than the rates of other cell types. This might be because membrane permeability of butane-grown cells allowed more substrate uptake than the other cell types. The results also showed that the alkane-grown cells could also oxidise ethene, propene and butene, which are not their growth substrates. The oxygen consumption rate in response to those alkenes was not detectable in glucose-grown cells. This suggested that those alkenes could be an energy source for *R. jostii* strain 8. There was no detectable oxidation rate of any type of cells in response to methane. This is correlated with growth tests that *R. jostii* strain 8 lacks the ability to grow on methane (see growth profile Table 3.3). Therefore, *R. jostii* strain 8 cannot use methane as its carbon and energy source.

The inducible alkane oxidation was also found in other bacteria containing alkane-degrading enzymes *e.g.* alkane monooxygenase. For example, the propane monooxygenase in *R. jostii* RHA1, the closest relative to *R. jostii* strain 8, was inducible during growth on propane (Sharp et al., 2007). However, other alkane- and

alkene-oxidising activity was not investigated in *R. jostii* RHA1. The oxidation activities with ethane, propane, butane and ethene were found in whole-cell *Mycobacterium smegmatis* MC² 155 containing a plasmid carrying a sMMO-like monooxygenase of *Mycobacterium* sp. NBB4 (MC² -155(pSmo)) (Martin et al., 2014). This sMMO-like monooxygenase belongs to the same family as the propane monooxygenase in *R. jostii* strain 8. Interestingly, the oxidation activities with small alkenes were inducible in alkane-grown cells of *R. jostii* strain 8 even though alkenes are not its growth substrates. This is different to the case of MC²-155(pSmo) that both small alkanes and alkenes could be metabolized in MC²-155(pSmo) (Martin et al., 2014).

3.4.2. Oxygen consumption by whole cells in response to alcohols

Alcohols which are intermediates in potential gaseous alkane metabolism were tested for their ability to induce oxygen consumption in *R. jostii* strain 8 cells grown on ethane, propane and butane. The substrate-induced rates with glucose-grown cells were carried out as a control. Oxidation rates of cells grown on glucose, ethane, propane and butane in response to primary alcohols are shown in Figure 3.6. The rates of those types of cells in response to secondary alcohols and diols are shown in Figure 3.7.

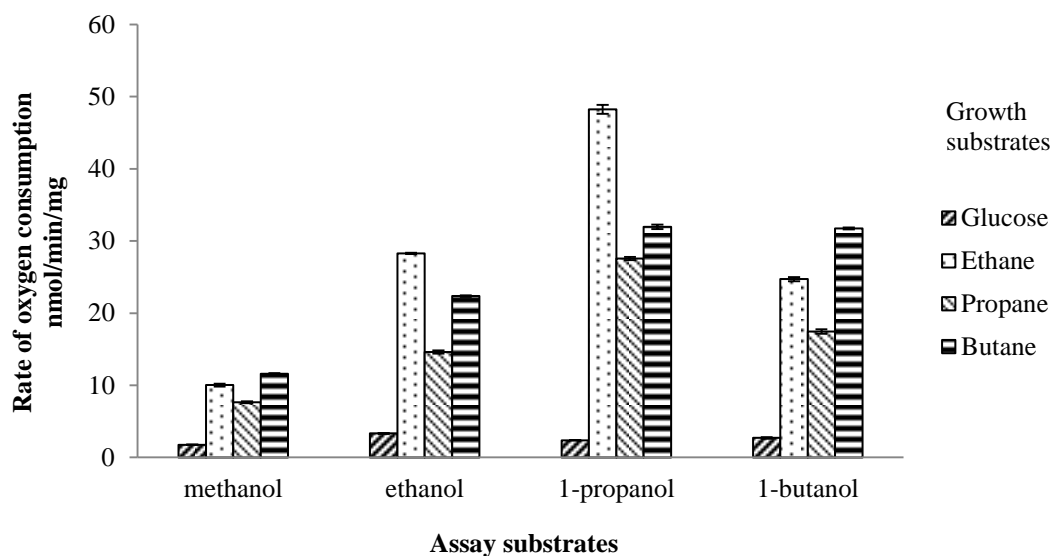


Figure 3.6: Oxygen consumption rates (nmol/min/mg dry cell weight) of whole-cell *R. jostii* strain 8 grown on glucose, ethane, propane and butane induced by primary alcohols which are potential intermediates in alkane metabolism pathways. Error bars indicated standard deviations of triplicate data.

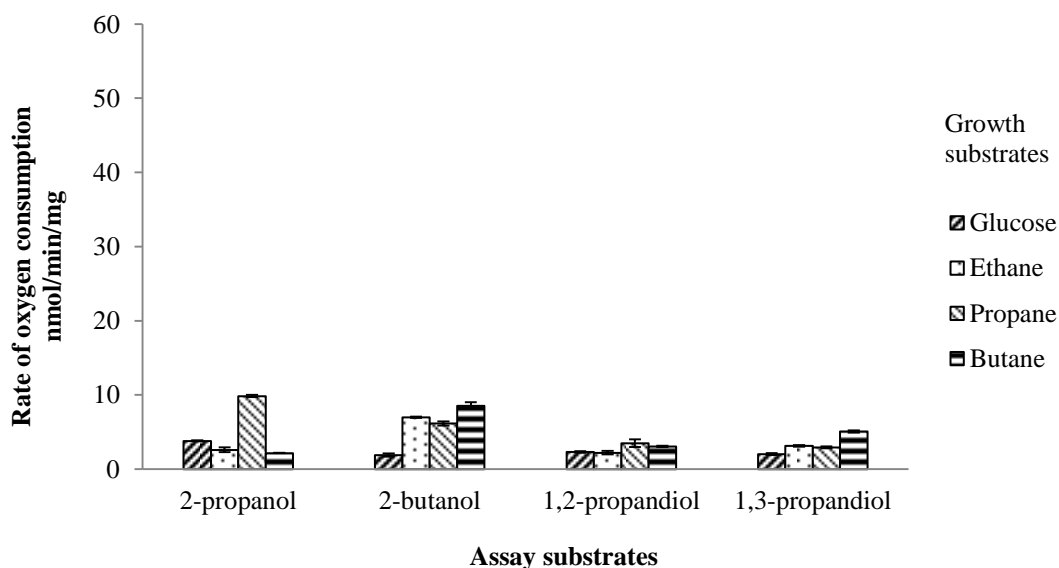


Figure 3.7: Oxygen consumption rates (nmol/min/mg dry cell weight) of whole-cell *R. jostii* strain 8 grown on glucose, ethane, propane and butane induced by secondary alcohols and diols which are potential intermediates in alkane metabolism pathways. Error bars indicated standard deviations of triplicate data.

The rates of oxygen consumption by cells grown on ethane, propane and butane in response to alcohols shared the same trend. This showed that ethane-, propane- and butane-grown cells probably contained similar enzymes responsible for oxidation of alcohols. Figure 3.6 showed that rates of oxygen consumption by *R. jostii* strain 8 with primary alcohols are outstanding in cells grown on ethane, propane and butane while the rates by glucose-grown cells in response to primary alcohols were significantly lower. This suggested that these primary alcohols could induce oxygen consumption rate when cells were grown on alkanes. In contrast, rates of oxygen consumption by cells grown on alkanes in response to secondary alcohols and diols (Figure 3.7) were low and relatively similar to the rate detected in glucose-grown cells. However, the substrate-induced rates by secondary alcohols were still significant. It was clear that primary alcohols could induce much higher rates of oxygen consumption by alkane-grown cells than secondary alcohols and diols. This suggested that primary alcohols were probably preferred substrates for alcohol dehydrogenases in alkane-grown cells.

Among primary alcohols, the oxidation rates by alkane-grown cells in response to ethanol were 2-fold higher than the rates in response to methanol. The oxidation rates were even higher when tested alkane-grown cells with 1-propanol and 1-butanol. This is unsurprising because ethanol, 1-propanol and 1-butanol are intermediates in the oxidation of ethane, propane and butane, which are growth substrates for *R. jostii* strain 8. Interestingly, the rates of oxygen consumption in response to methanol were much higher (approximately 10-fold) in alkane-grown cells than the rate in glucose-grown cells. This suggests that alcohol dehydrogenases in alkane-grown cells may have broad substrate specificity. Substrate specificity of alcohol dehydrogenase(s) in alkane-grown cells should be further investigated by assaying enzyme activities when a particular alcohol acted as a substrate. This will also confirm the ability of alkane-grown cells to oxidise methanol, which surprisingly was able to induce oxidation in alkane-grown cells. Alcohol dehydrogenase assay in cell-free extracts from cells grown on alkanes is described later in Section 3.5.

The oxidation rates in response to 1,2- and 1,3-propanediols with all type of cells were low, and had no significant difference among the rates of alkane-grown

cells and glucose-grown cells. This suggested that it is unlikely that *R. jostii* strain 8 could oxidise propane using dioxygenases to produce diols.

The oxidation activity with alcohols in whole-cell *R. jostii* strain 8 was different to a propane degrader, *Pseudomonas fluorescens* NRRL B-1244. In the case of *P. fluorescens* NRRL B-1244, 1,2-propandiol dehydrogenase activity was detected in cell-free extract from propane-grown cells (Hou et al., 1983b). Also, two different enzymes of this propane degrader were found during growth on propane. One of them preferred primary alcohols while the other preferred secondary alcohols (Hou et al., 1983a). In contrast, without purification of alcohol dehydrogenases, it was clear that the oxidation activity with diols in whole-cells of *R. jostii* strain 8 was significantly low and not inducible during growth on alkanes.

The inducible alcohol dehydrogenase activity was also found in other non-methanotrophs, alkane-degrading bacteria such as *Pseudomonas butanovora*, a butane degrader (Vangnai and Arp, 2001), *Mycobacterium vaccae* JOB-5, a propane degrader (Coleman and Perry, 1985), *Gordonia* sp. TY-5, a propane degrader (Kotani et al., 2003), *Rhodococcus rhodochrous* PNKb1, a propane degrader (Ashraf and Murrell, 1990).

3.4.3. Oxygen consumption by whole cells in response to other potential intermediates of alkane oxidation

Some aldehydes and ketones which are intermediates in subsequent steps in potential alkane oxidation pathways were tested for their ability to stimulate oxygen consumption in whole cells after growth of *R. jostii* strain 8 on ethane, propane and butane. The oxidation rates of cells grown on different carbon sources in response to those compounds are shown in Table 3.5.

Assay substrate	Growth substrate			
	Glucose	Ethane	Propane	Butane
Aldehydes				
propanal	5.4 ± 0.1	30.0 ± 0.2	28.7 ± 0.3	25.3 ± 0.2
pyruvaldehyde	5.8 ± 0.1	4.4 ± 0.0	8.4 ± 0.2	13.2 ± 0.2
acetaldehyde	5.1 ± 0.4	10.6 ± 0.7	8.8 ± 0.4	9.6 ± 0.6
butyraldehyde	3.5 ± 0.5	6.3 ± 0.6	10.9 ± 0.6	31.8 ± 0.0
Ketones				
acetone	0.9 ± 0.0	1.0 ± 0.0	7.7 ± 0.2	8.6 ± 0.0
acetol	2.5 ± 0.1	3.0 ± 0.1	11.8 ± 0.1	12.9 ± 0.3
2-butanone	1.3 ± 0.0	0.7 ± 0.4	15.5 ± 0.1	13.8 ± 0.2
Carboxylic acids				
propionate	3.5 ± 0.1	3.4 ± 0.2	13.1 ± 0.3	13.6 ± 0.1
acetate	14.8 ± 0.3	2.9 ± 0.3	5.5 ± 0.2	12.4 ± 0.3
succinate	1.5 ± 0.0	0.4 ± 0.1	0.6 ± 0.2	1.5 ± 0.2
methylacetate	4.2 ± 0.1	3.1 ± 0.0	7.2 ± 0.1	11.0 ± 0.4

Table 3.5: Oxygen consumption rates (nmol/min/mg dry cell weight) in response to potential intermediates in gaseous alkane metabolisms of whole-cell *R. jostii* strain 8 grown on glucose, ethane, propane and butane. Standard deviations of triplicate data are also indicated.

It should be noted that it is more sensible to consider substrate-induced rates among the same type of cells rather than to compare the rates across all cell types because each type of cell is likely to contain different enzymes. Also, an equal dry cell weight of each type of cells may correspond to different growth phase. The oxygen consumption rates in response to aldehydes were induced in cells grown on alkanes. This is probably because aldehyde dehydrogenases, enzymes responsible for the oxidation of aldehydes, in alkane-grown cells have broad substrate range. The oxygen consumption rates in response to ketones were significantly higher in propane- and butane-grown cells, while the rates were relatively similar in cells grown on ethane and glucose. This suggested that the oxidation of ketones was

induced only in cells grown on propane and butane. The oxygen consumption rates in response to propionate and methylacetate were induced during growth on propane and butane, but not ethane. In contrast, the substrate-induced rates by acetate and succinate in alkane-grown cells were negative. This is probably because acetate and succinate solutions are probably toxic to the cells in these concentrations. Also, cells may require specific transporters in order to uptake acetate and succinate into the cells. The overall trend suggested that it is probable that propane- and butane-grown cells contained similar enzymes which themselves are different from the enzymes in ethane-grown cells.

The oxidation rates in response to propanal and propionate, which are intermediates in potential terminal oxidation of propane, were higher than the rates in response to the other substrates. This suggested that *R. jostii* strain 8 is probably oxidizing propane via the terminal oxidation pathway. However, the oxygen consumption rates in response to intermediates of the sub-terminal oxidation of propane were still significant. This suggested that propane was also probably oxidised via the sub-terminal pathway. In addition, the substrate induced rates with the intermediates of the sub-terminal propane oxidation are higher in propane- and butane-grown cells than in glucose- and ethane-grown cells. This indicated that the sub-terminal propane oxidation was induced by growth on propane and butane.

Other compounds which *R. jostii* strain 8 could grow on such as naphthalene was also tested. The oxidation rate in response to naphthalene of all type of cells was not detectable. This may be because naphthalene is not very soluble in water. Also, *R. jostii* strain 8 may have a slow response to naphthalene as can be assumed from slow growth rate on naphthalene – it took at least two weeks to develop visible colonies on NMS agar incubated with a few crystals of naphthalene.

3.5. Alcohol dehydrogenase assays

Alcohol dehydrogenase assays (see Chapter 2, Section 18.1-18.3) on cell-free extracts of *R. jostii* strain 8 cells grown on glucose and gaseous alkanes were carried out in order to investigate a range of alcohols which are substrates for alcohol dehydrogenases in this bacterium.

In order to ensure that the amount of protein used in the assays was sufficient to allow maximum activities of the enzymes, the concentration of cell-free extract from propane-grown cells was varied from 5, 25 and 100 µg/1 ml reaction volume. The substrate used in this assay was 1-propanol at a final concentration of 1 mM. Each assay was conducted in duplicate. Specific enzyme activities when using 5, 25 and 100 µg of cell-free extract were approximately 325, 250 and 35 nmol NDMA/min/mg protein, respectively. This showed that there was a significant decrease in specific activity when added cell-free extract was added at a final concentration of 100 µg/ml. Specific activities from the assays containing 5 and 25 µg/ml of cell-free extract were not significantly different, but the activities were approximately 8-9-fold higher than the activity from the assay containing 100 µg/ml of the extract. This suggested that enzyme activity was inhibited by high (up to 100 µg/ml) concentrations of protein. Therefore, in this study, the concentration of cell-free extracts used was 25 µg/ml.

3.4.4. PQQ-dependent alcohol dehydrogenase assays

According to the literatures, most pyrroloquinoline quinone (PQQ)-dependent alcohol dehydrogenases are methanol dehydrogenases found in methylophilic bacteria (Anthony and Zatman, 1967). It was found that methanol dehydrogenase was sometimes able to oxidize ethanol (Anthony and Zatman, 1964). Ethanol dehydrogenase found in *Pseudomonas aeruginosa* ATCC17933 is PQQ-dependent (Groen et al., 1984; Görisch and Rupp, 1989). Since *R. jostii* strain 8 could oxidise methanol and ethanol, it was interesting to investigate whether enzymes responsible the oxidation of alcohols are PQQ-containing enzymes similar to those found in other bacteria. There are only a few PQQ-dependent alcohol dehydrogenases found in other types of bacteria. For example, butanol dehydrogenases in *Pseudomonas butanovora* are NAD⁺-independent and PQQ-containing (Vangnai et al., 2002b). Similar to *P. butanovora*, *R. jostii* strain 8 could grow on butane and also oxidise butanol. This became another reason why the PQQ-dependent alcohol dehydrogenase assay was carried out with *R. jostii* strain 8.

PQQ-dependent alcohol dehydrogenases were assayed using the artificial electron acceptor phenazine methosulfate (PMS) coupled to reduction of

dichlorophenolindophenol (DCPIP). The assay was performed as described in Chapter 2, section 18.1. Cell-free extract from *Methylocella silvestris* BL2 grown on methane was used as a control in order to ensure that the reaction was working as normal. This is because previous findings showed that this organism contains methanol dehydrogenase which is PQQ-dependent (Chen et al., 2010). Cell-free extracts from *R. jostii* strain 8 cultures grown on glucose, ethane, propane or butane were assayed. Substrates used in this assay were methanol, ethanol, 1- and 2-propanol and 1- and 2-butanol. Activities were calculated using a molar absorption coefficient for DCPIP at 600 nm of $19.1 \text{ mM}^{-1}\text{cm}^{-1}$ (ARMSTRONG, 1964).

Specific activities of PMS-link alcohol dehydrogenases relating to the reduction of DCPIP in *R. jostii* strain 8 grown on alkanes were not detectable. The activities were 100-fold lower than specific activity of methanol dehydrogenase in cell-free extract of *M. silvestris* BL2 grown on methane (approximately 100 nmol/min/mg protein) although the amount of cell-free extract of *M. silvestris* BL2 used in the assay was 5 times lower than that of *R. jostii* strain 8. This suggested that alcohol dehydrogenase(s) in *R. jostii* strain 8 did not depend on the reduction of DCPIP when PMS was used as electron acceptor. Therefore, it can be concluded that alcohol dehydrogenase(s) in *R. jostii* strain 8 is not PQQ-dependent. Another possible electron acceptor for alcohol dehydrogenase(s) is NADP^+ or NAD^+ , so an NAD(P)H-dependent ADH assay was then carried out.

3.4.5. NAD(P)H-dependent alcohol dehydrogenases

NAD^+ - and NADP^+ -dependent alcohol dehydrogenases were assayed by measuring the formation of NAD(P)H, which can be detected spectrophotometrically at 340 nm against a blank without substrate. The assays were carried out as described in Chapter 2, section 18.2. Substrates used in this assay were the same as these used in the PQQ-dependent alcohol dehydrogenase assays. The activities of enzymes were calculated using a molar extinction coefficient for NAD(P)H at 340 nm of $6.22 \times 10^3 \text{ M}^{-1}\text{cm}^{-1}$.

It is known that bacterial aldehyde dehydrogenase(s) used NAD^+ or NADP^+ as the coenzyme (Lindahl, 1992; Yoshida et al., 1998), so an aldehyde dehydrogenases assay was carried out to ensure that the reagents used in

NAD⁺/NADP⁺-dependent ADH assay were functioning. Instead of using alcohols as assay substrates, aldehydes were added in the reactions. Generally, aldehyde dehydrogenases have broad specificity, so only the aldehydes which are potential intermediates in gaseous alkane metabolisms were used in this experiment. Specific activities of NAD⁺-dependent aldehyde dehydrogenases in ethane cell-free extracts when acetaldehyde was used as substrate was 43 nmol/min/mg protein. Such high activity was also detected from the reaction containing propane cell-free extract with the addition of propanal as a substrate (specific activity was 33 nmol/min/mg protein). NAD⁺-dependent aldehyde dehydrogenase activity of butane cell-free extract was also significantly high (9 nmol/min/mg protein) although this was much lower than the activities detected from ethane and propane cell-free extracts. The fact that significant activities of aldehyde dehydrogenases were detected from ethane, propane and butane cell-free extracts suggested that this NAD⁺-dependent enzyme assay was functioning.

Cell-free extracts from cells grown on ethane, propane and butane were assayed for NAD⁺-dependent alcohol dehydrogenase activities in response to alcohols which are potential intermediates in corresponding alkane metabolism pathways. Specific activities detected from all types of cell-free extracts were very low (0-3 nmol/min/mg protein). This suggested that alcohol dehydrogenases in *R. jostii* strain 8 grown on alkanes were not NAD⁺-dependent. However, it should be noted that each type of cell-free extract may contain many different enzymes. Since alcohol dehydrogenases in *R. jostii* strain 8 were not NAD⁺-dependent, an NADP⁺-dependent alcohol dehydrogenase assay was carried out.

The results showed that specific activities of alcohol dehydrogenase(s) using NADP⁺ as electron carriers were very low (approximately 0-1 nmol/min/mg protein). This suggested that alcohol dehydrogenase(s) in *R. jostii* strain 8 was not dependent on the reduction of NADP⁺. Therefore, *R. jostii* strain 8 is likely to use another cofactor which mediates alcohol dehydrogenase activity in cells. However, optimisation of the assays in order to obtain higher activity could be carried out. Also, cell-free extract of *Rhodococcus rhodochrous* PNKb1 grown on propane could be used as a control for this experiment because a previous study showed that this bacterium contained NADPH-dependent alcohol dehydrogenases (Ashraf et al., 1994)

Another possible cofactor for ADHs in *R. jostii* strain 8 could be *N,N*-dimethyl-4-nitrosoaniline or NDMA. Evidence for a novel type of NDMA-linked ADH, has been reported by (Schenkels, 2000). These researchers suggested that NDMA could be an artificial cofactor for alcohol dehydrogenases in *Rhodococcus erythropolis* DSM 1069. Therefore, NDMA-dependent ADH assays were carried out.

3.4.6. NDMA-dependent alcohol dehydrogenases

NDMA-dependent alcohol dehydrogenase assays were carried out as described in Chapter 2, section 18.3. Activities were calculated using a molar absorption coefficient for NDMA at 440 nm of $35.4 \text{ mM}^{-1}\text{cm}^{-1}$. Specific activities for each type of cell-free extract corresponding to methanol, ethanol, 1- and 2-propanol and 1- and 2-butanol are shown in Figure 3.8-3.13.

According to the literature, primary alcohols are preferred substrates for NDMA-dependent ADHs rather than secondary alcohols and diols (Schenkels P., 2000). In order to estimate an appropriate substrate concentration for use throughout this assay, concentrations of 1-propanol used were 1, 2 and 10 mM. The assays were conducted with cell-free extract from propane-grown cells. Specific activities of NDMA-dependent ADHs corresponding to the increase in 1-propanol concentrations from 1 mM, 2 mM to 10 mM were approximately 400, 250 and 196 nmol/min/mg protein, respectively. This showed that activities of the enzyme decreased when the substrate was used at a concentration of 2 mM. The decrease in enzyme activity was even more significantly when using the substrate at a concentration of 10 mM. This suggested that the increase in final concentrations of the substrate up to 10 mM resulted in the inhibitory effect of the substrate on the enzyme. This inhibitory effect was also found when adding other substrates, e.g. ethanol, 2-propanol, 1-butanol, to the reaction containing cell-free extracts from glucose- and other alkane-grown cells. Therefore, for this study, a substrate concentration of 1 mM was used throughout the assays.

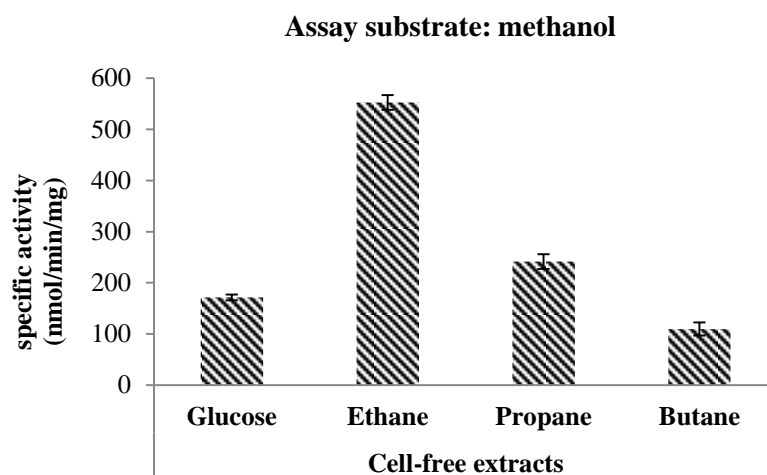


Figure 3.8: Specific activities of NDMA-linked enzymes in cell-free extracts, from glucose-, ethane-, propane- and butane-grown cells, corresponding to the addition of methanol. Error bars represented ranges of duplicate data.

Although methanol is not growth substrate for *R. jostii* strain 8, it was used as assay substrate in this experiment because it could induce oxygen consumption rates in cell-free extracts from cells grown on gaseous alkanes. NDMA-linked alcohol dehydrogenases in ethane-grown cells had significantly higher activity in response to methanol than the activities from other cell types. However, it should be noted that different types of cell-free extracts may contain different enzymes.

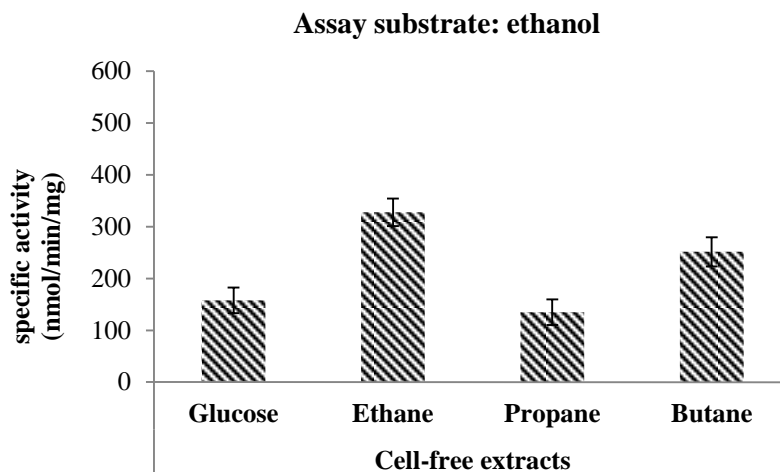


Figure 3.9: Specific activities of NDMA-linked enzymes in cell-free extracts, from glucose-, ethane-, propane- and butane-grown cells, corresponding to the addition of ethanol. Error bars represented ranges of duplicate data.

Specific activities of cell-free extracts of glucose- and propane-grown cells were in the same range, whereas the activities from cell-free extracts of ethane- and butane-grown cells were approximately 1.5 to 2-fold higher.

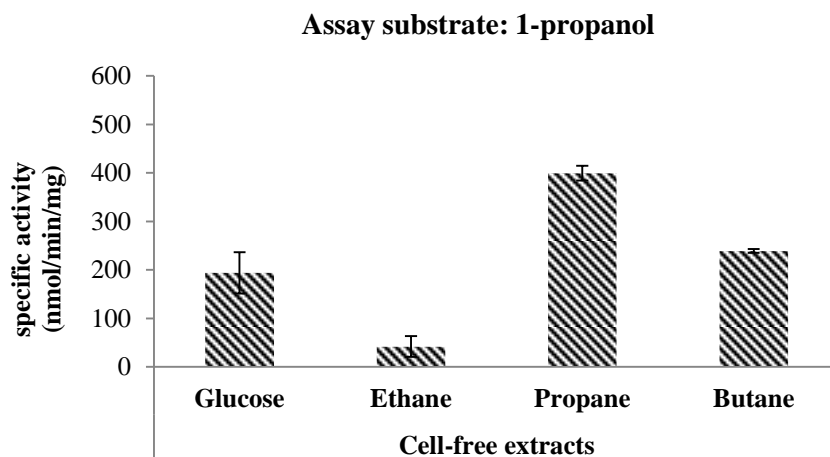


Figure 3.10: Specific activities of NDMA-linked enzymes in cell-free extracts, from glucose-, ethane-, propane- and butane-grown cells, corresponding to the addition of 1-propanol. Error bars represented ranges of duplicate data.

Specific activity of cell-free extract of ethane-grown cells in response to 1-propanol was significantly lower than that from the other types of cell-free extracts. There was no significant difference between the activity of cell-free extract of glucose-grown cells and that from the extract of butane-grown cells. The highest activity was detected from cell-free extract of propane-grown cells which was approximately 2-fold higher than the activities from glucose cell-free extract.

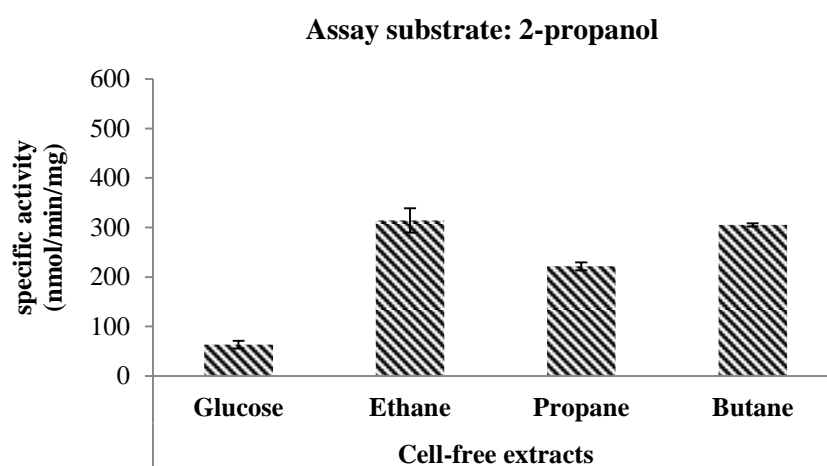


Figure 3.11: Specific activities of NDMA-linked enzymes in cell-free extracts, from glucose-, ethane-, propane- and butane-grown cells, corresponding to the addition of 2-propanol. Error bars represented ranges of duplicate data.

Specific activities of cell-free extracts of ethane, propane and butane-grown cells in response to 2-propanol were significantly higher (approximately 4-6 fold) than rates with cell-free extract from glucose-grown cells. However, the activities in cell-free extracts from alkane-grown cells were not significantly different.

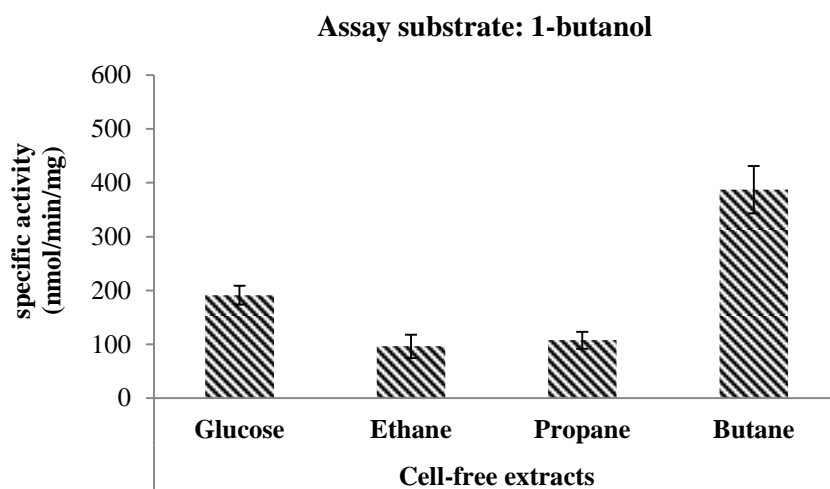


Figure 3.12: Specific activities of NDMA-linked enzymes in cell-free extracts, from glucose-, ethane-, propane- and butane-grown cells, corresponding to the addition of 1-butanol. Error bars represented ranges of duplicate data.

Cell-free extract of butane-grown cells had higher activity than the other types of cell-free extracts while there was no significant difference among the activities from cell extracts of ethane- and propane-grown cells. Specific activity of cell-free extract of glucose-grown cells was approximately 2-fold higher than the activities of ethane and propane cell-free extracts.

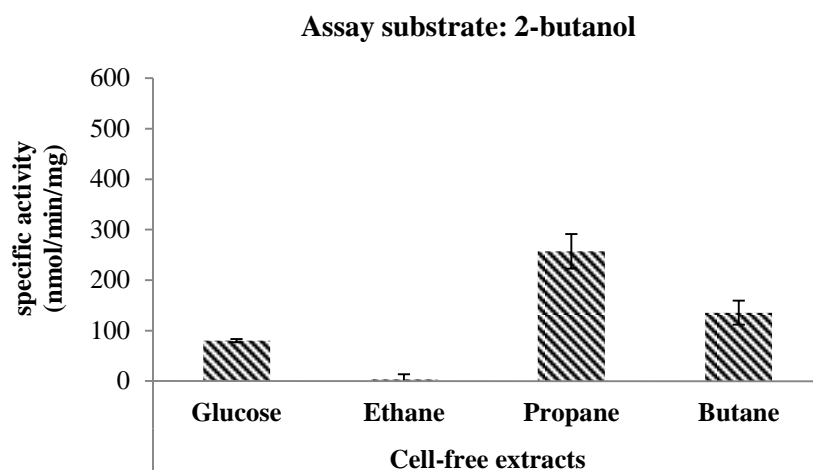


Figure 3.13: Specific activities of NDMA-linked enzymes in cell-free extracts from glucose-, ethane-, propane- and butane-grown cells, corresponding to the addition of 2-butanol. Error bars represented ranges of duplicate data.

There was no enzyme activity in response to 2-butanol with cell-free extract from ethane-grown cells. The highest activity was detected in cell-free extract of propane-grown cells which was 2.5-fold higher than the activity in cell-free extract from butane-grown cells and approximately 3-fold higher than the activity in cell-free extract from glucose-grown cells.

Although the results did not indicate the preferred substrates for alcohol dehydrogenases in *R. jostii* strain 8, NDMA-dependent enzyme activities were significantly high. This, not surprisingly, suggested that alcohol dehydrogenases in *R. jostii* strain 8 were NDMA-dependent. The first reported NDMA-dependent alcohol dehydrogenases were found in *Amycolatopsis methanolica* (Van Ophem et al., 1993). There were also some other bacteria which possess NDMA-dependent alcohol dehydrogenases. For example, it was found that ethanol dehydrogenase in *Rhodococcus erythropolis* EK-1 is NDMA-dependent (Pirog et al., 2009). NDMA-dependent alcohol dehydrogenases were also found in *Rhodococcus erythropolis* DSM 1069 (Schenkels and Duine, 2000). In order to study in more detail, the substrate specificity of alcohol dehydrogenases, optimal conditions for the enzyme assay may be required and purification of the enzymes could also be carried out.

3.5. Discussion and conclusion

At the start of this work, 26 alkane and alkene degraders had been isolated from petroleum contaminated soils. *Rhodococcus jostii* strain 8, which was isolated from propane enrichment, was selected for further study in this research because it contained more than one potential alkane-degrading enzymes and it could grow on various substrates. The 16S rRNA sequence of *R. jostii* strain 8 was closely related to the 16S rRNA sequence of *R. jostii* RHA1, a biphenyl degrader which its genome sequence was available, with 99% identity. Interestingly, *R. jostii* strain 8 could grow on ethane, butane, octane and naphthalene while *R. jostii* RHA1 could not. The other difference between these two strains was that *R. jostii* RHA1 could grow on biphenyl and ethylbenzene, but *R. jostii* strain 8 could not. Potential alkane-degrading enzymes found in *R. jostii* strain 8 were propane monooxygenase and an *alkB*-type alkane monooxygenase. Due to its distinctive alkane-degrading ability and the presence of more than one alkane-degrading enzyme systems in *R. jostii* strain 8, this bacterium was worthy of further study.

Oxidation studies on whole-cell *R. jostii* strain 8 were carried out using an oxygen electrode. Results suggested that the oxidation of ethane, propane and butane was inducible during growth on those alkanes. Interestingly, small alkenes such as ethene, propene and butene could also induce oxygen consumption rates in alkane-grown cells, although those alkenes were not growth substrates for *R. jostii* strain 8. Intermediates in potential alkane metabolism such as aldehydes, ketones and carboxylic acids could also induce oxygen consumption in whole cells. Alcohol dehydrogenases found in *R. jostii* strain 8 were inducible. It was found that substrate-induced rates with primary alcohols were significantly higher than the rates with secondary alcohols and diols. Similar to some other propane degraders such as *Mycobacterium vaccae* JOB-5 (Coleman and Perry, 1985), *Gordonia* sp. TY-5 (Kotani et al., 2003) and *Rhodococcus rhodochrous* PNKb1 (Ashraf and Murrell, 1990), alcohol dehydrogenases in *R. jostii* strain 8 could oxidise both primary and secondary alcohols. In contrast, an alcohol dehydrogenase activity with 1,2-propanediol was detected in cell-free extract of propane-grown *Pseudomonas fluorescens* NRRL B-1244 (Hou et al., 1983b). Alcohol dehydrogenase assays with cell-free extracts of alkane-grown *R. jostii* strain 8 showed that they are NDMA-dependent. This type of alcohol dehydrogenases was also found in other

Rhodococcus strains such as *Rhodococcus erythropolis* EK-1 (Pirog et al., 2009) and *Rhodococcus erythropolis* DSM 1069 (Schenkels and Duine, 2000). In order to further characterise alcohol dehydrogenases in *R. jostii* strain 8, establishment of optimal conditions for enzyme assays and purification of the enzymes could be carried out.

Chapter 4

The genome of *Rhodococcus jostii* strain 8

4.1. Introduction

Members of the genus *Rhodococcus* are widespread in the soil environment (Finnerty, 1992). Rhodococci have been of interest for biotechnological applications due to their metabolic versatility (Warhurst and Fewson, 1994). Genome sequencing has become one of the most useful tools to reveal potentially novel functional genes and also to understand specific metabolic pathways present in microbes. There are 12 non-pathogenic *Rhodococcus* strains whose genomes have been published (searched on 15 May 2014). A list of those *Rhodococcus* strains, to follow with substrates they were isolated on, is shown in Table 4.1.

According to the available genomes of non-pathogenic *Rhodococcus* strains listed in Table 4.1, none of them appear to use gaseous alkanes as their preferred growth substrates. Therefore, the genome of *Rhodococcus jostii* strain 8 is the first reported genome of a non-pathogenic *Rhodococcus* strain that utilizes gaseous alkanes as growth substrates. Study of the genome of *R. jostii* strain 8 will allow us to better understand its metabolic potential in the degradation of short-chain alkanes (C₂-C₄) and also other substrates.

Table 4.1: A list of non-pathogenic *Rhodococcus* strains whose genomes have been published.

Organism	Substrates which the organisms were enriched with	Size of genome (Mbp)	% GC content	References for published genomes
<i>Rhodococcus erythropolis</i> CCM2595	Phenol	6.4	62	(Strnad et al., 2014)
<i>Rhodococcus erythropolis</i> DN1	Crude oil	6.5	62	(Shevtsov et al., 2013)
<i>Rhodococcus erythropolis</i> PR4	C ₈ -C ₂₀ n-alkanes, branched alkanes including pristane	6.9	62	(Sekine et al., 2006)
<i>Rhodococcus erythropolis</i> XP	Gasoline (desulfurization)	7.2	62	(Tao et al., 2011)
<i>Rhodococcus opacus</i> B4	Benzene	8.8	68	(Na et al., 2005a; Na et al., 2005b)
<i>Rhodococcus opacus</i> PD630	Phenyldecane	9.3	67	(Holder et al., 2011a; Chen et al., 2014)

Table 4.1: continued

Organism	Substrates which the organisms were enriched with	Size of genome (Mbp)	% GC content	References for published genomes
<i>Rhodococcus opacus</i> M213	Naphthalene	9.2	67	(Pathak et al., 2013)
<i>Rhodococcus rhodochrous</i> ATCC 21198	Hydrocarbons	6.4	70	(Shields-Menard et al., 2014)
<i>Rhodococcus ruber</i> BKS 20-38	Cholesterol	6.1	69	(Bala et al., 2013b)
<i>Rhodococcus ruber</i> Chol-4	Steroids	5.4	71	(Fernández de Las Heras et al., 2013)
<i>Rhodococcus jostii</i> RHA1	Polychlorinated-biphenyl	9.7	67	(McLeod et al., 2006)
<i>Rhodococcus qingshengii</i> BKS 20-40	Cholesterol moiety	6.6	62	(Bala et al., 2013a)

4.2. Genome sequencing for *Rhodococcus jostii* strain 8

Rhodococcus jostii strain 8 cells were grown in a 250 ml flask containing 50 ml of NMS with 10% (v/v) of propane in the headspace. The culture was grown to an OD₅₄₀ of 0.8. Genomic DNA was extracted using a Fast DNA Spin Kit for Soil (MPBio, Solon, OH, USA) as described in Chapter 2, section 9.1. The DNA sample was sent to The Genome Analysis Center (TGAC) for Illumina MiSeq sequencing. Data were produced using 150 bp and 250 bp paired end reads. Both data sets were combined in order to obtain genome scaffolds. The total length of the 540 contigs was 8,509,286 bp. The average length of contigs was 15,757 bp. The number of possible missing genes was 128 genes. Annotation and analysis of the assembled data was carried out through RAST (Rapid Annotation using Subsystem Technology) (Overbeek et al., 2014). The size of the draft genome of *R. jostii* strain 8 was approximately 8.5 Mbp with a G+C content of 67%. The genome contains 8,283 open reading frames and 75 tRNAs.

4.3. Subsystems in the genome of *R. jostii* strain 8

All of the annotated genes in the genome were assigned into subsystems where the genes were categorized based on their related functions. Gene annotation within 429 subsystems, with subsystem coverage of 33%, was carried out using RAST. 67% of genes were not in subsystems. The numbers of genes in subsystems are shown in Table 4.2.

Subsystem category	Number of genes
Cofactors, vitamins, prosthetic groups, pigments	568
Cell wall and capsule	66
Virulence, disease and defense	100
Potassium metabolism	17
Photosynthesis	0
Miscellaneous	76
Membrane transport	71
Iron acquisition and metabolism	20
RNA metabolism	95
Nucleosides and nucleotides	144
Protein metabolism	245
Cell division and cell cycle	27
Motility and chemotaxis	5
Regulation and cell signaling	59
Secondary metabolism	10
DNA metabolism	134
Regulons	0
Fatty acids, lipids and isoprenoids	535
Nitrogen metabolism	57
Dormancy and sporulation	3
Respiration	246
Stress response	163
Metabolism of aromatic compounds	248
Amino acids and derivatives	876
Sulfur metabolism	76
Phosphorus metabolism	37
Carbohydrates	994

Table 4.2: The number of genes within each subsystem category in the genome of *Rhodococcus jostii* strain 8

4.4. Plasmids and transposable elements

The genes involved in the replication of the chromosome were found in the genome of *R. jostii* strain 8. The *gyrA*, *gyrB*, *recF*, *dnaN*, *dnaA*, *parA* and *parB* genes were present in the same contig of the genome of *R. jostii* strain 8. This is evidence for the presence of complete operon encoding enzymes necessary for chromosome replication. There are 41 genes which have been annotated as genes encoding probable transposases. Those transposases are belonged to various families such as IS4, IS6, IS6120, IS200 and Tn554.

The genome of *R. jostii* strain 8 consists of a chromosome and plasmids. The genes *repA* and *repB* which are usually found on small cryptic plasmids in most actinobacteria (De Mot et al., 1997) were found in the genome of *R. jostii* strain 8. Therefore, it is likely that *R. jostii* strain 8 possesses at least one plasmid. The *traA* gene encoding relaxase, an enzyme that initiates plasmid transfer, in *R. jostii* strain 8 is most closely related (450/1,506 amino acids) to the *traA* gene of *Rhodococcus erythropolis* (Yang et al., 2007). The disruption of the *traA* gene on a megaplasmid of *R. erythropolis* AN12 revealed that the mutant lacked the ability to transfer the plasmid into *R. erythropolis* SQ1 (Yang et al., 2007). It was found that the plasmid pRHL3 in *R. jostii* RHA1 containing *traA* is conjugative (Warren et al., 2004). The presence of *traA* in the genome of *R. jostii* strain 8 implied that *R. jostii* strain 8 is likely to be able to transfer conjugative plasmids to other strains.

In order to identify the presence of plasmid DNA in the genome of *R. jostii* strain 8, pulsed-field gel electrophoresis (PFGE) could be carried out. Deep sequencing could also be carried out in order to identify the origin of replication of a plasmid and some other genes which general sequencing methods might not.

According to the comparison between the growth profile of *R. jostii* strain 8 and growth profile of *R. jostii* RHA1 (Chapter 3, section 3.2), it was found that *R. jostii* strain 8 could grow on ethane, butane, naphthalene and octane, but *R. jostii* RHA1 cannot. Also, biphenyl and ethylbenzene are growth substrates for *R. jostii* RHA1, but not for *R. jostii* strain 8. *R. jostii* strain 8 is therefore different to *R. jostii* RHA1. Therefore, it was expected that *R. jostii* strain 8 genome should contain genes responsible for the degradation of ethane, butane, naphthalene and octane.

4.5. The genes encoding a putative naphthalene 1,2-dioxygenase

The genes encoding naphthalene 1,2-dioxygenase were present in the genome of *R. jostii* strain 8. The list of putative genes and proteins of naphthalene 1,2-dioxygenase in *R. jostii* strain8 and their close relatives is shown in Table 4.3. The naphthalene 1,2-dioxygenase gene clusters of *R. jostii* strain 8 and those of other *Rhodococcus* spp. are shown in Figure 4.1.

Gene name	Gene product	Close relative	% amino acid identity
<i>rubA</i>	rubredoxin	<i>R. opacus</i> B4	100 (86/86)
<i>narR1</i>	regulatory protein, GntR	<i>R. opacus</i> B4	100 (230/230)
<i>narR2</i>	putative naphthalene degradation regulator protein	<i>R. opacus</i> B4	100 (223/223)
<i>orf1</i>	auxiliary protein, nidF	<i>R. opacus</i> TKN14	100 (131/131)
<i>narAa</i>	naphthalene dioxygenase large subunit	<i>R. opacus</i> B4	99 (464/468)
<i>narAb</i>	naphthalene dioxygenase small subunit	<i>R. opacus</i> B4	100 (172/172)
<i>orf2</i>	hypothetical protein	<i>R. opacus</i> B4	100 (90/90)
<i>narB</i>	cis-naphthalene dihydrodiol dehydrogenase	<i>R. opacus</i> B4	100 (271/271)
<i>narC</i>	putative aldolase	<i>R. opacus</i> M213	100 (328/328)
<i>orf3</i>	hypothetical protein	<i>R. opacus</i> B4	100 (137/137)

Table 4.3: The list of putative genes and proteins of naphthalene 1,2-dioxygenase in *R. jostii* strain8 and their close relatives– *Rhodococcus opacus* B4 (Takarada et al., 2009), *Rhodococcus opacus* TKN14 (Maruyama et al., 2005) and *Rhodococcus opacus* M213 (Pathak et al., 2013).

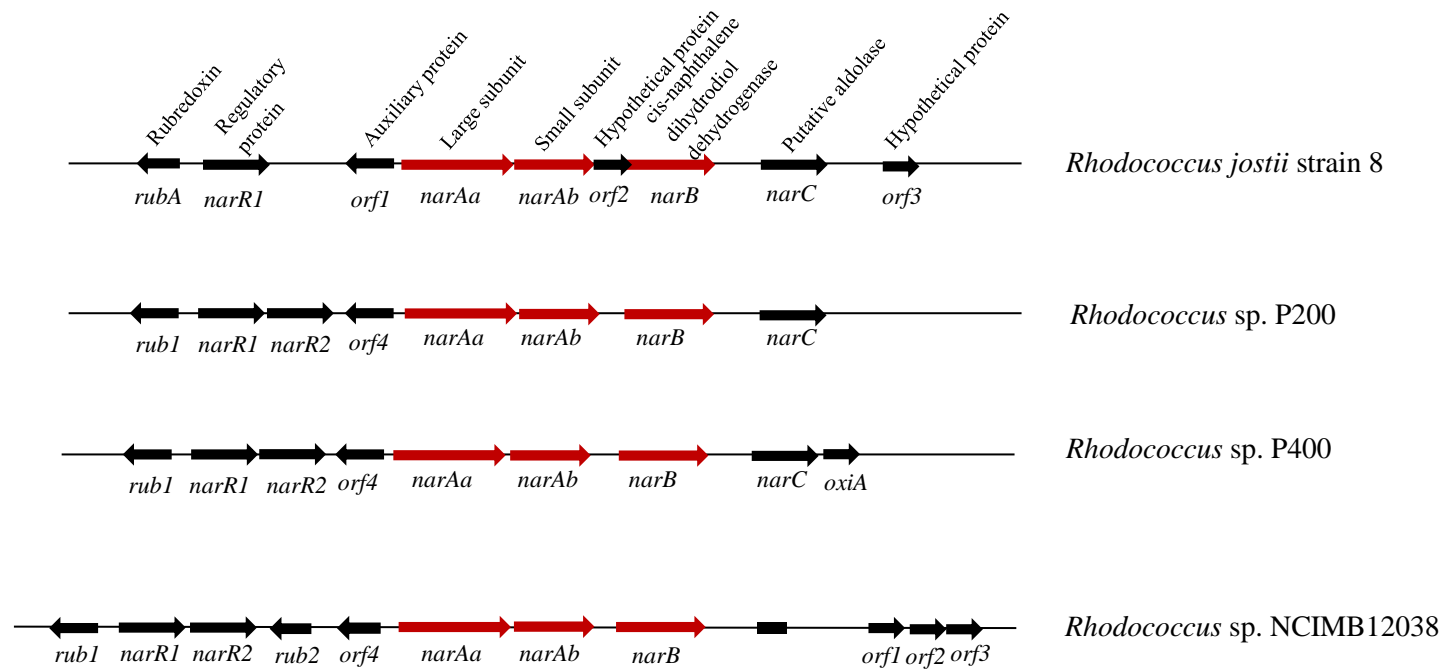


Figure 4.1: the naphthalene 1,2-dioxygenase gene clusters of *R. jostii* strain 8 and those of other *Rhodococcus* spp. – *Rhodococcus* sp. P200, *Rhodococcus* sp. P400 and *Rhodococcus* sp. NCIMB12038 (Kulakov et al., 2005)

Most of the genes involved in putative naphthalene 1,2-dioxygenase in *R. jostii* strain 8 were identical to the genes in *R. opacus* B4, a benzene-tolerant bacteria (Na et al., 2005a). The *orf1* gene was found between *narR2* and *narAa* similar to the *nar* gene cluster of *Rhodococcus* sp. P200 (Kulakov et al., 2005). Although the top BLAST hit of the amino acid sequence of *orf1* corresponded to the *nidF* product of *R. opacus* TKN14, it was found that the enzyme encoded by *nidF* is not necessary for the degradation of naphthalene (Maruyama et al., 2005). The *nidF* gene in *R. opacus* TKN14 encoded the enzyme responsible for the methyl oxidation reaction of *o*-xylene. The *nidF* homolog was also found in the *nar* genomic region of *Rhodococcus opacus* R7, which could grow on both naphthalene and *o*-xylene (Di Gennaro et al., 2010). It should be noted that *R. jostii* strain 8 may be able to grow on *o*-xylene due to the presence of high homology of *nidF* in the *nar* operon. Both *narR1* and *narR2* were typically found in the naphthalene 1,2-dioxygenase gene cluster of *Rhodococcus* sp. NCIMB12038, *Rhodococcus* sp. P200 and *Rhodococcus* sp. P400 (Kulakov et al., 2005). The *narAa*, *narAb*, *narB* and *narC* representing as central module of structural genes are arranged in the same order as the genes found in other naphthalene-degrading rhodococci such as *Rhodococcus* sp. NCIMB12038, *Rhodococcus* sp. P200, *Rhodococcus* sp. P400 and *R. opacus* R7 (Kulakov et al., 2005; Di Gennaro et al., 2010). The presence of a complete gene cluster encoding putative naphthalene 1,2-dioxygenase in the genome of *R. jostii* strain 8 suggested the ability of *R. jostii* strain 8 to grow on naphthalene.

It was found that *R. jostii* RHA1 lacks the complete *nar* operon encoding putative naphthalene 1,2-dioxygenase. In this research, growth tests indicated that *R. jostii* RHA1 could not grow on naphthalene. This is confirmed because *R. jostii* RHA1 does not have enzyme(s) responsible for the degradation of naphthalene. The inability of *R. jostii* RHA1 to grow on naphthalene has previously been reported (Patrauchan et al., 2008). Their study also suggested that biphenyl dioxygenase and ethylbenzene dioxygenase in *R. jostii* RHA1 cannot degrade naphthalene.

4.6. The biphenyl dioxygenase and ethylbenzene dioxygenase gene clusters

The genes encoding biphenyl and ethylbenzene dioxygenases in *R. jostii* strain 8 were searched for by using BioEdit tBLASTn with corresponding amino acid

sequences from *R. jostii* RHA1. The list of genes involved in the degradation of biphenyl and ethylbenzene in *R. jostii* RHA1 compared to the genes in *R. jostii* strain 8 is shown in Table 4.4.

Gene ID in the genome of <i>R. jostii</i> RHA1	Gene location in <i>R. jostii</i> RHA1	Gene name	Gene product	The presence of genes in the genome of <i>R. jostii</i> strain 8
ro08057	pRHL1	<i>bphAd</i>	biphenyl 2, 3-dioxygenase, reductase	N
ro08058	pRHL1	<i>bphAc</i>	biphenyl 2, 3-dioxygenase, ferredoxin component	N
ro08059	pRHL1	<i>bphAb</i>	biphenyl 2, 3-dioxygenase beta subunit	N
ro08060	pRHL1	<i>bphAa</i>	biphenyl 2, 3-dioxygenase alpha subunit	N
ro09018	pRHL1	<i>bphG1</i>	acetaldehyde dehydrogenase	Y
ro09019	pRHL1	<i>bphF1</i>	4-hydroxy-2-oxovalerate aldolase	Y
ro09021	pRHL1	<i>bphE1</i>	2-hydroxypenta-2, 4-dienoate hydratase	Y
ro10125	pRHL2	<i>etbAd</i>	ferredoxin reductase	Y
ro10126	pRHL2	<i>bphB2</i>	cis-3-phenylcyclohexa-3, 5-diene-1, 2-diol dehydrogenase	N
ro10133	pRHL2	<i>etbAa1</i>	ethylbenzene dioxygenase alpha subunit	Y
ro10134	pRHL2	<i>etbAb1</i>	ethylbenzene dioxygenase beta subunit	N
ro10135	pRHL2	<i>etbC</i>	2, 3-dihydroxybiphenyl 1, 2-dioxygenase	Y
ro10136	pRHL2	<i>bphD1</i>	2-hydroxy-6-oxo-6-phenylhexa-2, 4-dienoate hydrolase	Y
ro10137	pRHL2	<i>bphE2</i>	2-oxopent-4-enoate hydratase	Y
ro10138	pRHL2	<i>bphF2</i>	4-hydroxy-2-oxovalerate aldolase	Y
ro10143	pRHL2	<i>etbAa2</i>	ethylbenzene dioxygenase alpha subunit	Y
ro10144	pRHL2	<i>etbAb2</i>	ethylbenzene dioxygenase beta subunit	N
ro10145	pRHL2	<i>etbAc</i>	ethylbenzene dioxygenase, ferredoxin component	Y
ro10146	pRHL2	<i>etbD2</i>	2-hydroxy-6-oxohepta-2, 4-dienoate hydrolase	Y

Table 4.4: The list of genes involved in the degradation of biphenyl and ethylbenzene in *R. jostii* RHA1 (McLeod et al., 2006) compared to the genes in *R. jostii* strain 8. N: Not presence in the genome, Y: Presence in the genome

The major biphenyl dioxygenase gene cluster consisting of *bphA1A2A3A4-bphC-bphB* in *R. jostii* RHA1, which is located on the plasmid pRHL1, did not exist in the genome of *R. jostii* strain 8 (McLeod et al., 2006). The *bphDEF* genes which are located on the plasmid pRHL2 in *R. jostii* RHA1 were found in the genome of *R. jostii* strain 8. It was found that the *bphGF1E1* genes were responsible for the degradation of polychlorinated biphenyl in *R. jostii* RHA1 (Sakai et al., 2003). The similarity between the amino acid sequences of the *bphGF1E1* of *R. jostii* strain 8 and the amino acid sequences of *R. jostii* RHA1 was only 58-60%. The amino acid sequences of *bphGF1E1* genes are more similar (99-100% similarity) to the amino acid sequences of *bphGF1E1* genes in *Rhodococcus wratislaviensis* IFP 2016 (Auffret et al., 2012, unpublished), which have not been characterized. This suggested that the function of the *bphGF1E1* genes in *R. jostii* strain 8 is likely to be different from the function of these genes in *R. jostii* RHA1. The absence of the major biphenyl dioxygenase gene cluster, together with the low sequence similarity of *bphGF1E1* genes in *R. jostii* strain 8 are potentially the reasons why *R. jostii* strain 8 could not grow on biphenyl.

It was found that the *etbCbphD1E2F2* genes were involved in the degradation of biphenyl in *R. jostii* RHA1 (Seto et al., 1996). However, in order to allow the biphenyl dioxygenase enzyme to function, expression of the *etbAa1Ab1* genes are also required (Goncalves et al., 2006). *R. jostii* strain 8 possesses the *etbAa1*, *etbC*, *bphD1*, *bphE1* and *bphF2* genes, but it lacks the *etbAb1* gene. Therefore, a complete set of *etbAa1Ab1C-bphD1E2F2* genes are probably not expressed in *R. jostii* strain 8 resulting in the lack of biphenyl dioxygenase enzyme and lack of ability to grow on biphenyl.

An incomplete ethylbenzene dioxygenase gene cluster was found in the genome of *R. jostii* strain 8. *R. jostii* strain 8 lacks the gene homologs encoding ethylbenzene dioxygenase beta subunit (*etbAb1* and *etbAb2*). Therefore, ethylbenzene dioxygenase gene clusters are not expressed in *R. jostii* strain 8. This correlated with the growth profile of *R. jostii* strain 8 which could not grow on ethylbenzene.

Apart from naphthalene dioxygenase genes, there were 72 genes in the genome of *R. jostii* strain 8 which were annotated as probable aromatic dioxygenase genes.

4.7. Analysis of propane monooxygenase gene sequences in the genome of *Rhodococcus jostii* strain 8

The genome of *R. jostii* strain 8 was analysed for genes encoding hydroxylase subunits of alkane-degrading enzyme systems. There were 26 genes which were annotated as putative P450 monooxygenases. There was one gene cluster annotated as an *alkB*-type alkane monooxygenase. One gene cluster encoding propane monooxygenase was also found. In this study, the propane monooxygenase and an *alkB*-type alkane monooxygenase were particularly focused on because they were probably involved in the metabolism of gaseous alkanes which were growth substrates for *R. jostii* strain 8. In contrast, P450 monooxygenase was likely to be involved in the metabolism of long-chain alkanes (C₅-C₁₆) and aromatic compounds (van Beilen et al., 2006). The propane monooxygenase gene cluster in the genome of *R. jostii* strain 8 comprised of *prmABCD* is shown in Figure 4.2. The propane monooxygenase gene cluster of *R. jostii* strain 8 was compared with the propane monooxygenase gene clusters of the other two closely related strains, *Rhodococcus jostii* RHA1 (McLeod et al., 2006) and *Mycobacterium smegmatis* strain MC² 155 (accession no. NC 008596.1), the genome of which is not available.

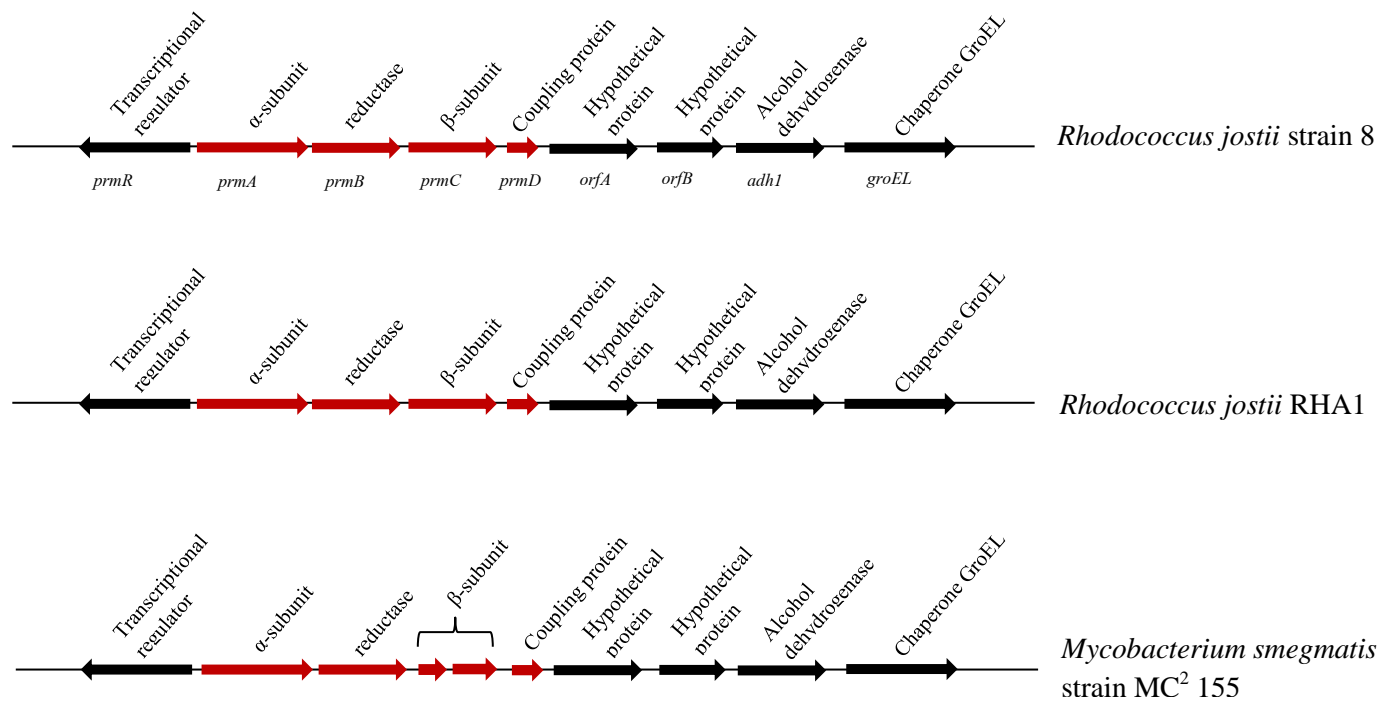


Figure 4.2: Gene arrangement of propane monoxygenase operon found in *R. jostii* strain 8 compared to its two close relatives. The genes which were expected to be essential for expression of the functional propane monoxygenase are shown in red. The names of each gene are indicated under the arrow representing the gene

There were four putative open reading frames in the propane monooxygenase gene cluster of *R. jostii* strain 8 (Figure 4.2). The propane monooxygenase gene cluster of *R. jostii* strain 8 (*prmACBD*) is closely related to the gene cluster of *R. jostii* RHA1 (*prmACBD*) and that of *M. smegmatis* MC² 155. The genes encoding the α -subunit, β -subunit, reductase and coupling protein in the *R. jostii* strain 8 genome shared the same arrangement as the genes in *R. jostii* RHA1. The arrangement of those genes expected to be responsible for the expression of active propane monooxygenase was different in the *M. smegmatis* strain MC² 155 genome. There were two genes encoding the β -subunit of propane monooxygenase found in the *M. smegmatis* MC² 155 genome while there was only one copy of the gene in the *R. jostii* strain 8 genome. Table 4.5 shows % identity of amino acid sequences of each structural gene in the propane monooxygenase gene cluster of *R. jostii* strain 8 compared to the sequences of its relatives.

Organism	Amino acid (% identity)			
	<i>prmA</i>	<i>prmB</i>	<i>prmC</i>	<i>prmD</i>
<i>Rhodococcus jostii</i> RHA1	543/544 (99)	341/347 (98)	366/368 (99)	113/113 (100)
<i>Mycobacterium smegmatis</i> MC ² 155	519/544 (95)	274/347 (79)	299/368 (81)	92/113 (88)

Table 4.5: The amino acid sequence identity of structural genes in the propane monooxygenase gene cluster of *R. jostii* strain 8 compared to its relatives, *R. jostii* RHA1 (Sharp et al., 2007) and *Mycobacterium smegmatis* MC² 155 (accession no. NC 008596.1).

The structural genes (*prmA*, *prmB*, *prmC* and *prmD*) in the propane monooxygenase gene cluster of *R. jostii* strain 8 were most closely related to the genes in the propane monooxygenase of *R. jostii* RHA1. Also, the gene encoding a putative transcriptional regulator (TetR family) located upstream of the propane monooxygenase of *R. jostii* strain 8 was 99% identical (205/208 amino acids) to the gene of *R. jostii* RHA1. However, it is unclear whether the probable transcriptional regulator is responsible for the transcription of propane monooxygenase. Therefore, further investigation by *prmR* knockout analysis could provide evidence for the correlation between this transcriptional regulator and the transcription of propane monooxygenase.

The amino acid sequence of *groEL* of *R. jostii* strain 8 was most closely related to the sequence of *R. jostii* RHA1 with 99% identity (547/549 amino acids). In *R. jostii* RHA1, *groEL* encoding a chaperone GroEL was linked with a stress response during cell starvation (LeBlanc et al., 2008). A study of *R. jostii* RHA1 also showed a correlation between the induction of the *prm* operon and desiccation-induced cell stress (LeBlanc et al., 2008). This suggested that *groEL* located downstream of the *prm* operon was involved in a stress response of *R. jostii* RHA1 cells. Due to the *groEL* amino acid sequence similarity, it is probable that this gene might also be involved in stress responses in *R. jostii* strain 8. Further investigation at the transcription level on the induction of the *prm* operon during cell starvation of *R. jostii* strain 8 could be interesting to study in the future.

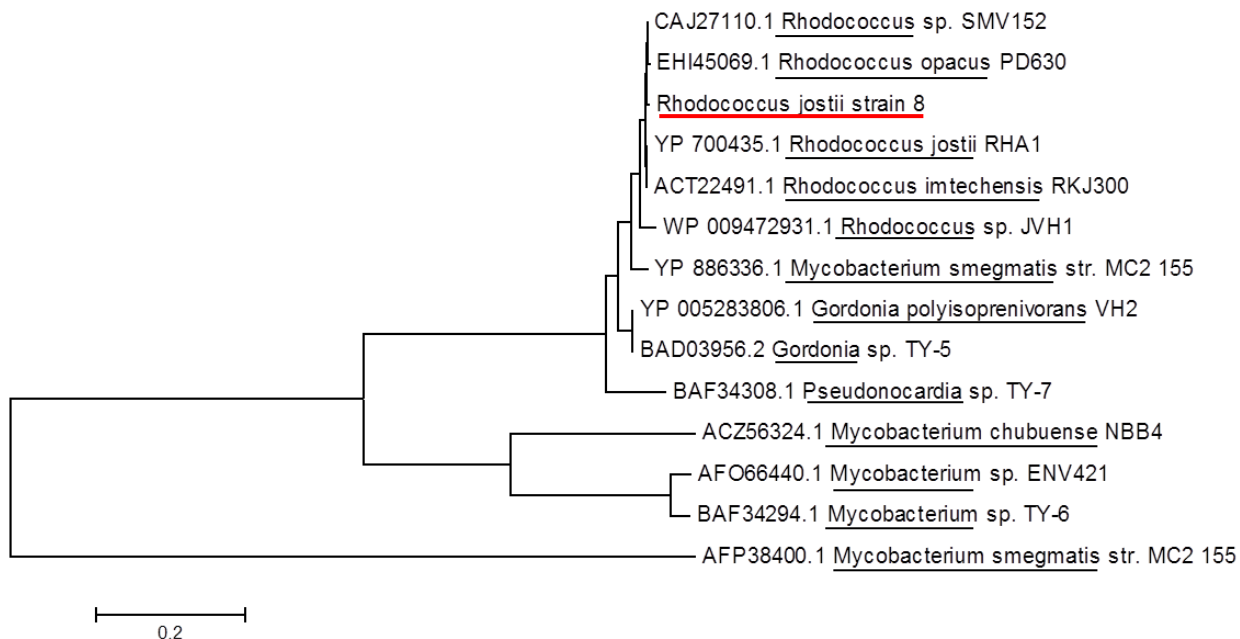


Figure 4.3: Neighbour-joining phylogenetic tree of the α -subunit hydroxylase (PrmA) of the propane monooxygenase in *R. jostii* strain 8 and its close relatives. Sequences covering 544 amino acids were aligned using ClustalW. The phylogenetic tree was created using MEGA5 (Tamura et al., 2011).

prmA encoding the α -subunit hydroxylase, which harbours the active site of the enzyme, was closely related to the corresponding protein of *Rhodococcus jostii* RHA1 with 99% identity (543/544 amino acids). The phylogenetic relationship between amino acid sequences of *prmA* from these rhodococci is shown in Figure 4.3. The presence of conserved amino acids in the amino acid sequence of *prmA* showed that this enzyme belongs to the family of soluble diiron monooxygenases (SDIMO) (Coleman et al., 2006). Those conserved amino acid residues corresponding to the binding sites for the two iron centres of the catalytic sites of the enzymes are shown in Figure 4.4 (Elango et al., 1997; Leahy et al., 2003).

mmoX, encoding the hydroxylase of soluble methane monooxygenase, a well-studied SDIMO, of *Methylosinus trichosporium* OB3b (Fox et al., 1989) and *Methylocella silvestris* BL2 (Chen et al., 2010; Crombie and Murrell, 2014) were included in order to show the well conserved amino acid residues at the two iron sites of the enzymes in SDIMO family. The residues in and around the iron ligands,

E114, E144, H147, E209, E243, H246 (according to numbering of the MMOX amino acid residues of *M. trichosporium* OB3b), are not surprisingly highly conserved (Coufal et al., 2000). The conserved residue T213, which is believed to be responsible for proton flux into the active site of soluble methane monooxygenase (Regnström et al., 1994), is also conserved among propane monooxygenases. There were several other amino acid residues conserved among these sequences (marked as asterisks in Figure 3). This strongly suggested that the propane monooxygenase of *R. jostii* strain 8 belongs to the SDIMO family and is also closely related to the propane monooxygenases of other *Rhodococcus* spp. such as *R. jostii* RHA1. However, the conserved residue C151 found in MMOX of soluble methane monooxygenases is not conserved among PrmA of propane monooxygenases (equivalent to position 154 based on consensus numbering). Interestingly, the differences between amino acid residues surrounding the diiron motifs of the propane monooxygenases and soluble methane monooxygenases may be an indication of differences in their substrate-binding sites. sMMO can oxidise both methane and propane but to our knowledge, the propane monooxygenase cannot oxidise methane (Murrell et al., unpublished observations).

Figure 4.4: Comparison of partial hydroxylase regions (residues 77-301) of the propane monoxygenase amino acid sequences of *R. jostii* strain 8 and the other known PrmA sequences -- *R. jostii* RHA1, *Gordonia* TY-5, *Mycobacterium* TY-6 and *Pseudonocardia* TY-7. Partial hydroxylase subunits (MMOX) of the soluble methane monoxygenases, a well-characterised soluble diiron monoxygenase (SDIMO), of *M. trichosporium* OB3b and *M. silvestris* BL2 are included to indicate conserved amino acid residues of enzymes among the SDIMO family. The number on the top indicated the consensus numbering and the bottom number is *M. trichosporium* OB3b residue number. The amino acid residues corresponding to the two iron centres of the enzymes are enclosed in red boxes. Other identical amino acid residues are marked by asterisks. Gaps were introduced due to sequence alignments.



Several gram-positive bacteria possess a putative propane monooxygenase gene cluster. *Gordonia* TY-5 is one of those bacteria whose propane monooxygenase gene cluster has been well-studied (Kotani et al., 2003). It was found that propane monooxygenase in *Gordonia* TY-5 was responsible for growth on propane. The study showed that *Gordonia* TY-5 could grow well only on propane among the gaseous alkanes. *Mycobacterium* TY-6, which could grow on C₃-C₆ alkanes, has a different propane monooxygenase gene organisation (*prmACDB*) to the gene cluster of *Gordonia* TY-5 (*prmABCD*) (Kotani et al., 2006). This study also showed that in *Pseudonocardia* TY-7, its two propane monooxygenase gene clusters (*prmABCD*) have the same gene arrangement as that of *Gordonia* TY-5, but *Pseudonocardia* TY-7 has a broader substrate range (C₂-C₆ alkanes). However, an expression study on the *prm* gene cluster from both *Mycobacterium* TY-6 and *Pseudonocardia* TY-7 (Kotani et al., 2006) suggested that propane monooxygenase was involved in their growth on propane. The propane monooxygenase of *Rhodococcus jostii* RHA1, which is the most closely related to that of *R. jostii* strain 8, is also well-studied. (Sharp et al., 2007) suggested that propane monooxygenase in *R. jostii* RHA1 was inducible in propane-grown cells, but a study of the substrate range of this enzyme was not carried out. It will therefore be interesting to further characterize the role of propane monooxygenase in *R. jostii* strain 8 as it is likely to be involved in growth on propane in *R. jostii* RHA1.

4.8. Analysis of *alkB*-type alkane hydroxylase gene sequences in the *Rhodococcus jostii* strain 8 genome

As previously mentioned, an *alkB*-type alkane monooxygenase was potentially involved in the metabolism of short-chain alkanes. The alkane monooxygenase gene cluster of *R. jostii* strain 8 is shown in Figure 4.5.

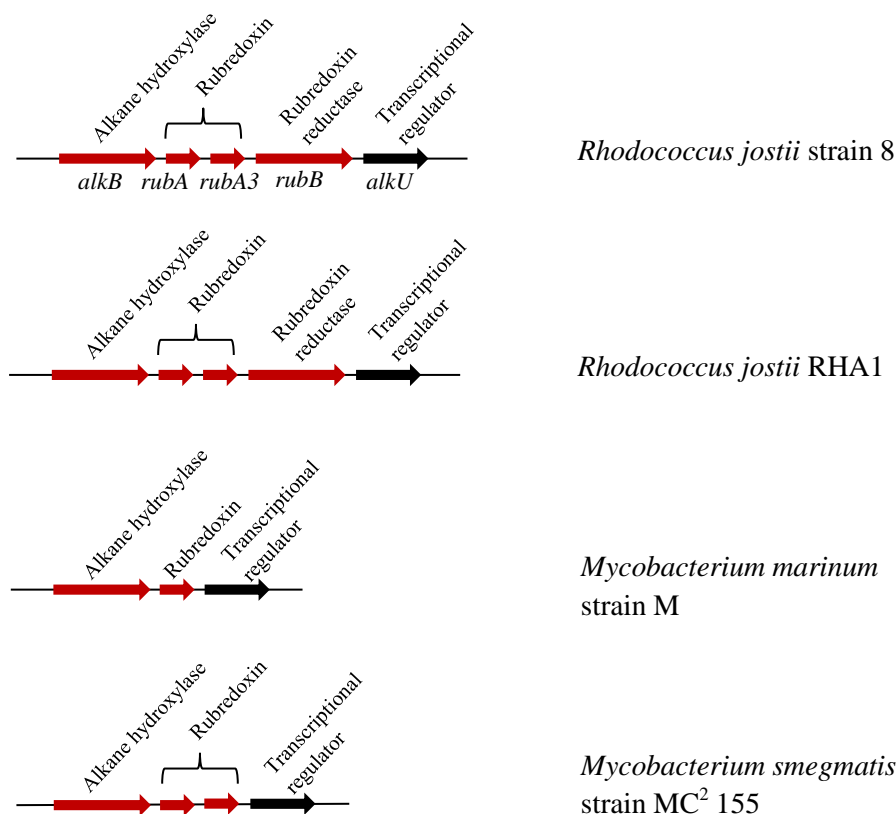


Figure 4.5: Gene arrangement of *alkB*-type alkane monooxygenase operon found in *R. jostii* strain 8 compared to its three close relatives. The genes which were expected to be essential for expression of the functional *alkB*-type alkane monooxygenase are shown in red.

Sequence analysis of *alkB*-type alkane monooxygenase gene cluster in the *R. jostii* strain 8 revealed four open reading frames. The number of genes in the alkane monooxygenase gene cluster of *R. jostii* strain 8 is the same as the gene cluster in *R. jostii* RHA1, which is the most closely related gene cluster. The arrangement of genes encoding alkane hydroxylase subunit, rubredoxin and ferredoxin reductase were similar in the genome of *R. jostii* strain 8 and the genome of *R. jostii* RHA1. The differences in the arrangement of genes essential for the expression of active alkane monooxygenase were found in *M. marinum* strain M (Stinear et al., 2008) and *M. smegmatis* strain MC² 155 (Gray et al., 2013), whose *alkB* gene cluster are the second and third close relative of the gene cluster of *R. jostii* strain 8. In the genome of *M. marinum* strain M, there was only one copy of the gene encoding rubredoxin

while there were two copies of the gene in the other three relatives. Also, the gene encoding ferredoxin reductase was absent in the *M. marinum* strain M. The absent of this gene was also noted in the genome of *M. smegmatis* strain MC² 155. Table 4.6 shows % identity of amino acid sequences of each structural gene in the *alkB*-type alkane monooxygenase gene cluster of *R. jostii* strain 8 compared to the sequences of its relatives.

Organism	Amino acid (% identity)			
	<i>alkB</i>	<i>rubA</i>	<i>rubA3</i>	<i>rubB</i>
<i>Rhodococcus jostii</i> RHA1	405/410 (98)	55/55 (100)	58/61 (95)	403/424 (95)
<i>Mycobacterium marinum</i> M	284/410 (70)	38/55 (75)	N/A	N/A
<i>Mycobacterium smegmatis</i> MC ² 115	296/410 (76)	42/55 (82)	47/61 (81)	N/A

N/A: Not available -- the genes were not present in the genome of that organism

Table 4.6: The amino acid sequence identity of structural genes in the *alkB*-type alkane monooxygenase gene cluster of *R. jostii* strain 8 compared to its relatives, *R. jostii* RHA1 (McLeod et al., 2006), *Mycobacterium marinum* M (Stinear et al., 2008) and *Mycobacterium smegmatis* MC² 155 (Gray et al., 2013).

Table 4.6 showed that the most closely related *alk* operon of *R. jostii* strain 8 was the *alk* operon of *R. jostii* RHA1. The study of the *alk* operon of *R. jostii* RHA1 showed that this operon was not up-regulated during growth on propane, so *alkB*-type alkane monooxygenase probably had no role in the growth of *R. jostii* RHA1 on propane (Sharp et al., 2007). It should be noted that a similar effect might be found in *R. jostii* strain 8 since the *alk* operon of this bacterium had significant identity to the *alk* operon of *R. jostii* RHA1.

The putative transcriptional regulator (*alkU*) of *R. jostii* strain 8 was 99% (205/208 amino acids) identical to the putative transcriptional regulator of *R. jostii* RHA1. However, there was no in-depth evidence showing whether this gene was involved in the transcription of the *alk* operon in this bacterium. Therefore, further investigation could be carried out.

The phylogenetic relationship between amino acid sequences of *alkB*, the gene encoding hydroxylase subunit of the enzyme, of *R. jostii* strain 8 and its relatives is shown in Figure 4.6.

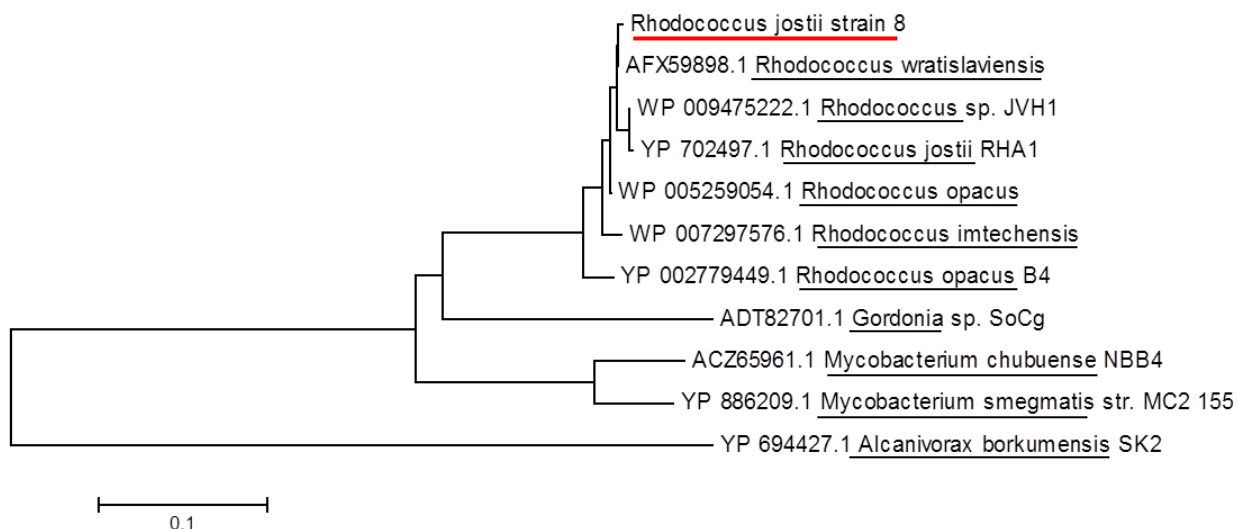
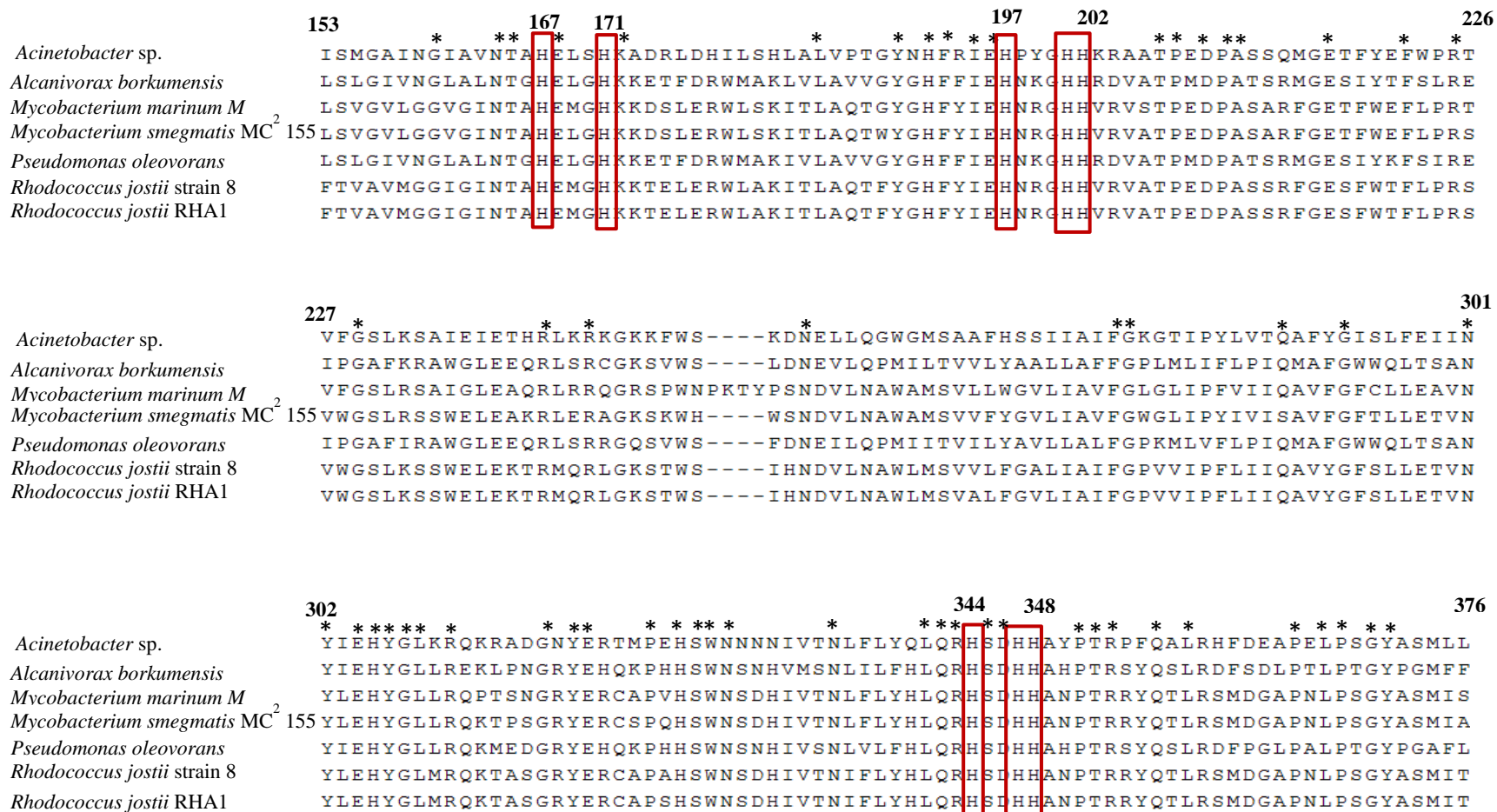


Figure 4.6: Neighbour-joining phylogenetic tree of the hydroxylase subunit of the *alkB*-type alkane monooxygenase in *R. jostii* strain 8 and its close relatives. Sequences covering 410 amino acids were aligned using ClustalW. Phylogenetic tree was created using MEGA5 (Tamura et al., 2011).

The amino acid sequences corresponding to catalytic sites of alkane monooxygenase, which are well conserved among most bacteria alkane monooxygenase were found in the AlkB sequence of *R. jostii* strain 8. Those conserved histidine residues (Shanklin et al., 1994; Shanklin et al., 1997; Smits et al., 1999) are shown in Figure 4.7. The amino acid sequence of *alkB*, encoding the α -subunit, in the alkane monooxygenase gene cluster of *R. jostii* strain 8 showed 98% (409/410 amino acids) identity to the corresponding protein in *Rhodococcus wratislaviensis* (accession no. AFX 59898.1), whose genome is not available and its alkane hydroxylase has never been characterised (accession AFX59898). The next close relative of the *R. jostii* strain 8 alkane hydroxylase is the alkane hydroxylase of *R. jostii* RHA1 (95% identity with 405/410 amino acids).

Figure 4.7: Comparison of partial hydroxylase regions (residue 153-376) of *alkB*-type alkane monooxygenases. Five conserved histidine residues are enclosed with red boxes. The top number indicated the consensus numbering. Other identical amino acid residues are indicated by asterisks. Gaps were introduced due to sequence alignments.



Although many of bacterial *alkB*-type alkane monooxygenases have been characterised, their substrate ranges are liquid alkanes (C₅-C₁₂ or C₁₂ or longer-chain alkanes for some bacteria) (van Beilen et al., 1994; Smits et al., 1999; Smits et al., 2002; Whyte et al., 2002; Hara et al., 2004). There have been only a few *alkB*-type alkane monooxygenases in Gram-positive bacteria investigated in detail (Whyte et al., 2002; Sameshima et al., 2008; Takei et al., 2008). Since the expression of alkane monooxygenase depends on substrate range (Hamamura et al., 2001), an expression study on *alkB*-type alkane monooxygenase in *R. jostii* strain 8 is needed to determine the substrate range of this enzyme. A study on alkane monooxygenase in *R. jostii* strain 8 will probably broaden our understanding of the role of this enzyme in Gram-positive bacteria.

4.9. Cytochrome P450 monooxygenases in *Rhodococcus jostii* strain 8

There were 26 different genes annotated as cytochrome P450 monooxygenases in the genome of *R. jostii* strain 8. The signature amino acid sequences corresponding to a heme ligand and a part of the oxygen-binding site of the cytochrome P450 monooxygenases (Graham and Peterson, 2002) were found in all of the 26 putative P450 enzymes. The patterns of those amino acid sequences are FXXGXXXCXG (a heme ligand) and A(A/G)X(E/D)T (a part of oxygen-binding site) (Graham and Peterson, 2002, Peterson and Graham, 1998). Studies on the role of bacterial cytochrome P450 monooxygenases in the degradation of alkanes are limited. Most of the enzymes in this family are likely to have a broad substrate range (C₆-C₁₁ alkanes), but none of them are known to oxidise gaseous alkanes (Maier et al., 2001; van Beilen et al., 2005; van Beilen et al., 2006).

4.10. Metabolic pathway analysis for *Rhodococcus jostii* strain 8

Potential metabolic pathways in *R. jostii* strain 8 were established using Kegg metabolic analysis from the SEED Viewer on the RAST website (<http://rast.nmpdr.org>). Relevant genes encoding enzymes in specific metabolic pathways were used to determine potential enzymes existing in the pathways. It is noteworthy that *R. jostii* strain 8 may possess genes which are not found in the correct genome sequence since the genome sequence is not completed. Therefore, those genes may not be present in Kegg recruitment plots.

According to RAST annotation, there are several key genes encoding enzymes potentially involved in central carbon metabolism of *R. jostii* strain 8. The central metabolism of *R. jostii* strain 8 includes glycolysis/ gluconeogenesis, carbon fixation, glyoxylate and dicarboxylate metabolism, the tricarboxylic acid (TCA) cycle and pentose phosphate pathway. *R. jostii* strain 8 also possesses genes encoding necessary enzymes for biosynthesis of nucleotides, nucleosides and amino acids. Nitrogen, sulfur, propanoate and butanoate metabolism in *R. jostii* strain 8 is described as follow.

4.10.1. Nitrogen metabolism: reduction and fixation

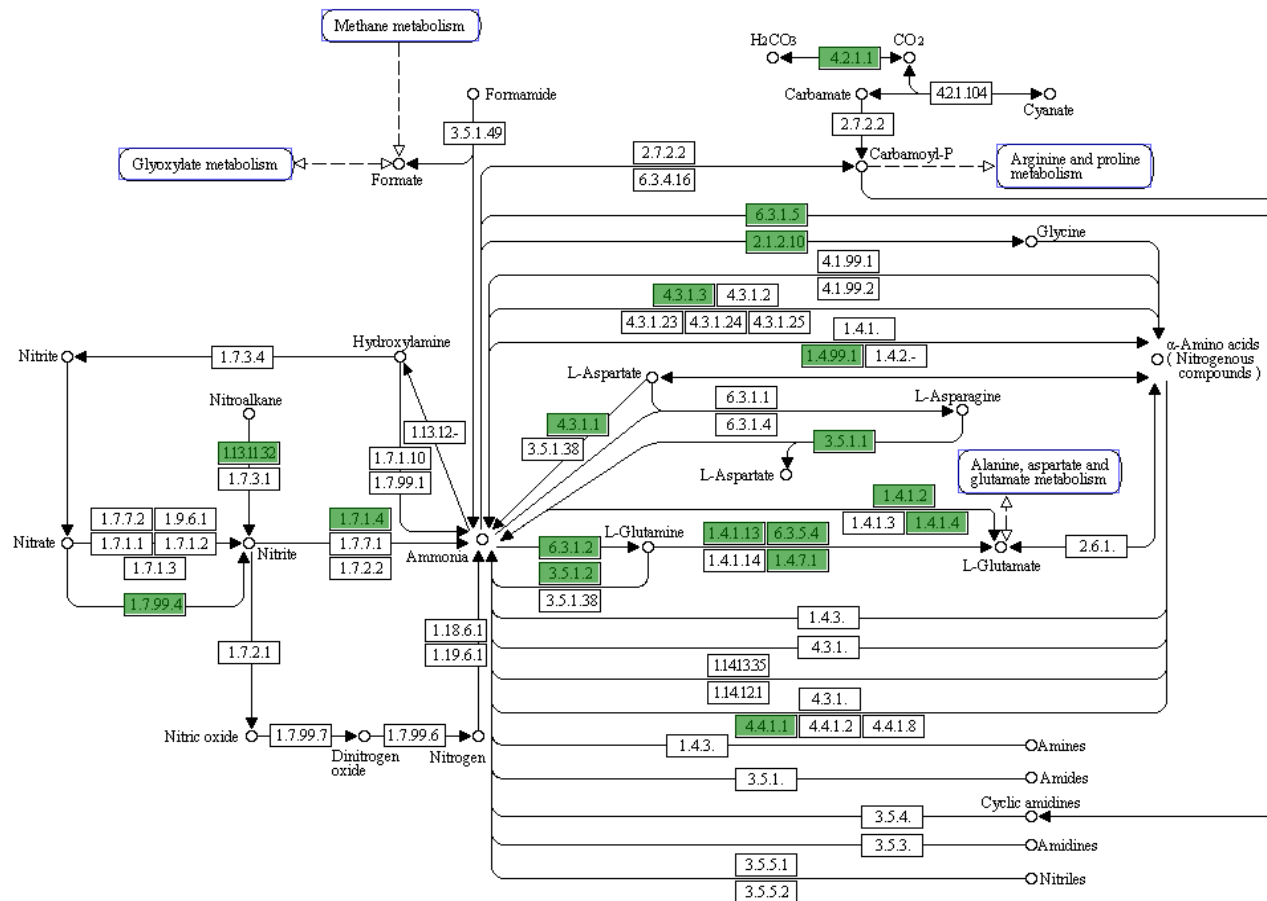


Figure 4.8: Kegg recruitment plot of genes involved in nitrogen metabolism: reduction and fixation from the *R. jostii* strain 8 genome. The enzymes (indicated in EC numbers) encoded by genes present in the genome are shown in green boxes.

The genome of *Rhodococcus jostii* strain 8 contains genes encoding several enzymes involved in nitrogen metabolism (Figure 4.8). *R. jostii* strain 8 can obtain nitrogen from nitrate and convert it to nitrite and then to ammonia by assimilatory nitrate reductase (EC 1.7.99.4) and nitrate reductase (EC 1.7.1.4), respectively. Ammonia can also be formed from the breakdown of L-aspartate by aspartate ammonia-lyase (EC 4.3.1.1) or L-glutamine by glutaminase (EC 3.5.1.2) or amino acids (nitrogenous compounds) by cystathionine gamma-lyase (EC 4.4.1.1). Ammonia can be used to synthesize L-glutamate which then goes into alanine, aspartate and glutamate metabolism. These steps are achieved by four enzymes (EC 6.3.1.2, 1.4.1.13, 6.3.5.4 and 1.4.7.1). Ammonia can also be converted to glycine by urea carboxylase-related aminomethyltransferase (EC 2.1.2.10) or cyclic amidines by NAD synthetase (EC 6.3.1.5). It was found that nitrogen metabolism in *R. jostii* strain 8 is similar to the nitrogen metabolism in *R. jostii* RHA1. *R. jostii* RHA1 used nitrate and nitrite as sole nitrogen sources (Iino et al., 2013). That study also showed that *R. jostii* RHA1 preferred ammonia as its nitrogen source than nitrite and nitrate.

4.10.2. Sulfur metabolism

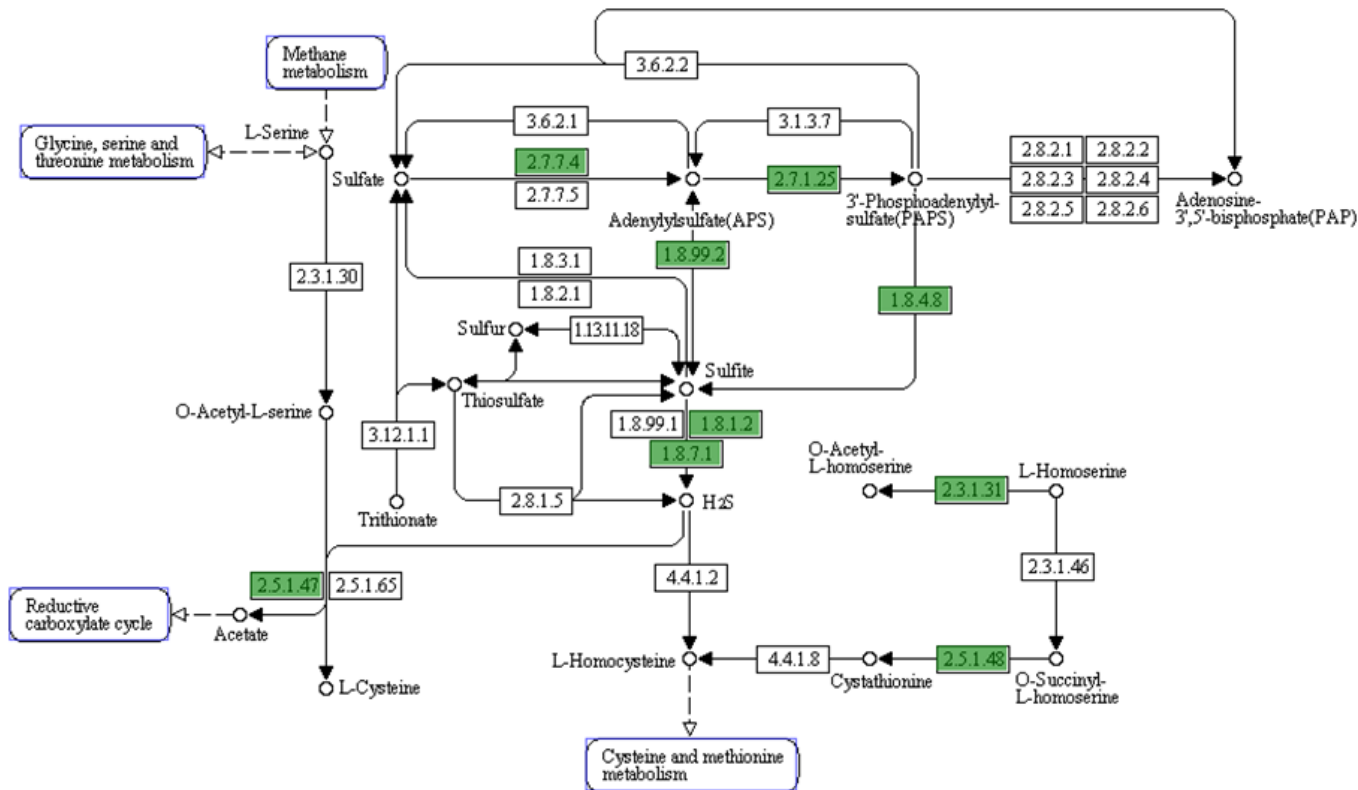


Figure 4.9: Kegg recruitment plot of genes involved in sulfur metabolism from the *R. jostii* strain 8 genome. The enzymes (indicated in EC numbers) encoded by genes present in the genome are shown in green boxes.

There are genes encoding several enzymes responsible for sulfur metabolism (Figure 4.9) present in the genome of *R. jostii* strain 8. The cycle starts with the conversion of sulfate into sulfite by sulfate adenylyltransferase (EC 2.7.7.4) and adenylylsulfate reductase (EC 1.8.99.2), respectively. Sulfite is then converted to hydrogen sulfide by two possible enzymes, sulfite reductase (EC 1.8.1.2) or ferredoxin-sulfite reductase (EC 1.8.7.1). Hydrogen sulfide together with O-acetyl-L-homoserine can be converted to L-cysteine and acetate, which then enters the reductive carboxylate cycle by cysteine synthase (EC 2.5.1.47). All the genes required for sulfur metabolism present in the genome of *R. jostii* strain 8 are also found in the genome of *R. jostii* RHA1. Moreover, *R. jostii* RHA1 also possesses the gene encoding serine O-acetyltransferase (EC 2.3.1.30) which converts L-serine together with acetyl-CoA into O-acetyl-L-serine, but this gene is absent in the genome of *R. jostii* strain 8.

4.10.3. Propanoate metabolism

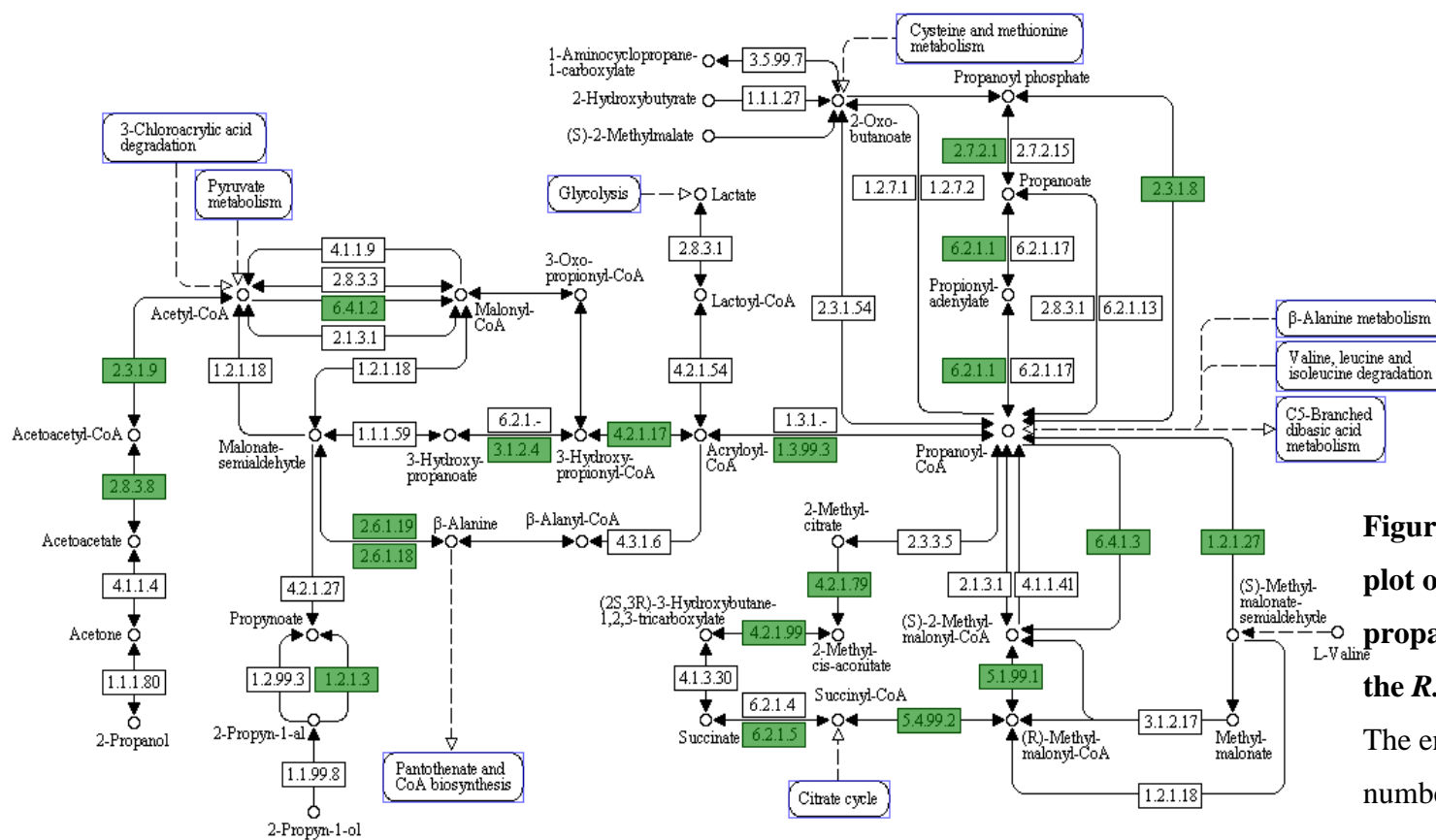


Figure 4.10: Kegg recruitment plot of genes involved in propanoate metabolism from the *R. jostii* strain 8 genome. The enzymes (indicated in EC numbers) encoded by genes present in the genome are shown in green boxes.

There are genes encoding enzymes necessary for the metabolism of propanoate found in the genome of *R. jostii* strain 8. Propanoate, an intermediate in propane metabolism, can be converted to propanoyl-CoA by acetyl-CoA synthetase (EC 6.2.1.1). Propanoyl-CoA is metabolised into (S)-2-methylmalonyl-CoA by propionyl-CoA carboxylase (EC 6.4.1.3). (S)-2-methylmalonyl-CoA is then transformed to succinyl-CoA and succinate by methylmalonyl-CoA epimerase (EC 5.1.99.1), methylmalonyl-CoA mutase (EC 5.4.99.2) and succinyl-CoA ligase (EC 6.2.1.5), respectively. Succinate and succinyl-CoA can then enter the TCA cycle. It should be noted that *R. jostii* strain 8 lacks the gene encoding isopropanol dehydrogenase (EC 1.1.1.80) which converts 2-propanol to acetone. However, *R. jostii* strain 8 possesses genes encoding alcohol dehydrogenases which can convert a wide range of alcohols to ketones. There are several genes in the genome of *R. jostii* RHA1 which are not present in the genome of *R. jostii* strain 8 and vice versa. It was found that those missing genes do not make any difference to the way these two strains probably metabolise propanoate.

4.10.4. Butanoate metabolism

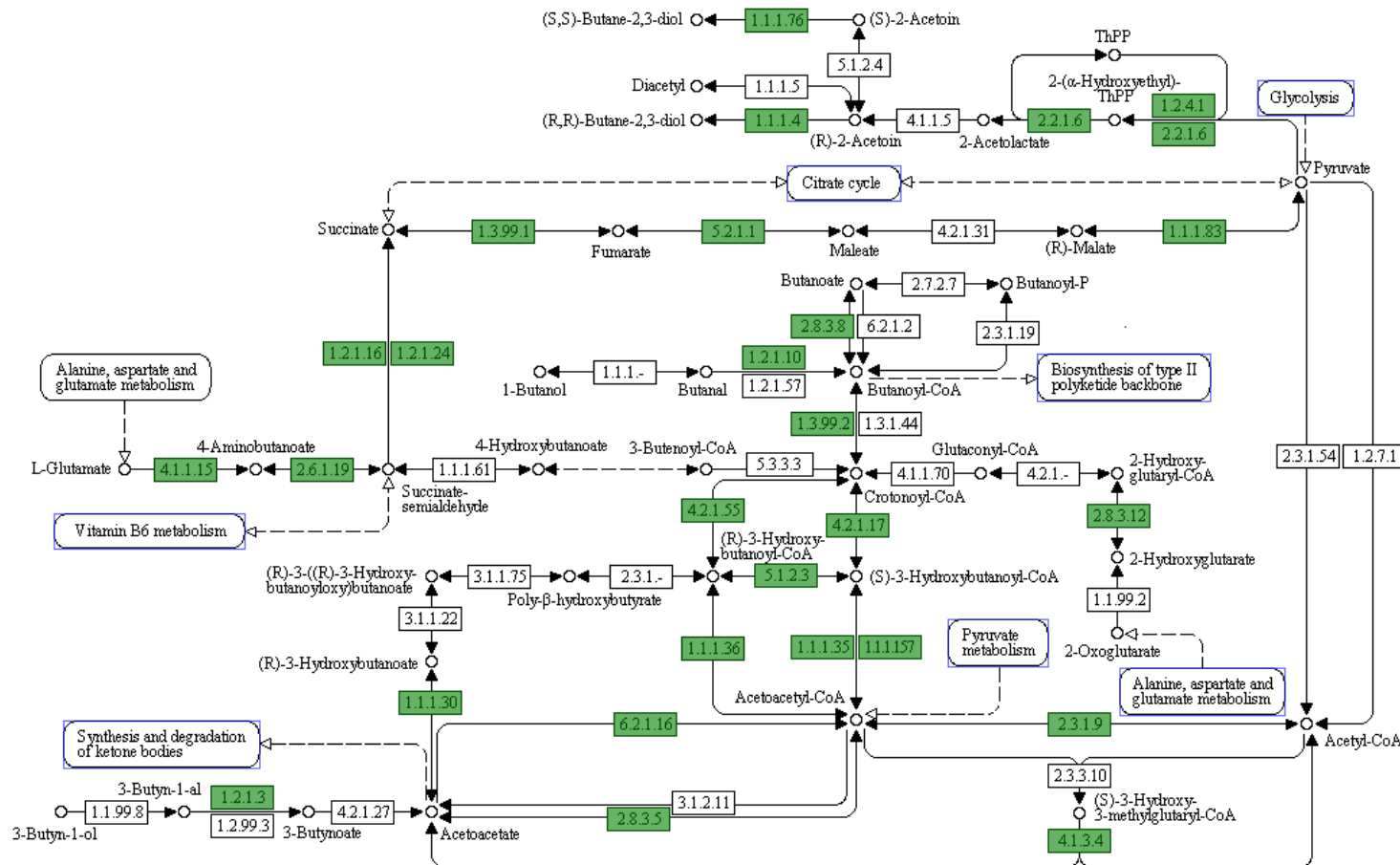


Figure 4.11: Kegg recruitment plot of genes involved in butanoate metabolism from the *R. jostii* strain 8 genome. The enzymes (indicated in EC numbers) encoded by genes present in the genome are shown in green boxes.

Because butanoate is one of the intermediates in butane metabolism, not surprisingly, there are genes encoding enzymes necessary for butanoate metabolism (Figure 4.11) present in the genome of *R. jostii* strain 8. The pathway starts with the conversion of butanoate into butanoyl-CoA by acetoacetyl-CoA transferase (EC 2.8.3.8). Butanoyl-CoA is then converted through crotonoyl-CoA to acetoacetyl-CoA by enoyl-CoA hydratase (EC 4.2.1.17) and 3-hydroxyacyl-CoA dehydrogenase (EC 1.1.1.35) or 3-hydroxybutyryl-CoA dehydrogenase (EC 1.1.1.157), respectively. Acetoacetyl-CoA is then metabolised into acetyl-CoA by acetyl-CoA acetyltransferase (EC 2.3.1.9). Acetyl-CoA then enters central metabolism. It was found that *R. jostii* strain 8 possesses several genes encoding enzymes in butanoate metabolism. There are also a few of these genes in the genome of *R. jostii* RHA1 which are not present in the genome of *R. jostii* strain 8, but, similar to propanoate metabolism, the absence of those genes does not affect the pathway by which these two strains could probably metabolise butanoate.

4.11. Discussion and conclusions

Rhodococcus jostii strain 8 is a gaseous alkane (C₂-C₄) degrader isolated from petroleum contaminated soil. The 16S rRNA gene sequence of *R. jostii* strain 8 is closely related to *R. jostii* RHA1, a biphenyl degrader whose complete genome is available (McLeod et al., 2006). Although the genome of *R. jostii* strain 8 was not complete, all key genes involved in central metabolism (e.g. TCA cycle and glycolysis pathway) and other specific pathways (e.g. alkane metabolism) were present and annotated.

It was found that the genome of *R. jostii* strain 8 carries a complete *nar* operon encoding putative naphthalene 1,2-dioxygenase, but this operon is absent in the genome of *R. jostii* RHA1. Moreover, *R. jostii* strain 8 lacks the genes necessarily required for the expression of biphenyl and ethylbenzene dioxygenases. In contrast, *R. jostii* RHA1 possesses complete operons encoding these two enzymes. This is confirmed by growth of *R. jostii* strain 8 on naphthalene and no growth on biphenyl or ethylbenzene. According to the presence of the complete gene clusters, there are two different monooxygenase systems, which are likely to be involved in the degradation of gaseous alkanes, found in the genome of *R. jostii* strain 8. One of the enzymes is propane monooxygenase which belonging to the soluble diiron monooxygenase family (Coleman et al., 2006). The propane monooxygenase gene cluster of *R. jostii* strain 8 is closely related to the propane monooxygenase gene cluster of *R. jostii* RHA1. The other enzyme system that might be responsible for the growth of *R. jostii* strain 8 on gaseous alkanes is an *alkB*-type alkane monooxygenase. All of the essential genes potentially responsible for the expression of an active *alkB*-type alkane monooxygenase are present in the genome.

The presence of enzymes necessary for propanoate metabolism suggested that *R. jostii* strain 8 may metabolise propane via propanoate which is also an intermediate in the terminal pathway in propane metabolism (see Figure 5, Section 4.1.2., Chapter 1) in *Rhodococcus rhodochrous* PNKb1 (Woods & Murrell, 1989). Similar to propane metabolism, *R. jostii* strain 8 probably oxidises butane via butanoate since essential genes required for the metabolism of butanoate were present in the genome. It was found that *R. jostii* RHA1 probably also metabolises

propanoate and butanoate through similar pathways as *R. jostii* strain 8. This remains to be tested in the future.

The genes encoding enzymes responsible for fixation of N₂ are absent, but *R. jostii* strain 8 has the genes necessary for the utilization of inorganic nitrogen such as ammonia, nitrite and nitrate. Throughout this research, potassium nitrate (KNO₃), included in NMS medium (see Chapter 2), was used as a nitrogen source for *R. jostii* strain 8. According to the sulfur metabolism pathways indicated by the genome sequence, *R. jostii* strain 8 is able to utilize sulfate as a sulfur source. Sulfate compounds such as magnesium sulfate (MgSO₄·7H₂O), Zinc sulfate (ZnSO₄·7H₂O) were also constituents of NMS medium.

In order to determine the role of propane monooxygenase and *alkB*-type alkane monooxygenase in the growth of *R. jostii* strain 8 on gaseous alkanes, physiological characterisation of these enzymes such as growth tests on a range of substrates, transcription of the key genes of these enzymes, profiling polypeptides from cell-free extracts of cells grown on different substrates and gene disruption analysis will be required (see discussion in Chapter 7).

Chapter 5

Expression of propane monooxygenase and alkane hydroxylase

5.1. Introduction

prmA encodes the large subunit of the hydroxylase component of the multi-component propane monooxygenase of the soluble diiron centre family. Propane monooxygenase is involved in the oxidation of propane, but is not involved significantly in the oxidation of other alkanes. For example, the transcription of the *prm* gene cluster in *Gordonia* sp. strain TY-5 is induced during growth on propane. Although the *prm* operon is induced weakly by ethane and butane, this organism lacks the ability to grow on ethane and butane (Kotani et al., 2003). In *R. jostii* RHA1, which can grow only on propane and not on the gaseous alkanes, the *prmA* gene was up-regulated during growth on propane (Sharp et al., 2007). Similar to *Gordonia* TY-5, *Rhodococcus* RHA1 does not grow on any other gaseous alkanes except propane (McLeod et al., 2006).

alkB encodes the large subunit of a membrane-bound alkane monooxygenase, the enzyme which typically oxidises liquid alkanes such as hexane and octane. This type of alkane monooxygenase can be induced by propane in some bacteria *e.g.* *Mycobacterium austroafricanum* and *Nocardia* sp. CF 8, but not in others (Hamamura et al., 2001; Lopes Ferreira et al., 2007). There are some reports describing the involvement of alkane hydroxylase in the growth of bacteria on *n*-alkanes including gaseous alkanes. *Pseudomonas putida* GPo1, a model organism for bacterial oxidation of alkanes other than methane, could grow on C₅ to C₁₃ *n*-alkanes and also the gaseous alkanes such as propane and butane. However, no growth on methane or ethane was observed (Johnson and Hyman, 2006). These researchers also found that there was no growth of an alkane hydroxylase-deficient strain GPo12 (Smith and Hyman, 2004) on propane or butane, even after incubating with the maximum concentrations (\approx 45% v/v gas phase) of these gases over 10 days (Johnson and Hyman, 2006). This suggested that alkane hydroxylase in *P. putida* GPo1 is responsible for growth on propane and butane. There was expression of the *alkB* gene, detected by RT-PCR, in *Mycobacterium austroafricanum* strains after growth on propane and a few other liquid alkanes such as hexane and hexadecane, which are growth substrates for these strains (Lopes Ferreira et al., 2007). These results suggested that alkane hydroxylase was induced during growth on propane and other liquid alkanes. *Mycobacterium vaccae* strain JOB-5 (Hamamura et al., 1999) which was capable of degrading propane does not possess a propane monooxygenase

homologue, but contains two functional alkane monooxygenases of the *alkB* type. However, transcription levels of these *alkB*-related alkane monooxygenases were not up-regulated after growth on propane (Sharp et al., 2010).

In this work, the expression of *prmA* and *alkB* in *R. jostii* strain 8 during growth on alkanes was investigated. Cell extracts from *R. jostii* strain 8 cells grown on alkanes were analysed on SDS-PAGE in order to identify polypeptides corresponding to monooxygenases involved in alkane oxidation. Transcription levels of *prmA* and *alkB* during growth on different carbon sources were quantified by RT-qPCR. Propane monooxygenase and alkane monooxygenase (*alkB*) gene clusters in *R. jostii* strain 8 have been identified from the genome. *prmA*, a key gene in the propane monooxygenase gene cluster, of *R. jostii* strain 8 is closely related to the gene of *Rhodococcus jostii* RHA1. *alkB* encoding the large subunit of alkane hydroxylase is closely related to the *alkB* gene of *Rhodococcus wratislaviensis* strain IFP 2016 (Auffret et al., 2009), whose alkane monooxygenase has never been characterised. The aim of experiments described in this chapter was to determine whether *prmA* and/or *alkB* is induced during growth of *R. jostii* strain 8 on ethane, propane, butane and octane.

5.2. Polypeptide analysis: Expression of propane monooxygenase polypeptides during growth on propane

The aim of this study was to investigate the presence of propane monooxygenase subunits in *R. jostii* strain 8 during growth on alkanes by analysing polypeptide profiles using SDS-PAGE. *R. jostii* strain 8 was grown to mid-exponential phase in flask cultures on 10 mM glucose, 10% (v/v) ethane, 10% (v/v) propane or 10% (v/v) butane. The cultures were harvested at mid-exponential phase. Cell-free extracts of *R. jostii* strain 8 were prepared using the French Press method (section 2.14) and then analysed on a 12.5% SDS-PAGE gel together with the extracts of *Methylocella silvestris* BL2 from cells grown on methane and propane. These were run as controls to determine the positions of the expected bands (*e.g.* the hydroxylase large subunit of propane monooxygenase) because *M. silvestris* BL2 possessed soluble methane monooxygenase and propane monooxygenase which belong to SDIMO family (Chen et al., 2010). Several distinct bands from each polypeptide profile (Figure 5.1 and 5.2) were excised into approximately 1 mm-thick gel slices for polypeptide analysis by tryptic digest and LC/EI-MS/MS at the University of Warwick Biological Mass Spectrometry and Proteomics Facility. The data were analysed against protein databases compiled from the *R. jostii* RHA1 (McLeod et al., 2006) and *R. jostii* strain 8 genomes (Chapter 4).

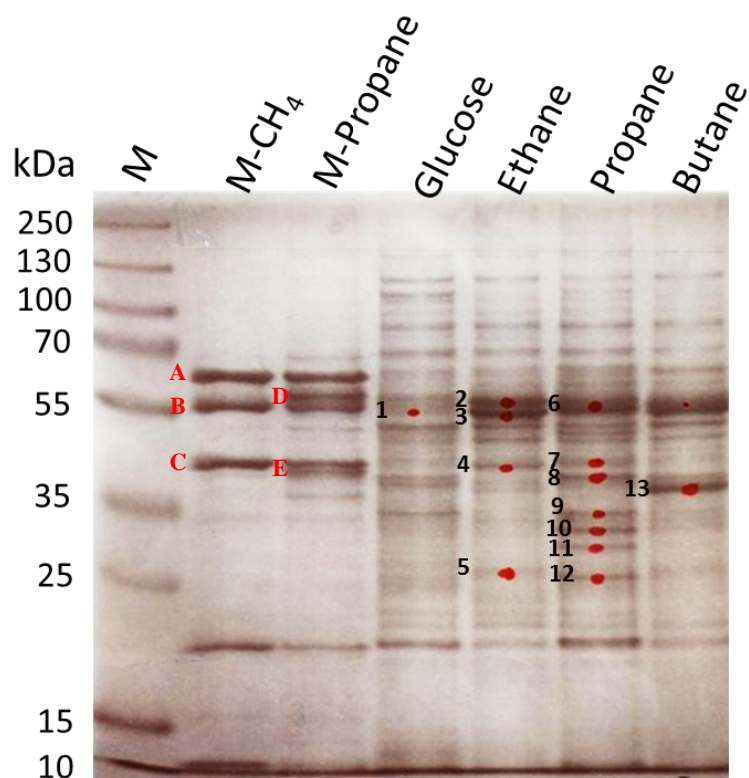


Figure 5.1: SDS-PAGE analysis of cell-free extracts from *R. jostii* strain 8 grown on glucose, ethane, propane and butane. 15 µg of protein were loaded in each lane. Bands which were excised for polypeptide identification by mass spectrometry analysis against the *Rhodococcus jostii* RHA1 genome are numbered. M: PageRuler Plus molecular mass marker (Fermentas); M-CH₄: cell-free extract of *Methylocella silvestris* BL2 grown on 10% (v/v) methane; M-propane: cell-free extract of *Methylocella silvestris* BL2 grown on 10% (v/v) propane. A: α-subunit of methanol dehydrogenase; B: α-subunit methane monooxygenase; C: β-subunit of methane monooxygenase; D: α-subunit of propane monooxygenase; E: β-subunit of propane monooxygenase.

Initially, polypeptide analysis was carried out against the *R. jostii* RHA1 genome because the *R. jostii* strain 8 was not yet available. However, the mass spectrometry data were re-analysed against the *R. jostii* strain 8 protein database later when the genome sequence of *R. jostii* strain 8 was obtained. PAGE analysis showed that the polypeptide patterns of cells grown on alkanes are different from those grown on glucose. This suggested that the enzymes involved in alkane degradation by *R. jostii* strain 8 are inducible. The polypeptide patterns of cell-free extracts from

cells grown on other alkanes were also different. This suggested that it was likely that *R. jostii* strain 8 used more than one enzyme system to grow on gaseous alkanes. Prior to the availability of the genome sequence of *R. jostii* strain 8, the excised bands present at approximately the size of propane monooxygenase subunits and other polypeptides which were distinct from those present in cell-free extract from glucose were initially analysed against the *R. jostii* RHA1 genome. The aim was to investigate if there were any soluble monooxygenase subunits in *R. jostii* RHA1, which corresponded to the excised polypeptides of *R. jostii* strain 8. A list of polypeptides corresponded to the excised bands analysed against the *R. jostii* RHA1 genome is shown in Table 5.1.

Table 5.1: Mass spectrometry analysis of polypeptides identifications of gel bands (shown in Figure 4.2.1.) after comparison with the *R. jostii* RHA1 genome. MM: theoretical molecular mass

Bands	Growth condition	Description	Peptides	MM (kDa)
1	Glucose	ATP synthase subunit beta	6	51984
		Glutamine synthetase	2	53450
2	Ethane	Chaperonin (1)	10	56617
		Glutamine synthetase	5	53450
		Aldehyde dehydrogenase	2	55135
3	Ethane	Chaperonin (2)	2	56168
		Chaperonin (1)	2	56617
4	Ethane	Phosphoserine aminotransferase	2	39574
		Elongation factor	2	43509
		Probable FMN dependent-S-2-hydroxy acid oxidase	2	41779
5	Ethane	Chaperonin (1)	3	56617
		50S ribosomal protein L4	2	24498
6	Propane	Propane monooxygenase hydroxylase large subunit	3	63181
		ATP synthase subunit beta	3	51984
		Ethylbenzene dioxygenase alpha subunit	2	51656
		Aldehyde dehydrogenase	2	55135
		Glutamine synthetase	2	53450
7	Propane	Succinyl-CoA ligase ADP forming subunit beta	5	40790
		Phosphoglycerate kinase	2	42075

Table 5.1: (continued)

Bands	Growth condition	Description	Peptides	MM (kDa)
8	Propane	Glyceraldehyde-3-phosphate dehydrogenase	8	35642
		Putative uncharacterized protein	2	40140
		Succinyl-CoA ligase ADP forming subunit beta	2	40790
9	Propane	Alcohol dehydrogenase	3	35743
		Elongation factor	3	29302
		propane monooxygenase hydroxylase small subunit	2	41669
		Cell division initiation protein	2	30370
10	Propane	2, 3-dihydroxybiphenyl 1, 2-dioxygenase	4	34005
11	Propane	2-hydroxy 6-oxo 6-phenylhexa 2, 4-dienoate hydrolase	10	31622
		Putative uncharacterized protein	2	28466
12	Propane	<i>Cis-3-phenylcyclohexa</i> 3, 5-diene 1, 2-diol dehydrogenase	6	28248
13	Butane	Alcohol dehydrogenase	6	38891
		Glyceraldehyde-3-phosphate dehydrogenase	3	35642

Note: chaperonin (1): accession number YP_702111.1, chaperonin (2): accession number WP_005253893.1

Some of the identified polypeptides corresponded to the polypeptides which are commonly found in membrane of cells *e.g.* ATP synthase, glutamine synthetase. This is because cell-free extracts contained both the soluble and membrane-bound components. Not surprisingly, band number 6 and 9, which were present in cell-free extracts from cells grown on propane, corresponded to the α - and β -subunits hydroxylase of a putative propane monooxygenase from *R. jostii* RHA1. This indicated that there was an expression of propane monooxygenase under growth of *R. jostii* strain 8 on propane. However, no polypeptides corresponding to propane monooxygenase or any of alkane-degrading enzymes, *i.e.* alkane hydroxylase were detected in cell-free extracts from cells grown on other substrates. This is probably because the *R. jostii* RHA1 genome was not an ideal database for an analysis of polypeptides from *R. jostii* strain 8. Identification of polypeptides by mass spectrometry using the *R. jostii* strain 8 genome was subsequently carried out.

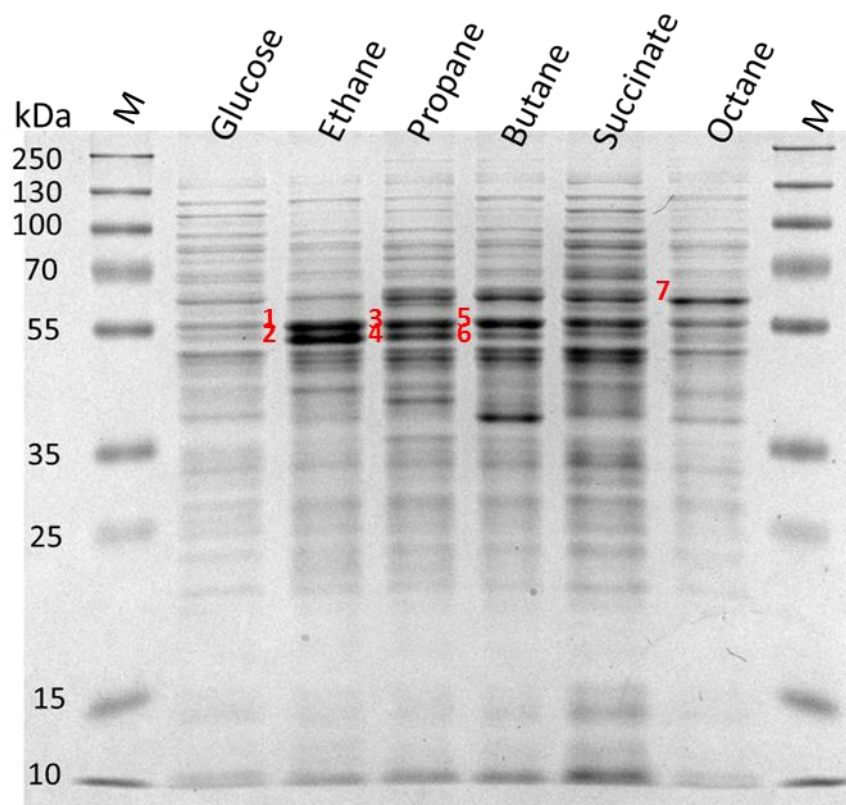


Figure 5.2: SDS-PAGE analysis of cell-free extracts from *R. jostii* strain 8 grown on glucose, ethane, propane, butane, succinate and octane. 15 μ g of cell extracts were loaded in each lane. M: PageRuler Plus molecular mass marker (Fermentas). Bands which were excised for polypeptide identification by mass spectrometry analysis against the *R. jostii* strain 8 genome are numbered.

Cell-free extracts of *R. jostii* strain 8 grown under different conditions were prepared as done previously. Cell-free extracts from *R. jostii* strain 8 grown on 5 mM succinate was included to serve as control cell-free extract from an alternative non-alkane substrate to glucose. Also, cell-free extract from octane-grown cells (0.1% (v/v) of octane in the culture) was included since it might induce a membrane-bound alkane hydroxylase subunit (AlkB) similar to what was found in *Pseudomonas putida* (Eggink et al., 1987). SDS-PAGE was repeated (Figure 5.2.) to obtain polypeptide patterns of cell-free extracts from each growth condition. Some distinct polypeptide bands (as numbered in Figure 4.2.2.) were excised for mass spectrometry analysis against the *R. jostii* strain 8 genome database. Identification of polypeptides using the *R. jostii* strain 8 genome database is shown in Table 5.2.

Table 5.2: Mass spectrometry analysis of polypeptides identifications of gel bands (shown in Figure 5.2) after comparison with the *R. jostii* strain 8 genome.

The five most abundant peptides are shown for each band, except some for which there were less than five peptides detected. MM: theoretical molecular mass

Band	Growth condition	Annotation	Peptides	MM (kDa)
1	Ethane	Aldehyde dehydrogenase (1)	25	55100
		Glutamine synthetase (1)	10	53450
		ATP synthase beta chain	7	51984
		Chaperone GroEL (1)	6	56617
		Chaperone GroEL (2)	3	56153
2	Ethane	Chaperone GroEL (1)	10	56617
		Aldehyde dehydrogenase (1)	10	55100
		Glutamine synthetase (2)	2	49650
		Dihydrolipoamide dehydrogenase	2	49781
3	Propane	Aldehyde dehydrogenase (1)	20	55100
		Glutamine synthetase (1)	11	53450
		ATP synthase beta chain	8	51984
		Chaperone GroEL (1)	4	56617
		Propane monooxygenase hydroxylase large subunit	2	63239
4	Propane	Aldehyde dehydrogenase (1)	8	55100
		Dihydrolipoamide dehydrogenase	5	49781
		Chaperone GroEL (3)	4	58087
		Branched-chain amino acid ABC transporter	4	44475

Table 5.2: (continued)

Band	Growth condition	Annotation	Peptides	MM (kDa)
5	Butane	Chaperone GroEL (1)	23	56617
		Long-chain-fatty-acid--CoA ligase	15	56148
		Acetoacetyl-CoA synthetase	11	59442
		Chaperone GroEL (2)	9	56153
		ATP synthase alpha chain	6	58475
6	Butane	Aldehyde dehydrogenase (2)	15	53009
		Aldehyde dehydrogenase (1)	14	55100
		Glutamine synthetase (1)	13	53450
		Chaperone GroEL (1)	10	56617
		Chaperone GroEL (2)	5	56153
7	Octane	Chaperone GroEL (1)	14	56617
		Hypothetical protein	9	61083
		Acetoacetyl-CoA synthetase	7	59442
		Chaperone GroEL (2)	5	56153
		Long-chain-fatty-acid-CoA ligase	3	56148

Note: The numbers in brackets indicated different forms of polypeptides in *R. jostii* strain 8. chaperone GroEL (1): accession number YP_702111.1, chaperone GroEL (2): accession number WP_005253893.1, chaperone GroEL (3): accession number WP_007297713.1, glutamine synthetase (1): accession number YP_002778076, glutamine synthetase (2): accession number YP_002778076.1, aldehyde dehydrogenase (1): accession number WP_005253809.1, aldehyde dehydrogenase (2): accession number WP_005251153.1

The main purpose of the identification of polypeptides using the *R. jostii* strain 8 genome as a database was to confirm that using the *R. jostii* strain 8 protein database as a reference for mass spectrometry analysis generated the same results as when using the *R. jostii* RHA1 genome as a reference. Seven bands (as numbered in Figure 4.2.2.) were excised for polypeptides analysis against the *R. jostii* strain 8 genome. According to the analysis of the *R. jostii* strain 8 genome, the molecular mass of propane monooxygenase large subunit (α -subunit hydroxylase) was approximately 64 kDa and the molecular mass of propane monooxygenase small subunit (β -subunit hydroxylase) was approximately 40 kDa. The α -subunit hydroxylase of propane monooxygenase was detected in cell-free extract from propane-grown cells. Unfortunately, there was no possible polypeptide relating to membrane-bound alkane-degrading enzyme subunits detected in cell-free extracts from ethane-, butane- and octane-grown cells. Cell-free extracts were then prepared by boiling whole cells in SDS (Chapter 2, section 2.25) in order to analyse both soluble proteins and membrane proteins which might include components of a membrane-bound alkane hydroxylase such as the alk system (alkB). This, in theory, should allow the visualisation of bands corresponding to membrane-bound polypeptides on the SDS-PAGE gel. The total amount of proteins in cell-free extracts was quantified by using the Bradford assay. Since the concentrations of cell-free extracts were very low (less than 2 $\mu\text{g}/\mu\text{l}$), maximum volume (35 μl) of the extracts mixed with loading dye were then run on the SDS-PAGE gel for polypeptide analysis. SDS-PAGE analysis of cell-free extracts using boiled whole cells of *R. jostii* strain 8 grown on glucose, ethane, propane, butane, succinate and octane is shown in Figure 5.3.

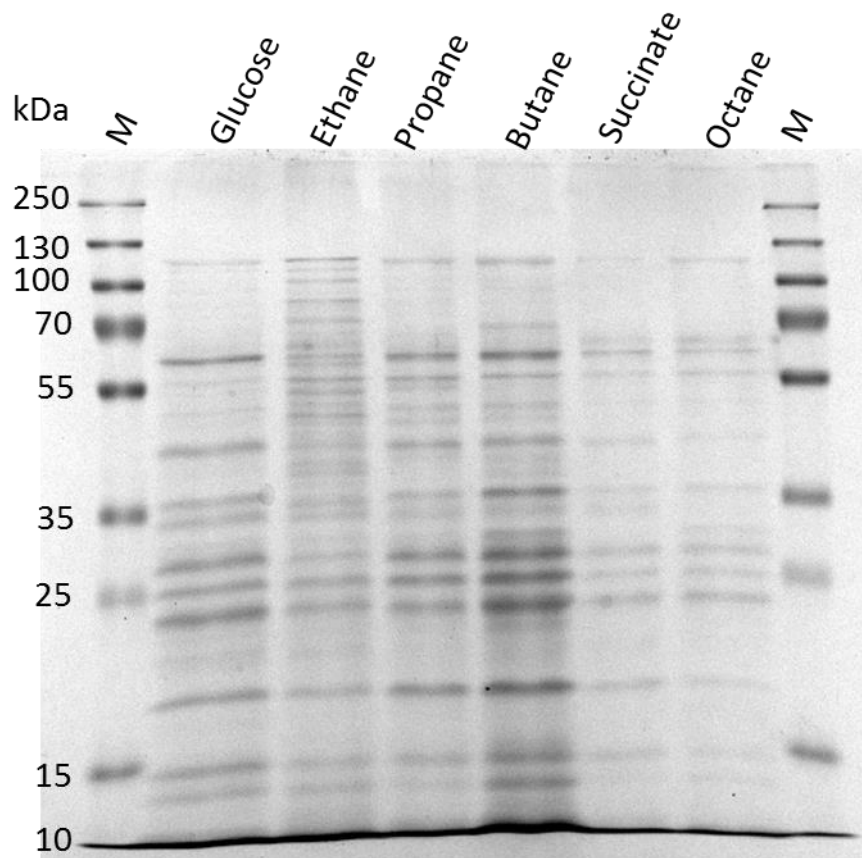


Figure 5.3: SDS-PAGE analysis of cell-free extracts (extracted by boiling preparation) from strain 8 grown on glucose, ethane, propane, butane, succinate and octane. 35 μ l of cell-free extracts were loaded in each lane. M: PageRuler Plus molecular mass marker (Fermentas).

Polypeptide profiles of *R. jostii* strain 8 grown on different growth conditions (Figure 5.3) were not obviously different. It was also found that the total protein concentration quantified by Bradford assay was not accurate. This could be observed when loading known amounts of protein of cell-free extracts from French Press extraction alongside the cell-free extracts from boiling preparation (data not shown). The total amount of proteins quantified by Bradford assay was not even close to the expected amount seen on the gel. This is probably because the buffer which was used in boiling preparation affected quantification by the Bradford assay. Also, protein extraction by the boiling preparation did not yield as much proteins as obtained from the extraction by the French Press method. Since the polypeptide profiles of cell-free extracts from boiling preparation was similar between different

growth conditions, mass spectrometry analysis of the polypeptide bands was not carried out. The polypeptide profiles in Figure 5.3 suggested that *R. jostii* strain 8 is likely to use alkane-degrading enzyme system(s) other than propane monooxygenase which enable it to grow on ethane, butane and octane. Although polypeptide profiles of cell-free extracts of *R. jostii* strain 8 grown on octane might have shown an alkane hydroxylase subunit corresponding to one found in the genome of *R. jostii* strain 8 which has a predicted molecular mass of approximately 41 kDa (Eggink et al., 1987), the bands appearing between 35-55 kDa were not distinct from those which appeared in cell-free extracts from cells grown on other substrates. In conclusion, propane monooxygenase was expressed in *R. jostii* strain 8 during growth on propane. However, the expression of other alkane-degrading enzyme(s) was still unclear.

5.3. Discussion for polypeptide analysis

The aim of this work was to investigate the induction of propane monooxygenase and alkane monooxygenase during growth of *Rhodococcus jostii* strain 8 on alkanes – ethane, propane, butane and octane. SDS-PAGE analysis of cell extracts from cells grown on different carbon sources showed that polypeptide profiles of cell extracts from cells grown on alkanes were different from the profile of cell extract from cells grown on glucose and succinate. This suggested that those polypeptides were inducible. The dominant polypeptide bands were excised and then analysed against the *R. jostii* RHA1 and the *R. jostii* strain 8 genomes. The analysis results will be discussed in more detail in the next paragraphs.

The polypeptides corresponded to the α - and β -subunits of the propane monooxygenase from *Methylocella silvestris* BL2 grown on propane were shown up at molecular masses of 64.2 and 40.2 kDa, respectively (Crombie and Murrell, 2014). Three major polypeptides with molecular masses of 69, 59 and 57 kDa were detected in cell extract from *Rhodococcus rhodochrous* PNKb1 cells grown on propane (Woods and Murrell, 1989). These polypeptides were then believed that they are components of propane monooxygenase. In *R. jostii* strain 8, the large and small subunits of propane hydroxylase were detected in cell extract from cells grown on propane (band 6 and 9 in Figure 5.1). The polypeptides with molecular masses of 63.2 and 41.7 kDa, similar size to the subunits found in *M. silvestris* BL2, corresponded to the α - and β -subunits of propane hydroxylase, respectively. The partially purified soluble butane monooxygenase from *Pseudomonas butanovora* were analysed on SDS-PAGE (Sluis et al., 2002). The researchers found that the multicomponent enzyme comprised of three polypeptides with molecular masses of 54, 43 and 25 kDa. Those polypeptides corresponded to the α -, β - and γ -subunits of the enzyme, respectively. SDS-PAGE analysis of polypeptides relating to soluble methane monooxygenase was carried out with purified enzymes from *Methylosinus trichosporium* OB3b (Fox et al., 1989). Polypeptides with molecular masses of 54.4, 43.0, 22.7, 39.7 and 15.8 kDa corresponded to the α -, β -, γ -subunits, reductase and coupling protein of the soluble methane monooxygenase. The prominent gel bands band 5 and 6 in Figure 5.2) with molecular masses of approximately 54 kDa, which were expected to correspond to the subunits of butane monooxygenase or an enzyme related to soluble methane monooxygenase (a soluble diiron centre monooxygenase),

were excised for mass spectrometry analysis. Unfortunately, those polypeptides did not correspond to the α -subunit of butane monooxygenase as was expected, but they were identified as chaperone GroEL and some other enzymes which do not directly relate to butane monooxygenase. The other gel bands from ethane-grown cell extract (band 1 and 2 in Figure 4.2.2) with a molecular mass of approximately 54 kDa were also excised for the analysis. Similar to the dominant band from butane-grown cell extract, these polypeptides did not correspond to any subunits of the soluble butane or methane monooxygenases. Therefore, propane monooxygenase was induced only during growth of *R. jostii* strain 8 on propane.

The appearance of a 58 kDa polypeptide from membrane fractions of *Pseudomonas* sp. IMT40 and *Rhodococcus* sp. IMT35 grown on propane and butane, but not in glucose- or nutrient broth-grown cell extracts suggested the involvement of this particular polypeptide in propane and butane utilisation in these organisms (Padda et al., 2001). A polypeptide with a similar molecular mass was also detected in cell extracts of *Pseudomonas butanovora* (recently re-named *Thauera butanivorans*) and *Mycobacterium vaccae* JOB-5 grown on butane (Hamamura et al., 1999). The researchers suggested that this polypeptide could be a component of butane monooxygenase, based on a [^{14}C] acetylene inhibition labelling experiment. In this research, a polypeptide in cell extract of butane-grown *R. jostii* strain 8 of approximately 58 kDa corresponded to chaperone GroEL. The role of chaperone GroEL in the function of soluble monooxygenases was studied in detail with butane monooxygenase and soluble methane monooxygenase (Kurth et al., 2008; Scanlan et al., 2009). Kurth and his team found that a *Pseudomonas butanovora* mutated in *bmoG*, a gene predicted to encode for chaperone GroEL, could not grow on C_2 - C_8 alkanes. They suggested that this chaperone GroEL may be involved in the assembly of an active butane monooxygenase. Similar result was also found with the soluble methane monooxygenase (sMMO) of *Methylosinus trichosporium* OB3b (Scanlan et al., 2009). These researchers suggested that MmoG, encoding a GroEL-like chaperone, may play a role in the transcription of soluble methane monooxygenase and/or is involved in sMMO enzyme assembly. Although the induction of particular enzyme systems during growth of *R. jostii* strain 8 on alkanes is yet unclear, a polypeptide corresponding to chaperone GroEL was prominent and detectable in cell extracts from cells grown on ethane, propane and

butane, but not glucose (Table 4.2.1.). This suggested that this chaperone GroEL may involve in the function of alkane-degrading enzyme in *R. jostii* strain 8. However, further studies could be carried out to determine whether or not the exact role of the chaperone GroEL in the degradation of alkanes in *R. jostii* strain 8 will be similar to those were found in *Pseudomonas butanovora* and *Methylosinus trichosporium* OB3b.

One of the polypeptides (38.9 kDa) in cell extract from butane-grown cells which corresponded to an alcohol dehydrogenase (band 13 in Figure 5.1) is also of interest since it was induced during growth of *R. jostii* strain 8 on butane. Therefore, it might be that this alcohol dehydrogenase is an enzyme involved in the oxidation of butane. In the work done by (Kotani et al., 2003), three alcohol dehydrogenases (ADH) in *Gordonia* sp. TY-5 were purified and analysed on SDS-PAGE. The polypeptide with a molecular mass of 39 kDa corresponded to NAD⁺-dependent alcohol dehydrogenase 1 (ADH1) in *Gordonia* sp. TY-5. These researchers found that secondary alcohols of up to five carbons in length were preferred substrates for this type of ADH. The ADH1 was also able to reduce acetone, acetol and 2-butanone which are intermediates in the oxidation of propane and butane.

Polypeptides corresponding to subunits of alkane hydroxylase were first studied in *Pseudomonas putida* (Benson et al., 1979; Owen et al., 1984). Alkane hydroxylase had a molecular mass of 40 kDa. Polypeptides with molecular masses of 54, 19, 47 and 59 kDa corresponded to rubredoxin reductase, rubredoxin and two components of alkanol dehydrogenase, respectively. A similar polypeptide with a molecular mass of 41 kDa, was also identified as an alkane hydroxylase, was found in *Pseudomonas oleovorans* (Eggink et al., 1987). These researchers suggested that alkane hydroxylase consisted of polypeptides with molecular masses of 41, 15, 49, 58, 59 and 20 kDa. The 15 and 49 kDa polypeptides were identified as rubredoxin and rubredoxin reductase. Polypeptides with similar molecular masses were not prominent in cell extracts from *R. jostii* strain 8 grown on any substrates (Figure 5.1 and 5.2). Although the 20 kDa polypeptide was visible, it was induced during all growth conditions including glucose. Thus, it is unlikely that this polypeptide will be specifically involved in the degradation of alkanes in *R. jostii* strain 8. The polypeptide with a molecular mass of approximately 58-59 kDa (band 7 in Figure 5.2) was identified as acetoacetyl-CoA synthetase, aldehyde dehydrogenase and

chaperone GroEL. Unfortunately, these enzymes were not particularly related to alkane hydroxylase. Therefore, alkane hydroxylase subunits such as *alkB* were not detected in cell extracts from *R. jostii* strain 8 grown on any alkanes. The reasons why alkane hydroxylase component was not detectable in cell extracts of *R. jostii* strain 8 maybe due to instability of the components (McKenna and Coon, 1970; Ruettinger et al., 1974) or alkane hydroxylase was not highly induced during mid- to late-exponential phase of growth, which is when the cells were harvested for use in this experiment.

The absence of polypeptides corresponding to the copper-containing monooxygenases, enzymes possessing similar function and structure to the particulate methane monooxygenase, in *R. jostii* strain 8 can be described as follows. There was no copper-containing monooxygenase gene homologue in the genome of *R. jostii* strain 8.

According to the [¹⁴C] acetylene inhibition assay in *Nocardia* sp. CF8, the covalent binding of ¹⁴C-acetylene to a 30 kDa polypeptide suggested that the enzyme involved in the growth of this bacterium on butane possesses copper-containing monooxygenase(s) (Hamamura et al., 1999). The molecular mass of this polypeptide was also similar to the polypeptide of particulate monooxygenase and ammonia monooxygenase (27 kDa) in *Methylococcus capsulatus* (Bath) and *Nitrosomonas europaea*, respectively (Hyman and Wood, 1985). Hamamura and colleagues then suggested that butane monooxygenase in *Nocardia* sp. CF8 is a copper-containing monooxygenase which is the same type of enzyme as particulate methane monooxygenase and ammonia monooxygenase. In the case of *R. jostii* strain 8, a 30 kDa polypeptide was not detectable in cell extracts from cells grown on any tested conditions (Figure 5.2). This suggested that the enzyme system which enabled *R. jostii* strain 8 to grow on alkanes was not a copper-containing monooxygenase.

The expression of propane monooxygenase and alkane hydroxylase during growth of *R. jostii* strain 8 on alkanes was also confirmed by investigating the transcription of *prmA* and *alkB* using reverse transcriptase PCR assay. The results were discussed in the next sections.

5.4. RT-qPCR: transcription of *alkB* and *prmA* in *Rhodococcus jostii* strain 8 grown on glucose, ethane, propane, butane and octane

5.4.1. RNA extraction and assessment of RNA quality

To investigate levels of transcription of propane monooxygenase and alkane hydroxylase in *R. jostii* strain 8 grown on alkanes, reverse transcription of total RNA followed by quantitative PCR was carried out. *R. jostii* strain 8 was grown in 50 ml NMS in 250 ml flasks with 10% (v/v) of ethane, propane or butane in the headspace, or 10 mM of octane or 10 mM final concentration of glucose. Cultures were harvested at late exponential phase ($OD_{540} \approx 1.0$). To avoid RNA degradation during cell harvesting, RNA was protected by treating the cultures with RNAProtect reagent (Qiagen) following the manufacturer's instruction. RNA extraction was carried out using the hot-phenol extraction method as described by Gilbert et al., 2000, followed by DNA removal using the RNeasy cleanup kit (Qiagen). DNA contamination of RNA was checked by PCR amplification of the 16S rRNA gene with 3 μ l of RNA as template using primers 27f/1492r. PCR was run for 35 cycles. The PCR products were checked on a 1% (w/v) agarose gel. The absence of a PCR product was an indication that the RNA was DNA-free. The RNA was then stored at -80°C until further use. RNA quality was assessed by agarose gel analysis and using a Nanodrop Spectrophotometer (BioRad). An agarose gel showing RNA extracted from cells grown on different carbon sources is shown in Figure 5.4.

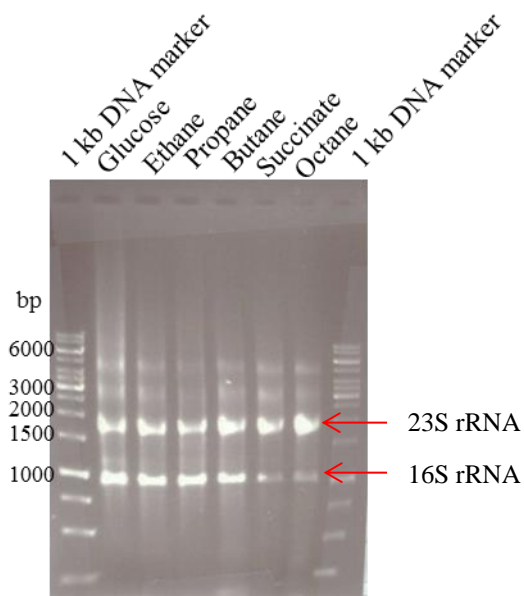


Figure 5.4: Total RNA (5 μ l each lane) extracted from cells grown on glucose, ethane, propane, butane, succinate and octane. Bands of 23S rRNA and 16S rRNA are indicated by the red arrows.

The appearance of two sharp bands of 23S rRNA and 16S rRNA, of which the 23S rRNA band is approximately twice as intense as the 16S rRNA, is judged as an indication of good intact RNA. The slight smear between the 23S and 16S rRNA bands is the area of mRNA migration and is considered as normal. No significant level of RNA degradation had occurred, which was indicated by the absence of smearing far below the 23S rRNA band. The lack of a smear in the upper part of the gel indicated the absence of DNA contamination. This was also confirmed by the absence of 16S rRNA PCR products. Therefore, these RNA samples were of high quality and were suitable for reverse transcription and qPCR assays.

5.4.2. Reverse Transcriptase PCR targeting *prmA* and *alkB*

Endpoint PCR assays targeting *prmA* and *alkB* using cDNA synthesized from cells grown on glucose, ethane, propane, butane, succinate and octane was carried out to investigate whether there was transcription of *prmA* and *alkB* under these different growth conditions. cDNA synthesis from 450 ng of RNA was carried out in 12 μ l total volume using random hexamer primers and the Superscript III reverse

transcriptase kit (Invitrogen) by following the manufacturer's instructions. Routine PCR on cDNA was carried out using PCR primers targeting *alkB* and *prmA*. PCR products were analysed on a 1% (w/v) agarose gel. The gels (Figure 5.5 and 5.6) indicated that there was transcription of both *prmA* and *alkB* in *R. jostii* strain 8 grown on all growth substrates.

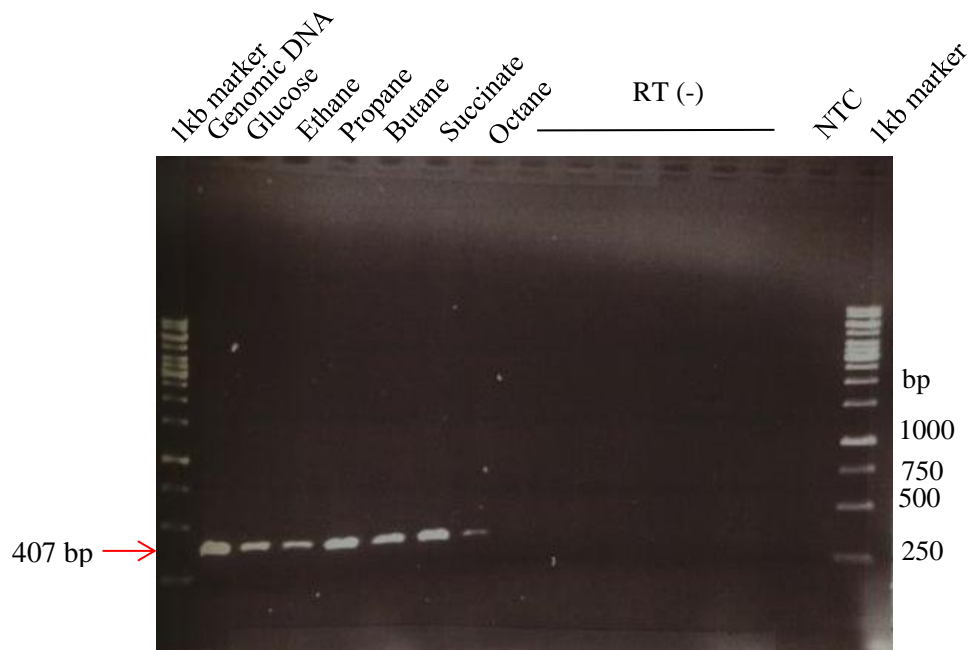


Figure 5.5: Reverse transcription followed by PCR reactions targeting *prmA*. To investigate the transcription of *prmA* in *R. jostii* strain 8 grown on glucose, ethane, propane, butane, succinate or octane. RT (-) represented PCR reactions using template from cDNA synthesis reactions where reverse transcriptase was omitted. NTC: no template control.

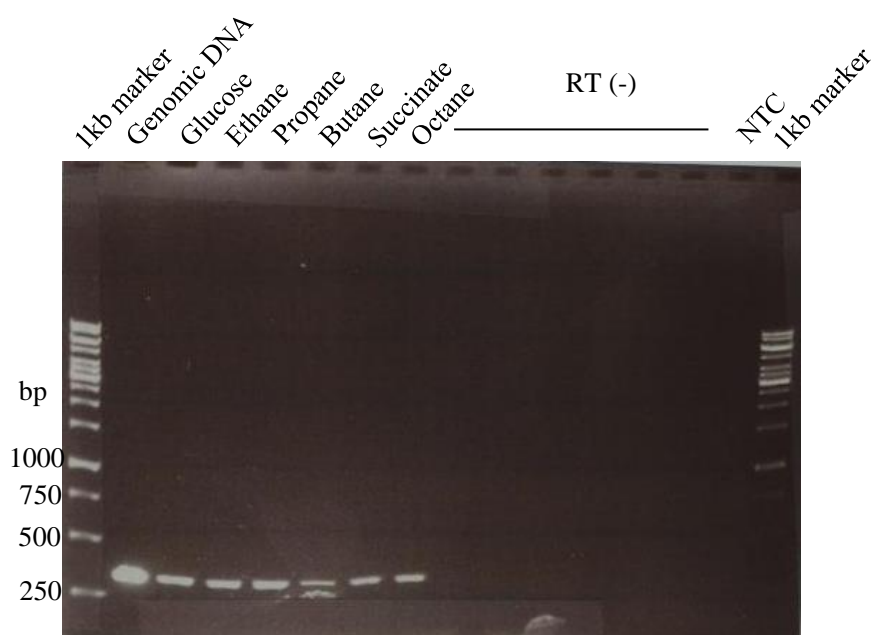


Figure 5.6: Reverse transcription followed by PCR reactions targeting *alkB*. To investigate the transcription of *prmA* in *R. jostii* strain 8 grown on glucose, ethane, propane, butane, succinate or octane. RT (-) represented PCR reactions using template from cDNA synthesis reactions where reverse transcriptase was omitted. NTC: no template control.

5.4.3. Primer optimisation for RT-qPCR

Primers used for RT-qPCR amplification of *alkB*, *prmA* and *rpoB* were designed using Primer Express 3.0.1 software (Applied Biosystems, Invitrogen, UK). A list of primers used is shown in Table 5.3.

Table 5.3: Primers used in RT-qPCR assays

Target gene	Primer sequences (5'-3')		Amplification length (bp)
	Forward primer	Reverse primer	
<i>alkB</i>	CCCGCACACAGCTGGAA	GCAGGTGGTACAGGAAGATGTTG	58
<i>prmA</i>	TCAAACAGATCATGCGGTCCTA	CGTACACGCGGTTGTCCTT	60
<i>rpoB</i>	CGGACCCGCGTTTCG	GCCGCGTAGGTCATGTCTTT	70

Primers targeting *prmA* were tested at final concentrations of 50, 100, 200 and 400 nM. Quantitative PCR reactions were performed in a total volume of 20 μ l containing 2 ng of genomic DNA as a template, SYBR Green Mastermix (Applied Biosystems, Invitrogen, UK) and the indicated concentration of primers. Each reaction was carried out in triplicate. Reactions with water in place of DNA template were included as a negative control. Amplification conditions were typically: enzyme activation (hot start) at 95°C, 20 s, denaturation at 95°C, 1s, annealing and extension at 60°C, 20 s. The data were analysed using StepOne software v 2.2.2. Melting curves for primer optimization are shown in Figure 5.7.

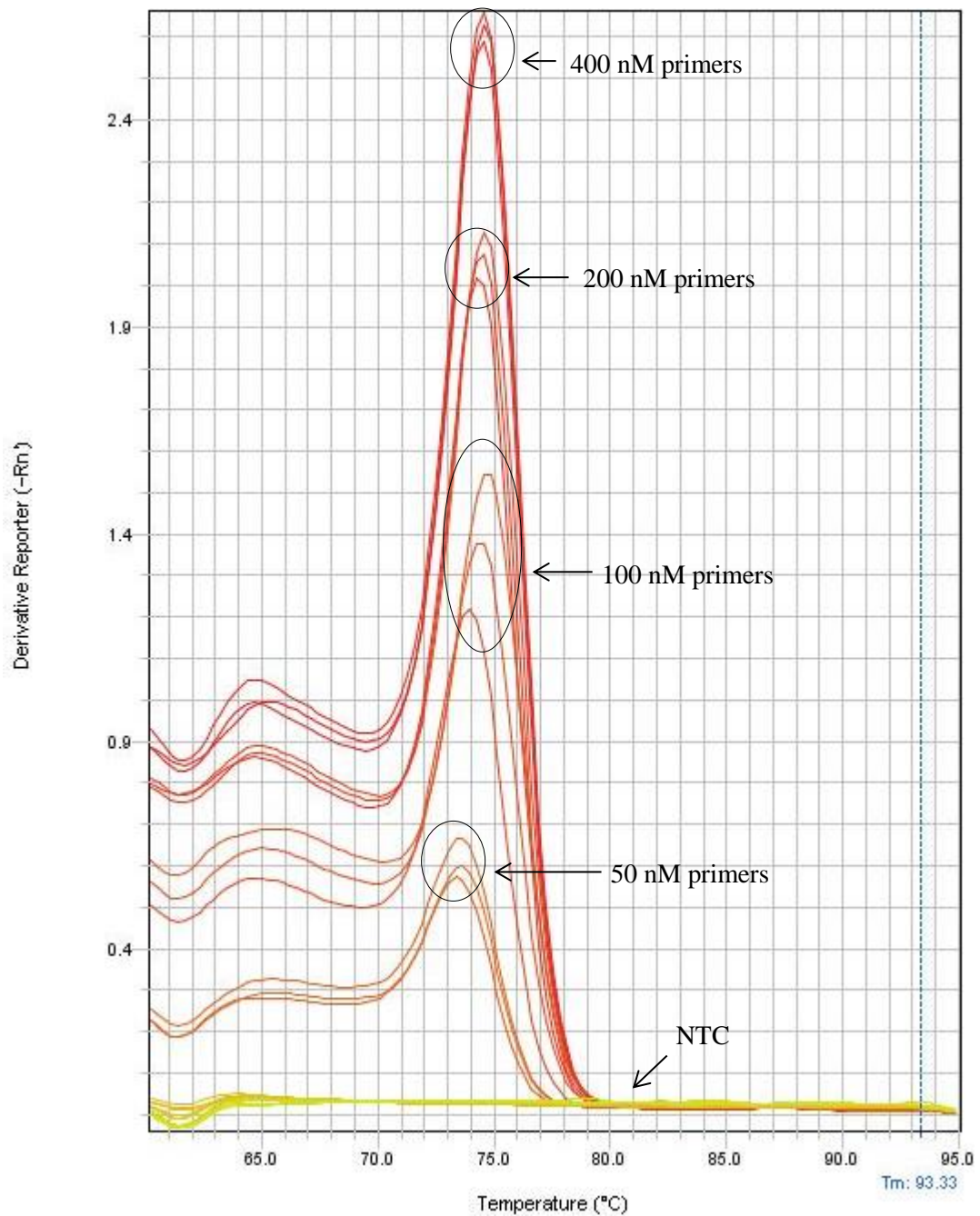


Figure 5.7: Melting curves showing fluorescent signals detected when using different concentrations of primers targeting *prmA*. Peaks corresponding to qPCR reactions containing different concentrations of primers are indicated as black arrows. NTC: no template control. C_T values (a relative indication of the concentration of amplification product) of a reaction with 50, 100, 200 and 400 nM primers are 23.5, 19.0, 18.1 and 17.8, respectively.

An acceptable level of product amplification (amplification efficiency) requires a certain minimum primer concentration. However, high primer concentrations tend to result in amplification of non-target sequences. The optimal primer concentration is thus a balance between these two factors. Non-specific amplification can be detected by melting-curve analysis (Figure 5.7).

The lowest concentration of primers resulting in high fluorescent peaks at the same relative melting temperature was considered as an optimal concentration. This is because amplification products of different lengths and sequences will melt at different temperatures. Therefore, melting peaks of triplicate amplifications appearing at the same temperature represented the specific product expected from a primer pair. In this case, a concentration of primers of 200 nM was optimal and was used for further qPCR assays.

5.4.4. Expression of propane monooxygenase and alkane hydroxylase in *R. jostii* strain 8 during different growth conditions

The expression of *prmA* and *alkB* during growth on alkanes compared to growth on glucose was investigated by using RT-qPCR assays. Quantitative PCR amplification on cDNA was carried out using the StepOnePlus Real-Time PCR system (Applied Biosystems, Invitrogen, UK). The reactions were performed in a total volume of 20 μ l containing 200 nM of forward and reverse primers, 2 μ l of cDNA templates and SYBR Green qPCR mastermix (Applied Biosystems, Invitrogen, UK) or Precision Fast 2x mastermix with SYBR Green (Primer Design, Southampton, UK). *rpoB* was also amplified and used as a reference gene because it is a housekeeping gene encoding the β subunit of bacterial RNA polymerase. The reactions with DNA template and with water in place of cDNA template were included as a positive and negative control, respectively. Negative controls which were the reactions with template from cDNA mix without reverse transcriptase were also included. Amplification conditions were typically: enzyme activation (hot start) at 95°C, 20 s, denaturation at 95°C, 1s, annealing and extension at 60°C, 20 s. The data were analysed using StepOne software v 2.2.2. Transcription of *rpoB* during different growth conditions is shown in Figure 5.8.

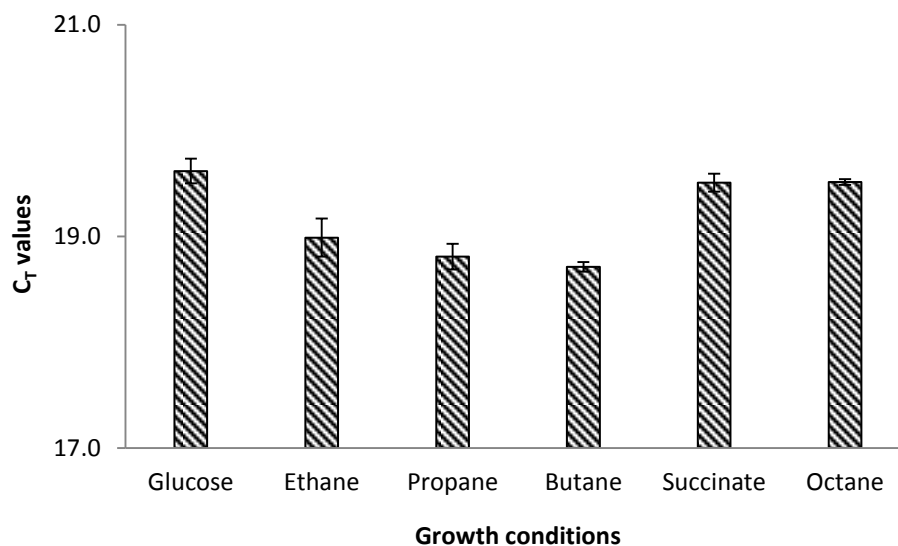


Figure 5.8: Transcription of *rpoB* during growth on glucose, ethane, propane, butane, succinate and octane. C_T (cycle threshold) values indicated a relative measure of the concentration of *rpoB* in PCR reactions. Error bars indicated standard deviations of triplicate assays. NB: C_T value is defined as the number of cycle required for the fluorescent signal to cross the background level.

rpoB was transcribed at a similar level (C_T values of 18.6-19.5) in all growth condition. Since the same amount of cDNA was used for analysis of each growth condition, this suggests that *rpoB* expression was relatively stable under these conditions. Therefore, transcription of *prmA* and *alkB* under different growth conditions was compared to *rpoB* as a reference gene.

Standard curves for amplification of *rpoB*, *alkB* and *prmA* was established using cDNA from octane-grown cells and propane-grown cells, respectively (shown in Figures 5.9 to 5.11). For all assays, sample transcripts were quantified by comparison with standard curves, generated by serial dilution of template, covering a concentration range of 1 to 10^{-5} . This also enabled assessment of the PCR efficiency from the slope of the standard curve. Standard curves were generated for all targets, both transcripts of interest (*prmA* or *alkB*) and reference transcripts (*rpoB*). Template for standard curves was prepared from cDNA predicted to contain appropriate amounts of relevant targets *i.e.* propane-grown cDNA for *prmA* and octane-grown cDNA for *alkB*). Transcripts were then quantified by comparing with the known

amount of genomic DNA in positive control reactions. The expression of *alkB* and *prmA* under the corresponding growth conditions is shown in Figure 5.12 and 5.13, respectively.

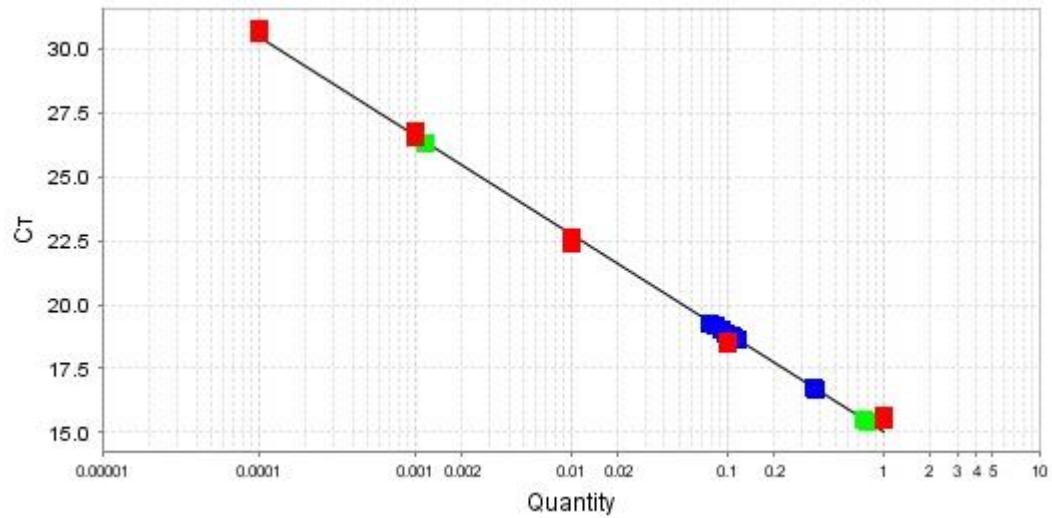


Figure 5.9: qPCR reactions targeting *rpoB*. Standard curve showing C_T value (y-axis) against quantity of template in log scale (x-axis) (red squares). Blue squares representing data from samples and green squares representing data which C_T standard deviation for the replicate group exceeds 0.5 are overlaid. The efficiency of PCR was 81.1%.

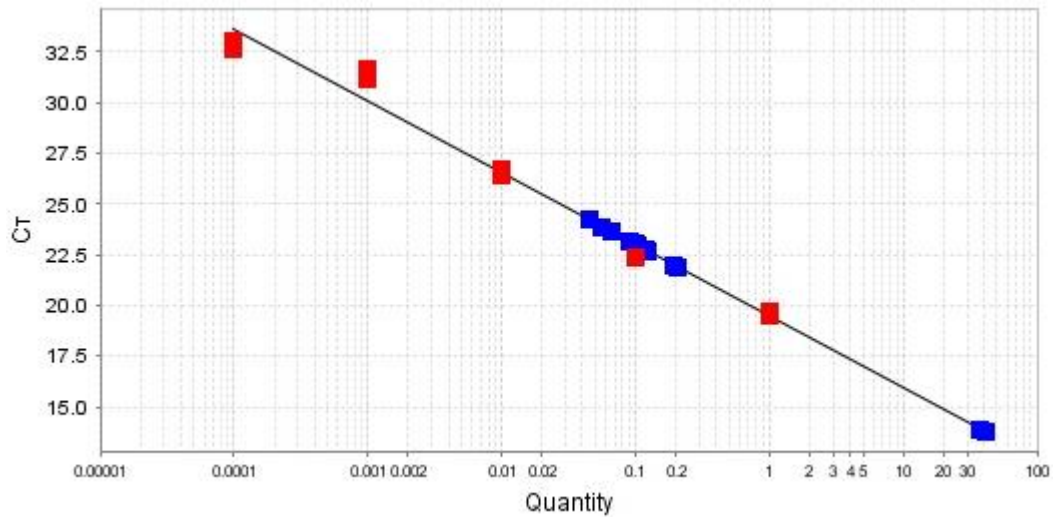


Figure 5.10: qPCR reactions targeting *alkB*. Standard curve showing Ct value (y-axis) against quantity of template in log scale (x-axis) (red squares). Blue squares representing data from samples are overlaid. The efficiency of PCR was 91.8%.

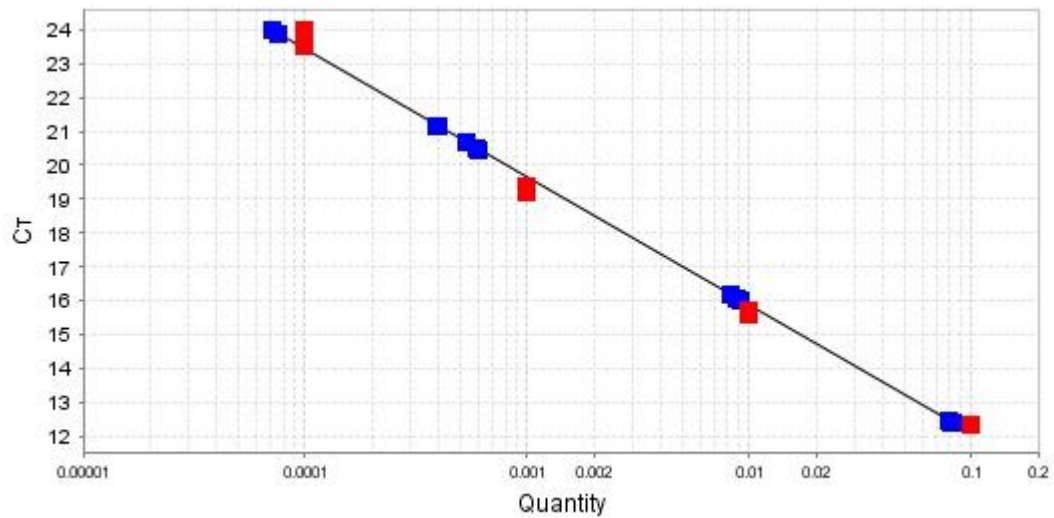


Figure 5.11: qPCR reactions targeting *prmA*. Standard curve showing Ct value (y-axis) against quantity of template in log scale (x-axis) (red squares). Blue squares representing data from samples are overlaid. The efficiency of PCR was 91.7%.

Standard curves from RT-qPCR targeting *rpoB*, *prmA* and *alkB* showed high PCR efficiencies (an ideal is 100%) indicating that inhibition and/or amplification errors did not significantly affected the assays. Most of the data from samples were placed within a range of standard data. This implied that data from samples were reliable.

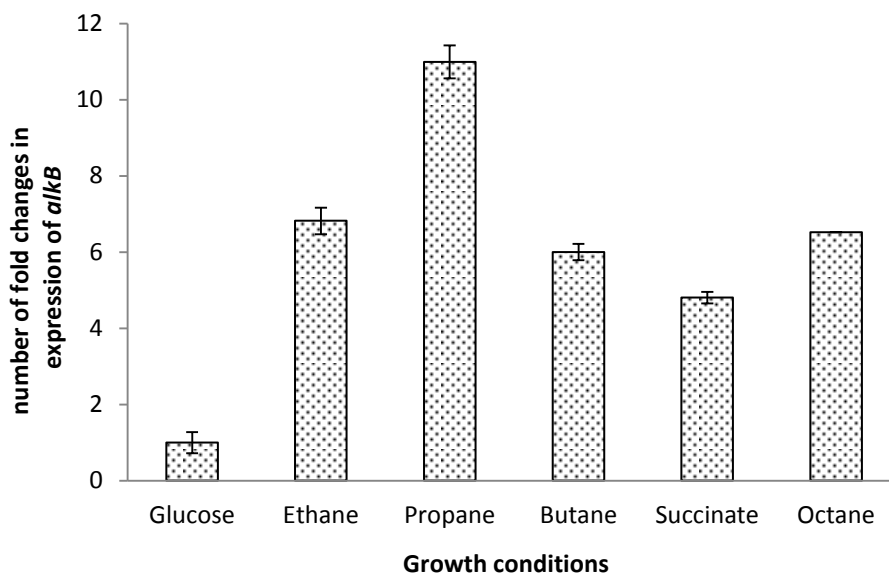


Figure 5.12: Fold changes in the expression of *alkB* in *R. jostii* strain 8 grown on ethane, propane, butane, succinate and octane compared to that of strain 8 grown on glucose. Error bars indicated the standard deviation of triplicate assays. The expression of *alkB* under growth of *R. jostii* strain 8 on alkanes was not highly significantly different (averagely less than 10 fold) from that of the growth on glucose. However, *alkB* gene expression was upregulated during growth on alkanes.

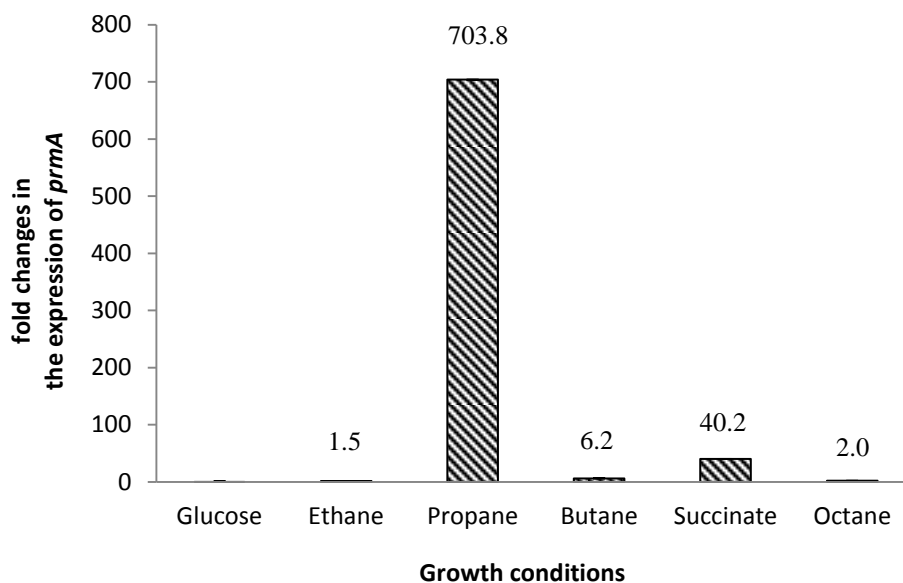


Figure 5.13: Fold changes in the expression of *prmA* in *R. jostii* strain 8 grown on ethane, propane, butane and octane compared to that of strain 8 grown on glucose. Error bars (which are non-visualised since the errors are very low) indicated the standard deviation of triplicate data. *prmA* was approximately 700-fold upregulated during growth on propane. In contrast, the expression of *prmA* was not significantly different in *R. jostii* strain 8 grown on glucose, succinate, ethane, butane and octane.

In investigating transcription of *alkB* and *prmA*, cDNA from succinate-grown cells was included in the RT-qPCR assays in order to serve as another non-alkane growth condition, apart from glucose. However, *prmA* transcripts were 700-fold more abundant in propane-grown cDNA than in cDNA from other growth conditions. This strongly suggested that *prmA* is involved in propane metabolism, but not in that of ethane, butane and octane. Interestingly, there is a distinctively significant transcription of *prmA* during growth on propane, while the transcription during growth on other substrates was approximately at the same level as for growth on glucose. This indicated that *prmA* was responsible for the growth of *R. jostii* strain 8 only on propane. According to the expression patterns for *alkB*, the *alkB* gene was expressed during growth on alkanes. Although the expression of *alkB* during growth on alkanes was not substantially high, alkane monooxygenase might still be involved in the growth of *R. jostii* strain 8 on ethane, propane, butane and octane

5.5. Discussion for expression of *prmA* and *alkB*

The purpose of the work described in this chapter was to quantify differential expression of the genes encoding propane monooxygenase and alkane hydroxylase during growth on alkanes, which then led to the understanding of the role of key enzymes involving in particular types of alkane metabolisms. A study on the expression of propane monooxygenase in *R. jostii* RHA1, which is a closely related strain to *R. jostii* strain 8, showed that the *prmA* gene was up-regulated during growth on propane. The expression of *prmA* was 2,450-fold higher during growth on propane compared to growth on pyruvate (Sharp et al., 2007). As with *R. jostii* RHA1, the *prmA* gene was up-regulated in *R. jostii* strain 8 during growth on propane, but not during growth on other alkanes. *prmA* gene had a propane/glucose expression ratio of 703, which is 3.5-fold less than the propane/pyruvate expression ratio of *R. jostii* RHA1. Conversely, the expression of *alkB* during growth of *R. jostii* RHA1 on propane was not very high. The *alkB* gene in *R. jostii* RHA1 had a propane/pyruvate expression ratio of 3.2. Similarly to *R. jostii* RHA1, the expression of *alkB* during growth of *R. jostii* strain 8 on propane and other alkanes was much lower. However, the expression of *alkB* during growth of *R. jostii* strain 8 on propane was approximately 3.5-fold higher than that of in *R. jostii* RHA1. The results showed that propane monooxygenase is inducible during growth on propane. Results suggested that this enzyme is involved in propane metabolism in *R. jostii* strain 8. Despite low expression of *alkB*, alkane monooxygenase is likely to be involved in ethane, propane, butane and octane catabolism in *R. jostii* strain 8. This assumption has been made based on the fact that it is clear that *prmA* is only responsible for the growth of *R. jostii* strain 8 on propane and that *alkB* is the only other monooxygenase that is likely to be present in *R. jostii* strain 8 as determined by analysis of its genome sequence. The genome of *R. jostii* strain 8 possesses only two alkane-degrading enzyme systems, propane monooxygenase and alkane hydroxylase, which are potentially involved in the degradation of gaseous alkanes. Alkane hydroxylase, responsible for degradation of short-chain alkanes, was also found in some other bacterial genus. For example, in *Pseudomonas putida* GPo1, this bacterium could grow on propane, butane and octane using an alkane hydroxylase (Johnson and Hyman, 2006). The ability of alkane hydroxylase to metabolise short-chain alkanes was also found in *Mycobacterium austroafricanum* strain IFP 2012

(Lopes Ferreira et al., 2007). These researchers demonstrated that the *alkB* gene, which is present as a single copy in the genome, was expressed during growth on propane, hexane and hexadecane. *Rhodococcus wratislaviensis* IFP 2016 contained an *alkB* gene and was able to degrade C₈-C₁₆ alkanes (Auffret et al., 2009). *Rhodococcus opacus* B4, a benzene-degrading bacterium, has two functional alkane hydroxylases with a substrate range of C₅-C₁₆ (Sameshima et al., 2008). The growth of *R. opacus* B4 on C₁-C₄ alkanes was not tested. However, *R. opacus* B4 can grow well on \geq C₇ alkanes while the growth on C₅-C₆ was low due to short-chain n-alkane (C₅-C₆) toxicity. There was no report of the ability of this strain to degrade gaseous alkanes. In *Rhodococcus* strains Q 15 and NRLL B-16531, these bacteria contain at least four alkane monooxygenase gene homologues, but there was no evidence to suggest that these enzymes were able to catalyse gaseous alkanes. Also, the growth of these *Rhodococcus* strains on C₁-C₄ alkanes has never been mentioned (Whyte et al., 2002). Interestingly, there is no research on any *Rhodococcus* strains whose expression of *alkB* is involved in the growth on gaseous alkanes (C₂-C₄). Therefore, *R. jostii* strain 8 is the first reported strain in the genus *Rhodococcus* whose *alkB* gene product is likely to be involved in the oxidation of C₂-C₄ gaseous alkanes. To confirm the role of alkane monooxygenase and propane monooxygenase in the oxidation of alkanes, mutagenesis of *alkB* and *prmA* genes was carried out. The results will be discussed in the next chapter.

5.6. Conclusions

Expression of propane monooxygenase and alkane monooxygenase in *R. jostii* strain 8 was studied by SDS-PAGE analysis and RT-qPCR. Polypeptides corresponded to the α - and β -subunits of propane monooxygenase were detected in cell extract from cells grown on propane, but were not detectable in cell extract from cells grown on other carbon compounds. This result correlated to the finding which *prmA* was highly expressed during growth on propane. Whereas there was no significant level of *prmA* expression during growth on ethane, butane and octane, the expression of *alkB*, which seemed to be constitutively expressed, was detectable by RT-qPCR during those growth conditions. This suggested that alkane monooxygenase was likely to be involved in gaseous alkane oxidation. Interestingly, this is the first report showing the involvement of alkane monooxygenase in the genus *Rhodococcus* in the degradation of the gaseous alkanes -- ethane, propane and butane. Unfortunately, polypeptide analysis of cell extracts from cells grown on ethane, propane, butane and octane did not show any components particularly related to alkane hydroxylase. This may be because the enzyme was instable during preparation of cell extracts or because the enzyme was not highly expressed when the cells were collected for preparation of cell extracts. Although major polypeptides corresponding to subunits of propane monooxygenase were detected only in cell extract from cells grown on propane and none of the detected polypeptides corresponded to subunits of alkane hydroxylase, polypeptide corresponded to chaperone GroEL, which was found to assist in the function of monooxygenases, was detected in all of the cell extracts from alkane-grown cells. Also, a polypeptide corresponded to alcohol dehydrogenase was detected in butane-grown cell extract. This alcohol dehydrogenase was likely to be involved in the oxidation of butane in *R. jostii* strain 8 because it was induced during growth on butane. According to analysis of the genome of *R. jostii* strain 8, there are propane and alkane monooxygenases which are potentially involved in the degradation of gaseous alkanes, so alkane monooxygenase was probably the enzyme responsible for the oxidation of ethane, butane and octane despite there being no detectable alkane hydroxylase subunits in cell extracts from cells grown on those alkanes. However, mutagenesis of *prmA* and *alkB* was carried out in order to clarify the role of these two monooxygenases (see Chapter 6).

Chapter 6
Mutagenesis of *prmA* and *alkB*

6.1. Introduction

The development of a genetic transformation strategy is necessary for detailed analysis of propane metabolism at the molecular level. *E.coli-Rhodococcus* shuttle vectors and electroporation methods were improved for cloning and expression of recombinant plasmid DNA in some *Rhodococcus* strains. Successful transformation of foreign DNA into *Rhodococcus jostii* RHA1, the most closely related strain to *R. jostii* strain 8, has been carried out by either conjugation or electroporation. The conjugation method was used for making mutants to investigate the role of genes responsible for rhodochelin synthesis and lignin degradation (Ahmad et al., 2011; Bosello et al., 2011). Both studies demonstrated successful introduction of DNA into *Rhodococcus jostii* RHA1 by conjugation. The use of pK18*mobsacB* (Schäfer et al., 1994) then allowed sucrose-counter selection for double-crossover mutants. Another potential approach for transferring foreign plasmid DNA into *R. jostii* RHA1 is electroporation. There has been a report showing successful electrotransformation, performed under high-voltage condition, in *R. jostii* RHA1 (Masai et al., 1995). Recently, the use of pK18*mobsacB* as a cloning vector and transformation of the plasmid by electroporation in *R. jostii* RHA1 was reported (Chen et al., 2013). Electrotransformation was also used in some other *Rhodococcus* spp. such as *R. equi*, *R. fascians*, *R. opacus*, *R. rhodochrous* etc. (Desomer et al., 1990; Sunairi et al., 1996; Sekizaki et al., 1998; Kalscheuer et al., 1999). The disadvantage of conjugation is that purification of transconjugants is required to eliminate *E. coli* prior to the selection of double-crossover mutants in the next step of mutagenesis experiments. In order to avoid that process, electroporation was selected as a potential tool in this study for mutagenesis of *prmA* and *alkB* in *R. jostii* strain 8.

Conditions for electroporation were established in order to introduce foreign plasmid and/or linear DNA into *Rhodococcus jostii* strain 8. It was hoped that evidence for the role of propane monooxygenase and *alkB*-type alkane monooxygenase in gaseous alkane metabolism in *R. jostii* strain 8 would be gained by the disruption of both *prmA* and *alkB* by marker exchange mutagenesis.

Prior to the construction of mutants, optimisation of electroporation conditions was carried out in order to investigate the most appropriate condition for transferring genetically modified genes into *R. jostii* strain 8. There are several parameters which affect transformation by electroporation, but, with limited time, a few parameters were optimised based on the method successfully achieved with other *Rhodococcus* strains in our lab.

6.2. Optimisation of electroporation conditions for use in mutagenesis of *prmA* and *alkB* in *R. jostii* strain 8

6.2.1. Optimal voltage for electroporation of *R. jostii* strain 8

Competent cells of *R. jostii* strain 8 were prepared as described in Chapter 2, section 12.1. The number of cells killed by increasing electroporation voltage was investigated. 50 µl of competent cell culture was aliquot and diluted to 10⁵. The diluted culture was plated on NMS medium containing 10 mM glucose. This was to check the total number of cells before electroporation. The rest of the competent cell culture was plated out (100 µl each plate) on NMS medium with 10 mM glucose after electroporation using different voltages.

Electroporation voltages used were varied over the range 1, 1.25, 1.5, 2 and 2.5 kV. The other electroporation conditions were set as follows: resistance 800Ω, capacitance 25 µF, 1mm-gap cuvette. Electroporation without DNA was carried out in order to determine the number of cells killed by an increased voltage. Each electroporation reaction was added with 50 ng of pNV18 (Chiba et al., 2007), a plasmid containing a kanamycin resistance gene, in order to determine the electroporation condition which allowed the maximum number of colonies to grow after electroporation. The transformants were recovered in NMS medium with glucose (10mM) overnight. The cultures were then plated out onto NMS medium with glucose (10 mM) and kanamycin (100 µg/ml). The viability of competent *R. jostii* strain 8 cells after electroporation using different voltages is shown in Table 6.1.

Electroporation voltage (kV)	Number of colonies	Time constant (ms)
Before electroporation	135	-
1	65	18.5
1.5	39	18.0
2	4	17.7
2.5	0	16.0

Table 6.1: The viability of competent *R. jostii* strain 8 cells after electroporation using different voltages. The number of colonies presented in the Table was an average number of colonies growing on triplicate plates.

Loss of cell viability normally occurred when cells were electroporated. This means that cell membranes were made porous in order to increase permeability of extracellular materials into the cell. In the case of Gram-negative bacteria, particularly *E. coli*, survivability of cells after standard electroporation conditions was approximately 30-40% (Dower et al., 1988). It should be noted that cell membranes of *E. coli* were certainly easier to damage than cell membranes of Gram-positive bacteria such as *Rhodococcus* spp. Therefore, in the case of *R. jostii* strain 8, higher cell viability after electroporation should be expected due to a lower number of damaged cells. The cell viability after using optimal electroporation conditions of *Rhizobium leguminosarum* was approximately 63% (Garg et al., 1999). The study showed that *R. leguminosarum* cells were more resistant to electroporation than *E. coli* although both organisms are Gram-negative bacteria. Similarly, cell viability after optimal electroporation of *Bradyrhizobium japonicum* was 75% (Hattermann and Stacey, 1990).

According to Table 6.1, the number of colonies growing after electroporation decreased by the increase in voltage. In the case of *R. jostii* strain 8, the optimum electroporation condition was considered as the one which resulted in approximately more than 30% and probably less than 75% of cell viability. Therefore, from the experiment above, the electroporation voltage which should be used was likely to be 1.5 kV. Growth of transformants on NMS containing 10 mM glucose and kanamycin

(100µg/ml) medium after different resistance settings during electroporation is shown in Table 6.2.

Electroporation voltage (kV)	Number of colonies	Transformation efficiency (cfu/µg DNA)	Time constant (ms)
1	0	0	18.2
1.25	12	240	18.4
1.5	2	40	18.5
1.75	0	0	17.4
2	0	0	18.0
2.25	0	0	17.0
2.5	0	0	16.0

Table 6.2: Growth of transformants on NMS containing 10 mM glucose and kanamycin (100µg/ml) medium after electroporation with pNV18 using different voltages. The number of colonies presented in the Table was an average number of colonies growing on triplicate plates.

There were colonies growing after electroporation using 1.25 and 1.5 kV. There were no colonies from the negative control cultures growing after electroporation. This suggested that there was no spontaneous mutation after electroporation. Although transformation efficiencies of the electroporation using 1.25 and 1.5 kV were not very high, both voltages were the most promising for electroporation conditions to be used with *R. jostii* strain 8.

6.2.2. Optimal resistance for electroporation conditions of *Rhodococcus jostii* strain 8

Similar to the optimisation for electroporation voltage, the experiment was carried out as described in section 6.2.1. Instead of varying voltages, resistances were varied (200, 400, 600 and 800 Ω). A resistance higher than 800 Ω caused shorting of the cuvette during electroporation and so could not be used. A resistance which was lower than 200 Ω was likely to have no effect on the cell membrane.

Therefore, the resistance was varied in the range 200 – 800 Ω . According to the result from Section 6.2.1, the most appropriate voltages for electroporation are likely to be 1.25 and 1.5 kV. Therefore, both voltages were selected for optimization of electroporation conditions. The other electroporation conditions were as follows: capacitance 25 μ F, 1mm-gap cuvette. The viability of competent *R. jostii* strain 8 cells before and after electroporation using different resistances is shown in Table 6.3.

Electroporation voltage (kV)	Electroporation resistance (Ω)	Number of colonies	Time constant (ms)
	Before electroporation	230	-
1.25	200	172	5.0
	400	140	10.0
	600	158	14.4
	800	104	17.3
1.5	200	163	5.1
	400	105	9.8
	600	57	14.5
	800	20	17.2

Table 6.3: The viability of competent *R. jostii* strain 8 cells after electroporation using different resistances. The number of colonies presented in the Table was the average number of colonies growing on triplicate plates.

Increasing the resistance did not seem to affect the growth of *R. jostii* strain 8 after electroporation using 1.25 kV. In contrast, an increase in resistance when using 1.5 kV electroporation resulted in a decrease in the number of cells grown after electroporation. This suggested that using 1.5 kV as a voltage in electroporation killed more cells after electroporation than when using 1.25 kV which is probably not surprising. Growth of transformants on NMS containing 10 mM glucose and kanamycin (100 μ g/ml) medium after different electroporation resistances with pNV18 is shown in Table 6.4.

Electroporation voltage (kV)	Electroporation resistance (Ω)	Number of colonies	Transformation efficiency (cfu/ μ g DNA)	Time constant (ms)
1.25	200	0	0	5.1
	400	4	80	10.0
	600	8	160	14.6
	800	26	520	17.5
1.5	200	0	0	5.0
	400	4	80	9.6
	600	5	100	14.1
	800	9	180	17.1

Table 6.4: Growth of transformants on NMS containing 10 mM glucose and kanamycin (100 μ g/ml) medium after electroporation with pNV18 using different resistances. The number of colonies presented in the Table was the average number of colonies growing on triplicate plates.

An increase in electroporation resistance when using 1.25 kV or 1.5 kV resulted in an increase in transformation efficiency. Using resistance at 200 Ω with 1.25 kV or 1.5 kV had no effect in transforming pNV18 into the cells. The highest transformation efficiency was obtained by electroporation using 1.25 kV/cm and 800 Ω , 25 μ F capacitance.

6.2.3. Optimal competent cell culture density, recovery medium and recovery time for transformants

Apart from electroporation voltage and resistance, competent cell culture density, recovery times after electroporation and recovery media were also optimized. Competent cell culture density was varied OD₅₄₀ 0.4-0.7, which is exponential growth phase of *R. jostii* strain 8. It appeared that the highest transformation efficiency was obtained using cells with an OD₅₄₀ of approximately 0.5, at mid-exponential phase. There was no growth after electroporation when using

cell culture densities of 0.6 and above. Fewer transformant colonies were obtained when using a cell culture density of 0.4, even when several attempts were made. Therefore, wild-type *R. jostii* strain 8 was grown to an OD₅₄₀ of approximately 0.5 for preparation of competent cells for electroporation.

Recovery times after electroporation were varied at 4, 8, 12, 16 and 24 hr. There were no colonies growing after 4 and 8 hr recovery. Only a few colonies grew after 12 hr incubation. The number of colonies growing after 16 and 24 hr recovery was not significantly different. Therefore, cells were recovered overnight (approximately 16-24 hr) before plating.

Media for recovery and growing transformant cultures were varied in order to investigate the medium which allowed the best growth of transformants. The selected media used were NMS containing 10 mM glucose with kanamycin (100µg/ml), Luria Bertani (LB) with kanamycin (100µg/ml) and nutrient broth (NB) with kanamycin (100µg/ml). It appeared that the maximum growth after electroporation was obtained when using NMS with 10 mM glucose and kanamycin (100µg/ml) as both recovery and growth medium. Therefore, the optimum electroporation condition used in this experiment was at 1.25 kV/cm, 800 Ω, 25 µF capacitance, using a single pulse. The recovery time after electroporation was overnight (16-24 hr). Cells were recovered in NMS containing 10 mM glucose. Transformants were grown on NMS medium with glucose (10mM) and gentamicin (5 µg/ml).

6.3. Marker exchange mutagenesis using the vector pK18*mobsacB* introduced by electroporation

6.3.1. Construction of mutants

The broad-host-range pK18*mobsacB* (Schäfer et al., 1994) is a suicide cloning vector carrying the levansucrase (*sacB*) gene. The pK18*mobsacB* also contains multiple cloning site, *lacZ* alpha sequence, kanamycin resistance gene and M13 primer binding sites. A diagram showing pK18*mobsacB* is shown in Figure 6.1. pK18*mobsacB* can only replicate in *E. coli*, but not in *Rhodococcus* spp. The use of

this vector facilitates cloning procedures in *E. coli* and forcing of a single homologous recombination event in *Rhodococcus* spp. The purpose of using pK18*mobsacB* as a vector to transfer mutated genes into the chromosome of *R. jostii* strain 8 was because this vector contains *sacB* which allows the construction of double-crossover mutants out of single-crossover mutants due to sucrose sensitivity of the single-crossover mutants. The expression of *sacB* in the presence of sucrose is lethal to cells due to toxicity of by-products from the reaction between levansucrase and sucrose (Steinmetz et al., 1983). Construction of the plasmids carrying disrupted *prmA* (pAGB) and *alkB* (pXGY) is shown in Figure 6.2.

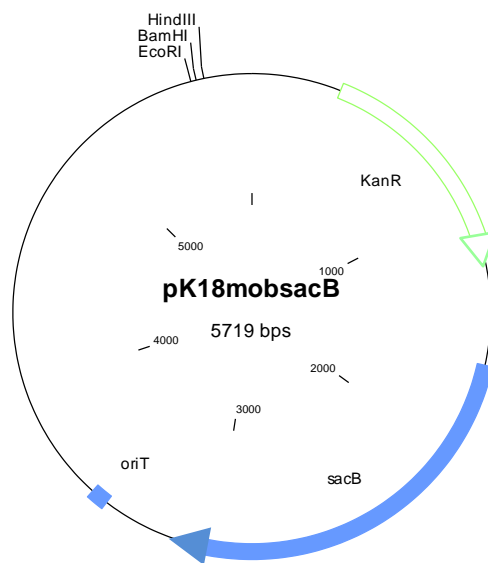


Figure 6.1: A diagram showing pK18*mobsacB*, a broad-host range vector which was used to carry mutated genes into *R. jostii* strain 8

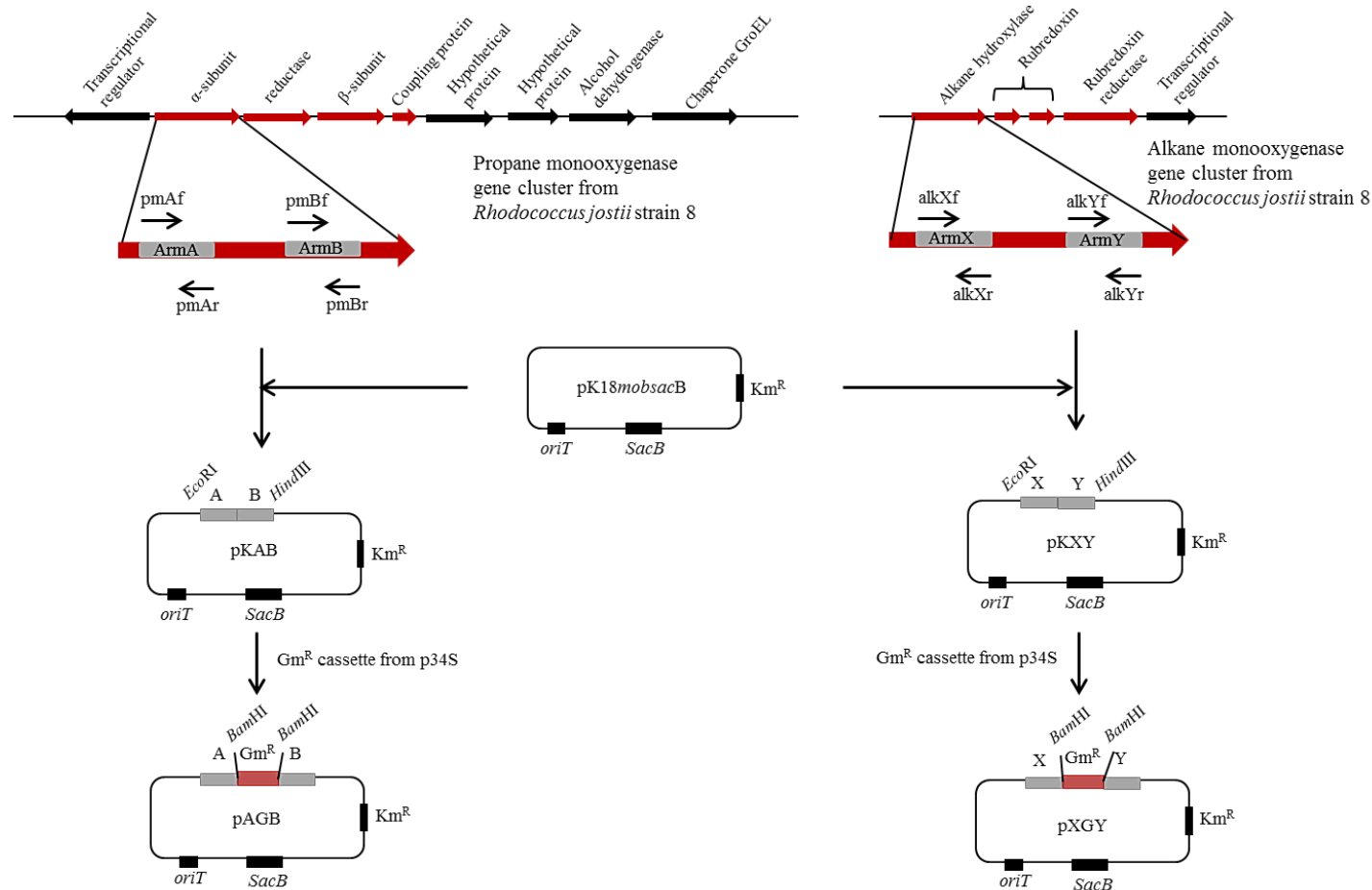


Figure 6.2: Construction of pAGB, a plasmid carrying a disrupted *prmA* and pXGY, a plasmid carrying a disrupted *alkB* gene. p34S (Dennis and Zylstra, 1998), a plasmid containing gentamicin resistance gene which can be inserted into other plasmids in either backward or forward sequence.

E. coli JM109 was used as host for all pK18*mobsacB*-relating cloning procedures. PCR amplification of a 489 bp ‘ArmA’ and a 502 bp ‘ArmB’ of *prmA* from genomic DNA was carried out using primers pmAf/r and pmBf/r, respectively. Each Arm was cloned into the pGEMT-Easy vector and transformed into *E. coli* Top 10 cells. *EcoRI/BamHI*-digested ArmA was ligated into pK18*mobsacB* plasmid and transformed into *E. coli* JM109. *BamHI/HindIII*-digested ArmB was then ligated, yielding pKAB (Figure 6.2). The gentamicin resistance cassette (Gm^R) from p34S plasmid, a cloning vector carrying gentamicin resistance gene, (Dennis and Zylstra, 1998) was digested with *BamHI* and then ligated into *BamHI*-digested pKAB, yielding pAGB. Construction of the mutated *alkB* plasmid was carried out through the same procedures as described for mutagenesis of *prmA* (see above). The only difference was that alkXf/r and alkYf/r primers were used to amplify ‘ArmX’ (362 bp) and ‘ArmY’ (371 bp), respectively. The mutated *alkB* construct was called pXGY (Figure 6.2).

The plan for construction of mutants was to introduce the mutagenic plasmids into the wild-type cells and subsequently allow single and then double homologous recombination events to occur. Single-crossover mutants were selected on NMS plates containing glucose (10mM) supplemented with gentamicin (5 µg/ml). The presence of kanamycin- and gentamicin-resistant genes, an indication of single-crossover mutants, was checked by PCR using DNA isolated from transconjugants. A colony of single-crossover mutants was grown in liquid NMS with glucose (10mM) and gentamicin (5 µg/ml) for 24 hr. The culture (100 µl) was plated onto NMS medium with 10% sucrose. The culture of wild-type *R. jostii* strain 8 grown in NMS with glucose (10mM) was plated onto NMS medium with 10% sucrose as a control. Single-crossover mutants were grown on NMS with 10% sucrose medium in order to allow a double recombination event. The counter selection by *sacB* allowed the removal of single-crossover mutants leaving only double-crossover mutants to grow. The double-crossover mutants could be distinguished from the wild-type strain by their ability to grow on medium supplemented with gentamicin. The presence of gentamicin-resistant gene was checked by PCR of DNA isolated from colonies. The absence of wild-type *prmA* and *alkB* in double-crossover mutants was checked by PCR of DNA isolated from

colonies using outAGBf/r and outXGYf/r primers. The results will be discussed later in this chapter.

6.4. Introduction of mutated *prmA* and *alkB* into the chromosome of *R. jostii* strain 8 by electroporation

6.4.1. Electroporation of pAGB and pXGY

Several attempts had been made to transfer pAGB and pXGY into *R. jostii* strain 8 in order to obtain *prmA*- and *alkB*-deficient strains, respectively. Unfortunately, it appeared that the transformation was not successful since there was no growth of transformants showing gentamicin resistant phenotype and the lack of *prmA* or *alkB* wild-type genes. Instead of transferring the whole plasmids, transformation of mutated gene fragments was then carried out to see if this would be a more efficient mutagenesis method.

6.4.2. Electroporation of mutated *prmA* and *alkB* fragments

The disrupted *prmA* and *alkB* genes were removed from the mutagenic plasmids by PCR amplification using pAf/pBr and AXf/AYr primers, respectively. The primers targeted both ends of the mutated genes, yielding 1,857 bp of the mutated *prmA* and 1,599 bp of the mutated *alkB* fragments. PCR products were purified using the PCR clean-up kit (Macherey Nagel, Düren, Germany) and quantified as described in Chapter 2 section 10.1-10.2. Purified PCR products were introduced into competent *R. jostii* strain 8 cells by electroporation using the optimal condition as previously described. Transformant cultures were plated on NMS medium containing glucose and gentamicin in order to select for *prmA*- and *alkB*-deficient mutants. Although NMS medium with glucose (10 mM) and kanamycin (100 µg/ml) was used to grow transformants in the optimization of electroporation condition experiments, it was found that using gentamicin (5 µg/ml) as a selective antibiotic in a medium had a similar effect in allowing the growth of transformants when using kanamycin as selective antibiotic. Colonies were subcultured twice onto

fresh NMS medium containing glucose supplemented with gentamicin before checking for the presence of the mutated gene in the chromosome by PCR. All of the colonies growing on gentamicin plates (after two subcultures) were checked for the presence of the gentamicin resistance gene and mutated *prmA* and *alkB* genes by colony PCR. The list of primers used for screening mutants is shown in Table 6.5.

Primer name	Target region	PCR product size (bp)		
		Wild-type DNA	Plasmid DNA	Double-crossover mutant
Gmf	gentamicin resistant gene	N	700	700
Gmr	gentamicin resistant gene			
out_AGBf	ArmA of <i>prmA</i>	750	1,495	1,495
out_AGBr	ArmB of <i>prmA</i>			
out_XGYf	ArmX of <i>alkB</i>	1,500	N	N
out_XGYr	ArmY of <i>alkB</i>			

Table 6.5: The list of PCR primers used for screening of colonies containing a gentamicin cassette and disrupted *prmA* and *alkB*. N: no PCR product was amplified due to the absence of the gene or the PCR extension time was not sufficiently long to amplify the product.

Only a few out of several electroporation attempts in transferring disrupted *prmA* and *alkB* fragments into *R. jostii* strain 8 resulted in the growth of putative mutants growing on gentamicin plates after recovery. The electroporation condition which resulted in the highest number of potential mutant colonies grown on gentamicin plates is shown in Table 6.6.

Type of DNA	Amount of DNA (ng)	Number of colonies
pNV18	50	565
disrupted <i>prmA</i> fragment	250	374
disrupted <i>alkB</i> fragment	250	339
pAGB	250	0
pXGY	250	0
Negative control	0	0

Table 6.6: Electroporation of disrupted *prmA* and *alkB* fragments, pAGB and pXGY into *R. jostii* strain 8. The number of colonies grown on antibiotic plates after recovery was counted after 3 days of incubation.

The electroporation efficiency calculated after electroporation with the control plasmid (pNV18) was 1.1×10^4 cfu/ μ g DNA. It appeared that using the same amount of DNA, the number of transformants obtained after electroporation of fragment DNA was much higher than the number of transformants obtained after electroporation of plasmid DNA. A similar experiment (data not shown) was carried out as a duplicate experiment. The results showed that more colonies were obtained from the electroporation of linear fragment DNA (approximately 10^2 cfu/ μ g DNA) than the colonies from electroporation of plasmid DNA (less than 10 cfu/ μ g DNA). This suggested that the electroporation of DNA into *R. jostii* strain 8 is likely to be more successful when introducing the DNA in a linear form than with circular DNA. After two subcultures, the colonies were checked for the presence of the gentamicin-resistant gene by PCR amplification using Gmf/r primers. The presence of the gentamicin-resistant gene in these colonies suggested that the mutated genes were successfully transferred into the cells. This provides evidence that an appropriate setting for transferring linear DNA into *R. jostii* strain 8 by electroporation is 1.25 kV/cm, 800 Ω , 25 μ F capacitance.

6.5. Screening for a *prmA*-deficient strain

PCR amplification to check for the presence of the gentamicin-resistant gene in *R. jostii* strain 8 was carried out directly on colonies using Gmf/r primers. The PCR reaction with pAGB DNA was used as a positive control. The reaction with wild-type DNA was included as a negative control. The reaction without DNA template was also included in order to ensure the absence of contamination in the PCR mixture. Gel analysis of PCR amplification reactions checking for the gentamicin resistance gene in colonies showed that PCR products from those colonies appeared at the same size as the product obtaining from pAGB DNA. This, as expected, suggested that those colonies contained the gentamicin-resistant gene. PCR on colonies (374 colonies) using outAGBf/r was then carried out in order to screen for the colonies containing mutated *prmA* and mutated *alkB*, respectively. The diagram showing primer binding sites on the wild-type and the mutated *prmA* fragments is illustrated in Figure 6.3.

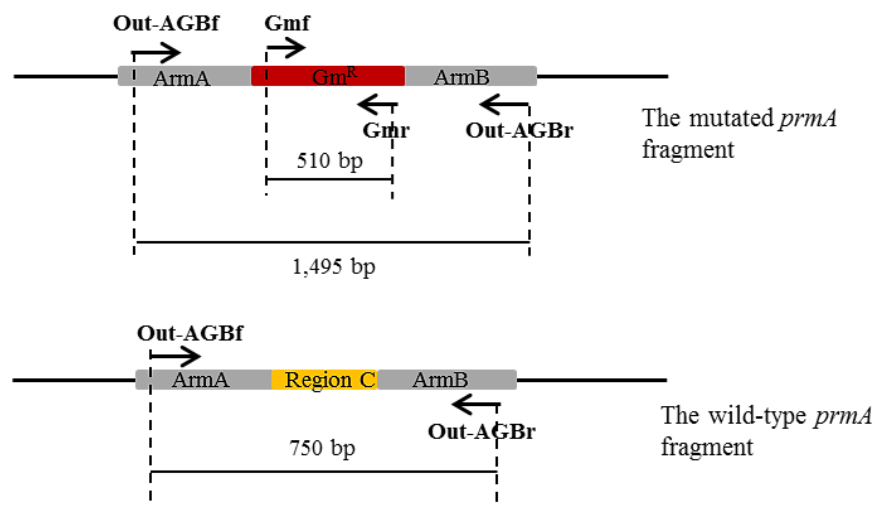


Figure 6.3: The diagram showing primer binding sites on the wild-type and the mutated *prmA* fragments. Scale bars indicated the sizes of PCR products. Region C, which is in the middle of ‘ArmA’ and ‘ArmB’ in the wild-type *prmA* fragment, represents the gene which was replaced by the gentamicin resistance gene in the mutated *prmA*.

The PCR assay with pAGB DNA was used as a positive control in the PCR amplification, checking for the mutated *prmA*. The PCR assay with wild-type DNA was included as a comparison. The PCR assay with no DNA template was included as a negative control. Gel analyses of PCR amplification checking for mutated *prmA* is shown in Figure 6.4. The gel shows PCR products of only 28 colonies since identical products were obtained from all 374 tested colonies.

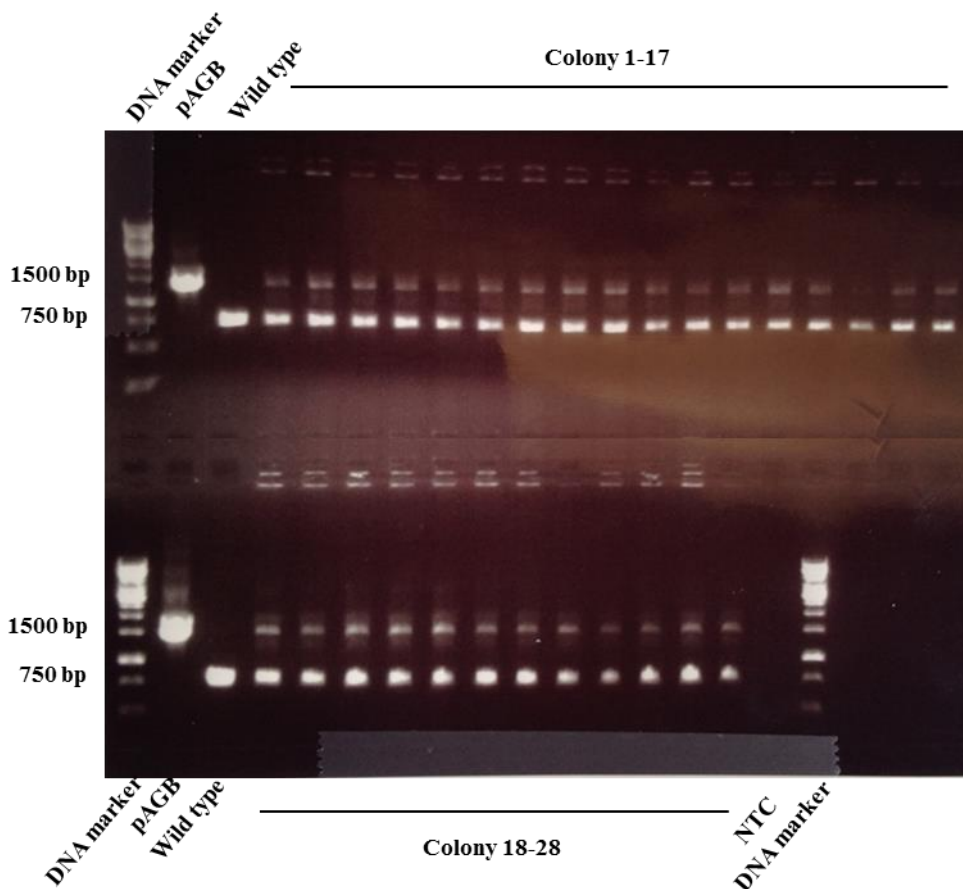


Figure 6.4: Gel analysis of PCR amplification using outAGBf/r primers on 28 colonies checking for mutated *prmA* using outAGBf/r primers.

PCR product from pAGB DNA was approximately 1,500 bp, which was as expected (see Table 6.5). The size of PCR product obtained with DNA from the wild-type *R. jostii* strain 8 was approximately 750 bp. This ensured that using these primers it was possible to distinguish the difference between the wild type and the

mutant. There were two different PCR products from those colonies tested. One of the products was at the same size as was obtained from pAGB. The other was at the same size as the PCR product from DNA from wild-type *R. jostii* strain 8. This suggested that both the non-mutated *prmA* and the mutated *prmA* were present in those 28 colonies. The presence of two PCR products in each colony was probably because the disrupted *prmA* was not integrated into the chromosome at the expected region. The other possibility to explain this event is that there was a mixture of the wild type strain and the *prmA*-deficient strain in the same colony.

In order to investigate whether or not the mutated *prmA* was replaced the wild-type *prmA* in the chromosome, three random colonies were grown in liquid NMS with glucose overnight. The cultures were diluted to 10^{-5} and were spread (50 μ l) onto NMS plus glucose plates and grown overnight in order to obtain individual colonies. Nine colonies were randomly selected and screened by PCR for *prmA*-deficient mutants. PCR amplification on colonies using outAGBf/r primers were carried out. Gel analyses of PCR amplification checking for *prmA* mutants from colonies grown from diluted cultures is shown in Figure 6.5.

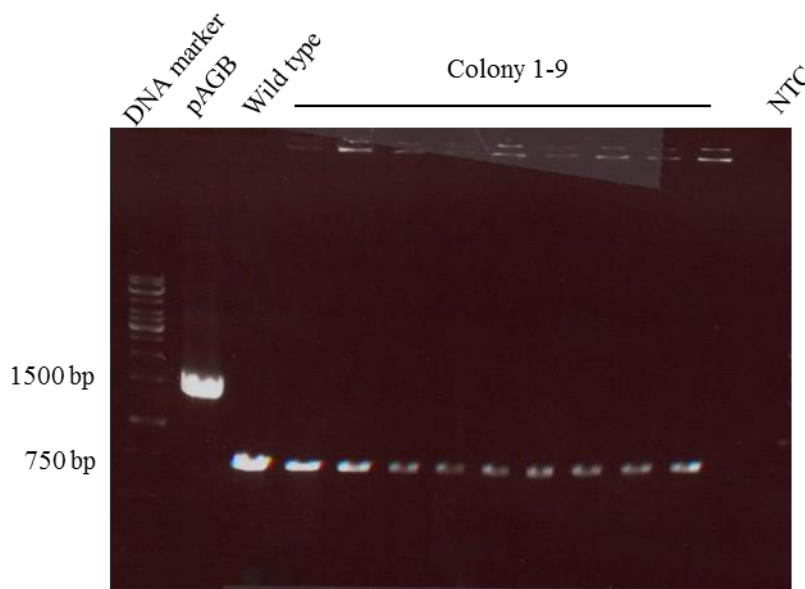


Figure 6.5: Gel analysis of PCR amplification using outAGBf/r primers on colonies grown from 10^5 -fold dilution cultures. NTC: No template control.

The result showed that PCR products from those selected colonies were the same size as the product from wild type DNA. This suggested that those ten colonies did not carry the *prmA* mutation.

6.6. Screening for *alkB* mutants

The presence of a mutated *alkB* in colonies grown on gentamicin plates was checked by PCR amplification using outXGYf/r primers. The diagram showing primer binding sites on the wild-type and the mutated *alkB* fragments is illustrated in Figure 6.6.

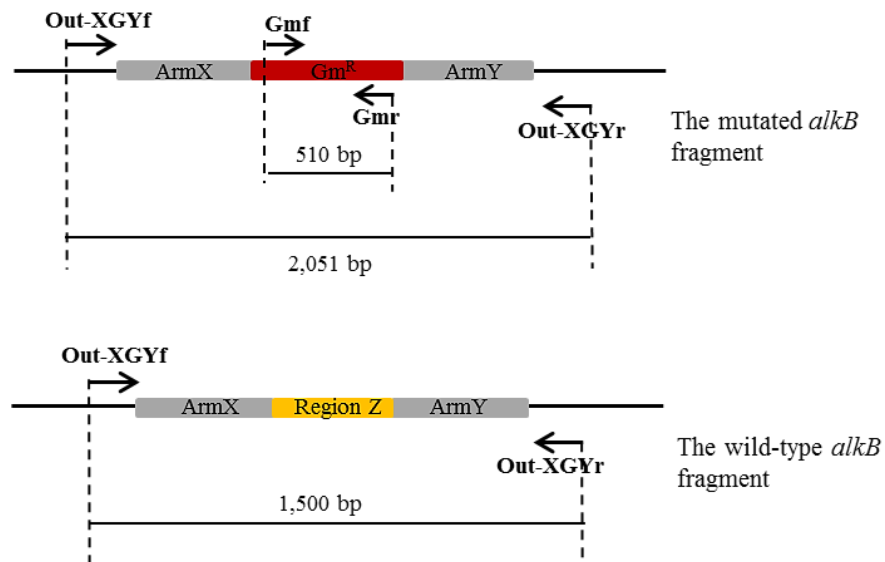


Figure 6.6: The diagram showing primer binding sites on the wild-type and the mutated *alkB* fragments. Scale bars indicated the sizes of PCR products. Region Z, which is in the middle of ‘ArmX’ and ‘ArmY’ in the wild-type *alkB* fragment, represents the gene which was replaced by the gentamicin resistance gene in the mutated *alkB*.

All of the colonies (339 colonies) grown on gentamicin plates were checked for the presence of mutated *alkB*. However, PCR products from only 28 colonies are shown below as representatives of 339 colonies, whose PCR products were identical.

Gel analyses of PCR amplification on 28 colonies checking for the presence of mutated *alkB* is shown in Figure 6.7.

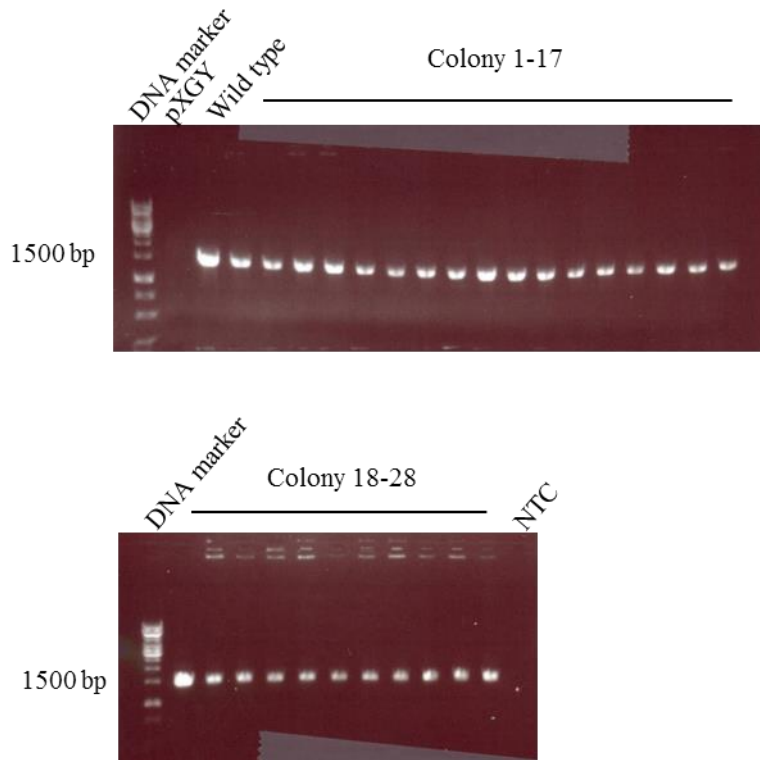


Figure 6.7: Gel analyses of PCR amplification on 28 colonies using outXGYf/r primers. NTC: No template control.

PCR product from wild-type DNA was approximately 1,500 bp, which was as expected. There was no PCR product from pXGY since the extension time was set at 1 min 30 sec, which was probably not sufficiently long to amplify the product (2,051 bp). The absence of PCR product from pXGY was also as expected. PCR products from all of the colonies grown on gentamicin appeared at the same size as the wild-type product. This suggested that the wild-type *alkB* was still present in those colonies. There were two possible explanations for this event. It could be because wild-type cells still co-existed in the colonies with the *alkB* mutant. Otherwise, the disrupted *alkB* was integrated into the chromosome at some other position and did not replace the wild-type *alkB*. In order to investigate which possibility explained this occurrence, three randomly selected colonies were grown

in liquid NMS with glucose. The overnight culture was diluted 10^5 -fold and grown on NMS with glucose plates. Individual colonies were assumed to be a collection of cells with single genotype and phenotype. PCR amplification on randomly selected 20 colonies was carried out using outXGYf/r primers. Gel analyses of PCR amplification products obtained using outXGYf/r primers on colonies grown from 10^5 -fold dilution cultures is shown in Figure 6.8.

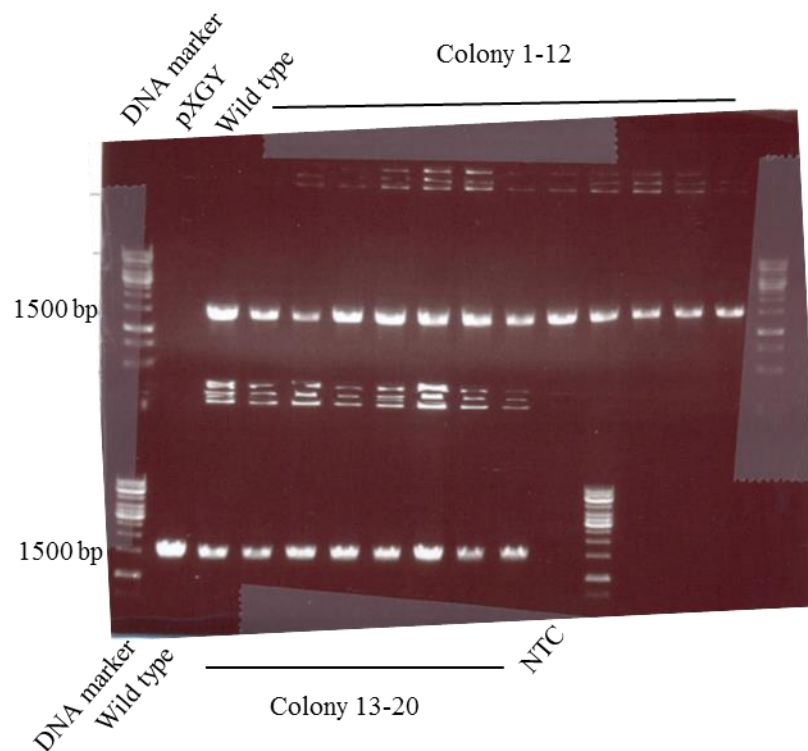


Figure 6.8: Gel analysis of PCR amplification using outXGYf/r primers on colonies grown from 10^5 -fold dilution cultures. NTC: No template control.

The result showed that PCR products from those 20 colonies appeared at the same size as the PCR product from wild-type DNA. This suggested that those colonies were not *alkB* mutant, and the mutated *alkB* did not replace the wild-type *alkB* in the chromosome.

6.7. Discussion and conclusion

In order to investigate the role of *prmA* and *alkB* in the degradation of gaseous alkanes in *R. jostii* strain 8, a genetic transformation system for transferring disrupted *prmA* and *alkB* was established. Electroporation was selected as the method of DNA transfer into *R. jostii* strain 8 since successful gene transfer by this method had been successful in *R. jostii* RHA1 (Takeda et al., 2004; Iwasaki et al., 2006; Chen et al., 2013), the most closely related strain to *R. jostii* strain 8. Also, the advantage of electroporation is that purification of transformants after gene transfer can be avoided, while it is required after conjugation in order to remove *E. coli*. Optimisation of electroporation conditions suggested that the best result was obtained using electroporation with the following conditions: 1.25 kV/cm, 800 Ω , 25 μ F capacitance. The highest transformation efficiency was approximately 10⁴ cfu/ μ g DNA. Unfortunately, although the transformation of linear fragments of DNA was successful, the mutated genes might have been integrated into the chromosome of the wild-type strain at the non-desired positions.

The voltage used for electroporation of *Rhodococcus* spp. varied considerably in previous reports in the literature. For example, electroporation at high voltage (25 kV/cm) was used to transform mutagenic plasmid into *R. jostii* RHA1 (Masai et al., 1995). Electroporation at a voltage of 2.5 kV/cm was used in *R. equi* (Sekizaki et al., 1998). In *Rhodococcus opacus* strains, lower voltage such as 2.5 kV/cm, 6.5 kV/cm and 10 kV/cm was applied (Kalscheuer et al., 1999; Na et al., 2005b; MacEachran et al., 2010). In *R. equi* RE1 (van der Geize et al., 2008), electroporation voltage was set to 12.5 kV/cm, which is equal to the voltage used for electroporation of *R. jostii* strain 8. However, the higher resistance (1,000 Ω) used in electroporation of *R. equi* RE1 was not applicable for *R. jostii* strain 8 since it resulted in shorting of the electroporation cuvettes.

In *R. equi*, the preparation of competent cells and the electroporation conditions were optimised to achieve efficient transformation (Sekizaki et al., 1998). The study demonstrated that the optimum electroporation conditions for transferring plasmid DNA into *R. equi* were 2.5 kV/cm, 400 Ω , 25 μ F capacitance. Increasing resistance to 600 Ω resulted in a decrease in the number of transformants. In

contrast, increasing electroporation resistance did not significantly affect transformation efficiency in *R. jostii* strain 8.

Since similar approaches in the construction of plasmid and electrotransformation were applied with other *Rhodococcus* strains in our lab, the results from those *Rhodococcus* strains were worthy of comparison with the result from *R. jostii* strain 8. In *Rhodococcus* sp. AD45, electrotransformation of *isoA*, a key gene responsible for isoprene degradation, was successful only when transforming the DNA in a circular form, not a linear form (A. Crombie, data not published). This also happened when transforming foreign DNA into *Rhodococcus opacus* PD630 (data not published). Interestingly, transformation of plasmid DNA into *R. jostii* strain 8 resulted in significantly lower number of transformant colonies than the number of transformant colonies obtaining by transformation of linear DNA.

The optimization of production of competent cells was reported as one of the crucial parameters in transformation of foreign DNA into *Rhodococcus* spp. For example, it was found that pretreatment of competent cells at 50°C for 9 min could increase transformation efficiency by approximately 10-fold compared to the result obtained from heating cells at 37°C (Sekizaki et al., 1998). Also, the addition of 1% glycerol, 0.2% Tween 80 and 2% glycine to growth medium resulted in an increase in transformation efficiency by approximately 20-fold compared to the result without addition of any growth supplement. However, it should be noted that the highest transformation efficiency obtaining from this experiment was 1.7×10^4 cfu/ μ g DNA, which is not much higher than the efficiency we obtained from electroporation of *R. jostii* strain 8 (1.1×10^4 cfu/ μ g DNA). Growth medium supplemented with 0.85% (w/v) glycine was used to grow competent *R. opacus* PD630 in order to facilitate DNA transfer into the cells (Kalscheuer et al., 1999). Supplementation of glycine in growth medium and pre-treatment for electrocompetent cells was also applied in *R. opacus* strains (Na et al., 2005b). The study suggested that successful electrotransformation was obtained when 0.5% (w/v) glycine was added in the growth medium, together with pre-incubation of competent cells at 40°C for 10 min. Therefore, the pretreatment of cells with heat may also be important for electrotransformation in *R. jostii* strain 8. Therefore, it will be interesting in the future to also optimize competent cell culture conditions in order to increase

transformation efficiency, which might then increase the chance of obtaining the desired transformants.

One possible explanation for the unsuccessful gene-knockout experiments was that the genome of *R. jostii* strain 8 contains several genes encoding transposons which could result in rearrangement of gene sequences in the chromosome. This could lead to the recombination of mutated genes at undesired positions in the chromosome and cause the unsuccessful gene-knockout experiments.

Chapter 7

Conclusions and future prospects

7.1. Conclusions

7.1.1. Growth and oxidation studies

The aim of this study was to investigate whether there was a versatile enzyme responsible for the degradation of gaseous alkanes or more than one enzyme which was involved in alkane metabolism in *R. jostii* strain 8. In this study, *Rhodococcus jostii* strain 8 was isolated from a propane enrichment culture of petroleum-contaminated soil. The 16S rRNA sequence of *R. jostii* strain 8 was closely related (99% identity) to the 16S rRNA sequence of *Rhodococcus jostii* RHA1, a biphenyl degrader for which the genome sequence was available. Growth of *R. jostii* strain on a variety of alkanes and alkenes was tested in order to distinguish differences between *R. jostii* strain 8 and *R. jostii* RHA1. It was found that *R. jostii* strain 8 could grow on ethane, propane and butane, but not on the other gaseous alkanes and alkenes. Interestingly, *R. jostii* strain 8 could grow on ethane, butane, octane and naphthalene while *R. jostii* RHA1 could not grow on those substrates. The other difference between these two strains was that *R. jostii* RHA1 could grow on biphenyl and ethylbenzene, but *R. jostii* strain 8 could not grow on those substrates. Substrate-induced oxygen consumption was examined with various types of carbon compounds particularly alcohols, aldehydes and ketones which are intermediates in potential alkane degradation pathways. It was found that oxygen consumption rates in response to the addition of ethane, propane and butane were induced in cells grown on ethane, propane and butane, but not in glucose-grown cells. This suggested that oxidation of ethane, propane and butane in *R. jostii* strain 8 was inducible. The oxidation studies also showed that rates of oxygen consumption in response to substrates which are intermediates in primary pathway of propane oxidation (via 1-propanol) were significantly higher than the rates in response to the substrates which are intermediates in the secondary pathway (via 2-propanol). This suggested that propane was likely to be metabolized via the primary oxidation pathway. However, oxygen consumption rates with intermediates of the secondary oxidation pathway were still significant. Therefore, propane oxidation via the secondary oxidation pathway may also occur in *R. jostii* strain 8 and mutants that are defective in for example growth on acetone or acetol (further oxidation intermediates of 2-propanol) would need to be isolated and examined to see if their metabolism was essential during growth on propane.

7.1.2. The genome of *Rhodococcus jostii* strain 8

A draft genome sequence of *R. jostii* strain 8 was obtained. In the genome, there are gene clusters potentially responsible for the degradation of ethane, propane and butane in *R. jostii* strain 8. One gene cluster encodes the propane monooxygenase which is closely related to the propane monooxygenase of *R. jostii* RHA1. Another gene cluster found in the genome of *R. jostii* strain 8 encodes an *alkB*-type alkane monooxygenase. A complete *nar* operon encoding putative naphthalene 1, 2-dioxygenase was found in the genome of *R. jostii* strain 8. In contrast, the *nar* operon is absent in the genome of *R. jostii* RHA1. This observation prompted experiments which confirmed the ability of *R. jostii* strain 8 to grow on naphthalene and lack of growth of *R. jostii* RHA1 on naphthalene. In the genome of *R. jostii* strain 8, the absence of genes necessarily required for the expression of biphenyl and ethylbenzene dioxygenases correlates with growth profiles which showed that this bacterium cannot grow on biphenyl and ethylbenzene. In contrast, *R. jostii* RHA1 possesses complete operons encoding these two enzymes and can grow on biphenyl and ethylbenzene.

7.1.3. Expression studies

The expression of *prmA*, a key gene in the propane monooxygenase gene cluster and *alkB*, a key gene in the *alkB*-type alkane monooxygenase gene cluster was investigated. RT-qPCR analysis showed that *prmA* was responsible for growth of *R. jostii* strain 8 on propane, but not on ethane or butane. It is still in doubt whether the *alkB*-type alkane monooxygenase was involved in the growth of *R. jostii* strain 8 on alkanes, particularly ethane and butane because the result showed that *alkB* was inducible during growth on ethane, propane and butane. It should be noted that polypeptide analysis of cell-free extracts from cells grown on alkanes did not clearly identify the enzyme responsible for ethane and butane degradation. Investigations on the role of *alkB*-type alkane monooxygenase and propane monooxygenase in the degradation of alkanes were then diverted at efforts to carry out by mutagenesis of *prmA* and *alkB*.

7.1.4. Mutagenesis of *prmA* and *alkB*

The construction of plasmids carrying disrupted *prmA* (pAGB) and *alkB* (pXGY) which were to be used in marker-exchange mutagenesis was successful. The electroporation conditions for transferring pAGB and pXGY into *R. jostii* strain 8 were established. The optimum condition was 1.25kV/cm, 800Ω, 40μF using a single pulse. The plasmid pAGB and pXGY were successfully constructed, but the transformation of these plasmids into the wild-type *R. jostii* strain 8 was not successful. Therefore, it is still unclear whether the *alkB*-type alkane monooxygenase is necessary for the degradation of ethane, propane and butane. However, based on expression studies, it was clear that propane monooxygenase in *R. jostii* strain 8 is required for growth on propane. Further studies on the ability of the disrupted *prmA* and disrupted *alkB* mutants to grow on alkanes and other hydrocarbons would provide more details about the function of these two monooxygenases in *R. jostii* strain 8.

7.2. Future prospects

The results from this study provide better understanding of the roles of multiple monooxygenases in the degradation of gaseous alkanes in a propane-degrading *Rhodococcus jostii* strain 8. It was clear that propane monooxygenase in *R. jostii* strain 8 is responsible for degradation of propane. However, the role of *alkB*-type alkane monooxygenase in the degradation of alkanes in this bacterium is still unclear. Therefore, it would be useful to continue these studies in order to resolve whether the *alkB*-type alkane monooxygenase is involved in the degradation of gaseous alkanes in *R. jostii* strain 8 by mutagenesis and further biochemical studies to identify the AlkB in cell-free extracts of *R. jostii* strain 8 grown on different alkanes.

It was found that the pathway of propane metabolism initiated by propane monooxygenase was branched at the second step in propane oxidation, which alcohol dehydrogenases play an important role in the conversion of alcohols to aldehydes or ketones (Ashraf and Murrell, 1992). Further studies on substrate specificity range of these primary and secondary alcohol dehydrogenases would

worth investigation in order to confirm the exact pathways for gaseous alkane oxidation in *R. jostii* strain 8. According to the results from alcohol dehydrogenase assays, alcohol dehydrogenases involved in the metabolism of gaseous alkanes in *R. jostii* strain 8 were NDMA-dependent. Characterisation of this type of alcohol dehydrogenases has not been extensive. Purification of alcohol dehydrogenases from alkane-grown cells could be carried out, followed by enzyme assays in order to determine activities of the enzymes in response to alcohols of interest (1-propanol, 2-propanol, 1-butanol, 2-butanol). The purification procedures for NDMA-dependent alcohol dehydrogenases that could be used are those used to purify NDMA-dependent alcohol dehydrogenases from *Methanosarcina barkeri* DSM 804 strain Fusaro (Daussmann et al., 1997). An investigation on potential inhibitors for these enzymes would also be useful to carry out because this would provide more insight about the stability of NDMA-dependent alcohol dehydrogenases, if they require metals and other cofactors etc.

Further studies on the genome of *R. jostii* strain 8 should be carried out to retrieve more information relating to the catabolic capacities of this bacterium. In order to analyse the size and organization of the genome of *R. jostii* strain 8, pulse-field gel electrophoresis (PFGE) would be a useful tool to be carried out. This technique would provide more details on any plasmids that might be present in the genome.

Polypeptide analysis by SDS-PAGE showed that propane monooxygenase is inducible during growth on propane, but the results was still unclear as to whether the *alkB*-type alkane monooxygenase is involved in the growth of *R. jostii* strain 8 on alkanes. This might be because *alkB*-type alkane monooxygenase was not present in cell-free extracts due to inappropriate extraction methods used in this study. Therefore, it would be useful to use other extraction methods. One possible method for extracting active alkane monooxygenase from the cell membrane fraction is to use detergent to solubilize membrane fraction using 0.23% lauryldimethylamine oxide (LDAO) under the conditions described in the work which was carried out with *Pseudomonas putida* GPo1 (Xie et al., 2011). This method would also allow direct assays for hydroxylation activity towards hydrophobic substrates. In addition, studies on growth profiles of mutants lacking active *prmA* or *alkB* would strongly support the polypeptide analysis.

In this study, electroporation conditions were optimized, resulting in successful transfer of linear DNA into *R. jostii* strain 8 at quite good transformation frequencies. Construction of *prmA*-disrupted plasmid and *alkB*-disrupted plasmid for marker-exchange mutagenesis were successfully carried out. Since the *prmA*-deficient mutant and *alkB*-deficient mutant were not successfully obtained in the final marker-exchange mutagenesis steps, mutagenesis studies would need to be continued in order to obtain such mutants for further studies. A study of the growth of the *prmA*-disrupted mutant and the *alkB*-disrupted mutant on a range of alkanes, alkenes and other hydrocarbons and assessment of the oxidation ability of the mutants with those substrates would reveal substrate specificity of both the propane monooxygenase and the *alkB*-type alkane monooxygenase. Moreover, polypeptide analysis of cell-free extracts from both mutants grown on alkanes should be carried out in order to investigate the expression of propane monooxygenase and *alkB*-type alkane monooxygenase during growth on those substrates. Any polypeptides that are expected specifically on propane (or other alkanes) could be excised from the gel and their identity confirmed by mass spectrometry (as the genome sequence of *R. jostii* strain 8 is now available). It would also be useful to compare the polypeptide profiles from cell-free extracts of both mutants with that of the wild-type strain. Such results would confirm whether the *alkB*-type alkane monooxygenase is involved in the growth of *R. jostii* strain 8 on ethane, propane and butane.

This PhD research suggested the potential use of *R. jostii* strain 8 in the degradation of gaseous alkanes including ethane, propane, butane and also other aromatic compounds such as naphthalene. The hydrocarbon-degrading ability of *R. jostii* strain 8 indicates that it could potentially be a biocatalyst for the remediation of hydrocarbon-contaminated environments. It has been found that immobilized microbial enzymes can be utilized as biocatalysts in order to degrade hydrocarbons in situ (Munnecke, 1984, Kennedy et al., 1987, Nannipieri et al., 1991).

In terms of realistic applications, research could be applied to solve, for example, hydrocarbon-contamination causing by the explosion and oil spill from the Deepwater Horizon disaster in April 2010. This event was considered as the world's largest marine oil spill in which at least 4 million barrels of oil were spilled in the Gulf of Mexico (reported in the On scene coordinator report Deepwater Horizon oil spill, 2011). Recently in 2013 a pipeline transferring oil undersea in the Gulf of

Thailand to a tanker burst. At least 50 tons of oil leaked from the pipeline into the sea (*Bangkok Post* 28 July 2013). Both events are likely to influence the change of the microbial community in marine environment as the spills released large amounts of natural gas. However, existing microorganisms such as methane degraders have limited ability to consume longer chain hydrocarbons. They cannot efficiently utilize other hydrocarbons found in natural gas such as ethane and propane, so some of these compounds remain in the environment. Even though bacteria which can degrade those compounds in marine environments are not well-characterised, it is likely that the degradation of natural gas possibly depends on the metabolism of non-methanotrophic bacteria such as propane- or ethane-degrading bacteria. This PhD thesis has shown that *R. jostii* strain 8 could be a good candidate for the degradation of hydrocarbons. It is therefore a potential biocatalyst for degrading components of natural gas, which is mostly made up of short-chain alkanes. However, adverse effects of the use of microbes in biodegradation are still a long-running debate because microorganisms such as bacteria can multiply rapidly and can lower the amount of oxygen at the remediated sites (Mascarelli, 2010). The study of whether or not the depletion of oxygen causes harm to other living organisms is also important. The combined investigations in the use of *R. jostii* strain 8 for the degradation of hydrocarbons and effects of the decrease in oxygen level could be a fundamental research project with a view to mitigating environmental damage arising from oil spills.

Another example of hydrocarbon-contaminated environments includes fracking sites. Basically, fracking or hydraulic fracturing is the process of applying extremely high-pressure water and rock-dissolving fluids directly into the rocks in order to channel them and release natural gas inside. For that purpose, water, sand and chemicals are injected into the rocks at high pressure so that natural gas can escape through the top of the well. An accumulation of natural gas and its constituents from fracking is one of the most concerned environmental problems regarding energy industries. This, undoubtedly, could be mitigated by gaining benefits from the capability of bacteria to degrade alkanes, alkenes and aromatic compounds. Due to the revolution of the energy industries, fracking has been extensively used in the US and Europe such as UK whereas there are also several environmental concerns (e.g. see Table 1 of Ridlington, 2013). The first concern is

that the large amount of water that is needed to inject to the fracking site will change geological properties of the site. The second is the worry that chemicals such as methanol, naphthalene, benzene and formaldehyde, which are potentially carcinogenic, used during fracking processes may release and contaminate groundwater around fracking sites (Schafer, 2012, Gilman et al., 2010, Arbelaez et al., 2014). Furthermore, since high pressure is applied to break apart hard shale rocks, there is also a concern that fracking can possibly cause small earthquake such as the 1.5 and 2.2 magnitude earthquakes in the Blackpool area in UK in 2011 (Marshall, 2011). Although the link between the shale gas drilling and earthquakes is still controversial, it is obvious that the environment could be contaminated only by toxic chemicals used in the fracking process but also by natural gas which is mostly comprised of gaseous alkanes such as methane, ethane and propane. The capability of bacteria to degrade alkanes, alkenes and aromatic compounds as part of this PhD research can therefore be applied to minimize the environmental impact during fracking process.

It should be noted that the ability of *Rhodococcus jostii* strain 8 to degrade ethane, propane and butane allows this bacterium to be a promising biocatalysts. A large amount of accumulation of, for example, short-chain alkanes around fracking sites could be mitigated by the use of gaseous alkane-degrading enzymes from *R. jostii* strain 8 or its whole cells. For that purpose, purification of alkane-degrading enzymes probably followed by encapsulation of the enzymes is worth carrying out and investigating further in the future. A better understanding of *R. jostii* strain 8 in the degradation of gaseous alkanes is essential in providing the solution for environmental damage caused by hydrocarbon contamination.

References

- Ahmad, M., Roberts, J.N., Hardiman, E.M., Singh, R., Eltis, L.D., and Bugg, T.D. (2011) Identification of DypB from *Rhodococcus jostii* RHA1 as a lignin peroxidase. *Biochemistry* **50**: 5096-5107.
- Allen, C. C. R., Boyd, D. R., Larkin, M. J., Reid, K. A., Sharma, N. D., and Wilson, K. (1997) Metabolism of naphthalene, 1-naphthol, indene and indole by *Rhodococcus* sp. strain NCIMB 12038. *Appl. Environ. Microbiol.* **63**: 151-155.
- Alonso, H., Kleifeld, O., Yeheskel, A., Ong, P.C., Liu, Y.C., Stok, J.E. et al. (2014) Structural and mechanistic insight into alkane hydroxylation by *Pseudomonas putida* AlkB. *Biochem J* **460**: 283-293.
- Anthony, C., and Zatman, L.J. (1964) The microbial oxidation of methanol. 2. The methanol-oxidizing enzyme of *Pseudomonas* sp. M 27. *Biochem J* **92**: 614-621.
- Anthony, C., and Zatman, L.J. (1967) The microbial oxidation of methanol. The prosthetic group of the alcohol dehydrogenase of *Pseudomonas* sp. M27: a new oxidoreductase prosthetic group. *Biochem J* **104**: 960-969.
- Arbelaez, J., Wolf, S. and Grinberg, A. (2014). Fracking, acidizing, and increased earthquake risk in California. *On Shaking Ground*.
- Arfman, N., and Dijkhuizen, L. (1990) Methanol dehydrogenase from thermotolerant methylotroph *Bacillus* C1. *Methods Enzymol* **188**: 223-226.
- Armstrong, J.M. (1964) The molar extinction coefficient of 2,6-dichlorophenol indophenol. *Biochim Biophys Acta* **86**: 194-197.
- Arp, D.J. (1999) Butane metabolism by butane-grown *Pseudomonas butanovora*. *Microbiology* **145**: 1173-1180.
- Ashraf, W., and Murrell, J.C. (1992) Genetic, biochemical and immunological evidence for the involvement of two alcohol dehydrogenases in the metabolism of propane by *Rhodococcus rhodochrous* PNKb1. *Arch Microbiol* **157**: 488-492.
- Ashraf, W., Mihdhir, A., and Murrell, J.C. (1994) Bacterial oxidation of propane. *FEMS Microbiol Lett* **122**: 1-6.
- Auffret, M., Labbé, D., Thouand, G., Greer, C.W., and Fayolle-Guichard, F. (2009) Degradation of a mixture of hydrocarbons, gasoline, and diesel oil additives by *Rhodococcus aetherivorans* and *Rhodococcus wratislaviensis*. *Appl Environ Microbiol* **75**: 7774-7782.
- Bala, M., Kumar, S., Raghava, G.P., and Mayilraj, S. (2013a) Draft genome sequence of *Rhodococcus qingshengii* strain BKS 20-40. *Genome Announc* **1**: e0012813.
- Bala, M., Kumar, S., Raghava, G.P., and Mayilraj, S. (2013b) Draft genome sequence of *Rhodococcus ruber* strain BKS 20-38. *Genome Announc* **1**: e0013913.

- Begoña Prieto, M., Hidalgo, A., Serra, J.L., and Llama, M.J. (2002) Degradation of phenol by *Rhodococcus erythropolis* UPV-1 immobilized on Biolite in a packed-bed reactor. *J Biotechnol* **97**: 1-11.
- Benson, S., Oppici, M., Shapiro, J., and Fennewald, M. (1979) Regulation of membrane peptides by the *Pseudomonas* plasmid alk regulon. *J Bacteriol* **140**: 754-762.
- Bobik, T.A. (2006) Polyhedral organelles compartmenting bacterial metabolic processes. *Appl Microbiol Biotechnol* **70**: 517-525.
- Bolt, H.M., Roos, P.H., and Thier, R. (2003) The cytochrome P450 isoenzyme CYP2E1 in the biological processing of industrial chemicals: consequences for occupational and environmental medicine. *Int Arch Occup Environ Health* **76**: 174-185.
- Borodina, E., Nichol, T., Dumont, M.G., Smith, T.J., and Murrell, J.C. (2007) Mutagenesis of the "leucine gate" to explore the basis of catalytic versatility in soluble methane monooxygenase. *Appl Environ Microbiol* **73**: 6460-6467.
- Bosello, M., Robbel, L., Linne, U., Xie, X., and Marahiel, M.A. (2011) Biosynthesis of the siderophore rhodochelin requires the coordinated expression of three independent gene clusters in *Rhodococcus jostii* RHA1. *J Am Chem Soc* **133**: 4587-4595.
- Bystrykh, L.V., Vonck, J., van Bruggen, E.F., van Beeumen, J., Samyn, B., Govorukhina, N.I. et al. (1993) Electron microscopic analysis and structural characterization of novel NADP(H)-containing methanol: N,N'-dimethyl-4-nitrosoaniline oxidoreductases from the Gram-positive methylotrophic bacteria *Amycolatopsis methanolica* and *Mycobacterium gastri* MB19. *J Bacteriol* **175**: 1814-1822.
- Bédard, C., and Knowles, R. (1989) Physiology, biochemistry, and specific inhibitors of CH₄, NH₄⁺, and CO oxidation by methanotrophs and nitrifiers. *Microbiol Rev* **53**: 68-84.
- Cardy, D.L., Laidler, V., Salmond, G.P., and Murrell, J.C. (1991) Molecular analysis of the methane monooxygenase (MMO) gene cluster of *Methylosinus trichosporium* OB3b. *Mol Microbiol* **5**: 335-342.
- Chakrabarty, A.M., Chou, G., and Gunsalus, I.C. (1973) Genetic regulation of octane dissimilation plasmid in *Pseudomonas*. *Proc Natl Acad Sci U S A* **70**: 1137-1140.
- Chase, H.H., Davis, J.B., and Raymond, R.L. (1956) *Mycobacterium paraffinicum* n. sp., a bacterium isolated from soil. *Appl Microbiol* **4**: 310-315.
- Chen, Y., Crombie, A., Rahman, M.T., Dedysh, S.N., Liesack, W., Stott, M.B. et al. (2010) Complete genome sequence of the aerobic facultative methanotroph *Methylocella silvestris* BL2. *J Bacteriol* **192**: 3840-3841.

- Chen, Y., Yang, L., Ding, Y., Zhang, S., He, T., Mao, F. et al. (2013) Tracing evolutionary footprints to identify novel gene functional linkages. *PLoS One* **8**: e66817.
- Chen, Y., Ding, Y., Yang, L., Yu, J., Liu, G., Wang, X. et al. (2014) Integrated omics study delineates the dynamics of lipid droplets in *Rhodococcus opacus* PD630. *Nucleic Acids Res* **42**: 1052-1064.
- Chiba, K., Hoshino, Y., Ishino, K., Kogure, T., Mikami, Y., Uehara, Y., and Ishikawa, J. (2007) Construction of a pair of practical *Nocardia-Escherichia coli* shuttle vectors. *Jpn J Infect Dis* **60**: 45-47.
- Coleman, J.P., and Perry, J.J. (1985) Purification and characterization of the secondary alcohol dehydrogenase from propane-utilizing *Mycobacterium vaccae* strain JOB-5. *J Gen Microbiol* **131**: 2901-2907.
- Coleman, N.V., Bui, N.B., and Holmes, A.J. (2006) Soluble di-iron monooxygenase gene diversity in soils, sediments and ethene enrichments. *Environmental Microbiology* **8**: 1228-1239.
- Coleman, N.V., Le, N.B., Ly, M.A., Ogawa, H.E., McCarl, V., LWilson, N., and Holmes, A.J. (2012) Hydrocarbon monooxygenase in *Mycobacterium*: recombinant expression of a member of the ammonia monooxygenase superfamily. *ISME Journal* **6**: 171-182.
- Coleman, N.V., Yau, S., Wilson, N.L., Nolan, L.M., Migocki, M.D., Ly, M.A. et al. (2011) Untangling the multiple monooxygenases of *Mycobacterium chubuense* strain NBB4, a versatile hydrocarbon degrader. *Environ Microbiol Rep* **3**: 297-307.
- Conrad, R. (1996) Soil microorganisms as controllers of atmospheric trace gases (H₂, CO, CH₄, OCS, N₂O, and NO). *Microbiol Rev* **60**: 609-640.
- Cooley, R.B., Dubbels, B.L., Sayavedra-Soto, L.A., Bottomley, P.J., and Arp, D.J. (2009) Kinetic characterization of the soluble butane monooxygenase from *Thauera butanivorans*, formerly *Pseudomonas butanovora*. *Microbiology* **155**: 2086-2096.
- Coufal, D.E., Blazyk, J.L., Whittington, D.A., Wu, W.W., Rosenzweig, A.C., and Lippard, S.J. (2000) Sequencing and analysis of the *Methylococcus capsulatus* (Bath) soluble methane monooxygenase genes. *Eur J Biochem* **267**: 2174-2185.
- Craft, D.L., Madduri, K.M., Eshoo, M., and Wilson, C.R. (2003) Identification and characterization of the CYP52 family of *Candida tropicalis* ATCC 20336, important for the conversion of fatty acids and alkanes to alpha,omega-dicarboxylic acids. *Appl Environ Microbiol* **69**: 5983-5991.
- Crombie, A.T., and Murrell, J.C. (2014) Trace-gas metabolic versatility of the facultative methanotroph *Methylocella silvestris*. *Nature* **510**: 148-151.
- Dabbs, E.R. (1998) Cloning of genes that have environmental and clinical importance from rhodococci and related bacteria. *Antonie Van Leeuwenhoek* **74**: 155-167.

Dabbs, E.R., Gowan, B., and Andersen, S.J. (1990) Nocardioform arsenic resistance plasmids and construction of *Rhodococcus* cloning vectors. *Plasmid* **23**: 242-247.

Dalton, H., S. D. Prior, D. J. Leak, and S. H. Stanley. (1984). Regulation and control of methane monooxygenase, p. 75–82. In R. L. Crawford and R. S. Hanson (ed.), *Microbial growth on C1 compounds. American Society for Microbiology*, Washington, D.C

Dalton, H. (2005) The Leeuwenhoek Lecture 2000 the natural and unnatural history of methane-oxidizing bacteria. *Philos Trans R Soc Lond B Biol Sci* **360**: 1207-1222.

Daussmann, T., Aivasidis, A., and Wandrey, C. (1997) Purification and characterization of an alcohol:N,N-dimethyl-4-nitrosoaniline oxidoreductase from the methanogen *Methanosarcina barkeri* DSM 804 strain Fusaro. *Eur J Biochem* **248**: 889-896.

Day, D., and Anthony, C. (1990) Methanol dehydrogenase from *Methylobacterium extorquens* AM1. *Methods Enzymol* **188**: 210-216.

De Mot, R., Nagy, I., De Schrijver, A., Pattanapitpaisal, P., Schoofs, G., and Vanderleyden, J. (1997) Structural analysis of the 6 kb cryptic plasmid pFAJ2600 from *Rhodococcus erythropolis* NI86/21 and construction of *Escherichia coli*-*Rhodococcus* shuttle vectors. *Microbiology* **143**: 3137-3147.

de Vries, G.E., Arfman, N., Terpstra, P., and Dijkhuizen, L. (1992) Cloning, expression, and sequence analysis of the *Bacillus methanolicus* C1 methanol dehydrogenase gene. *J Bacteriol* **174**: 5346-5353.

Dennis, J.J., and Zylstra, G.J. (1998) Plasposons: modular self-cloning minitransposon derivatives for rapid genetic analysis of Gram-negative bacterial genomes. *Appl Environ Microbiol* **64**: 2710-2715.

Desomer, J., Dhaese, P., and Van Montagu, M. (1988) Conjugative transfer of cadmium resistance plasmids in *Rhodococcus fascians* strains. *J Bacteriol* **170**: 2401-2405.

Desomer, J., Dhaese, P., and Montagu, M.V. (1990) Transformation of *Rhodococcus fascians* by high-voltage electroporation and development of *R. fascians* cloning vectors. *Appl Environ Microbiol* **56**: 2818-2825.

Di Gennaro, P., Terreni, P., Masi, G., Botti, S., De Ferra, F., and Bestetti, G. (2010) Identification and characterization of genes involved in naphthalene degradation in *Rhodococcus opacus* R7. *Appl Microbiol Biotechnol* **87**: 297-308.

Dower, W.J., Miller, J.F., and Ragsdale, C.W. (1988) High efficiency transformation of *E. coli* by high voltage electroporation. *Nucleic Acids Res* **16**: 6127-6145.

Duine, J.A., Frank, J., and Verwiel, P.E. (1980) Structure and activity of the prosthetic group of methanol dehydrogenase. *Eur J Biochem* **108**: 187-192.

Eastcott, L., Shiu, W.Y., and Mackay, D. (1988) Environmentally relevant physical-chemical properties of hydrocarbons: a review of data and development of simple correlations. *Oil Chem Pollut* **4**: 191–216.

Eggink, G., van Lelyveld, P.H., Arnberg, A., Arfman, N., Witteveen, C., and Witholt, B. (1987) Structure of the *Pseudomonas putida* alkBAC operon. Identification of transcription and translation products. *J Biol Chem* **262**: 6400-6406.

Elango, N., Radhakrishnan, R., Froland, W.A., Wallar, B.J., Earhart, C.A., Lipscomb, J.D., and Ohlendorf, D.H. (1997) Crystal structure of the hydroxylase component of methane monooxygenase from *Methylosinus trichosporium* OB3b. *Protein Sci* **6**: 556-568.

Federal register, 1987. Notice of the first priority list of hazardous substances that will be the subject of toxicological profiles. Fed. Reg. 52, 12866.

Fernández de Las Heras, L., Alonso, S., de la Vega de León, A., Xavier, D., Perera, J., and Navarro Llorens, J.M. (2013) Draft genome sequence of the steroid degrader *Rhodococcus ruber* strain Chol-4. *Genome Announc* **1**.

Finnerty, W.R. (1992) The biology and genetics of the genus *Rhodococcus*. *Annu Rev Microbiol* **46**: 193-218.

Fisher, M.B., Zheng, Y.M., and Rettie, A.E. (1998) Positional specificity of rabbit CYP4B1 for omega-hydroxylation of short-medium chain fatty acids and hydrocarbons. *Biochem Biophys Res Commun* **248**: 352-355.

Forney, F.W., and Markovetz, A.J. (1970) Subterminal oxidation of aliphatic hydrocarbons. *J Bacteriol* **102**: 281-282.

Fournier, D., Hawari, J., Halasz, A., Streger, S.H., McClay, K.R., Masuda, H., and Hatzinger, P.B. (2009) Aerobic biodegradation of N-nitrosodimethylamine by the propanotroph *Rhodococcus ruber* ENV425. *Applied and Environmental microbiology* **75**: 5088-5093.

Fox, B.G., Froland, W.A., Dege, J.E., and Lipscomb, J.D. (1989) Methane monooxygenase from *Methylosinus trichosporium* OB3b. Purification and properties of a three-component system with high specific activity from a Type II methanotroph. *J Biol Chem* **264**: 10023-10033.

Furuhashi, K. (1992) Biological routes to optically active epoxides. In chirality in industry. Collins, A.N., Sheldrake, G.N., and Crosby, J. (eds). London: John Wiley & Sons, pp. 167-186.

Garg, B., Dogra, R.C., and Sharma, P.K. (1999) High-efficiency transformation of *Rhizobium leguminosarum* by electroporation. *Appl Environ Microbiol* **65**: 2802-2804.

Gay, P., Le Coq, D., Steinmetz, M., Berkelman, T., and Kado, C.I. (1985) Positive selection procedure for entrapment of insertion sequence elements in Gram-negative bacteria. *J Bacteriol* **164**: 918-921.

Gerhardt, P. (1981). Diluents and biomass measurement. In: Manual of methods for general bacteriology, pp. 504-507. P. Gerhardt, R. Murray, R. Costilow, E. Nester, W. Wood, N. Kreig, G. Phillips (eds.). ASM publishers.

Gilman, J.B., de Gouw, J., Kuster, W., Bon, D., Warneke, C., Hooloway, J., Williams, E., Lerner, B., Pollack, I., Ryerson, T., Atlas, E., Blake, D., Vlasenko, A., Li, S-M., Alvarez, S., Flynn, Herndon, S., Zahniser, M., Rappengluck, B. and Lefer, B. (2010). "VOCs in the Greater Los Angeles Basin: Characterizing the gas-phase chemical evolution of air masses via multi-platform measurements during CalNEX". www.esrl.noaa.gov/csd/projects/calnex/meetings/datawkshpMay2011/monday/Gilman.pdf. Retrieved January 2015.

Goncalves, E.R., Hara, H., Miyazawa, D., Davies, J.E., Eltis, L.D., and Mohn, W.W. (2006) Transcriptomic assessment of isozymes in the biphenyl pathway of *Rhodococcus* sp. strain RHA1. *Appl Environ Microbiol* **72**: 6183-6193.

Goodfellow, M., Thomas, E.G., Ward, A.C., and James, A.L. (1990) Classification and identification of rhodococci. *Zentralbl Bakteriell* **274**: 299-315.

Goswami, M., Shivaraman, N., and Singh, R.P. (2005) Microbial metabolism of 2-chlorophenol, phenol and p-cresol by *Rhodococcus erythropolis* M1 in co-culture with *Pseudomonas fluorescens* P1. *Microbiol Res* **160**: 101-109.

Graham, D.W., Korich, D.G., LeBlanc, R.P., Sinclair, N.A., and Arnold, R.G. (1992) Applications of a colorimetric plate assay for soluble methane monooxygenase activity. *Appl Environ Microbiol* **58**: 2231-2236.

Graham, S.E., and Peterson, J.A. (2002) Sequence alignments, variabilities, and vagaries. *Methods Enzymol* **357**: 15-28.

Gray, T.A., Palumbo, M.J., and Derbyshire, K.M. (2013) Draft genome sequence of MKD8, a conjugal recipient *Mycobacterium smegmatis* strain. *Genome Announc* **1**: e0014813.

Green, J., and Dalton, H. (1989) Substrate specificity of soluble methane monooxygenase. Mechanistic implications. *J Biol Chem* **264**: 17698-17703.

Groen, B., Frank, J., and Duine, J.A. (1984) Quinoprotein alcohol dehydrogenase from ethanol-grown *Pseudomonas aeruginosa*. *Biochem J* **223**: 921-924.

Görisch, H., and Rupp, M. (1989) Quinoprotein ethanol dehydrogenase from *Pseudomonas*. *Antonie Van Leeuwenhoek* **56**: 35-45.

Hamamura, N., Yeager, C.M., and Arp, D.J. (2001) Two distinct monooxygenases for alkane oxidation in *Nocardioides* sp. strain CF8. *Appl Environ Microbiol* **67**: 4992-4998.

Hamamura, N., Storfa, R.T., Semprini, L., and Arp, D.J. (1999) Diversity in butane monooxygenases among butane-grown bacteria. *Appl Environ Microbiol* **65**: 4586-4593.

Hara, A., Baik, S.H., Syutsubo, K., Misawa, N., Smits, T.H., van Beilen, J.B., and Harayama, S. (2004) Cloning and functional analysis of *alkB* genes in *Alcanivorax borkumensis* SK2. *Environ Microbiol* **6**: 191-197.

Hattermann, D.R., and Stacey, G. (1990) Efficient DNA transformation of *Bradyrhizobium japonicum* by electroporation. *Appl Environ Microbiol* **56**: 833-836.

Hektor H.J., K.H., Dijkhuizen L. (2000) Nicotinoprotein methanol dehydrogenase enzymes in Gram-positive methylotrophic bacteria. *Journal of Molecular catalysis B: Enzymatic* **8**: 103-109.

Holder, J.W., Ulrich, J.C., DeBono, A.C., Godfrey, P.A., Desjardins, C.A., Zucker, J. et al. (2011) Comparative and functional genomics of *Rhodococcus opacus* PD630 for biofuels development. *PLoS Genetics* **7**: e1002219.

Holmes, A.J., and Coleman, N.V. (2008) Evolutionary ecology and multidisciplinary approaches to prospecting for monooxygenases as biocatalysts. *Antonie Van Leeuwenhoek* **94**: 75-84.

Holmes, A.J., Costello, A., Lidstrom, M.E., and Murrell, J.C. (1995) Evidence that particulate methane monooxygenase and ammonia monooxygenase may be evolutionarily related. *FEMS Microbiol Lett* **132**: 203-208.

Hopwood, D. A., Bibb, M. J., Chater, K. F., Kieser, T., Bruton, C. J., Keiser, H. M., Lydiate, D. J., Smith, C. P., Ward, J. M., and Schrempf, H. (1985) Genetic manipulation of *Streptomyces*: A laboratory manual. John Innes, Norwich, UK.

Hou, C.T., Patel, R.N., Laskin, A.I., Barist, I., and Barnabe, N. (1983a) Thermostable NAD-linked secondary alcohol dehydrogenase from propane-grown *Pseudomonas fluorescens* NRRL B-1244. *Appl Environ Microbiol* **46**: 98-105.

Hou, C.T., Patel, R.N., Laskin, A.I., Barnabe, N., and Barist, I. (1983b) Purification and properties of a NAD-linked 1,2-propanediol dehydrogenase from propane-grown *Pseudomonas fluorescens* NRRL B-1244. *Arch Biochem Biophys* **223**: 297-308.

Hughes, J., Armitage, Y.C., and Symes, K.C. (1998) Application of whole cell rhodococcal biocatalysts in acrylic polymer manufacture. *Antonie Van Leeuwenhoek* **74**: 107-118.

Hutchens, E., Radajewski, S., Dumont, M.G., McDonald, I.R., and Murrell, J.C. (2004) Analysis of methanotrophic bacteria in Movile Cave by stable isotope probing. *Environ Microbiol* **6**: 111-120.

Hyman, M.R., and Wood, P.M. (1985) Suicidal inactivation and labelling of ammonia monooxygenase by acetylene. *Biochem J* **227**: 719-725.

Iba, M.M., Fung, J., and Gonzalez, F.J. (2000) Functional CYP2E1 is required for substantial *in vivo* formation of 2,5-hexanedione from n-hexane in the mouse. *Arch Toxicol* **74**: 582-586.

Iino, T., Miyauchi, K., Kasai, D., Masai, E., and Fukuda, M. (2013) Characterization of nitrate and nitrite utilization system in *Rhodococcus jostii* RHA1. *J Biosci Bioeng* **115**: 600-606.

Inoue, H., Nojima, H., and Okayama, H. (1990) High efficiency transformation of *Escherichia coli* with plasmids. *Gene* **96**: 23-28.

Ivshina, I.B., Oborin, A.A., Nesterenko, O.A., and Kasumova, S.A. (1981) Bacteria of the *Rhodococcus* genus from the ground water of oil-bearing deposits in the Perm region near the Urals. *Microbiology* **50**: 709-717.

Ivshina, I.B., Kamenskikh, T.N, and Liapunov, Y.E. (1994) IEGM catalogue of strains of regional specialized collection of alkanotrophic microorganisms. Nauka, Moscow.

Iwasaki, T., Miyauchi, K., Masai, E., and Fukuda, M. (2006) Multiple-subunit genes of the aromatic-ring-hydroxylating dioxygenase play an active role in biphenyl and polychlorinated biphenyl degradation in *Rhodococcus* sp. strain RHA1. *Appl Environ Microbiol* **72**: 5396-5402.

Johnson, E.L., and Hyman, M.R. (2006) Propane and n-butane oxidation by *Pseudomonas putida* GPo1. *Appl Environ Microbiol* **72**: 950-952.

Jäger, W., Schäfer, A., Kalinowski, J., and Pühler, A. (1995) Isolation of insertion elements from Gram-positive *Brevibacterium*, *Corynebacterium* and *Rhodococcus* strains using the *Bacillus subtilis* *sacB* gene as a positive selection marker. *FEMS Microbiol Lett* **126**: 1-6.

Jörnvall, H., Persson, B., and Jeffery, J. (1987) Characteristics of alcohol/polyol dehydrogenases. The zinc-containing long-chain alcohol dehydrogenases. *Eur J Biochem* **167**: 195-201.

Kalscheuer, R., Arenskötter, M., and Steinbüchel, A. (1999) Establishment of a gene transfer system for *Rhodococcus opacus* PD630 based on electroporation and its application for recombinant biosynthesis of poly(3-hydroxyalkanoic acids). *Appl Microbiol Biotechnol* **52**: 508-515.

Kennedy, J.E; Cabral, J.M.S. (1987). Enzyme immobilization. *Enzyme Technology Biotechnology*. 7a; Kennedy, J.E, Ed.; Weinheim, Germany. VCH Verlagsgesellschaft. pp. 347-404.

Kotani, T., Yamamoto, T., Yurimoto, H., Sakai, Y., and Kato, N. (2003) Propane monooxygenase and NAD⁺-dependent secondary alcohol dehydrogenase in propane metabolism by *Gordonia* sp. strain TY-5. *Journal of Bacteriology* **185**: 7120-7128.

Kotani, T., Kawashima, Y., Yurimoto, H., Kato, N., and Sakai, Y. (2006) Gene structure and regulation of alkane monooxygenases in propane-utilizing *Mycobacterium* sp. TY-6 and *Pseudonocardia* sp. TY-7. *Journal of Bioscience and Bioengineering* **102**: 184-192.

- Kulakov, L.A., Chen, S., Allen, C.C., and Larkin, M.J. (2005) Web-type evolution of *Rhodococcus* gene clusters associated with utilization of naphthalene. *Appl Environ Microbiol* **71**: 1754-1764.
- Kulikova, A.K., and Bezborodov, A.M. (2000) Oxidation of organic compounds by *Rhodococcus erythropolis* 3/89 propanomonooxygenase. *Prikl Biokhim Mikrobiol* **36**: 267-271.
- Kunau, W.H., Dommès, V., and Schulz, H. (1995) Beta-oxidation of fatty acids in mitochondria, peroxisomes, and bacteria: a century of continued progress. *Prog Lipid Res* **34**: 267-342.
- Kurth, E.G., Doughty, D.M., Bottomley, P.J., Arp, D.J., and Sayavedra-Soto, L.A. (2008) Involvement of BmoR and BmoG in n-alkane metabolism in *Pseudomonas butanovora*. *Microbiology* **154**: 139-147.
- Labinger, J.A., and Bercaw, J.E. (2002) Understanding and exploiting C-H bond activation. *Nature* **417**: 507-514.
- Lane, D.J. (1991) 16S/23S rRNA sequencing. In *Nucleic acid techniques in bacterial systematics*. Stackebrandt, E. (ed). Chichester: Wiley & Sons, pp. 115 - 175.
- Larkin, M.J., Kulakov, L.A., and Allen, C.C. (2005) Biodegradation and *Rhodococcus*--masters of catabolic versatility. *Curr Opin Biotechnol* **16**: 282-290.
- Larkin, M.J., De Mot, R., Kulakov, L.A., and Nagy, I. (1998) Applied aspects of *Rhodococcus* genetics. *Antonie Van Leeuwenhoek* **74**: 133-153.
- Leahy, J.G., Batchelor, P.J., and Morcomb, S.M. (2003) Evolution of the soluble diiron monooxygenases. *FEMS Microbiol Rev* **27**: 449-479.
- LeBlanc, J.C., Gonçalves, E.R., and Mohn, W.W. (2008) Global response to desiccation stress in the soil actinomycete *Rhodococcus jostii* RHA1. *Appl Environ Microbiol* **74**: 2627-2636.
- Li, H.Y., Darwish, K., and Poulos, T.L. (1991) Characterization of recombinant *Bacillus megaterium* cytochrome P450 BM-3 and its two functional domains. *J Biol Chem* **266**: 11909-11914.
- Lindahl, R. (1992) Aldehyde dehydrogenases and their role in carcinogenesis. *Crit Rev Biochem Mol Biol* **27**: 283-335.
- Lloyd, J.S., De Marco, P., Dalton, H., and Murrell, J.C. (1999) Heterologous expression of soluble methane monooxygenase genes in methanotrophs containing only particulate methane monooxygenase. *Arch Microbiol* **171**: 364-370.
- Lopes Ferreira, N., Mathis, H., Labbé, D., Monot, F., Greer, C.W., and Fayolle-Guichard, F. (2007) n-Alkane assimilation and tert-butyl alcohol (TBA) oxidation capacity in *Mycobacterium austroafricanum* strains. *Appl Microbiol Biotechnol* **75**: 909-919.

- Lukins, H.B., and Foster, J.W. (1963) Methyl ketone metabolism in hydrocarbon-utilizing Mycobacteria. *J Bacteriol* **85**: 1074-1087.
- MacEachran, D.P., Prophete, M.E., and Sinskey, A.J. (2010) The *Rhodococcus opacus* PD630 heparin-binding hemagglutinin homolog TadA mediates lipid body formation. *Appl Environ Microbiol* **76**: 7217-7225.
- Maier, T., Förster, H.H., Asperger, O., and Hahn, U. (2001) Molecular characterization of the 56-kDa CYP153 from *Acinetobacter* sp. EB104. *Biochem Biophys Res Commun* **286**: 652-658.
- Marshall, M. (2011). “How fracking caused earthquake in the UK”. www.newscientist.com. New Scientist. 2 November 2011. Retrieved December 2014.
- Martin, K.E., Ozsvar, J., and Coleman, N.V. (2014) SmoXYB1C1Z of *Mycobacterium* NBB4: an sMMO-like monooxygenase, active on C₂-C₄ alkanes and alkenes. *Appl Environ Microbiol*.
- Maruyama, T., Ishikura, M., Taki, H., Shindo, K., Kasai, H., Haga, M. et al. (2005) Isolation and characterization of o-xylene oxygenase genes from *Rhodococcus opacus* TKN14. *Appl Environ Microbiol* **71**: 7705-7715.
- Masai, E., Yamada, A., Healy, J.M., Hatta, T., Kimbara, K., Fukuda, M., and Yano, K. (1995) Characterization of biphenyl catabolic genes of Gram-positive polychlorinated biphenyl degrader *Rhodococcus* sp. strain RHA1. *Appl Environ Microbiol* **61**: 2079-2085.
- Mascarelli, A. (2010). “Muddying the waters on Gulf oxygen data”. www.nature.com. 27 July 2010. Retrieved January 2015.
- McKenna, E.J., and Coon, M.J. (1970) Enzymatic omega-oxidation. IV. Purification and properties of the omega-hydroxylase of *Pseudomonas oleovorans*. *J Biol Chem* **245**: 3882-3889.
- McLeod, M.P., Warren, R.L., Hsiao, W.W., Araki, N., Myhre, M., Fernandes, C. et al. (2006) The complete genome of *Rhodococcus* sp. RHA1 provides insights into a catabolic powerhouse. *Proc Natl Acad Sci U S A* **103**: 15582-15587.
- Munnecke, D.M. (1984). Biotechnology approaches to hazardous waste. *Biotech '84 USA: World Biotech Report*; Online Publ. Pinner: U.K. pp 525-532.
- Murrell, J.C., Gilbert, B., and McDonald, I.R. (2000) Molecular biology and regulation of methane monooxygenase. *Arch Microbiol* **173**: 325-332.
- Na, K.S., Kuroda, A., Takiguchi, N., Ikeda, T., Ohtake, H., and Kato, J. (2005a) Isolation and characterization of benzene-tolerant *Rhodococcus opacus* strains. *J Biosci Bioeng* **99**: 378-382.
- Na, K.S., Nagayasu, K., Kuroda, A., Takiguchi, N., Ikeda, T., Ohtake, H., and Kato, J. (2005b) Development of a genetic transformation system for benzene-tolerant *Rhodococcus opacus* strains. *J Biosci Bioeng* **99**: 408-414.

Nagy, I., Verheijen, S., De Schrijver, A., Van Damme, J., Proost, P., Schoofs, G. et al. (1995) Characterization of the *Rhodococcus* sp. NI86/21 gene encoding alcohol: N,N'-dimethyl-4-nitrosoaniline oxidoreductase inducible by atrazine and thiocarbamate herbicides. *Arch Microbiol* **163**: 439-446.

Nannipieri, P.; Bollag, J.-M. (1991). Use of enzymes to detoxify pesticide-contaminated soils and waters. *Environ. Qual.* **20**, 510.

Nguyen, H.H., Elliott, S.J., Yip, J.H., and Chan, S.I. (1998) The particulate methane monooxygenase from *Methylococcus capsulatus* (Bath) is a novel copper-containing three-subunit enzyme. Isolation and characterization. *J Biol Chem* **273**: 7957-7966.

"Oil spill threatens Rayong beaches". www.bangkokpost.com. Bangkok Post. 28 July 2013. Retrieved 31 July 2013.

"On scene coordinator report Deepwater Horizon oil spill". http://www.uscg.mil/foia/docs/dwh/fosc_dwh_report.pdf. September 2011. Retrieved January 2015.

Overbeek, R., Olson, R., Pusch, G.D., Olsen, G.J., Davis, J.J., Disz, T. et al. (2014) The SEED and the Rapid Annotation of microbial genomes using Subsystems Technology (RAST). *Nucleic Acids Res* **42**: D206-214.

Owen, D.J., Eggink, G., Hauer, B., Kok, M., McBeth, D.L., Yang, Y.L., and Shapiro, J.A. (1984) Physical structure, genetic content and expression of the alkBAC operon. *Mol Gen Genet* **197**: 373-383.

Padda, R.S., Pandey, K.K., Kaul, S., Nair, V.D., Jain, R.K., Basu, S.K., and Chakrabarti, T. (2001) A novel gene encoding a 54 kDa polypeptide is essential for butane utilization by *Pseudomonas* sp. IMT37. *Microbiology* **147**: 2479-2491.

Paisio, C.E., Talano, M.A., González, P.S., Pajuelo-Domínguez, E., and Agostini, E. (2013) Characterization of a phenol-degrading bacterium isolated from an industrial effluent and its potential application for bioremediation. *Environ Technol* **34**: 485-493.

Paisio, C.E., Quevedo, M.R., Talano, M.A., González, P.S., and Agostini, E. (2014) Application of two bacterial strains for wastewater bioremediation and assessment of phenolics biodegradation. *Environ Technol* **35**: 1802-1810.

Paisio, C.E., Talano, M.A., González, P.S., Pajuelo-Domínguez, E., and Agostini, E. (2013) Characterization of a phenol-degrading bacterium isolated from an industrial effluent and its potential application for bioremediation. *Environ Technol* **34**: 485-493.

Paisio, C.E., Talano, M.A., González, P.S., Busto, V.D., Talou, J.R., and Agostini, E. (2012) Isolation and characterization of a *Rhodococcus* strain with phenol-degrading ability and its potential use for tannery effluent biotreatment. *Environ Sci Pollut Res Int* **19**: 3430-3439.

- Pathak, A., Green, S.J., Ogram, A., and Chauhan, A. (2013) Draft genome sequence of *Rhodococcus opacus* strain M213 shows a diverse catabolic potential. *Genome Announc* **1**.
- Patrauchan, M.A., Florizone, C., Eapen, S., Gómez-Gil, L., Sethuraman, B., Fukuda, M. et al. (2008) Roles of ring-hydroxylating dioxygenases in styrene and benzene catabolism in *Rhodococcus jostii* RHA1. *J Bacteriol* **190**: 37-47.
- Perry, J. J. (1980) Propane utilization by microorganisms. *Advance in Applied Microbiology* **26**: 89-115.
- Peterson, J.A., Basu, D., and Coon, M.J. (1966) Enzymatic omega-oxidation. I. Electron carriers in fatty acid and hydrocarbon hydroxylation. *J Biol Chem* **241**: 5162-5164.
- Phillips, W.E., and Perry, J.J. (1974) Metabolism of n-butane and 2-butanone by *Mycobacterium vaccae*. *J Bacteriol* **120**: 987-989.
- Pirnik, M.P., Atlas, R.M., and Bartha, R. (1974) Hydrocarbon metabolism by *Brevibacterium erythrogenes*: normal and branched alkanes. *J Bacteriol* **119**: 868-878.
- Pirog, T.P., Korzh, I.V., and Shevchuk, T.A. (2009) Dehydrogenases oxidizing ethanol and acetaldehyde in *Rhodococcus erythropolis* EK-1. *Mikrobiol Z* **71**: 34-41.
- Plaggenborg, R., Overhage, J., Loos, A., Archer, J.A., Lessard, P., Sinskey, A.J. et al. (2006) Potential of *Rhodococcus* strains for biotechnological vanillin production from ferulic acid and eugenol. *Appl Microbiol Biotechnol* **72**: 745-755.
- Pozzer, A., Pollmann, J., Taraborrelli, D., Jockel, P., Helmig, D., Tans, P., Hueber, J., and Lelieveld, J. (2010) Observed and simulated global distribution and budget of atmospheric C₂-C₅ alkanes. *Atmos. Chem. Phys.* **10**: 4403-4422.
- Prior, S. D., and H. Dalton. 1985. The effect of copper ions on membrane content and methane monooxygenase activity in methanol-grown cells of *Methylococcus capsulatus* (Bath). *J. Gen. Microbiol.* **131**:155–163.
- Proudfoot, A.T. (2003) Pentachlorophenol poisoning. *Toxicol Rev* **22**: 3-11.
- Raj J., Prasad S., Bhalla T.C. (2006) *Rhodococcus rhodochrous* PA-34 a potential catalyst for acrylamide synthesis. *Process Biochem* **41**:1359–1363.
- Raj, J., Sharma, N.N., Prasad, S., and Bhalla, T.C. (2008) Acrylamide synthesis using agar entrapped cells of *Rhodococcus rhodochrous* PA-34 in a partitioned fed batch reactor. *J Ind Microbiol Biotechnol* **35**: 35-40.
- Regnström, K., Aberg, A., Ormö, M., Sahlin, M., and Sjöberg, B.M. (1994) The conserved serine 211 is essential for reduction of the dinuclear iron center in protein R2 of *Escherichia coli* ribonucleotide reductase. *J Biol Chem* **269**: 6355-6361.
- Reid, M.F., and Fewson, C.A. (1994) Molecular characterization of microbial alcohol dehydrogenases. *Crit Rev Microbiol* **20**: 13-56.

- Ridlington, E. (2013). Fracking by the numbers: key impacts of dirty drilling at the state and national level.
- Rodrigues, A.o.S., and Salgado, B.V. (2009) Analysis of methane biodegradation by *Methylosinus trichosporium* OB3b. *Braz J Microbiol* **40**: 301-307.
- Rojo, F. (2009) Degradation of alkanes by bacteria. *Environ Microbiol* **11**: 2477-2490.
- Ruettinger, R.T., Olson, S.T., Boyer, R.F., and Coon, M.J. (1974) Identification of the omega-hydroxylase of *Pseudomonas oleovorans* as a nonheme iron protein requiring phospholipid for catalytic activity. *Biochem Biophys Res Commun* **57**: 1011-1017.
- Sainsbury, P.D., Hardiman, E.M., Ahmad, M., Otani, H., Seghezzi, N., Eltis, L.D., and Bugg, T.D. (2013) Breaking down lignin to high-value chemicals: the conversion of lignocellulose to vanillin in a gene deletion mutant of *Rhodococcus jostii* RHA1. *ACS Chem Biol* **8**: 2151-2156.
- Sakai, M., Miyauchi, K., Kato, N., Masai, E., and Fukuda, M. (2003) 2-Hydroxypenta-2,4-dienoate metabolic pathway genes in a strong polychlorinated biphenyl degrader, *Rhodococcus* sp. strain RHA1. *Appl Environ Microbiol* **69**: 427-433.
- Sambrook, J., and Russell, D.W. (2001) *Molecular cloning: A laboratory manual*. New York: Cold Spring Harbor Laboratory Press.
- Sameshima, Y., Honda, K., Kato, J., Omasa, T., and Ohtake, H. (2008) Expression of *Rhodococcus opacus alkB* genes in anhydrous organic solvents. *J Biosci Bioeng* **106**: 199-203.
- Sander, R. (1999). Compilation of Henry's Law constants for inorganic and organic species of potential importance in environmental chemistry (Version 3). URL <http://www.henrys-law.org>
- Sariaslani, F.S. (1991) Microbial cytochromes P450 and xenobiotic metabolism. *Adv Appl Microbiol* **36**: 133-178.
- Sayavedra-Soto, L.A., Hamamura, N., Liu, C.W., Kimbrel, J.A., Chang, J.H., and Arp, D.J. (2011) The membrane-associated monooxygenase in the butane-oxidizing Gram-positive bacterium *Nocardioides* sp. strain CF8 is a novel member of the AMO/PMO family. *Environ Microbiol Rep* **3**: 390-396.
- Scanlan, J., Dumont, M.G., and Murrell, J.C. (2009) Involvement of MmoR and MmoG in the transcriptional activation of soluble methane monooxygenase genes in *Methylosinus trichosporium* OB3b. *FEMS Microbiol Lett* **301**: 181-187.
- Schafer, D.D. (2012). Fracking attack: cracking the case against hydraulic fracturing. *Independence Institute*.

- Schenkels P., D.J.A. (2000) Nicotinoprotein (NADH-containing) alcohol dehydrogenase from *Rhodococcus erythropolis* DSM 1069: an efficient catalyst for coenzyme-independent oxidation of a broad spectrum alcohols and the interconversion of alcohols and aldehydes. *Microbiology*: 775-785.
- Schneiker, S., Martins dos Santos, V.A., Bartels, D., Bekel, T., Brecht, M., Buhrmester, J. et al. (2006) Genome sequence of the ubiquitous hydrocarbon-degrading marine bacterium *Alcanivorax borkumensis*. *Nat Biotechnol* **24**: 997-1004.
- Schwartz, R.D., and McCoy, C.J. (1973) *Pseudomonas oleovorans* hydroxylation-epoxidation system: additional strain improvements. *Appl Microbiol* **26**: 217-218.
- Schäfer, A., Tauch, A., Jäger, W., Kalinowski, J., Thierbach, G., and Pühler, A. (1994) Small mobilizable multi-purpose cloning vectors derived from the *Escherichia coli* plasmids pK18 and pK19: selection of defined deletions in the chromosome of *Corynebacterium glutamicum*. *Gene* **145**: 69-73.
- Sekine, M., Tanikawa, S., Omata, S., Saito, M., Fujisawa, T., Tsukatani, N. et al. (2006) Sequence analysis of three plasmids harboured in *Rhodococcus erythropolis* strain PR4. *Environ Microbiol* **8**: 334-346.
- Sekizaki, T., Tanoue, T., Osaki, M., Shimoji, Y., Tsubaki, S., and Takai, S. (1998) Improved electroporation of *Rhodococcus equi*. *J Vet Med Sci* **60**: 277-279.
- Selbitschka, W., Niemann, S., and Pühler, A. (1993) Construction of gene replacement vectors for Gram-negative bacteria using a genetically modified *sacRB* gene as a positive selection marker. *Appl Microbiol Biotechnol* **38**: 615-618.
- Semrau, J.D., Zolanz, D., Lidstrom, M.E., and Chan, S.I. (1995) The role of copper in the pMMO of *Methylococcus capsulatus* Bath: a structural vs. catalytic function. *J Inorg Biochem* **58**: 235-244.
- Seto, M., Kimbara, K., Shimura, M., Hatta, T., Fukuda, M., and Yano, K. (1995) A novel transformation of polychlorinated biphenyls by *Rhodococcus* sp. strain RHA1. *Appl Environ Microbiol* **61**: 3353-3358.
- Shanklin, J., Whittle, E., and Fox, B.G. (1994) Eight histidine residues are catalytically essential in a membrane-associated iron enzyme, stearoyl-CoA desaturase, and are conserved in alkane hydroxylase and xylene monooxygenase. *Biochemistry* **33**: 12787-12794.
- Shanklin, J., Achim, C., Schmidt, H., Fox, B.G., and Münck, E. (1997) Mössbauer studies of alkane omega-hydroxylase: evidence for a diiron cluster in an integral-membrane enzyme. *Proc Natl Acad Sci U S A* **94**: 2981-2986.
- Shao, Z., Dick, W.A., and Behki, R.M. (1995) An improved *Escherichia coli*-*Rhodococcus* shuttle vector and plasmid transformation in *Rhodococcus* spp. using electroporation. *Lett Appl Microbiol* **21**: 261-266.
- Sharp, J.O., Sales, C.M., and Alvarez-Cohen, L. (2010) Functional characterization of propane-enhanced N-nitrosodimethylamine degradation by two actinomycetales. *Biotechnol Bioeng* **107**: 924-932.

- Sharp, J.O., Sales, C.M., LeBlanc, J.C., Liu, J., Wood, T.K., Eltis, L.D. et al. (2007) An inducible propane monooxygenase is responsible for N-nitrosodimethylamine degradation by *Rhodococcus* sp. strain RHA1. *Appl Environ Microbiol* **73**: 6930-6938.
- Sheehan, M.C., Bailey, C.J., Dowds, B.C., and McConnell, D.J. (1988) A new alcohol dehydrogenase, reactive towards methanol, from *Bacillus stearothermophilus*. *Biochem J* **252**: 661-666.
- Shennan, J.L. (2006) Utilisation of C₂-C₄ gaseous hydrocarbons and isoprene by microorganisms. *Journal of Chemical Technology & Biotechnology* **81**: 237-256.
- Shevtsov, A., Tarlykov, P., Zholdybayeva, E., Momynkulov, D., Sarsenova, A., Moldagulova, N., and Momynaliev, K. (2013) Draft genome sequence of *Rhodococcus erythropolis* DN1, a crude oil biodegrader. *Genome Announc* **1**.
- Shields-Menard, S.A., Brown, S.D., Klingeman, D.M., Indest, K., Hancock, D., Wewelwela, J.J. et al. (2014) Draft genome sequence of *Rhodococcus rhodochrous* strain ATCC 21198. *Genome Announc* **2**.
- Simon, R., Priefer, U., and Puhler, A. (1983) A broad host range mobilization system for *in vivo* genetic engineering: transposon mutagenesis in Gram-negative bacteria. *Nat Biotechnol* **1**: 784-791.
- Singer, M.E., and Finnerty, W.R. (1988) Construction of an *Escherichia coli*-*Rhodococcus* shuttle vector and plasmid transformation in *Rhodococcus* spp. *J Bacteriol* **170**: 638-645.
- Sluis, M.K., Sayavedra-Soto, L.A., and Arp, D.J. (2002) Molecular analysis of the soluble butane monooxygenase from *Pseudomonas butanovora*. *Microbiology* **148**: 3617-3629.
- Smith, C.A., and Hyman, M.R. (2004) Oxidation of methyl tert-butyl ether by alkane hydroxylase in dicyclopropylketone-induced and n-octane-grown *Pseudomonas putida* GPo1. *Appl Environ Microbiol* **70**: 4544-4550.
- Smith, T.J., Slade, S.E., Burton, N.P., Murrell, J.C., and Dalton, H. (2002) Improved system for protein engineering of the hydroxylase component of soluble methane monooxygenase. *Appl Environ Microbiol* **68**: 5265-5273.
- Smits, T.H., Witholt, B., and van Beilen, J.B. (2003) Functional characterization of genes involved in alkane oxidation by *Pseudomonas aeruginosa*. *Antonie Van Leeuwenhoek* **84**: 193-200.
- Smits, T.H., Röthlisberger, M., Witholt, B., and van Beilen, J.B. (1999) Molecular screening for alkane hydroxylase genes in Gram-negative and Gram-positive strains. *Environ Microbiol* **1**: 307-317.
- Smits, T.H., Balada, S.B., Witholt, B., and van Beilen, J.B. (2002) Functional analysis of alkane hydroxylases from Gram-negative and Gram-positive bacteria. *J Bacteriol* **184**: 1733-1742.

Sotsky, J.B., Greer, C.W., and Atlas, R.M. (1994) Frequency of genes in aromatic and aliphatic hydrocarbon biodegradation pathways within bacterial populations from Alaskan sediments. *Can J Microbiol* **40**: 981-985.

Steffan, R.J., McClay, K., Vainberg, S., Condee, C.W., and Zhang, D. (1997) Biodegradation of the gasoline oxygenates methyl tert-butyl ether, ethyl tert-butyl ether, and tert-amyl methyl ether by propane-oxidizing bacteria. *Appl Environ Microbiol* **63**: 4216-4222.

Steinmetz, M., D. Le Coq, H. B. Djemia, and P. Gay. (1983). Analyse géne'tique de *sacB*, ge`ne de structure d'une enzyme secre'te'e, la le'vane-saccharase de *Bacillus subtilis* Marburg. *Mol. Gen. Genet.* **191**:138-144

Steinmetz, M., Le Coq, D., Aymerich, S., Gonzy-Tréboul, G., and Gay, P. (1985) The DNA sequence of the gene for the secreted *Bacillus subtilis* enzyme levansucrase and its genetic control sites. *Mol Gen Genet* **200**: 220-228.

Stinear, T.P., Seemann, T., Harrison, P.F., Jenkin, G.A., Davies, J.K., Johnson, P.D. et al. (2008) Insights from the complete genome sequence of *Mycobacterium marinum* on the evolution of *Mycobacterium tuberculosis*. *Genome Res* **18**: 729-741.

Stolyar, S., Costello, A.M., Peeples, T.L., and Lidstrom, M.E. (1999) Role of multiple gene copies in particulate methane monooxygenase activity in the methane-oxidizing bacterium *Methylococcus capsulatus* Bath. *Microbiology* **145**: 1235-1244.

Strnad, H., Patek, M., Fousek, J., Szokol, J., Ulbrich, P., Nesvera, J. et al. (2014) Genome sequence of *Rhodococcus erythropolis* strain CCM2595, a phenol derivative-degrading bacterium. *Genome Announc* **2**.

Strom, T., Ferenci, T., and Quayle, J.R. (1974) The carbon assimilation pathways of *Methylococcus capsulatus*, *Pseudomonas methanica* and *Methylosinus trichosporium* (OB3B) during growth on methane. *Biochem J* **144**: 465-476.

Sullivan, J.P., Dickinson, D., and Chase, H.A. (1998) Methanotrophs, *Methylosinus trichosporium* OB3b, sMMO, and their application to bioremediation. *Crit Rev Microbiol* **24**: 335-373.

Sunairi, M., Iwabuchi, N., Murakami, K., Watanabe, F., Ogawa, Y., Murooka, H., and Nakajima, M. (1996) Effect of penicillin G on the electroporation of *Rhodococcus rhodochrous* CF222. *Lett Appl Microbiol* **22**: 66-69.

Takahashi, J. (1980). Production of intracellular and extracellular protein from n-butane by *Pseudomonas butanovora* sp. nov. *Adv. Appl Microbiol* **26**: 117-127.

Takeda, H., Yamada, A., Miyauchi, K., Masai, E., and Fukuda, M. (2004) Characterization of transcriptional regulatory genes for biphenyl degradation in *Rhodococcus* sp. strain RHA1. *Journal of Bacteriology* **186**: 2134-2146.

Takei, D., Washio, K., and Morikawa, M. (2008) Identification of alkane hydroxylase genes in *Rhodococcus* sp. strain TMP2 that degrades a branched alkane. *Biotechnol Lett* **30**: 1447-1452.

Takeuchi, M., Hatano, K., Sedláček, I., and Páková, Z. (2002) *Rhodococcus jostii* sp. nov., isolated from a medieval grave. *Int J Syst Evol Microbiol* **52**: 409-413.

Tamura, K., Peterson, D., Peterson, N., Stecher, G., Nei, M., and Kumar, S. (2011) MEGA5: molecular evolutionary genetics analysis using maximum likelihood, evolutionary distance, and maximum parsimony methods. *Mol Biol Evol* **28**: 2731-2739.

Tao, F., Zhao, P., Li, Q., Su, F., Yu, B., Ma, C. et al. (2011) Genome sequence of *Rhodococcus erythropolis* XP, a biodesulfurizing bacterium with industrial potential. *Journal of Bacteriology* **193**: 6422-6423.

van Beilen, J.B., and Funhoff, E.G. (2005) Expanding the alkane oxygenase toolbox: new enzymes and applications. *Curr Opin Biotechnol* **16**: 308-314.

van Beilen, J.B., Wubbolts, M.G., and Witholt, B. (1994) Genetics of alkane oxidation by *Pseudomonas oleovorans*. *Biodegradation* **5**: 161-174.

van Beilen, J.B., Panke, S., Lucchini, S., Franchini, A.G., Röthlisberger, M., and Witholt, B. (2001) Analysis of *Pseudomonas putida* alkane-degradation gene clusters and flanking insertion sequences: evolution and regulation of the *alk* genes. *Microbiology* **147**: 1621-1630.

van Beilen, J.B., Holtackers, R., Lüscher, D., Bauer, U., Witholt, B., and Duetz, W.A. (2005) Biocatalytic production of perillyl alcohol from limonene by using a novel *Mycobacterium* sp. cytochrome P450 alkane hydroxylase expressed in *Pseudomonas putida*. *Appl Environ Microbiol* **71**: 1737-1744.

Van Beilen, J.B., Mourlane, F., Seeger, M.A., Kovac, J., Li, Z., Smits, T.H. et al. (2003) Cloning of Baeyer-Villiger monooxygenases from *Comamonas*, *Xanthobacter* and *Rhodococcus* using polymerase chain reaction with highly degenerate primers. *Environ Microbiol* **5**: 174-182.

van Beilen, J.B., Funhoff, E.G., van Loon, A., Just, A., Kaysser, L., Bouza, M. et al. (2006) Cytochrome P450 alkane hydroxylases of the CYP153 family are common in alkane-degrading eubacteria lacking integral membrane alkane hydroxylases. *Appl Environ Microbiol* **72**: 59-65.

van der Geize, R., de Jong, W., Hessels, G.I., Grommen, A.W., Jacobs, A.A., and Dijkhuizen, L. (2008) A novel method to generate unmarked gene deletions in the intracellular pathogen *Rhodococcus equi* using 5-fluorocytosine conditional lethality. *Nucleic Acids Res* **36**: e151.

van Ginkel, C. G., Welten, H. G. J., Hartmans, S. & de Bont, J. A. M. (1987). Metabolism of *trans*-2-butene and butane in *Nocardia* TB1. *J Gen Microbiol* **133**: 1713-1720.

van Hylckama Vlieg, J.E., Leemhuis, H., Spelberg, J.H., and Janssen, D.B. (2000) Characterization of the gene cluster involved in isoprene metabolism in *Rhodococcus* sp. strain AD45. *J Bacteriol* **182**: 1956-1963.

- Van Ophem, P.W., Van Beeumen, J., and Duine, J.A. (1993) Nicotinoprotein NAD(P)-containing alcohol/aldehyde oxidoreductases. Purification and characterization of a novel type from *Amycolatopsis methanolica*. *Eur J Biochem* **212**: 819-826.
- Vangnai, A.S., and Arp, D.J. (2001) An inducible 1-butanol dehydrogenase, a quinohaemoprotein, is involved in the oxidation of butane by *Pseudomonas butanovora*. *Microbiology* **147**: 745-756.
- Vangnai, A.S., Arp, D.J., and Sayavedra-Soto, L.A. (2002a) Two distinct alcohol dehydrogenases participate in butane metabolism by *Pseudomonas butanovora*. *J Bacteriol* **184**: 1916-1924.
- Vangnai, A.S., Sayavedra-Soto, L.A., and Arp, D.J. (2002b) Roles for the two 1-butanol dehydrogenases of *Pseudomonas butanovora* in butane and 1-butanol metabolism. *J Bacteriol* **184**: 4343-4350.
- Vonck, J., Arfman, N., De Vries, G.E., Van Beeumen, J., Van Bruggen, E.F., and Dijkhuizen, L. (1991) Electron microscopic analysis and biochemical characterization of a novel methanol dehydrogenase from the thermotolerant *Bacillus* sp. C1. *J Biol Chem* **266**: 3949-3954.
- Warhurst, A.M., and Fewson, C.A. (1994) Biotransformations catalyzed by the genus *Rhodococcus*. *Crit Rev Biotechnol* **14**: 29-73.
- Warren, R., Hsiao, W.W., Kudo, H., Myhre, M., Dosanjh, M., Petrescu, A. et al. (2004) Functional characterization of a catabolic plasmid from polychlorinated-biphenyl-degrading *Rhodococcus* sp. strain RHA1. *J Bacteriol* **186**: 7783-7795.
- Wegener, W.S., Reeves, H.C., Rabin, R., and Ajl, S.J. (1968) Alternate pathways of metabolism of short-chain fatty acids. *Bacteriol Rev* **32**: 1-26.
- West, C.A., Salmond, G.P., Dalton, H., and Murrell, J.C. (1992) Functional expression in *Escherichia coli* of proteins B and C from soluble methane monooxygenase of *Methylococcus capsulatus* (Bath). *J Gen Microbiol* **138**: 1301-1307.
- Whyte, L.G., Smits, T.H.M., Labbe, D., Witholt, B., Greer, C.W., and van Beilen, J.B. (2002) Gene cloning and characterization of multiple alkane hydroxylase systems in *Rhodococcus* strains Q15 and NRRL B-16531. *Applied and Environmental microbiology* **68**: 5933-5942.
- Willetts, A. (1979) Bacterial metabolism of propane-1,2-diol. *Biochem Biophys Acta* **588**: 302-309.
- Woods, N.R., and Murrell, J.C. (1989) The metabolism of propane in *Rhodococcus rhodochrous* PNKb1. *J Gen Microbiol* **135**: 2335-2344.
- Woods N.R., and Murrell, J.C. (1990) Epoxidation of gaseous alkenes by a *Rhodococcus* sp. *Biotechnol Letts* **12**:409-414.

Xie, M., Alonso, H., and Roujeinikova, A. (2011) An improved procedure for the purification of catalytically active alkane hydroxylase from *Pseudomonas putida* GP01. *Appl Biochem Biotechnol* **165**: 823-831.

Yam, K., van der Geize, R., and Eltis, L. (2010) in *The Biology of Rhodococcus* (Alvarez, H. M., ed) Springer, New York, in press.

Yang, J.C., Lessard, P.A., Sengupta, N., Windsor, S.D., O'brien, X.M., Bramucci, M. et al. (2007) TraA is required for megaplasmid conjugation in *Rhodococcus erythropolis* AN12. *Plasmid* **57**: 55-70.

Yoshida, A., Rzhetsky, A., Hsu, L.C., and Chang, C. (1998) Human aldehyde dehydrogenase gene family. *Eur J Biochem* **251**: 549-557.